

ADVANCES IN CHEMICAL PHYSICS
VOLUME III

EDITORIAL BOARD

- THOR A. BAK, Universitetets Fysik Kemiske Institut, Copenhagen, Denmark
- H. C. LONGUETT-HIGGINS, The University Chemical Laboratory, Cambridge, England
- V. MATHOT, Université Libre de Bruxelles, Brussels, Belgium
- P. MAZUR, Institut Lorentz, Leiden, Holland
- A. MÜNSTER, Laboratoire Chimie Physique, Université de Paris, Paris, France
- S. ONO, Institute of Physics, College of General Education, Tokyo, Japan
- B. PULLMAN, Laboratoire de Chimie Théorique, Université de Paris, Paris, France
- S. RICE, Department of Chemistry, University of Chicago, Chicago, Illinois
- M. V. VOL'KENShteIN, Institute of Macromolecular Chemistry, Leningrad, U.S.S.R.
- B. ZIMM, General Electric Research Laboratory, Schenectady, New York

ADVANCES IN CHEMICAL PHYSICS

Edited by I. PRIGOGINE

University of Brussels, Brussels, Belgium

VOLUME III

INTERSCIENCE PUBLISHERS, INC., NEW YORK
INTERSCIENCE PUBLISHERS LTD., LONDON

FIRST PUBLISHED 1961

ALL RIGHTS RESERVED

LIBRARY OF CONGRESS CATALOG CARD NUMBER 58-9935

INTERSCIENCE PUBLISHERS, INC., 250 Fifth Avenue, New York 1, New York
INTERSCIENCE PUBLISHERS LTD., 88/90 Chancery Lane, London W. C. 2, England

PRINTED IN THE NETHERLANDS

BIJ DIJKSTRA'S DRUKKERIJ, VOORHEEN BOEKDRUKKERIJ GEBR. HOITSEMA N.V., GRONINGEN

INTRODUCTION

In the last decades, chemical physics has attracted an ever increasing amount of interest. The variety of problems, such as those of chemical kinetics, molecular physics, molecular spectroscopy, transport processes, thermodynamics, the study of the state of matter, and the variety of experimental methods used, makes the great development of this field understandable. But the consequence of this breadth of subject matter has been the scattering of the relevant literature in a great number of publications.

Despite this variety and the implicit difficulty of exactly defining the topic of chemical physics, there are a certain number of basic problems that concern the properties of individual molecules and atoms as well as the behavior of statistical ensembles of molecules and atoms. This new series is devoted to this group of problems which are characteristic of modern chemical physics.

As a consequence of the enormous growth in the amount of information to be transmitted, the original papers, as published in the leading scientific journals, have of necessity been made as short as is compatible with a minimum of scientific clarity. They have, therefore, become increasingly difficult to follow for anyone who is not an expert in this specific field. In order to alleviate this situation, numerous publications have recently appeared which are devoted to review articles and which contain a more or less critical survey of the literature in a specific field.

An alternative way to improve the situation, however, is to ask an expert to write a comprehensive article in which he explains his view on a subject freely and without limitation of space. The emphasis in this case would be on the personal ideas of the author. This is the approach that has been attempted in this new series. We hope that as a consequence of this approach, the series may become especially stimulating for new research.

Finally, we hope that the style of this series will develop into

something more personal and less academic than what has become the standard scientific style. Such a hope, however, is not likely to be completely realized until a certain degree of maturity has been attained — a process which normally requires a few years.

At present, we intend to publish one volume a year, but this schedule may be revised in the future.

In order to proceed to a more effective coverage of the different aspects of chemical physics, it has seemed appropriate to form an editorial board. I want to express to them my thanks for their cooperation.

I. PRIGOGINE

CONTRIBUTORS TO VOLUME III

- THOR A. BAK, Institute for Physical Chemistry, University of Copenhagen, Copenhagen, Denmark
- O. BASTIANSEN, Universitetets Kyemiske Institutt, Blinderen Oslo, Norway
- C. F. CURTISS, Theoretical Chemistry Laboratory, University of Wisconsin, Madison, Wisconsin
- PHILIP J. ELVING, Laboratoire de Chimie Théorique, Université de Paris, Paris, France
- J. O. HIRSCHFELDER, Theoretical Chemistry Laboratory, University of Wisconsin, Madison, Wisconsin
- J. HOARAU, Laboratoire de Chimie Physique, Université de Bordeaux, Bordeaux, France
- HAROLD S. JOHNSTON, Department of Chemistry, University of California, Berkeley, California
- A. MARCHAND, Laboratoire de Chimie Physique, Université de Bordeaux, Bordeaux, France
- SYU ONO, College of General Education, University of Tokyo, Tokyo, Japan
- A. PACAULT, Laboratoire de Chimie Physique, Université de Bordeaux, Bordeaux, France
- BERNARD PULLMAN, Laboratoire de Chimie Théorique, Université de Paris, Paris, France
- P. N. SKANCKE, Universitetets Kyemiske Institutt, Blinderen Oslo, Norway
- WITOLD TOMASSI, Warsaw Polytechnic, Warsaw, Poland

CONTENTS

Mechanisms of Organic Electrode Reactions	
<i>By Philip J. Elving and Bernard Pullman</i>	1
Nonlinear Problems in Thermodynamics of Irreversible Processes	
<i>By Thor A. Bak</i>	33
Propagation of Flames and Detonations	
<i>By J. O. Hirschfelder and C. F. Curtiss</i>	59
Large Tunnelling Corrections in Chemical Reaction Rates	
<i>By Harold S. Johnston</i>	131
Aspects Récents du Diamagnétisme	
<i>Par A. Pacault, J. Hoarau, et A. Marchand</i>	171
Power Electrodes and their Applications	
<i>By Witold Tomassi</i>	239
Variational Principles in Thermodynamics and Statistical Mechanics of Irreversible Processes	
<i>By Syu Ono</i>	267
Electron Diffraction in Gasses and Molecular Structure	
<i>By O. Bastiansen and P. N. Skancke</i>	323

MECHANISMS OF ORGANIC ELECTRODE REACTIONS*

PHILIP J. ELVING† and BERNARD PULLMAN,
Laboratoire de Chimie Théorique, Faculté des Sciences, Paris

CONTENTS

I. Introduction	1
II. Reaction Mechanisms of Electrode Reactions	3
A. Bond Rupture	3
B. Processes Involving More Than Two Electrons	4
III. Chemical Reaction Mechanism	5
A. General Mechanism	8
B. Carbon-Halogen Bond Fission	11
C. Ketone Reduction	12
IV. Electrochemical Reaction Mechanism	13
A. Carbon-Halogen Bond Fission	14
B. Significance of pH-Dependence of Half-Wave Potential	15
C. Ketone Reduction	16
V. Energetic Reaction Mechanism	19
A. Thermodynamic-Kinetic Approach	19
B. Quantum Mechanical Approach	24
C. Rate Constant Calculation	29
References	30

I. INTRODUCTION

The primary aim of the present discussion is to summarize current approaches to the problem of the elucidation of the mechanism of the half-cell reaction for the electrolysis of an organic compound at an electrode. This reaction can be depicted in its simplest form as



* One of the authors (PJE) would like to thank the U.S. Atomic Energy Commission which has supported his investigations of organic electrochemical processes.

† Permanent address: Department of Chemistry, University of Michigan, Ann Arbor, Michigan, U.S.A.

where Ox represents the oxidized form, Red the reduced form and n the number of electrons transferred.

The stoichiometric form of Eq. 1 is usually quite simple, involving simple numerical ratios of oxidized and reduced forms with perhaps the addition of one or more of the species, hydrogen ions, hydroxyl ions and water, to balance the equation. However, the actual course of the reaction is quite complex since it is at least formally heterogeneous in nature, involving electron transfer between presumably a solution species or its adsorbed or otherwise altered form, and the electrode, and occurring in the interfacial region between bulk solution and electrode, which is distinguished as the electrical double layer.

Theoretically and experimentally, we have a relatively good picture of the mass transfer process, i.e., of the process of bringing an electroactive species from a point in the bulk solution "up to the electrode," although the latter phrase is often not too clearly defined in terms of the various subregions of the interfacial region between the physical electrode and the bulk solution. A number of treatments of more or less satisfactory nature have been made of the relations of the rates of the heterogeneous electron-transfer process to the observed potential and current values. (Treatments involving the effect of coupled chemical reactions preceding and following the electron-transfer step or steps have been described, e.g., Koutecký's excellent studies). However, these have not been systematically applied to the situations prevailing in organic electrode reactions. Many studies have been made of the reaction mechanisms of organic electrode reactions. Some of these studies have been very interesting and penetrating, but others have been lessened in value by such factors as generalizations based on data for too few compounds, failure to identify positively the reaction product or products, neglect of the effects of experimental conditions, overly naive treatment of the experimental data, and neglect of the kinetics and energetics of the electron-transfer process.

The further purposes of the present study are to indicate the physical bases and the interrelationships of the treatments of different aspects of organic electrode reactions, and to emphasize

the basis for a synthesis of the various treatments in so far as their presently revealed interrelationships permit this to be done.

The discussion is based primarily on data gathered by polarographic and derived voltammetric and electrolytic techniques and on the interpretations of such data. The use of known potential relations is essential to the interpretation of electron-transfer processes.

II. REACTION MECHANISMS OF ELECTRODE REACTIONS

Currently, three general approaches to the problem of organic electrode reaction mechanisms are being made: (1) The *chemical* reaction mechanism, in which the mechanism is stated in terms of the species involved on the basis usually used in describing organic chemical reaction mechanisms in homogeneous solution. (2) The *electrochemical* reaction mechanism, in which the processes occurring are described from the viewpoint of a more detailed analysis of the physical situation. (3) The *energetic* reaction mechanism, in which a more precise and, if possible, mathematical statement of the relation between the electron-transfer steps and the mechanistic picture is attempted.

In a sense, this sequence is a logical development in the elucidation of a mechanism and its interrelations with the factors involved. The three approaches will be discussed in that order.

Since the electrochemical reduction of organic compounds has been so much more extensively studied than the electrochemical oxidation of such compounds, the discussion will stress reductive processes, although the general ideas involved are equally well applicable to oxidative processes after due allowance is made for the change in direction of electron transfer.

A. Bond Rupture

Electrochemical reduction in the case of an organic compound involves, as in the reduction of an inorganic species, the net transfer of electrons from the electrode to the electroactive species; the essential difference is that in most inorganic reductions "normal" chemical bonds are rarely considered to be broken except, perhaps, in the cases where the electroactive element

either is present as an oxygenated species or has a lesser coordination number in the reduced state than in the oxidized state. On the other hand, organic reductions involve readily observed changes in the structure of functional groups or moieties with the concomitant feature that a single organic electrode reaction involves the transfer to the electroactive species of: (a) one electron, if a free radical is produced which dimerizes at the site of the electroactive moiety or at one derived from it through intramolecular electron rearrangement; (b) two electrons, if a bond is completely severed without formation of an intermediate free radical and its consequent dimerization preceding further electron transfer; or (c) combinations—simultaneous and/or successive—of one-electron and/or two-electron processes.

B. Processes. Involving More Than Two Electrons

The situation has been frequently described in the literature where the overall electrode reaction, e.g., that giving rise to a single polarographic wave, involves the transfer of more than two electrons per molecule of electroactive substance; such electrode reactions are due to either (a) a succession of processes whose potentials are so close together that a single reaction seems to be occurring, or (b) the occurrence of a one- or two-electron process at a certain potential to produce species which would be themselves reducible at a less energetic potential and which consequently immediately upon formation accept more electrons.

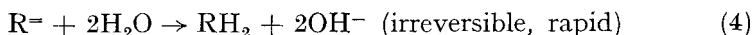
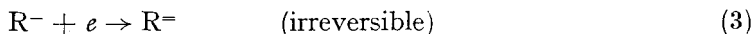
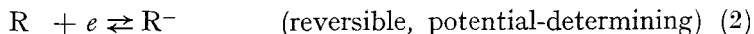
It is reasonable to assume on the basis of the considerable corpus of recent work on the mechanisms of inorganic and organic, homogeneous and heterogeneous (including electrode) reactions, that the occurrence of an electrode reaction involving the "simultaneous" transfer of more than two electrons is practically nil. Indeed, a question might be legitimately raised as to whether the apparently observed "simultaneous" two-electron transfer processes are not actually two one-electron processes which follow each other exceedingly rapidly in time, e.g., within, perhaps, less than either the life-time of an intermediate species or the time of a single molecular vibration. Since the previous argument

often is a nonoperational one and since dimers indicating one-electron processes do occur, we shall assume that a "simultaneous" two-electron process is the rapid succession of the reactions represented by subsequent Eqs. 14 and 18, with the amendment that the electrons may follow each other so rapidly that the transition state effectively represents a combination of the electroactive species and two electrons.

III. CHEMICAL REACTION MECHANISM

The chemical reaction type of mechanism is usually stated in terms of a set of chemical equations, certain ones of which may be specified as being "fast" or "slow" in order to emphasize potential-determining stages in the overall reaction. The only distinguishing characteristic is the treatment of the electron as one of the reactants with the often implied premise that an electron-transfer step must be the essential or determining stage.

Typical of such schemes is the one originally proposed by Laitinen and Wawzonek¹⁵ to explain their observations on the pH-independent polarographic reduction of styrene and stilbene:



Although this model was based on rather meager experimental evidence which has been shown to be—at least in part—in-sufficient to describe fully the behavior of the compounds involved,¹⁰ the reaction scheme of Eqs. 2 to 4 has been used to explain quite adequately the observed polarographic reduction of many organic compounds. The present discussion is obviously indebted to this pioneering and provocative suggestion.

Many attempts have been made to describe the experimental data in terms of substitution or free radical mechanisms, e.g., references 4 and 7. These mechanism deductions and the tests made of them have been based generally on the correlation of the

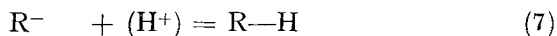
ease of reduction with structural factors and products* rather than on kinetic considerations as in the case of homogeneous solution reactions. Such attempts to explain or at least to describe a heterogeneous reaction in terms originally defined for homogeneous solution reactions are certainly open to criticism on that account. However, the success or lack of success of such treatments may help to indicate the extent to which the electrode reaction is explicable in such terms.

In the subsequent discussion, we shall consider the successive stages in the breaking of a bond, e.g., the bond between a carbon atom which can be taken as the reaction center and some other atom Y at the electroactive site, $R'_3C-YR''_m$, where R' and R'' represent any substituents including C and Y as in the particular cases of multiple bonds between C and Y, and of several Y connected to the same C center, and m is any number, including zero, which is necessary to define the species involved. For convenience, we shall represent the R'_3C- entity as R and $-YR''_m$ entity as X with the electroactive species being then written as $R-X$ or, if we assume a localized electron pair to describe adequately the bond, as $R:X$. Obviously, the reactive center can be an atom other than carbon; nitrogen, oxygen and sulfur have been found, *inter alia*, to function as reactive centers in organic electrode reactions.

The general approaches for the common types of organic reaction mechanisms can be summarized as in the following equations. Hydrogen and hydroxide ions, and water are not being shown except where necessary to indicate the final establishment of an electrically balanced species. The role of such species as reactants in potential-determining reactions is subsequently discussed. A similar statement applied to the situation where a multiple bond exists originally between R and X, and one or more bonds between them persist in the product of a step in the reaction or of the overall reaction.

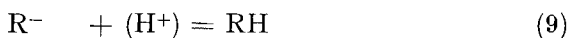
* E.g., expected ease of bond fission based on considerations of permanent polarization and polarizability, and compatibility of observed behavior on substitution with that predicted for different types of mechanisms.

S_N1 process:

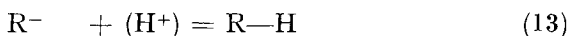
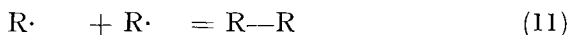
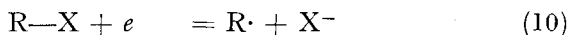


(The species, (H^+) , is intended to represent a proton source such as water or hydrogen ion.)

S_N2 process:



Free radical process:



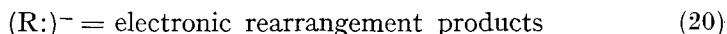
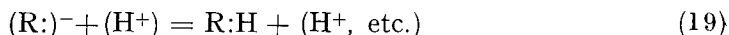
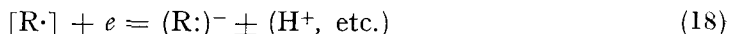
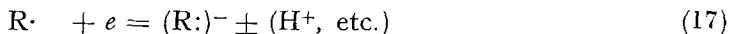
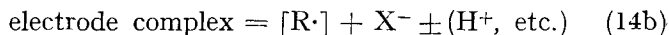
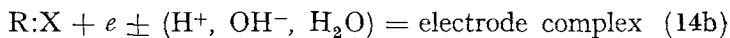
Operationally, there is often but little difference between the S_N1 and S_N2 mechanisms. In the use of the S_N1 description, one would like the electron-transfer step to be potential-determining. To do this, it is necessary to assume that the energy-controlling dissociation (Eq. 5) is due to the electrical field, i.e., the electrode potential, and that consequentially the electrons enter simultaneously. However, this is equivalent to the transition state that has to be postulated for the controlling stage of the S_N2 mechanism (Eq. 8). Consequently, it is probably more justifiable to speak of the *ionic* or *carbanion* mechanism, rather than of the S_N1 or S_N2 mechanism.

The ionic mechanism accommodates the data in the following respects: The slow step involves electron attack; there is simultaneous dissociation of the X entity so that the R—X bond strength must be involved in the potential required for reaction.

The free radical hypothesis is even more satisfactory and is considerably more popular. The isolation of dimer products (Eq. 11) is powerful evidence for this mechanism. The potential-determining step is usually assigned to the introduction of the first electron (Eq. 10), which is the step involving bond fission.

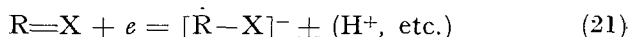
A. General Mechanism

A general sequence of reaction steps can be postulated, which will afford a basis for indicating the possibility of both ionic and free radical mechanisms. Such a general mechanism will facilitate the discussion of electrode processes, which, for example, may seem to change mechanism with experimental conditions or between members of a homologous series. The possible overall steps in a reaction occurring at an electrode may then be represented as follows:



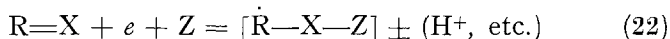
Equations 14a and 14b represent the formation of an electrode intermediate species, $[R\cdot]$, which may be converted to a more or less stable trigonal free radical (Eq. 15) or may be reduced to a carbanion (Eq. 18). The free radical formed may dimerize (Eq. 16) or be reduced to a carbanion (Eq. 17). The carbanion may then neutralize itself by acquisition of a proton from a solvent or interfacial species (Eq. 19) or by intramolecular electronic rearrangement (Eq. 20) with elimination of an anion.

If R and X are connected by multiple bonds, the combined initial reactions (Eqs. 14a and 14b) may be depicted as follows, where each horizontal line conventionally represents an electron pair,



However, since multiple bond reductions frequently, if not always, involve a third reactant, which is a solution component,

Z, such as hydrogen ion, it is probably better to use the following equation



Succeeding reactions of the intermediate species can still be depicted by Eqs. 15 to 20.

The general mechanistic scheme described will obviously be applicable to situations such as those which led to the mechanism proposed by Laitinen and Wawzonek¹⁵ which has been described, as well as being a more general formulation of the mechanism model used by Evans and Hush⁹ to interpret ionogenic reactions involving bond breaking at electrodes.

Certain qualifying and characterizing statements might be made about the proposed reaction scheme. For example, relative to the involvement of hydrogen (or hydroxyl) ion in the reactions as an energy-controlling component, the reaction of Eq. 19 is generally so rapid that it is not potential-controlling. It is safe to say on the basis of the many observations made on reactions whose potentials are pH-dependent, that such pH-dependence is commonly associated with the reaction of Eq. 14; there are few, if any, well-defined examples of the reaction represented by Eqs. 15 to 18 being pH-dependent. For example, in reductions such as those of ketones where two polarographic waves are observed with the first wave due to formation of a free radical species and the second to the reduction of the latter, the first wave may be pH-dependent but the second wave apparently never is. Such pH-dependence of the first wave may then be associated with hydrogen or hydroxyl ion being involved in formation of the energy-determining activated complex or transition state, whether the hydrogen or hydroxyl ion is involved in the final stoichiometry of the first step as in Eq. 22 or is not (Eq. 14, disregarding items in parentheses). This does not necessarily mean that every first reaction step representable by Eq. 22 is pH-dependent.*

However, this does not affect the principles of the text

* The importance of hydrogen ion in determining the state of the electroactive species involved and consequently the energy of the reaction is considerable in many situations, e.g., those involving acid-anion and keto-enol systems.

discussion. For example, the half-wave potential of the 2-bromoalkanoic acids is pH-dependent in the pH region where the shift from anion to more readily reduced acid form may be expected to be appreciable; the fundamental carbon-bromine bond fission process is pH-independent throughout the pH range involved.

The argument is a general one, since other solution components in addition to hydrogen ion may affect the reactive species; e.g., the studies of Zuman and Brezina on the effect of ammonia and amines on carbonyl group reductions. An analogous argument concerns the effect of possible ion pair formation between, e.g., a carbanion and a metallic cation.

Operationally, then, the chemical reaction mechanism for an organic electrode reaction can be summarized as follows (cf. Fig. 1):

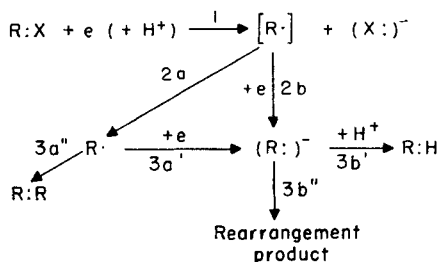


Fig. 1. Generalized chemical reaction mechanism. The initial reaction product may be, if R and X were connected by multiple bonds, $[\dot{\text{R}}-\text{X}-\text{Z}]$.

The initial step in the reaction is the addition of an electron to the electroactive species with hydrogen ion participating in this step if it can aid the process by chemical polarization of the R—X bond through formation of a more or less stable H—X bond (hydrogen ion is used in this discussion since it is the most common third participant in the initial step, although other species, e.g., another Lewis acid, may act similarly). This initial, generally potential-determining step is followed by step 2a or

2b, where 2a involves the discrete existence of a trigonal free radical, which will subsequently undergo (step 3a) a typical free radical reaction, e.g., (3a') addition of a second electron or (3a'') dimerization. Step 2b involves the immediate addition of a second electron to form a carbanion, followed by either (3b') acquisition of a Lewis acid, typically hydrogen ion, or (3b'') electronic rearrangement, which is usually followed by elimination of an atom or group from an atom adjacent to the original reactive site with consequent formation of a double bond between this atom and that of the reactive site. Obviously, the carbanion formed in step 3a' can then undergo the reactions of steps 3b' or 3b''.

The question as to whether the initial electron addition (and perhaps displacement of the X moiety) is completed by step 2a or 2b, depends on which route requires the less activation energy, i.e., on the difference in the free energies of the transition states.

The nature of the chemical reaction mechanisms can be conveniently illustrated by considering the ones advanced for the pH-independent carbon-halogen fission process and for the pH-dependent ketone carbonyl reduction. These two processes are examples of two fundamentally different types of electron addition processes (cf. subsequent discussion of Energetic Reaction Mechanism).

B. Carbon-Halogen Bond Fission

The voluminous experimental data on the reduction of organic halogen-containing compounds have been interpreted in various ways; some of the data indicate a free radical mechanism, whereas other data favor a carbanion mechanism.^{4,7,8} Any attempt to force all of the data into a strict carbanion or free-radical mechanism leads at best to an artificial picture of limited utility, due, it is believed, to the essentially dual nature of the process. The normal final products of the two-electron carbon-halogen fission process in R—X are the halide ion and the organic species in which hydrogen has replaced halogen, i.e., R—H, indicating the reaction of Eq. 19 to be the final step. In the case of compounds possessing halogens on adjacent carbon atoms, i.e.,

$R_1R_2CX-R_3R_4CX$, the products of the initial two-electron electrode reaction are the halide ions and a more unsaturated species, $R_1R_2C=CR_3R_4$. The dualistic nature of the reaction can be illustrated in terms of the reduction of the *meso*, α , α' -dibromosuccinic acid which forms only fumaric acid over the normal pH range and of the *racemic* α , α' -dibromosuccinic acid which also forms maleic acid in varying amount in the intermediate pH range associated with the presence of the mono anion.⁸

In the reduction of the *meso* acid over the whole pH range and of the *racemic* acid in the intermediate pH range, step 2b (Fig. 1) followed by 3b'' is the course pursued since the conformation of the molecules in these cases is such that the two bromine atoms are essentially *trans* and coplanar so that, as a pair of electrons is added to one carbon atom as its bromine departs as a bromide ion, a rearward displacement of the second bromine atom as a bromide ion and formation of a carbon-carbon double bond can occur simultaneously due to an electronic rearrangement, i.e., the electron pair on the original reactive center shifting towards the adjacent more positive carbon which still has a halogen attached to it. Such an action would have a relatively low activation energy. (Cf. the similar mechanism suggested for the chemical reduction of α , β dibromo compounds.^{26, 27})

The preferred configuration for the *racemic* acid at high pH and also probably at low pH, however, has the bromine atoms constrained in a *cis* position and single step elimination of the rearward type is not possible. In such a situation, a reaction involving step 2a is postulated; a planar free radical is formed and the second electron is then added in such a manner that the remaining bromine can be displaced at the same time.

C. Ketone Reduction

The general polarographic behavior of aromatic ketones and of aromatic alkyl ketones (acetophenone type) is distinguished by the presence in acidic solution of a first pH-dependent wave and a second pH-independent wave, which waves consequently merge at a pH of about 6 to form a single pH-dependent wave.⁶

Each of the waves in acid solution results from a one-electron process; the combined wave which reaches a magnitude at *ca.* pH 9 of that due to a two-electron process, declines in magnitude with increasing pH to near that expected for a one-electron process; a new more negative third wave appears above pH 9.

The free radical mechanism proposed essentially postulates (a) formation of a free radical as the fundamental process, (b) modification of this process with change in pH, i.e., formation of the corresponding free radical carbinolate ion in the alkaline region, and (c) possible reduction to the carbinol of the resultant free radical and its ion before dimerization occurs.

The detailed description of this process is given in the next section on the Electrochemical Reaction Mechanism.

IV. ELECTROCHEMICAL REACTION MECHANISM

The locus of the electrode reaction is the solution-electrode interface, i.e., the electrical double layer. The structure of the double layer is of importance in electrochemical kinetics and therefore in the potentials of irreversible processes, which include most organic electrode reactions, for at least two reasons: (a) it influences the effective potential difference which favors the electrochemical reaction, and (b) it causes the effective concentration of electroactive species to differ from the bulk concentration.²

The question as to whether the organic species *must* be adsorbed on the electrode in a type of chemisorption prior to electron transfer would seem to be now answered in the negative, although there are many cases in which adsorption of organic reactant, product or both seems to be an essential feature of the overall electrode reaction. It is likely that an orientation of the organic species in the interphase is necessary before electron transfer occurs; the energy for such a process would be likely to vary similarly to that for an adsorption process. Many investigators have considered the energy of adsorption, if involved, to be negligible compared to the other energies acting, although the possibility has been discussed that adsorption energy may be the

significant factor in the variation of $E_{\frac{1}{2}}$ for an aliphatic homologous series.²³

Attempts to define the physical path for the electrode reaction usually lead to a more detailed geometric description of the reaction and to the introduction of kinetic and energetic factors of the type discussed in the next main section. The basic problems in defining the complete electrochemical mechanism of an organic electrode reaction involve answers to the questions of (a) where is the molecule when electron transfer occurs, (b) what is its state of being, and (c) how does the electron transfer occur.

In the present section, two illustrative examples will be presented of the geometric treatment, which is essentially descriptive but does help to define the kinetic and energetic factors which must be considered and which will be examined in the next section.

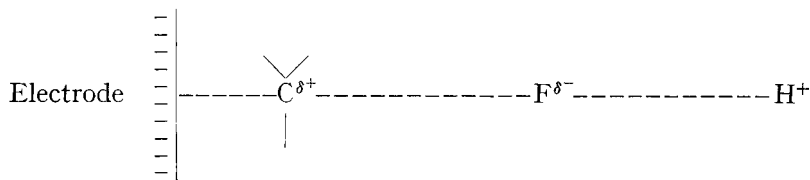
A. Carbon-Halogen Bond Fission

In the fission of a carbon-halogen bond, the dropping mercury electrode can be considered to function as an electron source and the carbon to which the halogen is attached as an electrophilic reaction center. We can then depict a type of nucleophilic displacement reaction on this carbon atom with electrons acting as the displacing agent.

As the species diffuses towards the electrode, there is an increased orientation of the carbon-halogen bond or dipole as it nears the electrode with the bond finally approaching in a direction normal to the electrode plane with the halogen, which is the more negative portion of the carbon-halogen bond, oriented away from the electrode. As the species comes into the immediate vicinity of the electrode, electrostatic repulsion will result in distortion of the species structure, especially in the direction of elongation of the carbon-halogen bond. Finally, a state is reached where the attractive forces between carbon and electrode and between carbon and halogen are in balance; this stage may be considered as the transition state since any movement of the carbon towards the halogen tends to reform the carbon-halogen bond, whereas a movement of the carbon towards the electrode results in the attractive forces between carbon and halogen being insufficient

to retain the halogen which separates as the negative halide ion since the electron pair which constituted the carbon-halogen bond has been driven even closer to it during the process described. Due to departure of the halogen with the electron pair, the carbon now is even more electropositive and an electron (or two electrons) will flow to it from the electrode to form a free radical or carbanion; the free radical, if formed, is normally rapidly converted to the carbanion by the addition of a second electron. The carbanion then either abstracts a proton from a solution or interfacial species to neutralize its charge or, as in the case of the vicinal dihalides, undergoes electronic rearrangement and expulsion of an anion to remove its charge.

Since the proton acquisition is not part of the rate-determining process, it is clear why the carbon-halogen bond fission process *per se* is normally pH-independent. The effect of pH in the case of carbon-fluorine bond fission serves to shed further light on the process.⁵ The half-wave potential for carbon-fluorine bond fission is pH-independent above pH 6, but shows a sigmoidal dependence on pH below pH 6. This is due to hydrogen ion being able to assist the electrode in the polarization of the C—F bond by hydrogen-fluorine bonding in the transition state or species, which may be depicted as follows:

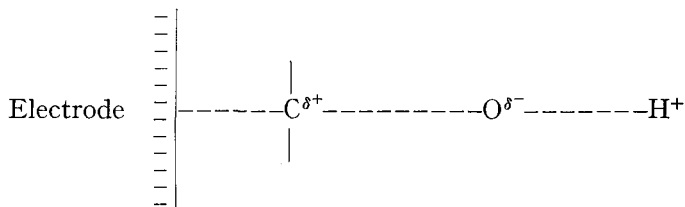


With decreasing hydrogen ion concentration, the effect decreases and the fission becomes pH-independent.

B. Significance of pH-Dependence of Half-Wave Potential

It is safe to generalize from the foregoing discussion that, *whenever an electrochemical bond fission process shows pH-dependence, the latter is due to hydrogen ion aiding the electrode in the polarization of the bond to be disrupted.* Thus, the pH-dependence of carbonyl

group reduction is ascribable to a transition species analogous for that described for carbon-fluorine bond fission:



It is likely that all multiple bond reductions in aqueous or partially aqueous solution are pH-dependent in the region of appreciable hydrogen ion activity. Unfortunately, reduction of certain types of multiple bonds, e.g., those of the phenyl-substituted olefins, occur at such negative potentials that, in solutions of appreciable hydrogen ion activity, hydrogen ion would be reduced at less negative potentials than the multiple bond and the resulting hydrogen wave would mask the desired wave.

C. Ketone Reduction

The behavior of the ketone pH-dependent wave I in the acidic region is best explained as follows (Fig. 2):⁶ (a) as the ketone diffuses into the field of the electrode, the latter initiates polarization of the carbonyl group; (b) simultaneously, the carbonyl oxygen is attracted by neighboring protons, thus favoring increased polarization (the possibility that some of the ketone may be protonated before diffusing into the electrode field can be overlooked in the general mechanism since the effect of ionic strength is negligible, indicating that little, if any, of the diffusing material possesses a charge before it comes within the field of the electrode); (c) the ketone, under the influence of both protons and field, completes the diffusion (now supplemented by electromigration) into the interphase and acquires an electron. The steps outlined are continuous and involve a transition state or species in which as an electron is transferred to the carbonyl carbon, a proton is simultaneously bonded to the carbonyl oxygen. The role of hydrogen ion in the potential-determining step and consequently

in the transition state or species is made apparent by the strong pH-dependence of the reduction process.

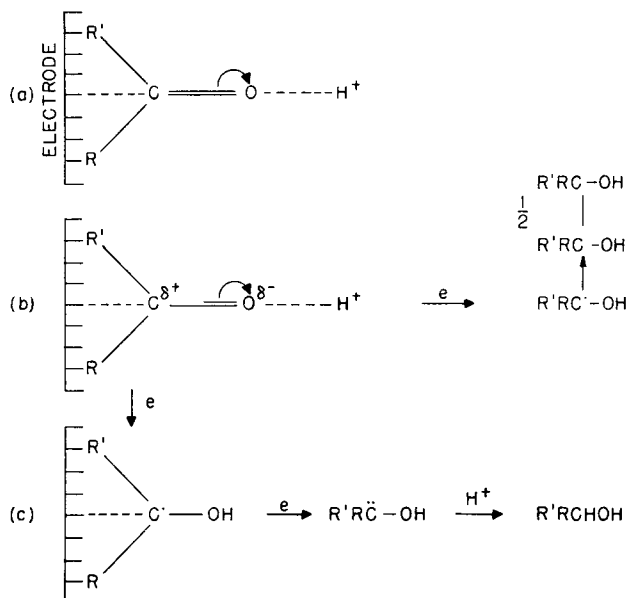


Fig. 2. Electrochemical reduction of a ketone in acidic, neutral and slightly alkaline media: (a) initial diffusion-polarization process, (b) formation of the carbinol-free radical (wave I), and (c) reduction of the carbinol-free radical (wave II) and subsequent acquisition of a proton. In neutral and slightly alkaline media the combined sequence of (b) and (c) produces the combined wave (taken from reference 6).

The free radical produced dimerizes to the pinacol until a potential is reached at which it is reducible; it can then either dimerize to pinacol or be reduced to carbinol; the latter process, which occurs almost exclusively depending on structure, is pH-independent and produces wave II. As pH increases, the shift of pH-dependent wave I results in its eventual merger with the pH-independent wave II to form the pH-dependent combined wave above *ca.* pH 6.

The pH-dependency observed in the alkaline region, even though lessened, indicates continued proton participation in the

potential-determining step. However, the decreased hydrogen ion concentration greatly diminishes the probability of forming an O—H bond simultaneously with electron transfer. Consequently, increasing amounts of carbinolate free radical ion are formed. The latter is not reduced at its formation potential and so dimerizes

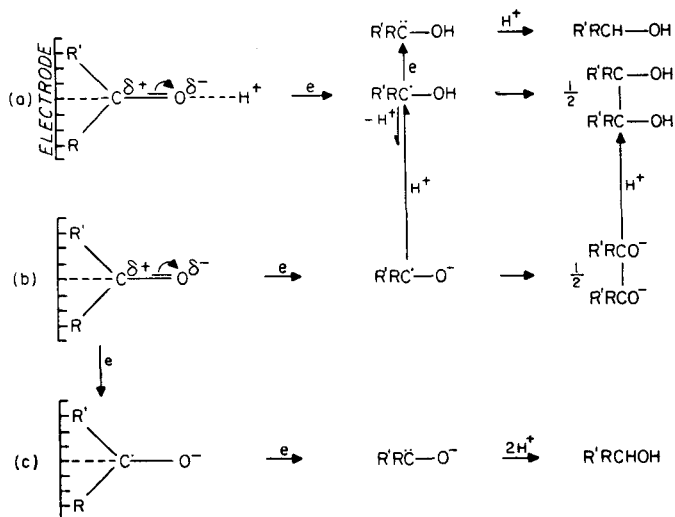


Fig. 3. Electrochemical reduction of a ketone in alkaline media above pH 9: (a) and (b) processes producing the combined wave, and (c) process (reduction of carbinolate-free radical ion) causing wave III; the steps shown should be considered as continuous. The position of the equilibrium between carbinol-free radical (a) and its anion (b) is dependent on pH (taken from reference 6).

until its reduction potential is reached. The need of additional energy for electroreduction of the anionic free radical arises from the coulombic repulsion between the electrode and the anion; further, the electron affecting the reduction now has to enter an area of increased electron density. The equilibrium shown in Fig. 3 is a possible source of carbinol free radical; if the carbinolate free radical ion is at the electrode when the proton is acquired, the resultant carbinol free radical will be reduced to carbinol and thereby contribute to the magnitude of the combined wave. Conversely, if the anionic free radical has diffused away from the

electrode, the carbinol free radical subsequently formed will not be reduced but will dimerize to pinacol.

Formation of the anionic free radical causes a decrease in magnitude of the combined wave above pH 9, while its reduction results in the appearance of wave III. Since reduction of the carbinol free radical is unaffected by pH, the combined wave height increases to a maximum at about pH 9 even though free radical formation becomes more difficult with increasing pH.

V. ENERGETIC REACTION MECHANISM

Two approaches to the problem of the energetic reaction mechanism may be conveniently distinguished: (a) the thermodynamic and kinetic, and (b) the quantum mechanical. These two approaches have been particularly applied in attempts to interpret and to correlate half-wave potential data for organic compounds. However, in order to do so, it has been necessary to construct or to postulate reaction mechanisms, upon which calculations can be based.

Current views concerning the irreversibility of electrode processes stress the irreversibility as due to the slowness of the rate-determining and hence potential-determining step in the sequence of steps in the electrochemical process.

In view of the nature of the electron and its behavior, it seems unlikely, *a priori*, that the physical transfer of an electron itself can be a slow process. However, it is readily possible to conceive of a variety of processes involving an atom or a group of atoms as electron-carrier or a readjustment under the influence of the electric field of atoms relative to one another prior or subsequent to electron transfer, which would be slow processes. Where the observed rate of electron transfer is governed by chemical processes, the laws of chemical kinetics should be applicable.

A. Thermodynamic-Kinetic Approach

The interpretation of $E_{\frac{1}{2}}$ for reversible organic half-cell reactions is relatively clear, since $E_{\frac{1}{2}}$ can then be simply related to the standard potential, E^0 , for the half-cell reaction as determined, for example, potentiometrically:

$$E_{\frac{1}{2}} = E^0 - (RT/nF) \ln (f_R D_O^{\frac{1}{2}} / f_O D_R^{\frac{1}{2}}) \quad (23)$$

where f and D refer to activity coefficient and diffusion coefficient, respectively, and the subscript O and R refer to oxidized and reduced forms, respectively.

Consequently, $E_{\frac{1}{2}}$ can be simply related to the free energy change of the electrode process for the situation in which a thermodynamically reversible equilibrium exists or, perhaps, is approached in the electrochemical reaction at the electrode.

For irreversible processes, which include most organic electrode reactions, the half-wave potential observed is a more complicated function, which is primarily controlled by the rate of the forward electrode reaction for the organic half-cell:



where $k_{f,h}$ and $k_{b,h}$ are the rate constants for the forward and backward heterogeneous reactions, respectively. This dependence at the dropping mercury electrode has been indicated³ to be

$$E_{\frac{1}{2}} = (RT/\alpha n_a F) \ln (t^{\frac{1}{2}} k_{f,h}^{\circ} / \lambda D^{\frac{1}{2}}) \quad (25)$$

where $k_{f,h}^{\circ}$ is the specific rate constant at an applied potential of zero *versus* the normal hydrogen electrode, α is the transfer coefficient as subsequently defined, n_a is the number of electrons involved in the activation step or complex of the half-cell reaction, t is the drop-time of the dropping mercury electrode and λ is a constant having the value of 0.76.

Equation 25 and other statements of the half-wave potential of irreversible processes in terms of the rate constant and transfer coefficient of the energy-controlling step are generally derived on the following basis.

The current resulting from the reaction of Eq. 24 at an electrode of area A is

$$i_{\text{obs}} = i_{\text{cathodic}} - i_{\text{anodic}} \quad (26)$$

or

$$i = k_{f,h} C_O nFA - k_{b,h} C_R nFA \quad (27)$$

where C refers to molar concentration. Equation 27 can be converted to a standard rate constant, $k_{s,h}$, via the Kimble-Eyring picture of the electrode reaction in terms of a potential energy-reaction coordinate of the type shown in Fig. 4. Two barriers are indicated, either of which may be the greater: (a) for transfer of the solvated species from the bulk solution to the

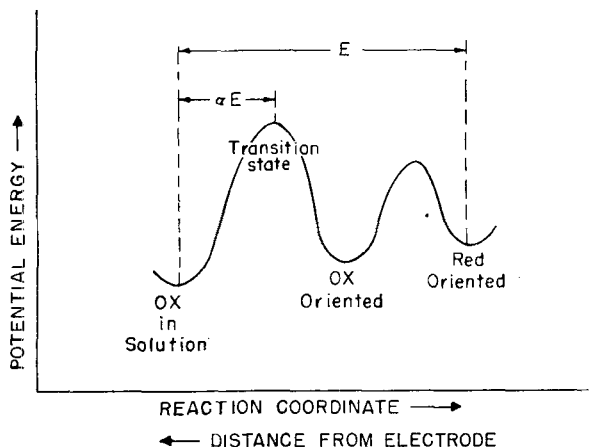


Fig. 4. Generalized reaction path for an electrode reaction. The reaction coordinate equals the distance from the electrode.

“electrode surface”, which may be accompanied by removal of solvent sheath, and (b) for transfer of an electron from electrode to “fixed”, e.g., adsorbed or oriented, species; obviously, more than two barriers may exist. At equilibrium, the potential, E , acts across all of the energy barriers with the fraction, αE , facilitating the reduction process and the fraction, $(1 - \alpha)E$, hindering the reoxidation of the product.* The resulting current

* Alpha, the transfer coefficient for the reaction, is consequently defined by the potential dependence of the rate constant for the reaction, i.e.,

$$\alpha = -(RT/F) \partial(\ln k_{f,h})/\partial\eta$$

where η is the overpotential at the particular potential at which $k_{f,h}$ applies.

Recent discussion has touched upon the possibility that the complementary coefficient, β , here shown as $(1 - \alpha)$, may in fact not always equal $(1 - \alpha)$.

equation is

$$i = nFAk_{s,h}\{C_O \exp[-\alpha nFE'/RT] - C_R \exp[(1-\alpha)nFE'/RT]\} \quad (28)$$

where E' is here the difference between the applied potential and potential E_e^0 which can often be identified with the standard potential. Equation 28 can be converted into the familiar Nernst-type equation of the polarographic wave involving the current i at any potential E .

The value of $k_{s,h}$ is useful in connection with the determination of the reversibility of half-cell reactions,³ which is taken to be indicated by $k_{s,h}^0$ equalling or exceeding 2×10^{-2} cm sec⁻¹. As of yet, it has not been of help in the detailed derivation of mechanism studies, although the effect of structure on $k_{s,h}$ may well be the dominant effect in the often noted systematic correlations of half-wave potential and structure for homologous series of organic compounds observed in a similar solution with the same or comparable capillaries. This would follow (Eq. 25) from the diffusion coefficient of such compounds being about the same (differences are minimized by the square root relation), t showing negligible variation over the potential range of $E_{\frac{1}{2}}$ for the series, n_a being identical unless the mechanism radically changes, and α probably being either similar for members of the series for the same mechanism or also varying slightly but systematically with structure.

Several interesting conclusions follow from the preceding discussion. First, α , the transfer coefficient, is related to the mechanism of the reaction by defining or by being controlled by the energy-determining barrier. Its effective use in reaction mechanism elucidation is predicated upon a general mechanistic interpretation of the physical steps in the electrode process as typified by an energy-reaction coordinate realization such as those of Figs. 4 or 5.

In the attempt to relate α to physical phenomena occurring at the solution-electrode interfacial region, cognizance has been taken of the fact that essentially all of the applied potential drops across the 10 or less Angstrom-thick electrical double layer.

Then α is considered to indicate the penetration of the

electroactive species into the double layer until it encounters the energy region of αE , which is sufficient to cause reaction.

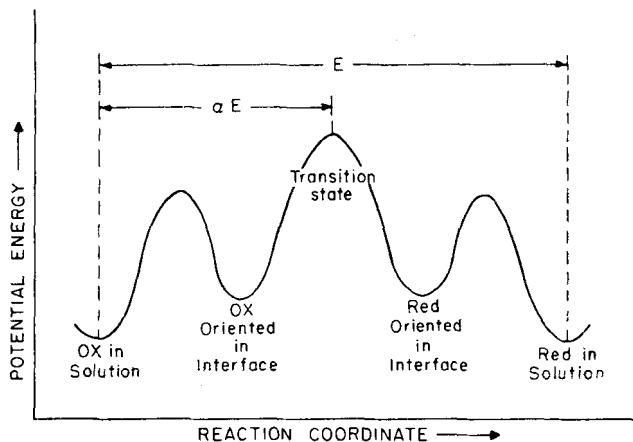


Fig. 5. Generalized reaction path for an organic electrode reaction. This representation is generally similar to that proposed by Hush.¹⁴

For example, there is Delahay's suggested generalization² that the effective potential, which favors and/or hinders the electrode reaction, equals the experimental electrode potential minus the potential difference between the plane of closest approach and the solution. This plane is taken to be the outer Helmholtz plane in the absence of specific adsorption and the inner Helmholtz plane in its presence.

$E_{\frac{1}{2}}$ for a member of homologous series is a composite function of the free energy change for the electrode process, and the activation energy and the rate of the slow step in the process, as well as, probably, of other factors such as an energy of adsorption or orientation. Correlations of geometric structure or of reactivity or energetic parameters with $E_{\frac{1}{2}}$ must recognize the possibility of more than one factor determining the half-wave potential.

Attempts to use $E_{\frac{1}{2}}$ as a measure of chemical reactivity for irreversible reactions would, *a priori*, be expected to be justified only if the mechanisms of the electrochemical and chemical reactions concerned involved fission of the same bonds by an

identical chemical reaction type. This is added justification for ascertaining whether organic electrode reactions are, e.g., free radical or substitution in nature. However, the obvious qualification must be made that if the half-wave potential and the chemical reactivity parameter or intensity used are both related in systematic fashion to some third quantity, the $E_{1/2}$ and reactivity can both be correlated directly, although the physical significance of the correlation will depend on the nature of the individual relations of each to the third quantity (cf. the subsequent discussion of correlation of $E_{1/2}$ and ionization potential).

B. Quantum Mechanical Approach

In the quantum mechanical treatment, emphasis is placed on the energies of atomic and molecular orbitals, to or from which electrons are to be transferred, and on the energies of the transition species provided by the overlap of orbitals of the two reactants, between which electron transfer is to occur. In electrode reactions, one reactant is the electrode which functions as the electron source in electroreductions.

In the electroreduction of organic functionalities, two basically different cases can be distinguished, according to whether single or multiple bonds are being broken.

In the reduction of multiple bonds as in polynuclear aromatic hydrocarbons and conjugated aliphatic unsaturated systems, the potential-determining reaction involves π bond reduction via addition of the electron to the lowest empty molecular orbital. In single bond reduction, e.g., carbon-halogen bonds, a σ bond is broken which generally requires a more negative potential. The essential step in the reaction consequently requires the overlap of the electron source with an antibonding π or σ orbital. Correlations of the half-wave potentials of organic compounds with other experimental or theoretical parameters must ultimately use the preceding fact as their basis.

It is this fundamental difference in the type of bond involved, which led to the previous discussions of the single carbon-halogen bond rupture and of the phenyl ketone carbonyl group reduction.

TABLE I. Half-wave potential and quantum mechanical data for aromatic hydrocarbons^a

Compound	Values of m_i		$-E_{1/2}$ v.
	h.o.m.o.	l.e.m.o.	
Benzene	0.8000	-1.3333	
Naphthalene	0.5353	-0.7309	2.50
Phenanthrene	0.5257	-0.7131	2.45
Pyrene	0.4005	-0.5008	2.10
1, 2, 5, 6-Dibenzanthracene	0.4234	-0.5871	2.07
9, 10-Dimethyl-1, 2-benzanthracene	0.3492	-0.5342	2.05
1, 2-Benzanthracene	0.4064	-0.5100	2.03
Anthracene	0.3753	-0.4620	1.94
Biphenyl	0.599	-0.855	2.70
Styrene	0.568	-0.793	2.34
Stilbene	0.448	-0.577	2.14
Tetraphenylethylene	0.337	-0.405	2.05
1, 4-Diphenylbutadiene	0.352	-0.427	1.98
Fulvene	0.5353	-0.2712	
Dimethylfulvene			1.89
Diphenylfulvene			1.57
Benzofulvene	0.5107	-0.3715	
Dimethylbenzofulvene			1.98
Diphenylbenzofulvene			1.61
Dibenzofulvene	0.5508	-0.4819	
Phenyldibenzofulvene (benzofluorene)			1.67
Diphenyldibenzofulvene			1.63
Biphenylenebutadiene	0.4312	-0.3281	
1-Biphenylene-3-phenylbutadiene (cinna- mylidene fluorene)			1.46
Indene	0.5665	-0.7628	2.54
Fluorene	0.5991	-0.8397	2.65
Dibiphenyleneethylene	0.4890	-0.1671	1.04
Triphenylmethyl	0.0000	0.000	1.05

^a Taken from references 21 and 22.

The general quantum mechanical approach is to postulate an energy-determining step in a possible mechanism, e.g., to consider Eq. 2 as a reversible step in the reaction sequence of Eqs. 2 to 4, and to calculate the energies of the reactant and of the product species, or of electron addition.

In the important area of the conjugated hydrocarbons, the most fruitful treatment^{16, 21, 22} is based on calculation of the energies of molecular orbitals of the mobile or π electrons. These energies are of the form

$$E_i = \alpha + k_i \beta = \alpha + m_i \gamma \quad (29)$$

where α is the coulomb integral and β or γ the resonance integrals with overlap, respectively, neglected or included. Their values are approximately 20 Kcal/mole for β and 40 Kcal/mole for γ .

Positive k_i or m_i values are associated with occupied (bonding) orbitals in the ground state of the molecule; the smallest numerical value is that of the highest occupied molecular orbital (h.o.m.o.) which, for a series of compounds, is related to the values of the ionization potential I ; the smaller k_i , the lower is I and, therefore, the greater is the electron donor capacity of the molecule.

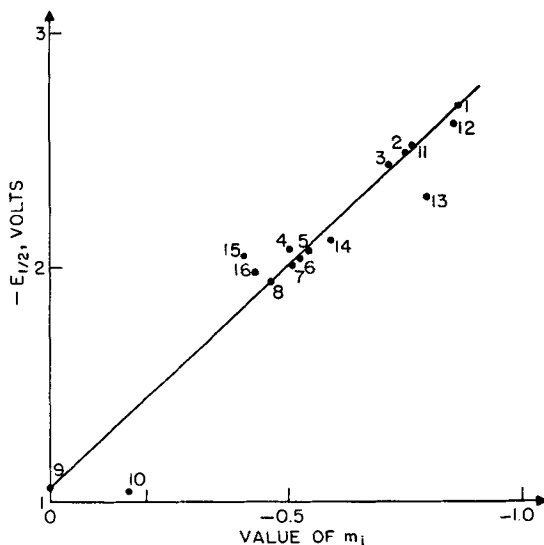


Fig. 6. Correlation of half-wave potentials of aromatic hydrocarbons with the coefficient m_i of the l.e.m.o. (taken from references 21 and 22): 1, biphenyl; 2, naphthalene; 3, phenanthrene; 4, pyrene; 5, 1, 2, 5, 6-dibenzanthracene; 6, 9, 10-dimethyl-1, 2-benzanthracene; 7, 1, 2-benzanthracene; 8, anthracene; 9, triphenylmethyl; 10, dibiphenyleneethylene; 11, indene; 12, fluorene; 13, styrene; 14, stilbene; 15, tetraphenylethylene; 16, 1, 4-diphenylbutadiene.

Negative values of k_i or m_i are associated with unoccupied (antibonding) orbitals which usually are occupied only in the excited state. The smallest numerical value is that of the lowest empty molecular orbital (l.e.m.o.) which is related to the relative electroaffinity of the compound. For a homologous series, the smaller k_i , the greater the electroaffinity and, therefore, the greater the electron acceptor properties of the molecule. *The half-wave potentials of organic compounds undergoing electroreduction have been shown to vary linearly with their l.e.m.o., e.g., Table I and Fig. 6 (both taken from reference 21).* In a more refined treatment, separate curves may be drawn for the different families of related hydrocarbons given in the table.^{11, 21, 22} The linear character of the relation is so well observed that the deviations from linearity may be successfully used for the establishment of deviations from molecular planarity.¹ A similar type of relation may be found in certain classes of derivatives of conjugated hydrocarbons, e.g., in aromatic aldehydes.²⁴

Due to the symmetry, observed in the classical L.C.A.O. molecular orbital calculations, of the h.o.m.o. (related to the ionization potential) and of the l.e.m.o. (related to the ease of acceptance of an electron in reduction) in certain types of compounds, e.g., conjugated hydrocarbons (complete symmetry when overlap is neglected, less complete when it is included), any property related, i.e., proportional, to one will be proportional to the other (this will not hold in more refined treatments). Thus, the theoretical π -ionization potentials of hydrocarbons¹⁸ are linearly proportional to the $E_{\frac{1}{2}}$ values for diphenyl, naphthalene, phenanthrene and anthracene; the point for butadiene deviates slightly from the straight line relation, while that for styrene deviates markedly. Such incidental correlations, due primarily to mathematical symmetry rather than to fundamental physical significance, must be watched for carefully. The same remark is valid for a proposed correlation²⁵ between absorption spectra and half-wave potentials (cf. reference 21).

There are complementary quantum mechanical approaches, which offer the possibilities of following the course of the reduction reaction, of deciding whether it is ionic or radical in nature, and of predicting the structure of the product which should be formed.

Thus, negative and positive ions would be expected to attack preferentially the most positive and the most negative carbons, respectively, in the compound as indicated by the calculated

distribution of electrical charge. The reactivity towards free radicals should, on the contrary, be governed by the distribution of free valence, which also, in fact, plays an important role in determining the relative polarizability of the different carbons towards any approaching reagents (cf., e.g., references 21 (Chapter X) and 20). The same considerations enable also the determination of the relative tendencies of a species, which has accepted one electron, to accept a second electron, i.e., to be further reduced, or to react with a second free radical, i.e., to dimerize. The chemical course of the reduction of conjugated hydrocarbons has effectively been successfully accounted for in this way.¹² (In the different although related problem of the oxydo-reduction reaction of the respiratory coenzymes, these types of considerations have enabled a clear-cut interpretation of the chemical aspects of the reduction.^{21a})

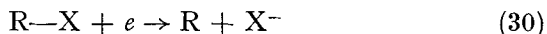
When possible, localization energies should be used preferentially for such interpretation of the course of the reduction. These quantities measure the relative values of the activation energies for different types of reactions which may occur at a conjugated system (cf. references 21 (Chapter X) and 20). They are thus characteristics of the reacting molecule and consequently are apt to be superior for the interpretation of chemical reactivity to indices characteristic of isolated molecules, like electrical charges and free valences. But, contrary to some propositions, no direct general relation may be expected between the localization energies and the half-wave potential.¹⁹

One of the currently most promising approaches to a quantitative theory of electron transfer at an electrode is that of Marcus,^{17,18} whose fundamental assumption is that only a weak electronic interaction of the two reactants is required for a simple electron transfer process to occur. Interesting and significant deductions have been made quantum mechanically for simple electrode reaction in which no rupture or formation of chemical bonds occurs in the electron transfer step. The elaboration of the theory to include bond rupture is of obvious importance for the treatment of organic electrode processes.

C. Rate Constant Calculation

Since the rate constant for the electron transfer reaction is related by definition to the free energy of activation of the electrode reaction, reaction rates could be predicted if adequate information about the structures of the reactant, transition states and product were available. Unfortunately, the meager data generally available concerning the structure and energies of these states do not readily permit such calculations. However, such rate constant calculations would likely not in themselves suffice to permit further calculation of $E_{\frac{1}{2}}$ via Eq. 25 even if α were known.

For example, Hush¹⁴ has calculated rate constants for the rate-determining step in the electrode reaction of the methyl halides



from the calculated standard potentials for the half-cell reactions of Eq. 30 and the experimental current-potential relations at the dropping mercury electrode. He interpreted the variation in equilibrium rate constants in terms of a model of the activation process for reaction 30, based on the assumptions that (a) the reaction is the exchange of an electron between a metallic orbital χ_1 of the electrode and the lowest vacant (antibonding) molecular orbital χ_2 in the RX molecule, (b) the electronic wave function, ϕ_λ , for any state λ in the range immediately preceding and following the transition state may be written in L.C.A.O. form as

$$\phi_\lambda = (1/N^{\frac{1}{2}}) (c_{1,\lambda} \chi_1 + c_{2,\lambda} \chi_2) \quad (31)$$

and (c) the overlap integral

$$\int \chi_1 \chi_2^* d\tau \quad (32)$$

is small, which leads to the conclusion that N , the normalization constant of Eq. 31, is 1. Hush concludes that no *direct* correlation exists between the energy of activation and the bond energy of the halide, the electron affinity of the halogen or the work function of the electrode. However, the latter three indirectly influence the adsorption and repulsion energies which cause the variation in activation energy between the members of the homologous series. From this and other factors, it is unlikely that calculations of the activation energy would be significant.

Adsorption phenomena and activation energy are apparently relatively constant factors with the determining factor being the entropy of activation.

References

1. Bergmann, E. D., Berthier, G., Pullman, A., and Pullman, B., *Bull. soc. chim.* **17**, 1079 (1950).
2. Breiter, M., Kleinerman, M., and Delahay, P., *J. Am. Chem. Soc.* **80**, 5111 (1958).
3. Delahay, P., "New Instrumental Methods in Electrochemistry," Interscience, New York, 1954.
4. Elving, P. J., *Record Chem. Progr.* **14**, 99 (1953).
5. Elving, P. J., and Leone, J. T., *J. Am. Chem. Soc.* **79**, 1546 (1957).
6. Elving, P. J., and Leone, J. T., *J. Am. Chem. Soc.* **80**, 1021 (1958).
7. Elving, P. J., Markowitz, J. M., and Rosenthal, I., *J. Electrochem. Soc.* **101**, 195 (1954).
8. Elving, P. J., Rosenthal, I., and Martin, A. J., *J. Am. Chem. Soc.* **77**, 5218 (1955).
9. Evans, M. G., and Hush, N. S., *J. chim. phys.* **49**, C159 (1952).
10. Hoiijtink, G. J., *et al.*, *Rec. trav. chim.* **73**, 355 (1954).
11. Hoiijtink, G. J., *et al.*, *Rec. trav. chim.* **72**, 903 (1953); **74**, 1525 (1955); **75**, 487 (1956).
12. Hoiijtink, G. J., and van Schooten, J., *Rec. trav. chim.* **71**, 1089 (1952); **72**, 691 (1953); **76**, 885 (1957).
13. Hush, N. S., *J. Chem. Phys.* **27**, 612 (1957).
14. Hush, N. S., *Z. Elektrochem.* **61**, 734 (1957).
15. Laitinen, H. A., and Wawzonek, S., *J. Am. Chem. Soc.* **64**, 1765 (1942).
16. Maccoll, A., *Nature* **163**, 178 (1949).
17. Marcus, R. A., *O.N.R. Tech. Report* No. 12, Project NR-051-331, 1957; *Am. Chem. Soc.*, 132nd Natl. Meeting, New York, 1957.
18. Marcus, R. A., *Can. J. Chem.* **37**, 155 (1959).
19. Pullman, A., and Pullman, B., *Compt. rend.* **243**, 1632 (1956).
20. Pullman, B., and Pullman, A., *Progr. in Org. Chem.* **4**, 31 (1954).
21. Pullman, B., and Pullman, A., *Les théories électroniques de la chimie organique*, Masson et Cie., Paris, 1952, pp. 259-272.
- 21a. Pullman, B., and Pullman, A., *Proc. Nat. Acad. Sci.* **45**, 136 (1959).
22. Pullman, A., and Pullman, B., and Berthier, G., *Bull. soc. chim. France* **1950**, 591.
23. Rosenthal, I., Albright, C. H., and Elving, P. J., *J. Electrochem. Soc.* **99**, 227 (1952).
24. Schmid, R. W., and Heilbronner, E., *Helv. Chim. Acta* **37**, 1453 (1954).

25. Watson, A. T., and Matsen, F. A., *J. Chem. Phys.* **18**, 1305 (1950).
26. Winstein, S., Pressman, D., and Young, W. G., *J. Am. Chem. Soc.* **61**, 1645 (1939).
27. Young, W. G., Pressman, D., and Coryell, C. D., *J. Am. Chem. Soc.* **61**, 1640 (1939).

Nonlinear Problems in Thermodynamics of Irreversible Processes*

THOR A. BAK,

Institute for Physical Chemistry, University of Copenhagen

CONTENTS

I.	Introduction	33
II.	Thermodynamics of Linear Systems	35
III.	Thermodynamics of Nonlinear Systems	39
IV.	Oscillating Reactions	47
V.	Conclusion	56
	References	57

I. INTRODUCTION

The thermodynamic description of nonequilibrium systems rests on the assumption that the usual thermodynamic functions can be defined for nonequilibrium states so that the relationship between them is that known from equilibrium systems.

The range of validity of this thermodynamic hypothesis can be determined by considering a definite statistical-mechanical model of the irreversible process, and this has been done among others by Prigogine^{17,18} who used the Chapman-Enskog solution of the Maxwell-Boltzmann equation. The investigation revealed the fact that there is indeed a large class of nonequilibrium systems for which the assumption is justified. This class of systems is conveniently subdivided into linear and nonlinear systems in the following way.

Let an isolated system be described by the thermodynamic variables A_k ($k = 1, 2, \dots, n$) and let

$$\alpha_k = A_k - A_k^\dagger$$

* The research on which this review is based was supported in part by the United States Air Force through the European Office of the Air Research and Development Command.

be their deviations from equilibrium. Then we define the thermodynamic forces as

$$X_k = \partial S / \partial \alpha_k \quad (1)$$

and the thermodynamic fluxes as

$$J_k = \dot{\alpha}_k \quad (2)$$

so that we have

$$\sigma \stackrel{\text{def}}{=} dS/dt = \sum_k X_k J_k \quad (3)$$

For a system which is not isolated σ is the rate of production of entropy, that is, the rate of change of the entropy due to internal sources only.

The thermodynamic system is called linear when

$$J_i = \sum_k L_{ik} X_k \quad (4)$$

where L_{ik} is a matrix with constant coefficients. For such a system it is of course also possible to choose the forces as linear combinations of the derivatives of S with respect to α_k , provided the fluxes are redefined so that (3) still holds. For a linear system Onsager¹¹ showed that the reciprocity relations

$$L_{ik} = L_{ki}$$

are valid (neglecting magnetic fields and Coriolis forces). That is, the matrix \mathbf{L} is symmetric. In his derivation Onsager used microscopic reversibility and furthermore assumed that on the average the decay of fluctuations follow the ordinary phenomenological laws.

A system for which there are no linear relations between the forces and fluxes as defined above will be called nonlinear even if the system may be described by linear differential equations in the α -variables such as

$$\dot{\alpha}_k = -\alpha_k \sum_{i \neq k} w_{ki} + \sum_{i \neq k} w_{ik} \alpha_i \quad (5)$$

where the w_{ki} 's are constant transition probabilities, which we shall discuss below.

In many cases the assumption of linearity is an excellent approximation, valid seemingly within the same range as that

for which the thermodynamic functions exist, but in the case of chemical reactions or diffusion or in general processes which are governed by a "master equation" like (5) this is not so. This discussion of the irreversible thermodynamics of nonlinear systems will therefore solely be concerned with systems of chemical reaction and diffusion.

In the following discussion we will throughout assume the existence of macroscopic transport equations like (5) without trying to justify them from statistical mechanical models.

II. THERMODYNAMICS OF LINEAR SYSTEMS

The main results from the thermodynamics of linear systems are the Onsager relations. To give a simple example of the Onsager relations we consider, following Onsager,¹¹ a closed system at constant temperature and pressure in which three substances M_1 , M_2 and M_3 , with concentrations c_1 , c_2 and c_3 are transformed into each other by first order chemical reactions. We have then

$$(d/dt) c_1 = -(w_{12} + w_{13})c_1 + w_{21}c_2 + w_{31}c_3 \quad (6)$$

and analogous equations for c_2 and c_3 . We shall only consider first order reactions, since the generalization to an arbitrary order of reaction is trivial.

We take $-\alpha_k$ to be $c_k - c_k^\dagger$ and we must then determine the forces X_k such that the rate of entropy production is

$$\sigma = - \sum_k X_k \dot{c}_k \quad (7)$$

Comparing this with the expression for the Gibbs function

$$dG = \sum_k \mu_k dc_k$$

valid for unit volume at constant temperature and pressure, we see that the force equals

$$(\mu_k - \mu_k^\dagger)/RT$$

where μ_k^\dagger is the chemical potential of M_k at equilibrium, and S is measured in units of R , the gas constant.

Assuming ideality we have

$$\mu_k = RT \log c_k + \text{const}$$

and near equilibrium we obtain approximatively:

$$X_k = (\mu_k - \mu_k^\dagger)/RT = (c_k - c_k^\dagger)/c_k^\dagger \quad (8)$$

We have therefore

$$\dot{\alpha}_i = \sum_k L_{ik} X_k \quad (9)$$

with

$$\mathbf{L} = \begin{bmatrix} (w_{12} + w_{13})c_1^\dagger & -w_{21}c_2^\dagger & -w_{31}c_3^\dagger \\ -w_{12}c_1^\dagger & (w_{23} + w_{21})c_2^\dagger & -w_{32}c_3^\dagger \\ -w_{13}c_1^\dagger & -w_{23}c_2^\dagger & (w_{31} + w_{32})c_3^\dagger \end{bmatrix}$$

The \mathbf{L} -matrix is symmetric when we have

$$w_{ij}c_j^\dagger = w_{ji}c_j^\dagger$$

i.e., when we have detailed balance. This parallels the more general derivation of the Onsager relation, in which microscopic reversibility is assumed.

The fluxes with which we operate here are linearly dependent, since

$$\sum_i \dot{c}_i = 0$$

It is easily shown that if \mathbf{L} is symmetric for one set of forces and fluxes, it will remain symmetric when the forces (or fluxes) are changed by a linear transformation, even if this transformation changes the number of variables, if only the fluxes (or forces) are transformed so that the entropy production is invariant under the transformation.

To see this we set

$$\mathbf{X} = \mathbf{Q}\mathbf{X}' \quad (10)$$

where \mathbf{X}' is the vector formed by the new forces and \mathbf{Q} is the transforming matrix. To be specific we can assume that \mathbf{X} is a vector formed by linearly independent forces and that \mathbf{X}' is formed by a set of linearly dependent forces. \mathbf{Q} is then a rectangular matrix. We set

$$\mathbf{J}' = \bar{\mathbf{Q}}\mathbf{J} \quad (11)$$

and have therefore

$$\sigma = \bar{\mathbf{X}}\mathbf{J} = \bar{\mathbf{X}}'\mathbf{J}' \quad (12)$$

from which we see that the entropy production is invariant under the transformation. Furthermore we have that if

$$\mathbf{J} = \mathbf{L}\mathbf{X}$$

the new fluxes are related to the new forces by

$$\mathbf{J}' = \tilde{\mathbf{Q}}\mathbf{L}\mathbf{Q}\mathbf{X}' = \mathbf{L}'\mathbf{X}' \quad (13)$$

and it is seen that \mathbf{L}' is symmetric if \mathbf{L} is.

Since \mathbf{L} is symmetric, we can find an orthogonal transformation which will diagonalize it, leaving σ invariant. This possibility forms the basis for treating irreversible thermodynamics, using "transport complexes," as particularly stressed by Koefoed⁹ and Rice.¹⁹ The main interest in this approach lies in the fact that in some cases it may be intuitively clear what is the composition of the transport complex.

We shall now see that the Onsager relations permit us to assert for the above discussed example that sufficiently near equilibrium the concentrations will decay monotonically towards their equilibrium values. We have

$$\mathbf{X} = \begin{bmatrix} 1/c_1^\dagger & 0 & 0 \\ 0 & 1/c_2^\dagger & 0 \\ 0 & 0 & 1/c_3^\dagger \end{bmatrix} \begin{bmatrix} c_1 - c_1^\dagger \\ c_2 - c_2^\dagger \\ c_3 - c_3^\dagger \end{bmatrix} = \mathbf{C}^{\dagger-1} \begin{bmatrix} c_1 - c_1^\dagger \\ c_2 - c_2^\dagger \\ c_3 - c_3^\dagger \end{bmatrix} \quad (14)$$

and therefore

$$\dot{\alpha} = \mathbf{L}\mathbf{X} = -\mathbf{L}\mathbf{C}^{\dagger-1} \alpha \quad (15)$$

using that $-\alpha_k = c_k - c_k^\dagger$.

If the eigenvalues of $-\mathbf{L}\mathbf{C}^{\dagger-1}$ are negative, the concentrations therefore will decay monotonically towards their equilibrium values. To see that this is so we consider the characteristic equation

$$|-\mathbf{L}\mathbf{C}^{\dagger-1} - \lambda\mathbf{E}| = 0$$

or

$$|\mathbf{L} + \lambda\mathbf{C}^\dagger| = 0 \quad (16)$$

Since \mathbf{L} and \mathbf{C}^\dagger can be diagonalized simultaneously and all equilibrium concentrations are positive, we have the result that $-\mathbf{L}\mathbf{C}^\dagger$ has negative eigenvalues.

$$\sigma = \sum_{i,k} L_{ik} X_i X_k$$

is a positive definite form, and therefore if we impose certain constraints on the system such as keeping some forces constant, we shall find that when the system reaches a stationary state, this state minimizes σ . Let us assume that the k first forces are kept constant. We then ask whether it is possible to choose one and only one set of forces $\{X_{k+1}, \dots, X_n\}$ so that σ has an extremum. The necessary condition is

$$\partial\sigma/\partial X_i = 2\sum_j L_{ij} X_j = 2J_i = 0 \quad (i = k+1, \dots, n) \quad (17)$$

that is, it is necessary that all fluxes between non-fixed forces vanish. It is easily verified that the equation

$$\sum_j L_{ij} X_j = 0 \quad (i = k+1, \dots, n) \quad (18)$$

has a unique solution, and we see therefore, that a set of forces exists $\{X_{k+1}, \dots, X_n\}$ for which σ has a minimum.

Since the concentrations will decay monotonically towards their equilibrium values, if possible, it can be asserted that they will also decay monotonically towards a stationary state, when the stationary state is inside the linear domain. This is so, because the inhomogeneous differential equation which describes the approach to the stationary state has (15) as its homogeneous part. As there is only one stationary state of the system corresponding to a given set of fixed forces or fluxes, and this state is a state of minimum entropy production, we have seen that the system in time approaches a state of minimum entropy production. This is sometimes formulated as a direct consequence of the existence of a state of minimum entropy production, but it is clear that in that case one always assumes in addition to the existence of the minimum a relationship between α and $\dot{\alpha}$ such as (15), since only then do the equations give a temporal description of the system.

It is useful to think of this principle of minimum entropy production in a more geometrical way. The equation

$$\dot{\alpha} = -\mathbf{LC}^{\dagger-1}\alpha$$

which was derived for the triangular reaction discussed above, can be written as

$$\dot{\alpha} = \nabla_{\alpha}(-\tfrac{1}{2}\alpha\mathbf{L}\mathbf{C}^{\dagger-1}\alpha) \quad (19)$$

where the operator ∇_{α} is used for forming the n -dimensional gradient in the space with coordinates $(\alpha_1, \dots, \alpha_n)$. Analogously we can write

$$\mathbf{J} = \nabla_{\mathbf{X}}(\tfrac{1}{2}\mathbf{X}\mathbf{L}\mathbf{X}) \quad (20)$$

On the right hand side of these equations we have gradients of positive functions with a single minimum, and the equations can be considered as equations of motion for the projection of a point sliding on the surface

$$z = -\tfrac{1}{2}\alpha\mathbf{L}\mathbf{C}^{\dagger-1}\alpha$$

in an $n + 1$ -dimensional space towards the minimum of z .

The minimum property of the entropy production can also be formulated as the statement that for a natural process in a linear system $d\sigma \leq 0$, where the equality sign is valid for the final stationary state.

In connection with this it is useful to write $d\sigma$ as

$$d\sigma = \sum_k X_k dJ_k + \sum_k J_k dX_k \quad (21)$$

the first of the differential forms on the right hand side is denoted $d_J\sigma$ and the second is denoted $d_X\sigma$. In the linear domain they are numerically equal and are the total derivatives of the so-called dissipation functions Φ and Ψ which play an important rôle in Onsager's formulation of the thermodynamics of irreversible processes^{11,12}. In the nonlinear approximation they are no longer equal, nor are they total differentials. Since for a natural linear process one has $d\sigma \leq 0$ one has also $d_J\sigma \leq 0$ and $d_X\sigma \leq 0$. In a nonlinear system, as we shall see below, the approach to a stationary state does not proceed so that $d\sigma \leq 0$. A closer analysis due to Glansdorff and Prigogine⁵ shows, however, that one of the inequalities, namely $d_X\sigma \leq 0$ remains true.

III. THERMODYNAMICS OF NONLINEAR SYSTEMS

In the previous section we have indicated the results one may obtain for near-equilibrium systems. The first problem for the thermodynamics of nonlinear systems is to see if any of these

results can be generalized to be valid for systems far from equilibrium. Although for such systems there are no linear relations between the forces and fluxes, it is of course possible to linearize the equations for approach to a stationary state in the vicinity of such a state, and we start by investigating if these linear equations have symmetry properties analogous to the Onsager relations.

As an example we consider the triangular reaction, discussed above, in a stationary state. Let c_i^* ($i = 1, 2, 3$) be the stationary concentrations so that

$$\gamma_i = c_i - c_i^*$$

is the deviation from the stationary state. Furthermore we must introduce three fluxes into the system and three rate constants w_i for substance leaving the system. We then have

$$\dot{c}_1 = -(w_{12} + w_{13} + w_1)\gamma_1 + w_{21}\gamma_2 + w_{31}\gamma_3 \quad (22)$$

and analogous equations for \dot{c}_2 and \dot{c}_3 .

Taking the fluxes j_i as $-\dot{c}_i$ and the forces

$$x_i = \log(c_i/c_i^*) \approx \gamma_i/c_i \quad (23)$$

we have

$$\sigma - \sigma^* = \sum_i j_i x_i$$

where

$$j_i = \sum_k l_{ik} x_k$$

with

$$l_{ik} = \begin{bmatrix} (w_{12} + w_{13} + w_1)c_1^* & -w_{21}c_2^* & -w_{31}c_3^* \\ -w_{12}c_1^* & (w_{21} + w_{23} + w_2)c_2^* & -w_{32}c_3^* \\ -w_{13}c_1^* & -w_{23}c_2^* & (w_{31} + w_{32} + w_3)c_3^* \end{bmatrix} \quad (24)$$

Here we have

$$w_{ij}c_i^* \neq w_{ji}c_j^*$$

since there is no detailed balancing for a nonequilibrium state. Therefore the \mathbf{l} -matrix is not symmetric, but contains an anti-symmetric part

$$\frac{1}{2}(l_{ik} - l_{ki}) = \begin{bmatrix} 0 & J_{12}^* & J_{13}^* \\ -J_{12}^* & 0 & J_{23}^* \\ -J_{13}^* & -J_{23}^* & 0 \end{bmatrix} \quad (25)$$

which increases proportional to the flux in the stationary state. When one wants to use the Onsager formalism these fluxes must be negligibly small compared to quantities like $w_{12}c_1^*$.

It is also easy to show that the dissipation functions Φ and Ψ do not exist far from equilibrium, since $d_J\sigma$ and $d_X\sigma$ are not total differentials. Neither do they in general possess integrating multipliers. Therefore the variational principle of Onsager^{11,12} cannot be used, but as we shall see it is possible to generalize Prigogine's principle of minimum entropy production in the stationary state to be valid outside near-equilibrium states in the sense that we can construct a function which is minimized in the stationary state and which near equilibrium reduces to the entropy production.

To show how such a function is constructed we shall first consider the case of one-dimensional diffusion without external field for which the entropy production in the diffusion column between cross-sections at x_1 and x_2 is:

$$\sigma = -(1/RT) \int_{x_1}^{x_2} J d\mu = \int_{x_1}^{x_2} (D/c) (\partial c / \partial x)^2 dx = \int_{x_1}^{x_2} (1/Dc) J^2 dx \quad (26)$$

We seek a variational principle which will characterize the time-independent state of this diffusion. Let us first consider the principle originally suggested by Prigogine,¹⁴ $\delta\sigma = 0$. The Euler equation is

$$-(D/c^2)(dc/dx)^2 - (d/dx)^2 (D/c)(dc/dx) = 0$$

or

$$-(2/c)(d/dx)D(x)(dc/dx) + D[(1/RT)(\partial\mu/\partial x)]^2 = 0 \quad (27)$$

In order that this be the equation for time-independent diffusion, viz.

$$(d/dx) [D(x) (dc/dx)] = 0 \quad (28)$$

we must have $\partial\mu/\partial x = 0$, that is, the diffusion process must have reached equilibrium.

For systems in which the time-independent state is not an equilibrium state (or very close to equilibrium) this variational principle cannot be used. However, Prigogine¹⁵ showed that when

the diffusion constant depends only on concentration the variational principle

$$\delta \int_{x_1}^{x_2} J^2 dx = 0 \quad (29)$$

will characterize the steady states.

It is easily verified that a similar principle also holds when the diffusion constant depends on geometrical coordinates only. Here we shall investigate the case where it depends both on x and c .

We have to construct a variational problem whose Euler equation is

$$(d/dx) [D(c, x)(dc/dx)] = 0$$

The left hand side of this equation is not a linear differential operator operating on c , so that in general we cannot do much about it. If, however, we can write $D(c, x)$ as $D_1(x)D_2(c)$ we can introduce a new variable by

$$U = \int D_2(c) dc \quad (30)$$

We now have to find a variational principle whose Euler equation is

$$(d/dx) [D_1(x)(dU/dx)] = 0 \quad (31)$$

Accordingly, our variational principle reads

$$\delta \int D_1(x) (dU/dx)^2 dx = 0 \quad (32)$$

Since

$$J = -D_1(x)D_2(c) dc/dx = -D_1(x) dU/dx$$

this can also be written as

$$\delta \int D_1^{-1}(x) J^2 dx = 0 \quad (33)$$

and we see that we have a variational principle which will characterize any stationary state for this diffusion process.

The expression under the integral sign has the form of a "resistance" times a flux squared, since $D_1^{-1}(x)$, the reciprocal of the geometrical factor in the diffusion constant, can be considered a resistance against diffusion. This resistance is a function of x , only if D depends on x . When D is a constant or depends

$$J_i = w_{i,i+1} c_i - w_{i+1,i} c_{i+1}$$

and equating all derivatives of $\sum_i r_i J_i^2$ with respect to c_i to zero we get

$$r_i J_i w_{i,i+1} - r_{i-1} J_{i-1} w_{i,i-1} = 0$$

For the stationary state $J_i = J_{i-1}$ and we have therefore the following recursion formula for r_i

$$r_i = (w_{i,i-1}/w_{i,i+1}) r_{i-1} \quad (38)$$

which, aside from a constant factor, determines r_i as being identical with the resistance R_i .

The quantity R_i is what we should compare with $D_1^{-1}(x)$. Since we saw in the calculations for diffusion that $D_2(c)$ does not occur at all in the final integral in the variational principle, we shall now consider a system of chemical reactions with arbitrary reaction order. For the flux we may write

$$J_i = w_{i,i+1} c_i^{q_{i,i+1}} - w_{i+1,i} c_{i+1}^{q_{i+1,i}} \quad (39)$$

where, as above, J_i is the flux from species i to species $i+1$, the w_{ij} 's are transition probabilities (or rate constants), c_i concentration and $q_{i,j}$ the power to which the concentration is raised in the kinetic equation. We now investigate whether all values of $q_{i,j}$ are permissible by again forming the function

$$\sum_i r_i J_i^2$$

and requiring that this function be a minimum for the steady state, i.e., for

$$J_i = J_{i+1} \quad (\text{all } i)$$

The derivatives of the function are

$$\begin{aligned} (\partial/\partial c_i) \sum_k r_k J_k^2 = & 2w_{i,i+1} q_{i,i+1} c_i^{q_{i,i+1}-1} r_i J_i \\ & - 2w_{i,i-1} q_{i,i-1} c_i^{q_{i,i-1}-1} r_{i-1} J_{i-1} \end{aligned} \quad (40)$$

When we equate this to zero for $J_i = J_{i-1}$ we get the following recursion formula for r_i

$$r_i = (w_{i,i-1} q_{i,i-1} / w_{i,i+1} q_{i,i+1}) c_i^{q_{i,i-1} - q_{i,i+1}} r_{i-1}$$

which for

$$q_{i,i-1} = q_{i,i+1}$$

determines r_i to be equal to the above-mentioned R_i except for a constant factor. This shows that the power of c need only be the same for the forward and reverse reaction for each species separately.

We could now try to generalize these results further, for instance, to a set of reactions where transitions between any pair of the N species is possible. Since we have

$$\sigma = (1/RT) \sum_{i=1 < j}^N \mu_{ij} J_{ij}$$

we have near equilibrium, as shown above

$$\sigma = \sum_{i=1 < j}^N (1/c_j^\dagger w_{ij}) J_{ij}^2 \quad (41)$$

The entropy production has a minimum for a stationary state near equilibrium, but neither σ nor the expression derived from it by linearizing μ_{ij} has a minimum for a stationary state far from equilibrium. This is seen by equating the derivatives of

$$\sum_{i=1 < j}^N (1/c_j^\dagger w_{ij}) J_{ij}^2$$

with respect to c_k to zero. Only for a system where the stationary state is a state where all fluxes are equal, i.e., the linear chain of reactions discussed above, will such a form have a minimum in the stationary state.

This means that although there still is an expression $\sum R_{ij} J_{ij}^2$ which is minimized in the stationary state, the coefficients R_{ij} are now functions of the stationary state concentrations rather than the equilibrium concentrations. This still explains the stability of the stationary state as discussed below, but the intuitive meaning of the coefficient is lost and we shall therefore not pursue generalizations of this kind further.

To see how the question of stability is connected with the minimum principle let us consider the linear chain of reactions discussed above in a state for which

$$\Gamma = \sum_i r_i J_i^2$$

has a minimum. If we perturb the system by introducing a small amount of compound i so that its concentration is increased by Δc_i we have

$$\Delta F = \sum' R_i J_i^2 - \sum R_i J_i^2 > 0 \quad (42)$$

where $\sum' R_i J_i^2$ is the value of F after the perturbation. Carrying out the algebra we get

$$\begin{aligned} \Delta F = & (R_i J'_i w_{i,i+1} - R_{i-1} J'_{i-1} w_{i,i-1}) \Delta c_i \\ & + (R_i J_i w_{i,i+1} - R_{i-1} J_{i-1} w_{i,i-1}) \Delta c_i \end{aligned}$$

Since $R_i w_{i,i+1} = R_{i-1} w_{i,i-1}$ and $J_i = J_{i-1}$, the second bracket vanishes, and we have

$$\Delta F = R_i w_{i,i+1} (J'_i - J'_{i-1}) \Delta c_i > 0 \quad (43)$$

and, since $R_i w_{i,i+1} > 0$, we have

$$(J'_i - J'_{i-1}) \Delta c_i > 0 \quad (44)$$

When $J'_i - J'_{i-1}$ is positive, it follows from the continuity equation that c_i is decreasing so that we see that this inequality ensures us that the fluxes will arrange themselves in such a way as to diminish the perturbation. This we have in a way already shown above by proving that the concentrations in a system of this kind decay monotonically towards the stationary state. Therefore the present formulation contains no more information about stability than does the original kinetic equations, but it gives a simple physical picture of how the stability arises.

An especially simple geometrical picture of the stability arises when as in the previous section we consider the expression for the time derivative of the vector

$$\mathbf{c} = (c_1, c_2, \dots, c_N)$$

as the negative gradient of a function with a single minimum. This picture can formally be extended to the continuous case by considering the right hand side of the diffusion equation

$$(\partial c / \partial t) = (\partial / \partial x) [D (\partial c / \partial x)]$$

as a gradient in function space of the functional

$$\frac{1}{2} \int D_1^{-1}(x) J^2 dx$$

Since σ is not minimized in a stationary state far from equilibrium $d\sigma$ is no longer negative for a natural process, but Glansdorff and Prigogine⁵ have shown that for a rather wide class of systems it still holds that $d_X \sigma \leq 0$. To see this for a system of the kind we have considered here, we consider again the triangular reaction and using

$$\dot{c}_1 = J_3 - J_1$$

and analogous expressions we obtain

$$\begin{aligned} (d_X \sigma / dt) &\stackrel{\text{def}}{=} \sum_i J_i \dot{X}_i = -(1/c_1)(J_3 - J_1)^2 - (1/c_2)(J_1 - J_2)^2 \\ &\quad - (1/c_3)(J_2 - J_3)^2 \leq 0 \end{aligned} \quad (45)$$

The only direct physical interpretation of the differential form $d_X \sigma$ seems to be that in the case of oscillating reactions, which we shall now consider, it may be said to fix the sense of rotation in the space with coordinates (c_1, c_2, \dots, c_N) .

IV. OSCILLATING REACTIONS

So far we have have primarily considered systems which, although thermodynamically nonlinear, are described by linear differential equations in terms of the α -variables. For such systems we have shown in (15), using the Onsager relations, that the matrix which determines the approach to equilibrium has real negative eigenvalues, and oscillatory behaviour therefore is not possible. This result can also be obtained in a slightly different way starting directly with the equations for detailed balance as done for instance by Hearon⁷ and Bak.²

For reactions described by differential equations which are nonlinear in the α -variables oscillations are, however, possible, and we shall now investigate the conditions for the occurrence of such oscillations and a method for solving the differential equations in these cases.

Until recently the primary interest in such an investigation would have been to explain the oscillating reactions which are known to occur in biological systems either inside an organism or

as a result of the interaction between different species. In recent years the interest has been shifted somewhat, since reactions of the types which possibly can lead to oscillations occur also in the thermonuclear reactions in a plasma.

Of the equations proposed for biological systems those of Volterra²⁰ have attracted most interest, and we shall therefore treat them in some detail. They do not correspond to any chemical reaction in a closed system, but formally one can give an interpretation of them as describing reactions in an open system. It should perhaps be remarked at this place that exceedingly few chemical reactions in homogeneous phases proceed in a periodic way, and in no case is the detailed mechanism known. A good example of these puzzling reactions is the reduction of hydrogen-peroxide in aqueous solution catalyzed by iodic acid.³

To find the condition for the occurrence of undamped oscillations during a chemical reaction or another process described by nonlinear first order differential equations in some variables A_1, A_2, \dots we use the fact that if the oscillations are around some stationary point the equations can always be linearized near that point to give

$$\dot{\alpha} = \mathbf{W}_L \alpha \quad (46)$$

where \mathbf{W}_L is a constant matrix. The condition for undamped oscillations is that \mathbf{W}_L has purely imaginary eigenvalues, and let us for simplicity consider only the condition that all eigenvalues are imaginary. We can rule out the cases where N is odd, since in these cases the matrix will have at least one real eigenvalue.

The secular equation is

$$\lambda^N + \mathcal{A}_1 \lambda^{N-1} + \dots + \mathcal{A}_N = 0 \quad (47)$$

where the coefficients $\mathcal{A}_1, \mathcal{A}_2, \dots$ can be expressed in terms of the matrix elements of \mathbf{W}_L , and since all the coefficients are real, the purely imaginary roots must occur in conjugated pairs. That is, the secular equation can be factorized to give

$$\prod_{k=1}^{N/2} (\lambda - i\zeta_k)(\lambda + i\zeta_k) = 0$$

where the ζ_k 's must be real numbers. From this we see immediately that

$$\mathcal{A}_1 = \mathcal{A}_3 = \dots = \mathcal{A}_{N-1} = 0$$

and introducing the new variable $z = \lambda^2$ we have the equation

$$\eta(z) = z^n + \mathcal{A}_2 z^{n-1} + \dots + \mathcal{A}_{N-2} z + \mathcal{A}_N = 0 \quad (48)$$

where n equals $N/2$.

The necessary and sufficient condition that the ζ_k 's are real is now that the roots of this equation are real and positive.

If it is known that all the roots are real, it is easy to give the condition that they are all positive. We use the theorem of Descartes which is:

In any equation the number of positive roots cannot exceed the number of changes of signs of the coefficients, and in any complete equation the number of negative roots cannot exceed the number of continuations in the sign of the coefficients.

Therefore, provided the roots of $\eta(z)$ are all real, the conditions

$$\mathcal{A}_2 < 0; \mathcal{A}_4 > 0; \mathcal{A}_6 < 0 \text{ etc.} \quad (49)$$

ensures that they are positive.

To decide whether or not the roots of $\eta(z)$ are real is more complicated, except for small values of n .

For the case $n = 1$ ($N = 2$) we see immediately that the conditions

$$\mathcal{A}_1 = 0, \mathcal{A}_2 < 0$$

are sufficient, but for the case of $n = 2$ ($N = 4$) we find that in addition to

$$\mathcal{A}_1 = \mathcal{A}_3 = 0, \mathcal{A}_2 < 0, \mathcal{A}_4 > 0$$

we must require $\mathcal{A}_2^2 \geq 4\mathcal{A}_4$. The case of $n = 3$ ($N = 6$) can still be handled by elementary methods, but we shall rather use it as an example of the more general method. To investigate the number of real roots of $\eta(z)$ in a certain interval one forms the sequence of functions $\eta(z)$, $\eta'(z)$, $\eta_2(z)$, \dots where $\eta_2(z)$ is minus the remainder in the division $\eta(z)/\eta'(z)$, $\eta_3(z)$ is minus the remainder in the division $\eta'(z)/\eta_2(z)$ and so on. The criterion of Sturm then

states that the number of distinct real roots between $z = a$ and $z = b$ is equal to the excess of the number of changes of sign in the sequence

$$\eta(z), \eta_1(z), \eta_2(z), \dots$$

when $z = a$ over the number of changes of sign when $z = b$. We are interested in the interval

$$-\infty < z < \infty$$

and therefore the signs of the functions in the sequence only depend on the sign of the coefficient to the highest power of z in the function. To ensure that all roots are real, it is therefore a requirement that the coefficient of the leading term in all the η -polynomials, including the last one which is a constant, is positive.

When we use it on the example

$$\eta(z) = z^3 + \mathcal{A}_2 z^2 + \mathcal{A}_4 z + \mathcal{A}_6$$

it is convenient to introduce the usual transformation

$$\begin{aligned} z &= x - \frac{1}{3}\mathcal{A}_2 \\ a &= \mathcal{A}_4 - \frac{1}{3}\mathcal{A}_2^2 \\ b &= \frac{2}{27}\mathcal{A}_2^3 - \frac{1}{3}\mathcal{A}_2\mathcal{A}_4 + \mathcal{A}_6 \end{aligned}$$

We then have to find the condition that the roots of

$$f(x) = x^3 + ax + b = 0$$

are real. We have

$$\begin{aligned} f(x) &= x^3 + ax + b \\ f'(x) &= 3x^2 + a \\ f_2(x) &= -\frac{2}{3}ax - b \\ f_3(x) &= -27b^2/4a^2 - a \end{aligned}$$

and the condition for real roots reduces to the well known inequality

$$4a^3 + 27b^2 < 0$$

Substituting the expressions for a and b in terms of \mathcal{A}_2 , \mathcal{A}_4 and \mathcal{A}_6 in this inequality we get the condition which together with the conditions

$$\mathcal{A}_2 < 0, \mathcal{A}_4 > 0, \mathcal{A}_6 < 0, \mathcal{A}_1 = \mathcal{A}_3 = \mathcal{A}_5 = 0$$

ensures that the system will execute undamped oscillations around some stationary point.

We have thus found a criterion for oscillations which in principle can be applied to systems with reactions between any number of substances. For large values of N , however, the inequalities between the rate-constants become extremely complicated as do the calculations leading to them.

So far we have only considered oscillations around a stationary point, but it is also possible that the original nonlinear equations for two components A_1 and A_2 may give a curve in A_1A_2 -space which, when time increases, approaches a limiting cycle. Such a system will only be strictly periodic in the limit $t \rightarrow \infty$, but already after a relatively short time it can be so close to the limiting cycle that experiments cannot discern between its path and the limiting cycle.

To our knowledge so far no thermodynamic system with equations of this type has been found, but it is well to bear in mind, especially when experimental results have to be explained, that the above discussed oscillations are not the only possible type. This last type of cyclic behaviour, which is of a more complicated nature than oscillation around a stationary point, has primarily been investigated for the case of only two variables A_1 and A_2 . We refer to the book by Hurewicz⁸ for the proof of the necessary and sufficient conditions for the existence of such limiting cycles.

As an example of an oscillating reaction we shall finally discuss the equations of Volterra from a thermodynamic point of view, and see how the method of Kryloff and Bogoliouboff¹⁰ can be used to solve the differential equations.

It was assumed by Volterra²⁰ that the interaction between two biological species, 1 and 2, of which 2 feeds on 1, can be described by the equations

$$\begin{aligned} \dot{A}_1 &= w_1 A_1 - w_2 A_1 A_2 \\ \dot{A}_2 &= w_3 A_1 A_2 - w_4 A_2 \end{aligned} \quad (50)$$

in which A_1 and A_2 are concentrations and w_i ($i = 1, 2, 3, 4$) are constants. Below we give an interpretation of these equations in four partial reactions. J_i ($i = 1, 2, 3, 4$) are the corresponding flows and X_i ($i = 1, 2, 3, 4$) are the thermodynamic forces defined such that

$$\sigma = \sum_i X_i J_i$$

is the entropy production of R per second.

Reaction	Flow	Force
$A_1 \rightarrow 2A_1$	$J_1 = k_1 A_1$	$X_1 = \ln (k_1/k_{-1} A_1)$
$A_1 + A_2 \rightarrow A_2$	$J_2 = k_2 A_1 A_2$	$X_2 = \ln (k_2 A_1/k_{-2})$
$A_1 + A_2 \rightarrow 2A_2$	$J_3 = k_3 A_1 A_2$	$X_3 = \ln (k_3 A_1/k_{-3} A_2)$
$A_2 \rightarrow M$	$J_4 = k_4 A_2$	$X_4 = \ln (k_4 A_2/k_{-4})$

where M is an inert substance.

The four reactions correspond biologically to growth of species 1, species 2 feeding on 1, species 2 propagating faster the more food there is, species 2 dying.

If the four reactions are considered as chemical reactions, it is evident that they do not conserve matter, i.e., other substances, whose concentrations are kept constant, must be involved.

We see that with $k_1 = w_1$, $k_2 + k_3 = w_2$, $k_3 = w_3$, and $k_4 = w_4$ we have

$$\dot{A}_1 = J_1 - J_2 - J_3$$

and

$$\dot{A}_2 = J_3 - J_4$$

We must now eliminate k_{-1} , k_{-2} , k_{-3} , k_{-4} from the expressions for the forces. To do so we observe that the original equations have a stable stationary point

$$(A_1^s, A_2^s) = (w_4/w_3, w_1/w_2)$$

It is known from the investigations of Volterra that the representative point in the A_1, A_2 -plane moves in closed curves counter-

clockwise around this stationary point. This suggests introducing relative forces $\Delta X_i = X_i - X_i^s$ in which X_i^s is the force at the stationary point.

We find

$$\Delta X_1 + \Delta X_3 + \Delta X_4 = 0 = \Delta X_1 + \Delta X_2$$

so that

$$\theta \stackrel{\text{def}}{=} \sum \Delta X_i J_i = (J_1 - J_2 - J_3) \Delta X_1 + (J_3 - J_4) (\Delta X_1 + \Delta X_3) = \sum j_i x_i \quad (52)$$

with

$$\begin{aligned} x_1 &= \Delta X_1 = \ln w_4 / (w_4 + w_3 \alpha_1) \approx - (w_3 / w_4) \alpha_1 \\ x_2 &= \Delta X_1 + \Delta X_3 = \ln w_1 / (w_1 + w_2 \alpha_2) \approx - (w_2 / w_1) \alpha_2 \end{aligned} \quad (53)$$

In these equations j_i is the time derivative of A_i (or α_i) and $\alpha_i = A_i - A_i^s$. The approximate values given are valid for $\alpha_i \approx 0$. In terms of the α_i 's the original equations read

$$\begin{aligned} \dot{\alpha}_1 &= (w_2 w_4 / w_3) \alpha_2 - w_2 \alpha_1 \alpha_2 \\ \dot{\alpha}_2 &= (w_1 w_3 / w_2) \alpha_1 + w_3 \alpha_1 \alpha_2 \end{aligned} \quad (54)$$

and we see that when $\alpha_1 \alpha_2$ can be neglected compared with α_1 or α_2 , i.e., when we linearize the equations, the representative point describes an ellipse around the stationary point (0, 0) in the α_1, α_2 -plane. θ is the closest analogy to the entropy-production we can find, which can be expressed using only the rate-constants which enter in the final equation for \dot{A}_1 and \dot{A}_2 .

The system so far described has no tendency to approach the stationary state, and this state is therefore, thermodynamically speaking, not a stable state. If $w_1 A_1$ is replaced by a constant, as suggested by Lotka, or if terms containing A_1^2 and A_2^2 are included in the equations, the representative point in the A_1, A_2 -plane will spiral in towards the stationary state. This is seen by linearizing the equations. Arbitrarily close to the stationary state there will, however, exist states with $\theta < 0$ and therefore the approach to the stationary state does not minimize θ . Nor does it seem possible to construct a physically meaningful function which is minimized. We have, therefore, here a thermodynamically stable state which seemingly is not governed by a minimum

principle related to the principle of minimum entropy production.

It is possible, however, to give a simple interpretation of the differential form

$$\sum_i j_i dx_i = w_2 \alpha_2 d\alpha_1 - w_3 \alpha_1 d\alpha_2 \quad (55)$$

which was shown by Glansdorff and Prigogine⁵ to be always negative. Since the rotation is counter-clockwise, this is immediately verified, and the theorem of Glansdorff and Prigogine can be said to fix the sense of rotation, as pointed out by Prigogine and Balescu.¹⁶

If one tries to solve the non-linear equations of Volterra by usual iteration-methods, starting from the solution of the linearized equation, one immediately gets terms which diverge strongly as $t \rightarrow \infty$. It is possible, however, to express the frequency as an integral, but this integral cannot be expressed in terms of elementary functions. To solve the equations we must use an iterative procedure where, at each step, the occurrence of divergent terms is prevented. Such a method has been devised by Kryloff and Bogoliubov,¹⁰ and we refer to their book for details.

It is convenient to introduce new variables y_1 and y_2 by

$$\alpha_1 = w_2 \sqrt{(w_4)} y_1$$

and

$$\alpha_2 = w_3 \sqrt{(w_1)} y_2$$

We then have

$$\dot{y}_1 = -\nu y_2 - a y_1 y_2$$

$$\dot{y}_2 = \nu y_1 + b y_1 y_2$$

with

$$\nu = \sqrt{(w_1 w_4)}; a = w_2 w_3 \sqrt{w_1}; b = w_2 w_3 \sqrt{w_4}$$

or:

$$\ddot{y}_1 + \nu^2 y_1 = b y_1 \dot{y}_1 - a \nu y_1^2 + a \dot{y}_1^2 / (\nu + a y_1) \quad (56)$$

and an analogous equation for y_2 .

In the first approximation the representative point in y_1, y_2 -space now moves on a circle around $(0, 0)$. We see that the right-hand side of the last equation contains terms which, when expanded in power series near $(0, 0)$, are smaller than the terms

on the left-hand side by increasing orders of magnitude. Expanding the fraction on the right-hand side we rewrite the equation as:

$$\begin{aligned}\ddot{y}_1 + \nu^2 y_1 &= \varepsilon(b y_1 \dot{y}_1 - a \nu y_1^2 + (a/\nu) \dot{y}_1^2) - \varepsilon^2 (a/\nu)^2 \dot{y}_1^2 y_1 + \dots \\ &= -\varepsilon f_1(y_1, \dot{y}_1) - \varepsilon^2 f_2(y_1, \dot{y}_1) - \dots\end{aligned}\quad (57)$$

where the factor ε indicates the smallness of the perturbation. This separation of the right-hand side into terms of increasing order of smallness appears to be necessary for the successful application of the Kryloff-Bogoliubov method. In the final solution we shall of course put $\varepsilon = 1$.

We want to find a solution of the form $y_1 = z(\tau)$, with $\tau = \omega t + \varphi$, where $z(\tau)$ is a function with period 2π . Substituting we get

$$\omega^2 z'' + \nu^2 z = -\varepsilon f_1(z, \omega z') - \varepsilon^2 f_2(z, \omega z') - \dots$$

and we now assume

$$z = z_0(\tau) + \varepsilon z_1(\tau) + \varepsilon^2 z_2(\tau) + \dots$$

$$\omega = \omega_0 + \varepsilon \omega_1 + \varepsilon^2 \omega_2 + \dots$$

Using the above assumption and collecting powers of ε we have the recursive system:

$$\begin{aligned}1. \quad & \omega_0^2 z''_0 + \nu^2 z_0 = 0 \\ 2. \quad & \omega_0^2 z''_1 + \nu^2 z_1 = -f_1(z_0, \omega_0 z'_0) - 2\omega_0 \omega_1 z''_0 \\ 3. \quad & \omega_0^2 z''_2 + \nu^2 z_2 = -f'_1(z_0, \omega_0 z'_0) - f_2(z_0, \omega_0 z'_0) \\ & \quad - (\omega_1^2 + 2\omega_0 \omega_2) z''_0 - 2\omega_0 \omega_1 z_1\end{aligned}\quad (58)$$

etc.

These linear differential equations are solved, and at each step in the iterative procedure we adjust ω so that secular terms do not develop, i.e. we adjust ω so that the Fourier-expansion of the right-hand side does not contain terms with $\sin \omega t$ or $\cos \omega t$. We obtain:

$$\begin{aligned}1. \quad & y_1 = r \cos(\nu t + \varphi); \quad \nu = \sqrt{(w_1 w_4)} \\ & y_2 = r \sin(\nu t + \varphi)\end{aligned}$$

$$\begin{aligned}
2. \quad y_1 &= r \cos(\nu t + \varphi) + (a/3\nu)r^2 \cos 2(\nu t + \varphi) + (b/6\nu)r^2 \sin 2(\nu t + \varphi) \\
y_2 &= r \sin(\nu t + \varphi) - (b/3\nu)r^2 \cos 2(\nu t + \varphi) + (a/6\nu)r^2 \sin 2(\nu t + \varphi) \\
\omega_1 &= 0
\end{aligned}$$

i.e., the frequency is as in the first approximation.

$$3. \quad w_2 = -(r^2/12)(a^2 + b^2)$$

i.e., the frequency is

$$\nu - (r^2/12)(a^2 + b^2) = \sqrt{(w_1 w_4) - (w_2^2 w_3^2 r^2/12)(w_1 + w_4)} \quad (59)$$

It is hardly worth while to go on to higher approximations for y_1 and y_2 , since the most important result certainly is the expression for the frequency. Experimentally the frequency will be easily accessible even for very fast reactions, and if the chemical reactions leading to the Volterra equations could be realized, it would be easy to check this expression, since at least one rate-constant can be changed at will, simply by adding the substance which must serve as "food" for A_1 to conserve matter.

V. CONCLUSION

In the previous section we have first tried to show how far one can go with respect to using thermodynamic concepts in chemical kinetics and similar processes. Only in very few cases, if any, has this formulation up till now given information about the systems which could not as readily have been extracted directly from the kinetic equations, and the primary use of the formalism is therefore to express in a more abstract way certain general properties of the thermodynamic system.

Although, as we have seen, the principle of minimum entropy production can be generalized to be valid for a fairly large class of thermodynamically nonlinear systems, the most general result still appears to be the differential principle of Glansdorff and Prigogine, which states that

$$d_X \sigma \leq 0$$

under the natural motion of the system. In that case, however, the physical implications of the statement still seem to be rather

obscure, except possibly for the case of oscillating reactions, where it may be said to determine the sense of rotation.

One of the most interesting properties of nonlinear systems is the possibility of oscillating reactions. Thanks to the method of Kryloff and Bogoliubov and related methods these oscillations can now be investigated in detail, and one may hope that this will finally lead to a conclusion about the exact nature of the oscillations found in some chemical systems.

References

1. Bak, T. A., *J. Phys. Chem.* **60**, 1611 (1956).
2. Bak, T. A., *Contributions to the Theory of Chemical Kinetics*, Munksgaard, Copenhagen, 1959.
3. Bray, W. C., *J. Am. Chem. Soc.* **43**, 1262 (1921).
4. Frank-Kamenetzki, D. A., *Diffusion and Heat Exchange in Chemical Kinetics*, Princeton Univ. Press, Princeton, 1955.
5. Glansdorff, P., and Prigogine, I., *Physica* **20**, 773 (1954).
6. de Groot, S. R., *Thermodynamics of Irreversible Processes*, North Holland, Amsterdam, 1951.
7. Hearon, J. Z., *Bull. Math. Biophys.* **15**, 121 (1953).
8. Hurewicz, W., *Lectures on Ordinary Differential Equations*, Wiley, New York, 1958.
9. Koefoed, J., *J. Coll. Sci.* **12**, 131 (1957).
10. Kryloff, N., and Bogoliubov, N., *Introduction to Non-Linear Mechanics*, Princeton Univ. Press, Princeton, 1947.
11. Onsager, L., *Phys. Rev.* **37**, 405; **38**, 2265 (1931).
12. Onsager, L., and Machlup, S., *Phys. Rev.* **91**, 1505, 1512 (1953).
13. Peard, M. G., and Cullis, C. F., *Trans. Faraday Soc.* **47**, 616 (1951).
14. Prigogine, I., *Bull. classe des Sci. Acad. roy. Belg.* **31**, 600 (1945).
15. Prigogine, I., *Bull. classe des Sci. Acad. roy. Belg.* **40**, 417 (1954).
16. Prigogine, I., and Balescu, R., *Bull. classe des Sci. Acad. roy. Belg.* **42**, 256 (1956).
17. Prigogine, I., and Mahieu, M., *Physica* **16**, 51 (1950).
18. Prigogine, I., and Xhrouet, E., *Physica* **15**, 931 (1949).
19. Rice, O. K., *J. Phys. Chem.* **61**, 622 (1957).
20. Volterra, V., *Théorie Mathématique de la lutte pour la Vie*, Gautiers Villars, Paris, 1931.

PROPAGATION OF FLAMES AND DETONATIONS*

J. O. HIRSCHFELDER and C. F. CURTISS, *Theoretical Chemistry
 Laboratory, University of Wisconsin*

CONTENTS

I.	Introduction	60
II.	Hydrodynamic Equations	60
	A. Equations of Change	60
	B. One-Dimensional Time-Dependent Equations	63
	C. One-Dimensional Steady-State Equations.	65
	D. Boundary Conditions	66
III.	Flames Produced by an Exothermic Unimolecular Reaction.	68
	A. The Flame Equations	69
	B. Ignition Temperature Model	74
	C. Arrhenius Kinetics	76
	D. The Effect of the Kinetic Energy Terms	86
	E. Approximate Solutions	88
	(1) Ignition Temperature Approximation	88
	(2) Corner Approximation	89
	(3) Adams and Wilde Approximations	91
	(4) Hirschfelder Approximations	93
	(5) The Klein Approximation	95
IV.	Flames Supported by Complex Systems of Chemical Reaction Chains.	96
V.	Single Step, Unimolecular Reaction Detonation	104
	A. The Detonation Equations	110
	B. Ignition Temperature Model	115
	C. Arrhenius Kinetics and Detonations in Real Gases	121
	References	128

* This work was carried out at the University of Wisconsin Theoretical Chemistry Laboratory under Contract NOrd 15884 with the Naval Bureau Ordnance.

I. INTRODUCTION

The study of chemical kinetics is often limited to reactions taking place in a vessel at constant temperature and either constant volume or constant pressure. However, it is sometimes more convenient to carry out the reactions under other conditions where the mathematical analysis may be somewhat complicated. For example, the study of reactions carried out in a shock tube is becoming most useful. There is a large mass of precise experimental data available on the behaviour of flames and detonations which would provide a wealth of information regarding chemical kinetics if one could unravel the complicated mathematical relationships which tie the chemical kinetics to the fluid flow properties.

In the present paper we write down the general equations which govern the detailed structure of flames and detonations. Indeed, these relations should apply to chemical reactions taking place under any conditions of fluid flow. The mathematical solution of these equations is sufficiently difficult that for the present time we are content to restrict ourselves to steady state problems in which the flow is not only laminar but takes place in one-dimension. Under these conditions, we obtain exact solutions for a hypothetical unimolecular reaction $A \rightarrow B$, and indicate the mathematical procedure required to treat an arbitrary system of chemical kinetics.

II. HYDRODYNAMIC EQUATIONS

The theory of propagation of flames and detonations is based on the hydrodynamic equations of change. These equations represent the overall conservation of momentum and energy in molecular collisions and the rate of change of molecular species due to chemical reactions and diffusion. In this way, we obtain the most general description of nonequilibrium processes in fluids.

A. Equations of Change

The state of gas mixture may be described by the temperature, T , the velocity, \mathbf{v} , and the molar density of each species, n_i , at

each point \mathbf{r} . In addition, it is convenient to introduce the overall density,

$$\rho = \sum_i n_i m_i \quad (1)$$

where m_i is the molecular weight of species i . The equations of change are then:*

1. The equations of continuity of each chemical species,

$$(\partial/\partial t) n_i + (\partial/\partial \mathbf{r}) \cdot n_i (\mathbf{v} + \mathbf{V}_i) = K_i \quad (2)$$

where \mathbf{V}_i is the diffusion velocity and K_i is the net rate of formation of molecules of i due to chemical reactions.

2. The overall equation of continuity (which is the sum of the individual equations, each weighted with its corresponding molecular weight) is given by

$$(\partial/\partial t) \rho + (\partial/\partial \mathbf{r}) \cdot \rho \mathbf{v} = 0 \quad (3)$$

3. The equation of motion

$$(\partial/\partial t) \mathbf{v} + \mathbf{v} \cdot (\partial/\partial \mathbf{r}) \mathbf{v} = -(1/\rho) (\partial/\partial \mathbf{r}) \cdot \mathbf{p} + (1/\rho) \sum_i n_i \mathbf{X}_i \quad (4)$$

where \mathbf{p} is the pressure tensor (including the effects of viscous forces) and \mathbf{X}_i is the external force on a mole of particles of species i .

4. The energy balance equation,

$$\begin{aligned} & (\partial/\partial t) \hat{U} + \mathbf{v} \cdot (\partial/\partial \mathbf{r}) \hat{U} \\ &= -(1/\rho) (\partial/\partial \mathbf{r}) \cdot (\mathbf{q} + \mathbf{q}_R) - (1/\rho) \mathbf{p} : (\partial/\partial \mathbf{r}) \mathbf{v} + (1/\rho) \sum_i n_i \mathbf{V}_i \cdot \mathbf{X}_i \end{aligned} \quad (5)$$

where \hat{U} is the thermodynamic internal energy of the mixture per unit mass, \mathbf{q} is the energy flux due to molecular motions and \mathbf{q}_R is the radiation contribution to the energy flux.

These equations are essentially incomplete until expressions are given for the K_i and the various fluxes. For simplicity, we restrict the discussion of these expressions to forms applicable to mixtures of perfect gases. The chemical kinetics of a reacting mixture may be described in terms of a set of chemical reactions, which may be written symbolically in the form

* Hirschfelder *et al.*, *Molecular Theory of Gases and Liquids*, (reference 11). Henceforth this is referred to as MTGL.

$$\beta_{1j}[1] + \beta_{2j}[2] + \dots \rightleftharpoons \eta_{1j}[1] + \eta_{2j}[2] + \dots \quad (6)$$

where the β_{ij} and the η_{ij} are integers and the $[i]$ indicate the molecular species. Let the rate constant for the j -th forward reaction be k_j and that for the reverse reaction be k'_j . Then in a mixture of perfect gases the rate of the forward reaction is

$$k_j n_1^{\beta_{1j}} n_2^{\beta_{2j}} \dots \quad (7)$$

and a similar expression gives the rate of the reverse reaction. The total rate of formation of i due to chemical reactions is then

$$K_i = \sum_j (\eta_{ij} - \beta_{ij}) [k_j n_1^{\beta_{1j}} n_2^{\beta_{2j}} \dots - k'_j n_1^{\eta_{1j}} n_2^{\eta_{2j}} \dots] \quad (8)$$

This is the expression for the K_i which is used in the equation of continuity of species i , Eq. (2).

In a mixture of perfect gases, the diffusion velocities are¹¹

$$\mathbf{V}_i = \langle n^2/n_i \rho \rangle \sum_j m_j D_{ij} \mathbf{d}_j - (D_i^T/n_i m_i) \partial \ln T / \partial \mathbf{r} \quad (9)$$

where

$$\begin{aligned} \mathbf{d}_j = & (\partial / \partial \mathbf{r}) (n_j/n) + (n_j/n - n_j m_j / \rho) \partial \ln p / \partial \mathbf{r} \\ & - (n_j m_j / p \rho) [(\rho / m_j) \mathbf{X}_j - \sum_k n_k \mathbf{X}_k] \end{aligned} \quad (10)$$

and

$$p = nRT \quad (11)$$

Here n is the total number of moles per unit volume and R is the gas constant. The D_{ij} are the multicomponent diffusion coefficients and the D_i^T are the multicomponent thermal diffusion coefficients. Both the D_{ij} and the D_i^T are rather complicated functions of the temperature and the composition. In the study of flames and detonations it is usually more convenient to use the implicit expressions for the diffusion velocities given by the "diffusion equations," obtained by combining Eq. (10) with the relation

$$\begin{aligned} \mathbf{d}_i = & \sum_j (n_i n_j / n^2 \mathcal{D}_{ij}) (\mathbf{V}_j - \mathbf{V}_i) \\ & + (\partial \ln T / \partial \mathbf{r}) \sum_j (n_i n_j / n^2 \mathcal{D}_{ij}) (D_j^T / n_j m_j - D_i^T / n_i m_i) \end{aligned} \quad (12)$$

where the \mathcal{D}_{ij} are the binary diffusion coefficients associated with the interdiffusion of species i and j . The binary diffusion coefficients are to a good approximation independent of the composition. This set of equations is not sufficient to give all of the

diffusion velocities, since the sum of the equations is zero, but the diffusion velocities are defined relative to the mass average velocity \mathbf{v} so that

$$\sum_i n_i m_i \mathbf{V}_i = 0 \quad (13)$$

Thus, Eqs. (12) together with the condition Eq. (13) are equivalent to the set Eqs. (9).

In any isotropic, Newtonian fluid the pressure tensor is

$$\mathbf{p} = p\mathbf{U} - 2\eta\mathbf{S} - \kappa' ((\partial/\partial\mathbf{r}) \cdot \mathbf{v})\mathbf{U} \quad (14)$$

where \mathbf{S} is the rate of shear tensor

$$\mathbf{S} = \frac{1}{2} ((\partial/\partial\mathbf{r})\mathbf{v}) + \frac{1}{2} ((\partial/\partial\mathbf{r})\mathbf{v})^\dagger + -\frac{1}{3} ((\partial/\partial\mathbf{r}) \cdot \mathbf{v})\mathbf{U} \quad (15)$$

The \dagger indicates the transpose of the vector gradient*. The η and κ' are the coefficients of shear and bulk viscosity, respectively, and p is the static pressure, which for a perfect gas is, of course, given by Eq. (11).

In a mixture of perfect gases, the contribution of the molecular motions to the energy flux is

$$\mathbf{q} = -\lambda \partial T / \partial \mathbf{r} + \sum_i n_i H_i \mathbf{V}_i + (RT/n) \sum_{ij} (n_j D_i^T / m_i \mathcal{D}_{ij}) (\mathbf{V}_i - \mathbf{V}_j) \quad (16)$$

In this expression, λ is the coefficient of thermal conductivity, H_i is the enthalpy per mole of species i , and R is the gas constant. The energy flux due to radiation processes, \mathbf{q}_R , often depends in an important way on the exact chemical nature of the medium, and will not be discussed here.¹¹

When the expressions for the K_i and the various fluxes are used in the equations of change, Eqs. (2), (4), and (5), one obtains a set of differential equations which describe the time and space variation of the variables n_i , \mathbf{v} , and T . These equations involve the rate constants $k_j(T)$ and $k'_j(T)$ for the chemical reactions and the transport coefficients \mathcal{D}_{ij} , D_i^T , η , κ' , and λ .

B. One-Dimensional Time-Dependent Equations

The discussion of flames and detonations will be restricted entirely to one-dimensional systems. We, thus, consider the

* The ij element of tensor $(\partial/\partial\mathbf{r})\mathbf{v}$ is $(\partial/\partial r_i)v_j$. The corresponding element of the transpose tensor $((\partial/\partial\mathbf{r})\mathbf{v})^\dagger$ is $(\partial/\partial r_j)v_i$.

equations of change, described above, in the special case in which the flow is only in the z direction and in which all variables are independent of the x and y coordinates.

Before discussing the equations, it is convenient to define several additional quantities:

1. M is the total mass flux,

$$M = \rho v \quad (17)$$

2. x_i is the mole fraction of component i ,

$$x_i = n_i/n \quad (18)$$

3. G_i is the fraction of the mass flux due to component i ,

$$G_i = n_i m_i (v + V_i)/M \quad (19)$$

Sometimes the G_i are referred to as chemical progress variables. It is convenient to consider the G_i as dependent variables and to use the diffusion equations, Eqs. (12), as part of the hydrodynamic equations.

The expressions for the various fluxes and the above definitions may now be used in the equations of change, and the equations reduced to the one-dimensional form. With some rearrangement, one then obtains the following set of equations:

1. The equation of continuity of each chemical species

$$(\partial/\partial t)(n x_i) = -(\partial/\partial z)(M G_i/m_i) + K_i \quad (20)$$

2. The overall equation of continuity

$$(\partial/\partial t)\rho = -(\partial/\partial z)M \quad (21)$$

3. The equation of motion

$$(\partial M/\partial t) = -(\partial/\partial z)[p + Mv - (\frac{4}{3}\eta + \kappa')\partial v/\partial z] + \sum_i n_i x_i X_i \quad (22)$$

4. The energy balance equation

$$\begin{aligned} & (\partial/\partial t)[n \sum_i x_i m_i \hat{H}_i - p + \frac{1}{2}\rho v^2] \\ & = (\partial/\partial z)\{\lambda \partial T/\partial z - M \sum_i G_i \hat{H}_i - \frac{1}{2}Mv^2 + (\frac{4}{3}\eta + \kappa')v \partial v/\partial z \\ & - q_R + (pM/n^2) \sum_{ij} (D_i^T/m_i m_j \mathcal{D}_{ij}) [G_j - (m_j x_j/m_i x_i) G_i]\} \\ & + M \sum_i G_i X_i/m_i \end{aligned} \quad (23)$$

5. The diffusion equations

$$\begin{aligned} \partial x_i / \partial z = & (M/n) \sum_j (x_i m_i G_j - x_j m_j G_i) / m_i m_j \mathcal{D}_{ij} - x_i (1 - nm_i / \rho) \partial \ln p / \partial z \\ & + (\partial \ln T / \partial z) \sum_j (x_i m_i D_i^T - x_j m_j D_i^T) / nm_i m_j \mathcal{D}_{ij} \\ & + (x_i n / p) [X_i - (nm_i / \rho) \sum_j x_j X_j] \quad (24) \end{aligned}$$

These are the equations which would be used in the study of time dependent phenomena, such as ignition problems, stability questions, and the possible transformation of a flame into a detonation. The present discussion, however, is limited to the steady state propagation of flames and detonations.

C. One-Dimensional Steady-State Equations

One-dimensional steady state flames and detonations travel with constant velocity into the unburned gas. If the unburned gas is stationary, such a wave actually moves in space with a constant velocity. On the other hand, if the unburned gas moves with the proper constant velocity, the wave may be maintained at a constant position in space. In either case, it is convenient to make use of a coordinate system fixed with respect to the wave and consider the stationary state solutions of the equations. This is possible because the hydrodynamic equations apply in any system of coordinates moving with constant velocity (Galilean invariance).

To obtain the time-independent equations we require that all time derivatives in the hydrodynamic equations, Eqs. (20) to (24), be zero. Let us also restrict the consideration to systems which are not subject to any external force, so that all the $X_i = 0$. The overall equation of continuity, Eq. (21), the equation of motion, Eq. (22), and the energy balance equation, Eq. (23), may then be integrated with respect to z . The result is that the mass rate of flow, M , is a constant and that the remaining equations are as follows:

1. The equation of continuity of each chemical species

$$dG_i/dz = m_i K_i / M \quad (25)$$

2. The equation of motion

$$(\frac{4}{3}\eta + \kappa') dv/dz = p + Mv + L_1 \quad (26)$$

3. The energy balance equation

$$\begin{aligned} & \lambda dT/dz + (\frac{4}{3}\eta + \kappa') v dv/dz \\ &= M \sum_i G_i \hat{H}_i + \frac{1}{2} M v^2 + q_R \\ &+ L_2 - (pM/n^2) \sum_{ij} (D_i^T/m_i m_j \mathcal{D}_{ij}) [G_j - (m_j x_j/m_i x_i) G_i] \end{aligned} \quad (27)$$

where L_1 and L_2 are the constants of integration. The diffusion equations as given by Eq. (24) are unchanged (except for omission of the terms due to the external forces, X_i).

D. Boundary Conditions

We are interested in flames and detonations in which the burned gases are free to flow undisturbed infinitely far in the positive z direction. The various properties of the burned gas then asymptotically approach limiting values as $z \rightarrow \infty$. We refer to these limiting values as the "hot boundary" values and indicate the quantities by a subscript ∞ . The constants L_1 and L_2 may then be expressed in terms of the hot boundary values of the various quantities by noting that in this limit dv/dz and dT/dz are zero.

In most problems involving flames and detonations, one may neglect radiation effects (take $q_R = 0$), neglect thermal diffusion and the Dufour effects (take the $D_i^T = 0$), and neglect pressure diffusion (drop the corresponding term in the diffusion equations). These are, however, effects which should be investigated explicitly when the results are applied to any particular example. When these terms are dropped from the hydrodynamic equations and the constants of integration evaluated in terms of the hot boundary conditions, one obtains the following "flame and detonation equations:"

1. The equations of continuity

$$dG_i/dz = m_i K_i/M \quad (28)$$

2. The equation of motion

$$(\frac{4}{3}\eta + \kappa') dv/dz = (p - p_\infty) + M(v - v_\infty) \quad (29)$$

3. The energy balance equation

$$(\lambda/M)dT/dz = \sum_i G_i \hat{H}_i - \sum_i G_{i\infty} \hat{H}_{i\infty} - (1/\rho)(p - p_\infty) - (1/2)(v - v_\infty)^2 \quad (30)$$

4. The diffusion equations

$$dx_i/dz = (M/n) \sum_j (x_i m_i G_j - x_j m_j G_i) / m_i m_j \mathcal{D}_{ij} \quad (31)$$

The problem is then one of obtaining solutions of these equations which satisfy the required boundary conditions.

At the hot boundary, $z \rightarrow \infty$, the various quantities approach finite limits corresponding to complete chemical and thermal equilibrium. Accordingly, the derivatives of all of the quantities approach zero as $z \rightarrow \infty$.

The cold boundary conditions are somewhat more difficult to specify. First, let us consider the case in which all of the K_i are identically zero at the cold boundary temperature, T_0 . In this case, we can consider an "unattached" flame or detonation and let $z \rightarrow -\infty$. The boundary conditions at the cold boundary are then completely analogous to those at the hot boundary: the various quantities approach finite limits as $z \rightarrow -\infty$, and the derivatives approach zero. Equations relating the values of the quantities at the two boundaries are obtained from Eqs. (29), (30), and (31) by setting the derivatives equal to zero.

In practice it is usual to use Arrhenius type expressions for the temperature dependence of the rate constants. These expressions lead to small but finite values of the K_i at the cold boundary temperature T_0 . In this case, solutions of the type mentioned above do not exist and it is necessary to invoke the concept of a flameholder. The flameholder acts primarily as a heat sink and as a semipermeable membrane which passes only the fuel molecules and prevents the back diffusion of the product molecules.

The cold boundary conditions at the flameholder, which is taken to be at the origin of the z coordinate system, are: (1) the G_i are the mass fractions of the various components in the unburned fuel, and (2) the heat transfer to the heat sink or the value of energy flux at $z = 0$ is

$$q_0 = -\lambda_0(dT/dz)_0 \quad (32)$$

In general, Eq. (29) would lead to a finite value of dv/dz at $z = 0$ and a small but finite thrust on the flameholder.

The concept of the flameholder is apparently necessary if the rate constants are taken to be finite at T_0 . The concept is, however, useful even if the K_i are identically zero at T_0 since the heat transfer to the flameholder determines the quenching distance. It is interesting to speculate on the relation of this mathematical flameholder to physical flameholders, but such a discussion involves three dimensional hydrodynamics, radiation, and turbulence.

Solutions of the flame and detonation equations, Eqs. (28) to (31), satisfying the boundary conditions discussed above are described in the succeeding sections. Two qualitatively distinct types of solutions are obtained. One type of solution represents the structure of flames; the other is associated with detonations.

If the initial temperature, pressure, and composition of the fuel are specified along with the strength of the heat sink, q_0 , a flame type solution of the equations exists (and satisfies all of the boundary conditions) only for a single value of the mass rate of flow, M . This value of M is the product of the flame velocity v_0 (the value of v at the flameholder ($z = 0$)) and ρ_0 , the gas density at the flameholder. The problem then is an eigenvalue problem for obtaining the proper value of M . In practice, it is usually found that the value of M is very insensitive to the value of q_0 over a large range of values of q_0 . If the K_i are not zero at T_0 , this range does not include zero. On the other hand, detonation type solutions of the equations satisfying all of the boundary conditions exist for a wide range of values of M . It is interesting to determine both the steady state flame and the steady state detonation solutions from the same set of equations with the same boundary conditions.

III. FLAMES PRODUCED BY AN EXOTHERMIC UNIMOLECULAR REACTION*

The equations and boundary conditions discussed in the preced-

* Flames supported by unimolecular reactions have been discussed in many places, including MTGL. However, the most complete treatment is given by Hirschfelder and McCone, (reference 13).

ing section apply to any steady state, laminar, one dimensional flame or detonation. Flames in which the chemical reactions occur in one step have only one linearly independent G_i and are therefore much easier to consider than flames supported by a complex set of reactions. In this section, we consider the application of the equations to a particularly simple flame system. This is the flame supported by a single step unimolecular reaction,



As a first step, we introduce some simplifying notation and consider the equations of the preceding section as applied to this special case. We then consider two types of kinetic rate expressions, an "ignition temperature" model and the more realistic Arrhenius type expressions. The advantage of the ignition temperature model is that it leads to simpler solutions and hence the effect of the various parameters may be better understood. The effects of fuel dilution, a back reaction, and the kinetic energy terms (which become important in unusually high velocity flames) are then discussed. Several approximate solutions of the flame equations are then considered. These approximate solutions also lead to a better understanding of the effects of the various parameters.

A. The Flame Equations

The equation of motion, Eq. (29), indicates that the pressure is nearly constant throughout an ordinary flame. The derivative, dv/dz , is zero at the hot boundary and very nearly zero at the cold boundary. Thus,

$$p_0 - p_\infty = M(v_\infty - v_0) \quad (33)$$

or

$$(p_0 - p_\infty)/p_0 = \gamma v_0 (v_\infty - v_0)/c_0^2 \quad (34)$$

where c_0 is the velocity of sound in the cold gas,

$$c_0 = (\gamma p_0/\rho_0)^{1/2} \quad (35)$$

and γ is the ratio of the heat capacity at constant pressure, C_p , to the heat capacity at constant volume, C_v ,

$$\gamma = C_p/C_v \quad (36)$$

Typical values of the various quantities are: $\gamma = 1.25$, $v_0 = 30$ cm/sec, $v_\infty = 300$ cm/sec, and $c_0 = 30,000$ cm/sec. Using these values in Eq. (34) we find that

$$(p_0 - p_\infty)/p_0 = 1.13 \times 10^{-5}$$

Furthermore, it may be shown that the variation of pressure through the flame is monotone. Thus, for most purposes, we may neglect the variation of pressure and ignore the equation of motion. Similar numerical considerations indicate that in most flames the last two terms in the energy balance equation, Eq. (30), (the terms associated with the pV work and with the kinetic energy) may be neglected. Hence, we first neglect these terms, and then later discuss their effect in more detail.

It follows from the definitions, Eqs. (18) and (19), that the sum over all components of the x_i , and also of the G_i , is unity. In the simple two component system associated with the reaction $A \rightarrow B$, only two x_i functions appear, and hence one may readily be expressed in terms of the other. It is convenient to use x_A and for notational simplicity to neglect the subscript. Similar considerations apply to the G_i . Hence in this section

$$x \equiv x_A = 1 - x_B \quad (37)$$

and

$$G \equiv G_A = 1 - G_B \quad (38)$$

Clearly, A and B have the same molecular weight, m . Let us assume that A and B have the same specific heat \hat{C}_p per unit mass and further assume that \hat{C}_p is independent of the temperature. Then the enthalpies per unit mass of the two species are

$$\hat{H}_A = \hat{H}_{A0} + \hat{C}_p T \quad (39)$$

$$\hat{H}_B = \hat{H}_{B0} + \hat{C}_p T \quad (40)$$

The enthalpy per unit mass of a mixture of A and B is then

$$\hat{H} = x\hat{H}_A + (1 - x)\hat{H}_B = \hat{H}_{B0} + \hat{Q}x + \hat{C}_p T \quad (41)$$

where

$$\hat{Q} = \hat{H}_{A0} - \hat{H}_{B0} \quad (42)$$

is the heat of reaction per unit mass.

From chemical kinetic considerations, it follows that the rate of production of A by the unimolecular reaction $A \rightarrow B$ is of the form

$$K_A = -xnk(T) \quad (43)$$

where $k(T)$ is the specific reaction rate and is a function of temperature only. It is convenient to introduce the dimensionless reaction rate parameter

$$R_\infty = nm\lambda k(T_\infty)/M^2\hat{C}_p \quad (44)$$

where $k(T_\infty)$ is the specific reaction rate, $k(T)$ at the hot boundary temperature. It is assumed that the product $n\lambda$ is constant so that R_∞ is constant. From Eq. (17), we find that the velocity of approach of the gas on the cold side is

$$v_0 = (1/\rho_0)(nm\lambda k(T_\infty)/\hat{C}_p R_\infty)^{\frac{1}{2}} = (\mathcal{D}_0 k(T_\infty)/R_\infty \delta)^{\frac{1}{2}} \quad (45)$$

This is the velocity with which the flame would move into unburned cold gas and is known as the flame velocity. In the Eq. (45), δ is the Lewis number

$$\delta = nm\hat{C}_p \mathcal{D}/\lambda \quad (46)$$

It is convenient to express the flame equations entirely in terms of dimensionless variables and dimensionless groups. The reduced temperature is defined by

$$\theta = T/T_\infty \quad (47)$$

and the reduced distance variable is defined by

$$\xi = M \int_0^z (\hat{C}_p/\lambda) dz \quad (48)$$

The energy released by the chemical reaction may be expressed in terms of either of the parameters

$$\varepsilon = 1 + (\hat{Q}/\hat{C}_p T_0) \quad (49)$$

or

$$a = \hat{Q}/\hat{C}_p T_\infty = (\varepsilon - 1)\theta_0 \quad (50)$$

The use of ε or a depends on whether T_0 or T_∞ is specified.

The flame equations, Eqs. (28) to (31), may now be written for the special case of a flame supported by the simple unimolecular

reaction. As discussed above, we take the pressure to be constant so that the equation of motion can be ignored. At this point, we also neglect the kinetic energy (last two) terms in the energy balance equation. The effect of these terms is discussed later. In terms of the reduced variables and dimensionless groups the flame equations are then:

1. The equation of continuity of species A ,

$$dG/d\xi = -Rx \quad (51)$$

where

$$R = nm\lambda k(T)/M^2 \hat{C}_p = R_\infty k(T)/k(T_\infty) \quad (52)$$

2. The energy balance equation

$$d\theta/d\xi = aG - (1 - \theta) \quad (53)$$

3. The diffusion equation

$$\delta(dx/d\xi) = x - G \quad (54)$$

From Eq. (32) and the definition of the dimensionless quantities, it follows that the energy flux to the flameholder is

$$-q_0 = (M\hat{Q}/a)(d\theta/d\xi)_0 = (M\hat{Q}/a)[aG_0 - (1 - \theta_0)] \quad (55)$$

The product $M\hat{Q}$ is the total flux of chemical energy into the flame. Thus the quantity multiplying this factor in the above equation is the fraction of the total chemical energy which is lost at the flameholder to the heat sink.

The structure of the flame is described by the particular solution of the Eqs. (51), (53), and (54) which satisfies the hot and cold boundary conditions. The hot boundary conditions are simply that the derivatives on the left of these equations approach zero as $\xi \rightarrow \infty$. It follows from the equations that in this limit,

$$x_\infty = 0, \quad G_\infty = 0, \quad \theta_\infty = 1$$

At the cold boundary $G = G_0$, the mass (or mole) fraction of A in the fuel mixture. If the energy flux to the flameholder, $-q_0$, (q_0 is negative for a heat sink) is specified, the value of θ at the cold boundary, i.e. θ_0 , is given by Eq. (55). The cold boundary condition is then that $G = G_0$ when $\theta = \theta_0$. In most of the present

discussion, G_0 is taken to be unity corresponding to a fuel of pure A . If, in addition, ε and δ are specified, then a satisfactory solution exists for only one value of R_∞ . The eigenvalue R_∞ is thus a function of ε , δ , $q_0/M\hat{Q}$, G_0 , and any dimensionless groups necessary to specify the temperature dependence of the specific rate constant $k(T)$.

The flame equations are particularly simple in the special case in which the Lewis number, δ , is unity. Since for most non-polar substances the Lewis number is about 0.89, taking $\delta = 1$ is a reasonable approximation. From Eq. (41) it follows that the enthalpy of the gas is

$$\hat{H} = \hat{H}_{B0} + \hat{C}_p T_\infty (ax + \theta) \quad (56)$$

If δ is taken to be unity, the energy balance equation and the diffusion equation, Eqs. (53) and (54), lead to an equation for the enthalpy,

$$d\hat{H}/d\xi = \hat{H} - \hat{H}_{B0} - \hat{C}_p T_\infty = \hat{H} - \hat{H}_\infty \quad (57)$$

The only solution of this equation which satisfies the hot boundary condition is

$$\hat{H} = \hat{H}_\infty \quad (58)$$

The assumption that $\delta = 1$ thus leads to the conclusion that the enthalpy is constant throughout the flame or that

$$ax = 1 - \theta \quad (59)$$

This linear relation between x and θ is a partial solution of the flame equations.

One may now express x in Eq. (51) in terms of θ and consider the pair of coupled differential equations, Eqs. (51) and (53), for $G(\xi)$ and $\theta(\xi)$. Since the space variable ξ does not appear explicitly, one may also divide Eq. (51) by Eq. (53) to obtain a single differential equation for $G(\theta)$. In order to proceed further with the solution of these equations it is necessary to specify the temperature dependence of the specific rate constant, $k(T)$, in order to determine the function $R(\theta)$. This requires a knowledge of the chemical kinetics of the unimolecular reaction. In the

following two sections, we consider first an oversimplified model referred to as the ignition temperature model and then the more realistic Arrhenius expression.

B. Ignition Temperature Model⁹

In the ignition temperature model, the specific reaction rate $k(T)$ is taken to be a simple step function of the temperature; it is taken to be zero for T less than the ignition temperature T_i , and a constant, k_i , for $T > T_i$. The simplicity of this model leads to a better understanding of the structure of the flame front and the dependence of the burning velocity on the various parameters. The results of this treatment are also used later, in Section (III-E), in the development of an approximate solution to the more realistic problem involving Arrhenius kinetics.

The simplicity of the ignition temperature model arises from the piecewise uncoupling of the equations for $G(\xi)$ and $x(\xi)$ from the equation for $\theta(\xi)$. The problem is then reduced to one of properly joining the solutions at the ignition temperature.

Let us first consider the equations for $\theta > \theta_i$. In this region, $R = R_\infty^{(ig)}$ (a constant) and Eqs. (51), (53), and (54) are a set of coupled linear equations. It may readily be shown that the most general solution of these equations which satisfies the hot boundary conditions is

$$G = G_i \exp [-\alpha(\xi - \xi_i)] \quad (60)$$

$$x = (\alpha/R_\infty^{(ig)})G_i \exp [-\alpha(\xi - \xi_i)] \quad (61)$$

$$\theta = 1 - [aG_i/(1 + \alpha)] \exp [-\alpha(\xi - \xi_i)] \quad (62)$$

where

$$\alpha = (2\delta)^{-1}[-1 + (1 + 4\delta R_\infty^{(ig)})^{\frac{1}{2}}] \quad (63)$$

and G_i and ξ_i are arbitrary constants. It is convenient to take ξ_i as the value of ξ at the ignition temperature, so that G_i is the corresponding value of G . Then the values of x and θ at the ignition temperature are

$$x_i = (\alpha/R_\infty^{(ig)})G_i \quad (64)$$

$$\theta_i = 1 - [aG_i/(1 + \alpha)] \quad (65)$$

In the low temperature region, when $\theta < \theta_i$, $R = 0$. The solution of the equations in this region, which takes on the values G_i , x_i , and θ_i at ξ_i , is easily shown to be

$$G = G_i \quad (66)$$

$$x = G_i - (1 - x_i) \exp \{(\xi - \xi_i)/\delta\} \quad (67)$$

$$\theta = 1 - aG_i + (\theta_i - 1 + a) \exp (\xi - \xi_i) \quad (68)$$

In order that the solutions in the two regions join properly when $T = T_i$ the values of G_i , x_i , and θ_i in these equations must, of course, be identical with those given by Eqs. (64) and (65).

If the fuel is taken to be pure A , then $G_i = 1$. The remaining cold boundary conditions require that at the flameholder (at $\xi = 0$), $\theta = \theta_0$, and that Eq. (55) be satisfied, i.e.

$$\theta_0 = 1 - a + (\theta_i - 1 + a) \exp (-\xi_i) \quad (69)$$

$$-q_0/M\hat{Q} = 1 - [(1 - \theta_0)/a] \quad (70)$$

or

$$\theta_0 = 1 - a + [a\alpha/(1 + \alpha)] \exp (-\xi_i) \quad (71)$$

$$-q_0/M\hat{Q} = [\alpha/(1 + \alpha)] \exp (-\xi_i) \quad (72)$$

From Eq. (71) and the definition Eq. (50), it follows that

$$a = (\varepsilon - 1) \{ \varepsilon - [\alpha(\varepsilon - 1)/(1 + \alpha)] \exp (-\xi_i) \}^{-1} \quad (73)$$

Since, in this model, the reaction rate is identically zero at the initial temperature, it is possible to take the rate of heat transfer to the flameholder to be zero. This is accomplished by taking $\xi_i = +\infty$, i.e. by moving the flameholder to $-\infty$. We then find from Eqs. (64), (71), and (73) that

$$\theta_i/\theta_0 = T_i/T_0 = \varepsilon - [(\varepsilon - 1)/(1 + \alpha)] \quad (74)$$

If this is combined with Eq. (63), one obtains an expression for the eigenvalue

$$R_{\infty}^{(ig)} = [(T_i/T_0) - 1][\varepsilon - \delta + (\delta - 1)(T_i/T_0)][(T_i/T_0) - \varepsilon]^{-2} \quad (75)$$

This is an explicit expression for $R_{\infty}^{(ig)}$ in terms of ε , δ , and T_i/T_0 .

If the heat transfer to the flameholder, $-q_0$, is not zero, it is not possible to obtain an explicit expression for $R_\infty^{(ig)}$. A parametric solution in terms of α is formed by the two equations

$$R_\infty^{(ig)} = (T_i/T_0 - 1)[1 + (\varepsilon - 1)q_0/M\hat{Q}][\varepsilon - \delta + (\delta - 1)T_i/T_0 + (1/\alpha)(1 + \alpha)(\varepsilon - 1)(T_i/T_0)(q_0/M\hat{Q}) - (\varepsilon - 1)(\delta - 1)(1 - T_i/T_0)q_0/M\hat{Q}] \div [T_i/T_0 - \varepsilon + (\varepsilon - 1)(T_i/T_0 - 1)q_0/M\hat{Q} - (1/\alpha)(1 + \alpha)(\varepsilon - 1)(T_i/T_0)(q_0/M\hat{Q})]^2 \quad (76)$$

and

$$R_\infty^{(ig)} = \alpha(1 + \alpha\delta) \quad (77)$$

This pair of equations determines $R_\infty^{(ig)}$ as a function of ε , δ , T_i/T_0 and $q_0/M\hat{Q}$.

Three characteristic distances arise in the description of the structure of a flame front. These are the quenching distance, ξ_Q , the temperature flame thickness, ξ_θ , and the reaction flame thickness, ξ_G .

In the ignition temperature model the quenching distance may be defined as the distance from the flameholder to the point where the temperature has risen to the ignition temperature. From Eq. (72) it is easily seen that the quenching distance is

$$\xi_Q = \xi_i = \ln [-\alpha M\hat{Q}/(1 + \alpha)q_0] \quad (78)$$

The temperature flame thickness may be defined as the distance between the points where $\theta = \theta_0 + 0.1$ and $\theta = 0.9$. If $\theta_i > \theta_0 + 0.1$ we find from Eqs. (62) and (68) that

$$\xi_\theta = -(1/\alpha) \ln \{ (1 + \alpha)\varepsilon/10(\varepsilon - 1) - (\alpha/10) \exp(-\xi_i) \} - \ln \{ \varepsilon/10 + [9\alpha(\varepsilon - 1)/10(1 + \alpha)] \exp(-\xi_i) \} \quad (79)$$

The reaction flame thickness is defined, in an analogous manner, as the distance between the points where $G = 0.9$ and $G = 0.1$. From Eq. (60), it follows simply that

$$\xi_G = (1/\alpha) \ln 9 \quad (80)$$

C. Arrhenius Kinetics

In a considerably more realistic model, the specific reaction rate is taken to vary with the temperature in a continuous manner

according to an Arrhenius type rate law; that is, $k(T)$ is taken to be of the form

$$k(T) = k' \exp(-E^\ddagger/RT) \quad (81)$$

where k' is the steric factor (usually about $10^{-13} \text{ sec}^{-1}$) and E^\ddagger is the activation energy. The function R as defined by Eq. (51) is then

$$R = R_\infty \exp[-(1 - \theta)/\tau_\infty \theta] \quad (82)$$

where

$$\tau_\infty = E^\ddagger/RT_\infty \quad (83)$$

and the constant

$$R_\infty = [(nm\lambda k')/(M^2 \hat{C}_p)] \exp(-E^\ddagger/RT_\infty) \quad (84)$$

is again the eigenvalue of the problem.

It is not possible to obtain an explicit solution of the flame equations, Eqs. (51), (53), and (54) with R given by the above expression. For the special case in which $\delta = 1$, however, Eq. (59) represents a partial solution. Thus in the present treatment we take $\delta = 1$ and discuss only this case. As mentioned earlier, for most non-polar substances δ has a value around 0.89 and thus $\delta = 1$ is a reasonable approximation.

If x is eliminated from Eq. (51) by means of Eq. (59) and the result divided by Eq. (53) one obtains

$$a(aG - 1 + \theta)(dG/d\theta) = -R(1 - \theta) \quad (85)$$

as the differential equation for $G(\theta)$. The conditions on the solution of this equation are the hot and cold boundary conditions. The hot boundary condition is simply that $G(1) = 1$. The cold boundary condition as given by Eq. (54) may be stated more explicitly as follows. First, θ_0 is defined by

$$\theta_0 = 1 - aG_0 - aq_0/M\hat{Q} = \{1 + (\varepsilon - 1)[G_0 + q_0/M\hat{Q}]\}^{-1} \quad (86)$$

where G_0 is the mass fraction of A in the fuel. We discuss primarily the case in which the fuel is pure A , so that $G_0 = 1$. The cold boundary condition is then

$$G(\theta_0) = G_0 \quad (87)$$

These boundary conditions determine R_∞ as a function of ε , δ , $q_0/M\dot{Q}$, G_0 , and τ_∞ .

The first order ordinary differential equation, Eq. (85), is an Abel equation of the second kind. With the functional form of R as given by Eq. (82), the solutions of this equation cannot be expressed in terms of analytic or simple transcendental functions. The solutions must be obtained numerically.

The hot boundary is a singular point of the differential equation, and two solutions cross at this point. Applying L'Hospital's rule to the expression for the derivative, we find that at the hot boundary

$$a^2(dG/d\theta)_\infty^2 + a(dG/d\theta)_\infty - R_\infty = 0 \quad (88)$$

or

$$a(dG/d\theta)_\infty = -(1/2) \pm (1/2)[1 + 4R_\infty]^{1/2} \quad (89)$$

Clearly, one slope is negative and the other is positive. In the flame solution, G decreases and θ increases with increasing ξ . Thus

$$a(dG/d\theta)_\infty = -b \quad (90)$$

where

$$b = (1/2) + (1/2)[1 + 4R_\infty]^{1/2} \quad (91)$$

It may be shown that the solution with the other slope cannot satisfy the cold boundary condition, and corresponds to solutions $G(\xi)$ and $\theta(\xi)$ of the original equations which diverge as $\xi \rightarrow \infty$.

Once the first derivative of G with respect to θ is known, the higher derivatives at the singular point may readily be evaluated. Thus, one may obtain a Taylor's series about $\theta = 1$ for the solution which satisfies the hot boundary condition,

$$\begin{aligned} aG = & b(1-\theta) - R_\infty(1-\theta)^2/(3b-2)\tau_\infty \\ & - \{[(3b-2)^2(2\tau_\infty-1)R_\infty + 2R_\infty^2]/2(3b-2)^2(4b-3)\tau_\infty^2\}(1-\theta)^3 + \dots \end{aligned} \quad (92)$$

With this series approximation near the hot boundary, the differential equation Eq. (85) may be integrated numerically from $\theta = 1$ toward smaller values of θ .

The numerical procedure for obtaining the eigenvalue, R_∞ , is as follows: First, a trial value of R_∞ is guessed and Eq. (85)

integrated numerically from the hot boundary toward lower values of θ to obtain a trial value of $G(\theta_0)$. If this value is larger than G_0 , the calculation is repeated with a smaller value of R_∞ ; if the value is too small, a larger value of R_∞ is used. In this way one obtains the value of R_∞ which leads to a solution which satisfies the cold boundary condition, Eq. (87). Usually, the value of R_∞ is insensitive to the θ_0 , that is, to the rate of heat transfer to the flameholder, $-q_0$, since along a solution curve G is nearly constant when θ is less than about 0.5. This constancy of G arises from the very small reaction rate at low temperatures.

TABLE I. Results of Numerical Integration, $\delta = 1$

$1/\tau_\infty$	ε	R_∞	ξ_θ	ξ_G
2	12.3046	3.6427	3.0214	2.1553
2	10.5864	3.4693	3.0486	2.2297
2	7.2605	2.9142	3.1755	2.5248
3	11.4103	6.7591	2.6230	1.5435
3	9.7304	6.4372	2.6274	1.5936
4	11.0302	10.705	2.4395	1.2122
4	9.3466	10.196	2.4333	1.2500
5	10.8530	15.475	2.3378	1.0021
5	9.1482	14.738	2.3260	1.0325
7	10.7457	27.467	2.2342	0.7463
7	8.9839	26.160	2.2163	0.7680
7	5.7887	27.188	2.1555	0.8520
10	10.8189	51.566	2.1702	0.5406
10	8.9589	49.111	2.1485	0.5558
10	5.6702	41.253	2.0722	0.6142
15	11.1370	107.98	2.1350	0.3700
15	9.1033	102.83	2.1107	0.3800
20	11.5446	184.66	2.1253	0.2809
20	9.3300	175.87	2.1000	0.2883
20	5.6605	147.73	2.0095	0.3168

Equation (85) has been integrated numerically for a wide range of the parameters.^{13,14} The results of the integrations are given in Table I and in Figs. 1, 2, and 3. In Table I the eigenvalue R_∞ is given for $G_0 = 1$, $\delta = 1$, and a range of values of τ_∞ and ε . The heat loss to the flameholder is taken to be small but non-zero.

As indicated above, for these values of the parameters the solution is insensitive to the magnitude of this heat loss.

Two characteristic distances associated with the structure of

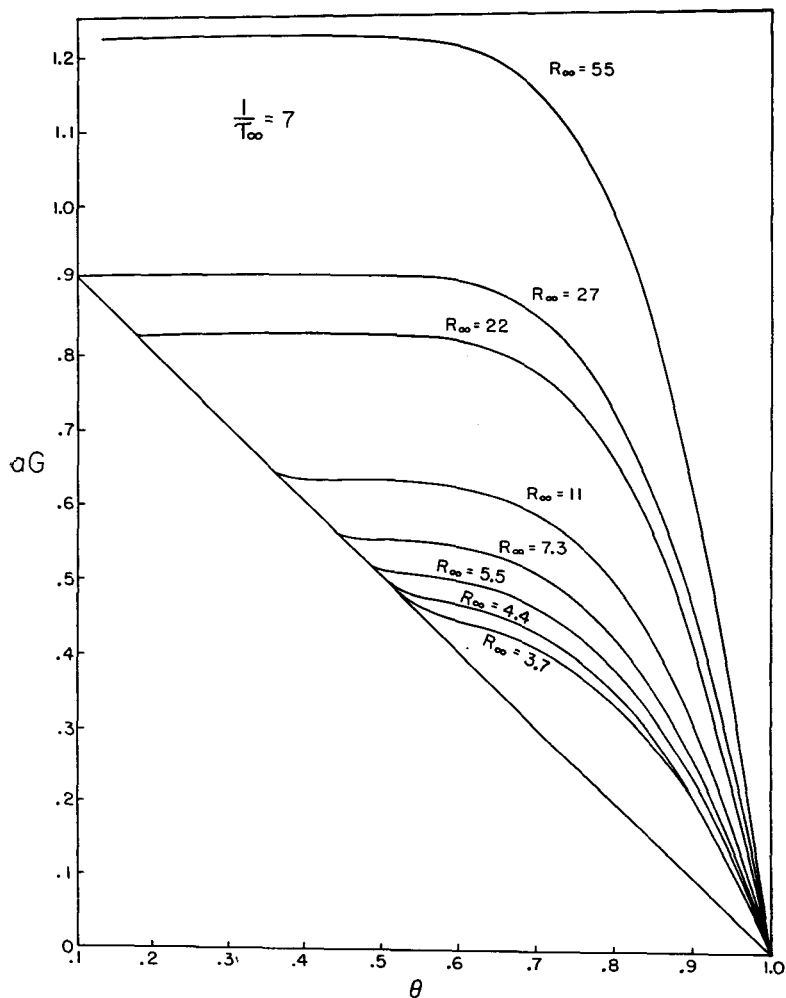


Fig. 1. Solution curves of aG versus θ for $1/\tau_\infty = 7$ and $\delta = 1$. For practical flames the value of a lies between 0.8 and 0.9. Such solutions have a long plateau. This results in a lack of sensitivity of R_∞ (or the flame velocity) to the heat transfer to the flameholder.

the flame are also given in the table. These distances are defined as in the discussion of the ignition temperature model. That is, the temperature thickness, ξ_θ , is defined as the distance, in terms of the reduced distance parameter ξ , between the points where $\theta = \theta_0 + 0.1$ and $\theta = 0.9$, and the reaction thickness is defined as the distance between the points where $G = G_0 - 0.1$ and $G = 0.1$.

Fig. 1 illustrates the way in which one determines R_∞ for given values of a and θ_0 . At $\theta = \theta_0$, $G = 1$, so that the correct value of R_∞ corresponds to the curve which passes through the point

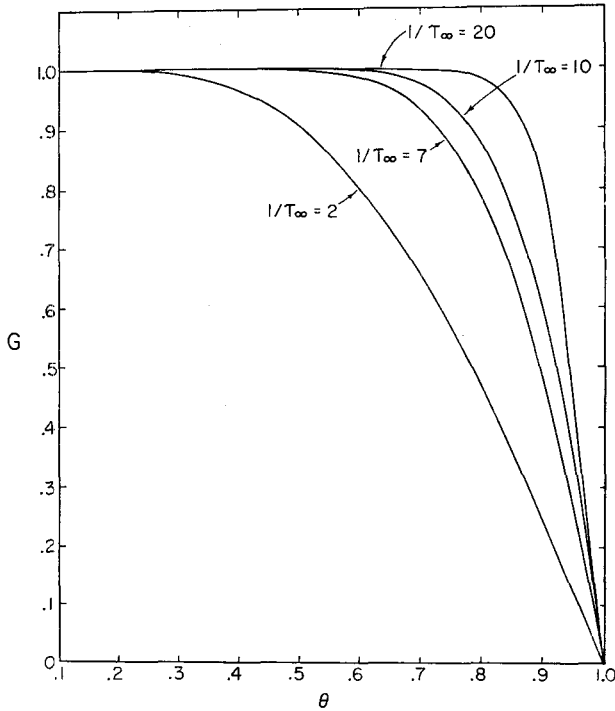


Fig. 2. The variation of G with the reduced temperature θ for $\theta_0 = 0.1$ and various values of $1/\tau_\infty$.

$\theta = \theta_0$ with $aG = a$. If too large a value of R_∞ is assumed, the value of aG for θ_0 is too large. If R_∞ is too small, aG for θ_0 is

too small. Thus the correct value is found by successive approximations. For extremely small values of heat loss to the flameholder, the initial conditions lie close to the line $aG = 1 - \theta$ and the value of R_∞ becomes dependent on the precise amount of the minuscule heat transfer to the flameholder. This effect becomes more important for larger values of θ_0 or smaller values of $1/\tau_\infty$.

Figure 2 shows the variation of G with θ for various values of $1/\tau_\infty$. The larger the value of $1/\tau_\infty$, the larger the slope at the hot boundary.

Figure 3 shows the variation of G and θ with the reduced distance ξ for various values of $1/\tau_\infty$. Note that the variation in G depends strongly on the value of $1/\tau_\infty$, whereas the variation

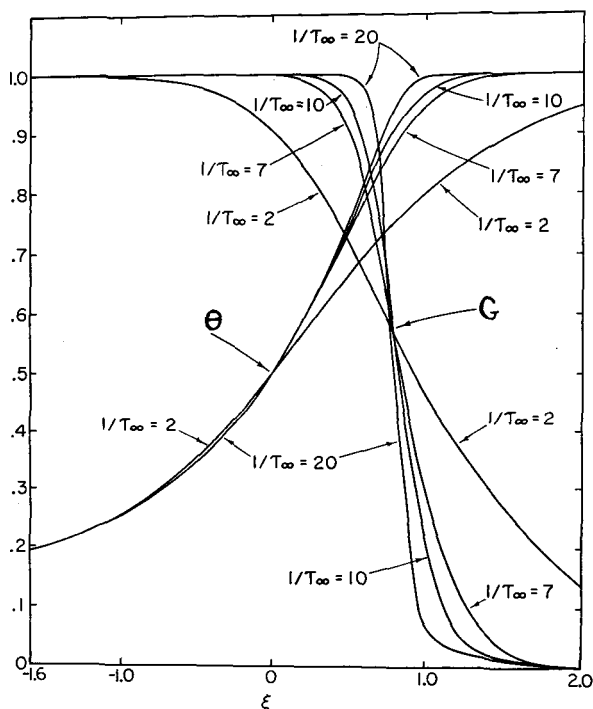


Fig. 3. The variation of θ and G with the reduced distance ξ for $\theta_0 = 0.1$ and various values of $1/\tau_\infty$.

in θ is independent of $1/\tau_\infty$ except at the highest temperatures.

Let us now consider the effect of heat transfer to the flame-holder. It can be shown that $(-q_0)$ must lie between a minimum and a maximum value. From Eqs. (50) and (53), it follows directly that

$$\theta_0 = [1 + (d\theta/d\xi)_0][(\varepsilon - 1)G_0 + 1]^{-1} \quad (93)$$

Then from Eq. (55), we find that the heat transfer may be written in the form

$$-q_0 = [\rho_0 \hat{Q} v_0 / (\varepsilon - 1)][(\varepsilon - 1)G_0 + 1](d\theta/d\xi)_0 [1 + (d\theta/d\xi)_0]^{-1} \quad (94)$$

The existence of minimum heat transfer follows from the existence of a minimum value of the initial slope, $(d\theta/d\xi)_0$. From the rate equation, Eq. (51), we find that, for $G_0 = 1$,

$$(d\theta/d\xi)_0 = (dG/d\xi)_0 / (dG/d\theta)_0 = -R_0 / (dG/d\theta)_0 \quad (95)$$

It can be shown by simple arguments that along a solution curve

$$-(\varepsilon - 1)\theta_0]^{-1} < (dG/d\theta)_0 \quad (96)$$

Thus

$$(d\theta/d\xi)_0 > (\varepsilon - 1)\theta_0 R_0 \quad (97)$$

Then, since R_0 is small but non-zero, the minimum value of the heat transfer, $-q_0$, must be finite.

Solutions of the flame equations exist for all values of the initial slope $(d\theta/d\xi)_0$ greater than the minimum value given by Eq. (97). From several approximate solutions of the flame equations, it is found that v_0 varies approximately as $\exp(-1/2\tau_\infty)$ or $\exp[-\theta_0(E^\ddagger/2RT_0)]$. This variation of v_0 with θ_0 , along with Eqs. (93) and (94), would then lead to a maximum value of $(-q_0)$ when

$$\theta_0 = \{1 + [1 + 8\theta_0 \tau_\infty (1 + (\varepsilon - 1)G_0)]^{\frac{1}{2}}\} / 2[1 + (\varepsilon - 1)G_0] \quad (98)$$

Actual numerical calculations lead to a maximum close to this point.

When the heat transfer is less than the maximum, there are two possible modes of steady state flame propagation—one corresponds to a low value of the flame velocity and the other to a high value. Spalding²² has studied these modes experimentally and discussed them from a quasi-theoretical point of view.

Apparently the low flame velocity mode is unstable while the high velocity mode is stable. A complete transient analysis is necessary to prove this and no such analysis has been made. However, from an intuitive standpoint, this is reasonable. Suppose that the flame were blown so as to increase the quenching distance and hence decrease the heat transfer to the flameholder. For the low velocity unstable mode, this would decrease the flame velocity and hence further increase the quenching distance. Thus flame would blow off. However, in the stable high velocity mode, the decrease in the heat transfer would increase the flame velocity tending to restore the normal quenching distance.

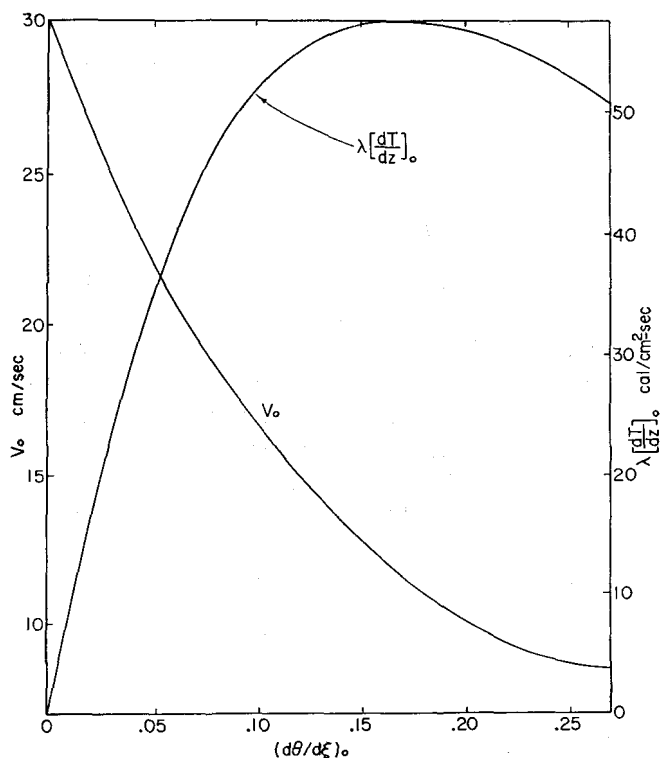


Fig. 4. The flame velocity, v_0 , and the heat transfer to the flameholder $-q_0 = \lambda_0(dT/dz)_0$ plotted as a function of $(d\theta/d\xi)_0$. Note the maximum value of the heat transfer.

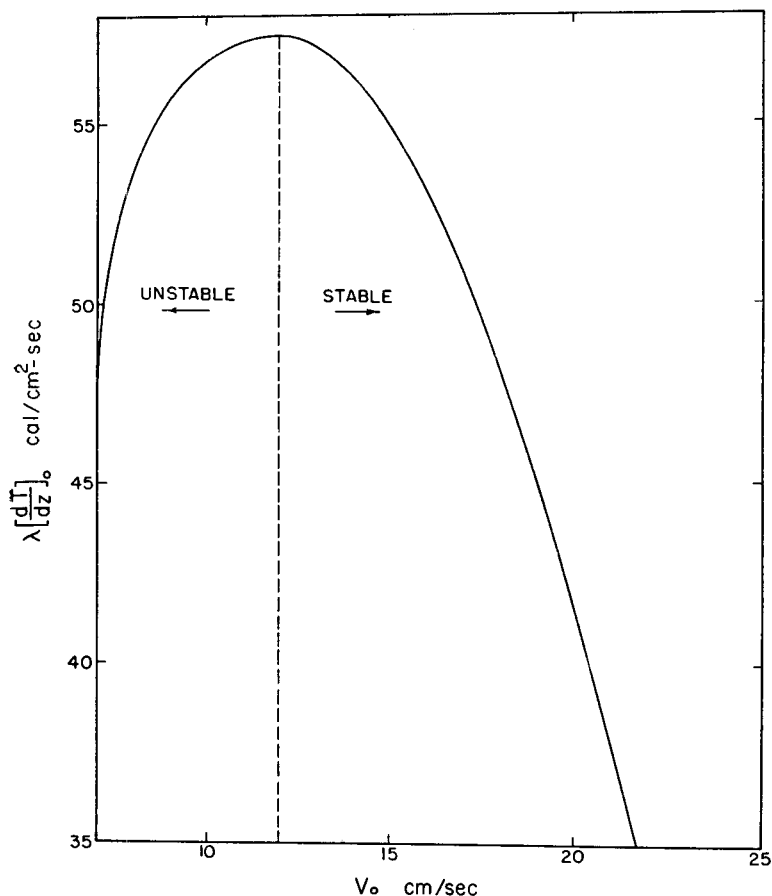


Fig. 5. The heat transfer to the flameholder, $-q_0 = \lambda_0(dT/dz)_0$ versus the flame velocity, v_0 . Note the minimum value of $v_0 = 12$ cm/sec for stable flame propagation.

Figures 4 and 5 show the numerical results which are obtained for an example in which it is assumed that: $\delta = 1$, $T_0 = 300^\circ K$, $Q = 25000$ cal/mole, $C_p = 10$ cal/mole, $\rho_0 = 0.00122$ gm/cm³, $\lambda_0 = 6 \times 10^{-5}$ cal/cm/sec/deg, $\varepsilon = 28/3$, $E^\ddagger = 37000$ cal/mole, and $k' = 3.12 \times 10^9$ sec⁻¹. Figure 4 is obtained directly by assuming specific values of $(d\theta/d\xi)_0$, using Eq. (93) to obtain θ_0

and solving the resulting flame equations to obtain v_0 , and then using Eq. (94) to obtain the heat transfer to the flameholder. This process is then repeated for a number of different values of $(d\theta/d\xi)_0$ to obtain the curves for v_0 and $(-q_0)$ as functions of $(d\theta/d\xi)_0$. Figure 5 is then the result of cross-plotting the two curves in Fig. 4.

The ignition temperature model leads to no minimum value of the heat transfer to the flameholder. However, the ignition temperature model does lead to a maximum value of the heat transfer, together with the same double valued nature of the solutions.

D. The Effect of the Kinetic Energy Terms

The flame velocity, for flames supported by a unimolecular reaction, varies inversely as the square root of the ambient pressure. Thus, the lower the pressure, the greater the burning rate. At extremely low pressure, the flame velocity becomes so large that the kinetic energy of the gases must be considered. This leads to a lowest ambient pressure, p_m , which will support steady state flame propagation.^{11,9} At this lowest pressure, the velocity of the hot burned gas has a Mach number of unity. However, this lowest ambient pressure is so very small that the rate of any normally unimolecular chemical reaction would depend upon the frequency of bimolecular collisions. Thus, from a chemical kinetics standpoint, the discussion of flames with appreciable kinetic energy is academic. The most surprising feature of these calculations is the small range in ambient pressure over which the kinetic energy is important, i.e., between p_m and $2p_m$. Apparently kinetic energy is negligible if the flame velocity is less than $0.1 c_0$.

The kinetic energy terms appear in the energy balance equation and the equation of motion. At sufficiently low ambient pressures their effects become important and the entire structure of the flame zone depends on the ambient pressure. Under these conditions, the pressure drop through the flame front is also significant. Two sets of detailed calculations have been carried out. One set of calculations⁴ is based on the ignition temperature model, the simple unimolecular reaction $A \rightarrow B$, and $\delta = 1$.

The other set of calculations¹² is based on an Arrhenius expression for the reaction rate and the reversible unimolecular reaction $A \rightleftharpoons B$, but neglects diffusion (i.e. $\delta = 0$). The results of the ignition temperature model calculations are given in Table II. The value of p_m is simply p_0 when $\kappa^2 = 1.0000$. It is

TABLE II. Effect of Kinetic Energy Terms,^{7,9} Ignition Temperature Model

$\kappa^2 =$ $(v_\infty/c_\infty)^2$	$\theta_0 =$ T_0/T_∞	p_0/p_∞	v_0/c_0	$\frac{p_0 \bar{C}_p \gamma}{\lambda_0 [k(T_\infty)]_{\text{ig}}}$	$R_\infty^{(\text{ig})}$
$\varepsilon = 7, \gamma = 1.25, \theta_i = 0.6$					
0.0000	0.1429	1.0000	0.0000	∞	2.449
0.5000	0.1517	1.5850	0.1761	15.94	2.024
1.0000	0.1606	2.1570	0.1856	17.83	1.627
$\varepsilon = 12.2, \gamma = 1.25, \theta_i = 0.6$					
0.0000	0.08197	1.0000	0.0000	∞	2.972
0.5000	0.08708	1.5908	0.1312	23.51	2.473
1.0000	0.09220	2.1976	0.1382	26.09	2.007

seen that R_∞ decreases as the ambient pressure decreases and the Mach number κ of the hot gases increases. The results of the calculations based on the Arrhenius kinetics are given in Table III. In this case R_∞ passes through a slight maximum and again decreases as κ approaches unity.

TABLE III. Effect of Kinetic Energy Terms, Arrhenius Model, when $\varepsilon = 10$, $Q/E^\ddagger = 1.0848$, $\theta_0 \tau_\infty = 0.02$, $\gamma = 1.2$, and $\delta = 0$

$\kappa^2 =$ $(v_\infty/c_\infty)^2$	$\theta_0 =$ T_0/T_∞	p_0/p_∞	v_0/c_0	$p_0 \frac{\bar{C}_p \gamma}{k' \lambda}$	R_∞
0.0000	0.10000	1.0000	0.0000	∞	4.528
0.2778	0.10270	1.3064	0.1293	0.07429	4.740
0.8230	0.10803	1.9295	0.1545	0.03969	4.757
1.0000	0.10977	2.1349	0.1552	0.03846	4.466

E. Approximate Solutions⁹

Several approximate solutions of the flame equations have been suggested. The simplest approximate solution is based on the ignition temperature model. The Corner³ approximation has been used for some time but it leads to flame velocities which are too small by a factor which may be as large as 1.5. The Adams^{4,8} and Wilde²⁵ approximations are much better. A recent approximation introduced by Hirschfelder⁹ gives the flame velocity within a few percent and gives an excellent approximation to the variation of the flame variables with temperature and distance.

(1) Ignition Temperature Approximation

The ignition temperature model may be used as the basis of an approximate solution of the problem involving Arrhenius kinetics. The approximation is based on an estimate of θ_i and the relation of the $R_{\infty}^{(ig)}$ of the ignition temperature model to the R_{∞} of the Arrhenius model. It is to be expected that the constant reaction rate of the ignition temperature model should be the Arrhenius rate at some average temperature, T_{av} , somewhat less than the temperature at the hot boundary, i.e., (see Eq. (82))

$$R_{\infty}^{(ig)} = R_{\infty} \exp [-(1 - \theta_{av})/\tau_{\infty} \theta_{av}] \quad (99)$$

The parameter θ_i may be chosen so that the reaction thickness ξ_G is the same when calculated by the two methods. The parameter θ_{av} is then chosen so that $R_{(ig)}^{\infty}$ and R_{∞} are related in accordance with Eq. (99). The approximate agreement between the two values of the temperature thickness, ξ_{θ} , as calculated by the two methods, is then a measure of the accuracy of the spatial relations given by the ignition temperature model as an approximation to the Arrhenius model.

Values of θ_i and θ_{av} obtained in this manner are given in Table IV for a range of values of the other parameters. In this table, the values of the temperature thickness ξ_{θ} calculated by the two methods are compared. The agreement of these numbers within a few percent is an indication that the ignition temperature approximation is very good for reproducing many of the characteristic features of flame propagation.

TABLE IV. The Ignition Temperature Model as an Approximation to the Arrhenius Kinetics for Flames with $\delta = 1$

$1/\tau_\infty$	ε	ξ_G	$R_\infty^{(ig)}$	θ_i	θ_{av}	$\xi_\theta^{(ig)}$	ξ_θ
2	12.3046	2.1553	2.05875	0.54506	0.77802	2.97912	3.0214
2	10.5864	2.2297	1.95652	0.54391	0.77737	3.03040	3.0486
2	7.2605	2.5248	1.62761	0.53896	0.77445	3.23540	3.1755
3	11.4103	1.5435	3.45004	0.62355	0.81688	2.58666	2.6230
3	9.7304	1.5936	3.27975	0.62282	0.81647	2.61692	2.6274
4	11.0302	1.2122	5.09825	0.67669	0.84355	2.39951	2.4395
4	9.3466	1.2500	4.84733	0.67618	0.84325	2.41974	2.4333
5	10.8530	1.0021	7.00057	0.71565	0.86308	2.29411	2.3378
5	9.1482	1.0325	6.65721	0.71527	0.86286	2.30857	2.3260
7	10.7457	0.7463	11.61295	0.77006	0.89049	2.18499	2.2342
7	8.9839	0.7680	11.04598	0.76983	0.89034	2.19324	2.2163
7	5.7787	0.8520	9.23026	0.76886	0.88975	2.22528	2.1555
10	10.8189	0.5406	20.58135	0.82078	0.91588	2.11872	2.1702
10	8.9589	0.5558	19.58078	0.82064	0.91579	2.12275	2.1485
10	5.6702	0.6142	16.37584	0.82007	0.91542	2.13485	2.0722
15	11.1370	0.3700	41.21401	0.86883	0.93967	2.08538	2.1350
15	9.1033	0.3800	39.21758	0.86875	0.93961	2.08662	2.1107
20	11.5446	0.2809	69.02876	0.89648	0.95311	2.07945	2.1253
20	9.3300	0.2883	65.69784	0.89644	0.95308	2.07957	2.1000
20	5.6605	0.3168	55.04385	0.89625	0.95296	2.08005	2.0095

(2) Corner Approximation

The Corner³ approximation is one of the earliest of the approximate solutions of the flame equations. To illustrate the nature of this approximation we consider here only the special case of $\delta = 1$.

According to Eqs. (82) and (85), G as a function θ is the solution of

$$dG/d\theta = -\{(1-\theta)R_\infty/a[aG-1+\theta]\} \exp[-(1-\theta)/\tau_\infty\theta] \quad (100)$$

Also, from Eqs. (90) and (91), we find that the limiting slope of

the solution at the hot boundary is

$$(dG/d\theta)_\infty = -b/a \quad (101)$$

where

$$b = (1/2) + (1/2)[1 + 4R_\infty]^\dagger \quad (102)$$

The Corner approximation consists simply of replacing G in the denominator on the right of Eq. (100) by the high temperature limiting form

$$G = -(1 - \theta)(dG/d\theta)_\infty = (1 - \theta)b/a \quad (103)$$

The approximation to Eq. (100) is then

$$\begin{aligned} dG/d\theta &= -[R_\infty/a(b - 1)] \exp [-(1 - \theta)/\tau_\infty \theta] \\ &= -(b/a) \exp (\tau_\infty^{-1}) \exp [(\tau_\infty \theta)^{-1}] \end{aligned} \quad (104)$$

This equation may be integrated directly to give

$$G = (b/a) (1 - \varphi_\infty) - (b\theta/a) (1 - \varphi) \exp [-(1 - \theta)/\tau_\infty \theta] \quad (105)$$

where

$$\varphi = -(\theta\tau_\infty)^{-1} \exp [(\theta\tau_\infty)^{-1}] E_i [-(\theta\tau_\infty)^{-1}] \quad (106)$$

and φ_∞ is the value of φ when $\theta = 1$. The function $E_i(x)$ is the usual exponential integral.

For reasonable values of τ_∞ , the second term on the right of Eq. (105) is negligible for values of θ appreciably less than unity. Thus, by setting the limiting form (for $\theta \rightarrow 0$) of the expression on the right of Eq. (105) equal to $G_0 = 1$,

$$(b/a)(1 - \varphi_\infty) = 1 \quad (107)$$

An approximation to R_∞ is then obtained by using Eq. (107) and Eq. (102) to give

$$R_\infty = a(a - 1 + \varphi_\infty)(1 - \varphi_\infty)^{-2} \quad (108)$$

Values of R_∞ calculated by the Corner approximation for $a = 0.9$ and a range of values of τ_∞ , along with values obtained by numerical integration of the exact equation, are given in Table V. The approximate values of R_∞ are too large by a factor of about 2.1.

TABLE V. Values of $(R_\infty)_c$ Computed by the Corner Approximation Compared with Values of R_∞ Computed by Numerical Integration of the Flame Equations, with $a = 0.9$

$1/\tau_\infty$	$(R_\infty)_c$	R_∞	$(R_\infty)_c/R_\infty$
2	7.28546	3.398	2.144
3	13.51819	6.496	2.081
4	21.41093	10.41	2.057
5	30.94937	15.13	2.045
7	54.93499	26.96	2.037
10	103.13253	50.59	2.039
15	215.95115	104.9	2.058
20	369.32217	178.9	2.064

(3) Adams and Wilde Approximations

In the Adams^{1,8} and Wilde²⁵ approximate solutions of the flame equations, the heat transfer to the flameholder is also neglected. Thus, $a = 1 - \theta_0$, and it is convenient to define a new reduced temperature,

$$\theta' = (\theta - \theta_0)/a = (\theta - \theta_0)/(1 - \theta_0) \quad (109)$$

which takes on values between 0 and 1. In terms of θ' , the flame equation, Eq. (100), is

$$\begin{aligned} dG/d\theta' = -\{ & (1 - \theta')R_\infty/[G - (1 - \theta')] \} \\ & \times \exp[-a(1 - \theta')/\tau_\infty(1 - a + a\theta')] \end{aligned} \quad (110)$$

This equation may easily be written in the form

$$\begin{aligned} (d/d\theta') [(1/2)G^2 - (1 - \theta')G] \\ = G - (1 - \theta')R_\infty \exp[-a(1 - \theta')/\tau_\infty(1 - a + a\theta')] \end{aligned} \quad (111)$$

and formally integrated to give

$$-(1/2)G^2 + (1 - \theta')G = \int_{\theta'}^1 G d\theta' - R_\infty F(\theta') \quad (112)$$

where

$$F(\theta') = \int_{\theta'}^1 (1 - \theta') \exp[-a(1 - \theta')/\tau_\infty(1 - a + a\theta')] d\theta' \quad (113)$$

Since $G = 1$ when $\theta' = 0$, it follows from Eq. (113) that

$$R_{\infty} = [-(1/2) + \int_0^1 G d\theta'] / F(0) \quad (114)$$

Any method of estimating the two integrals which appear in this expression leads to an approximation of the eigenvalue.

Adams approximated G in the integral of Eq. (114) by

$$G = 1 - (\theta')^{b'} \quad (115)$$

where b' is a constant. Thus

$$\int_0^1 G d\theta' = b' / (b' + 1) \quad (116)$$

Furthermore, Adams approximated the exponential in the integral for $F(\theta')$, Eq. (113), by a simple power of θ' ,

$$\exp [-a(1 - \theta') / \tau_{\infty} (1 - a + a\theta')] \approx (\theta')^s \quad (117)$$

where the constant s is evaluated by the condition that the temperature derivative of the exponential be correct at the flame temperature. This condition leads to

$$s = a / \tau_{\infty} \quad (118)$$

and the approximation to $F(0)$ is

$$F(0) = (s + 1)^{-1} (s + 2)^{-1} \quad (119)$$

When the approximations for the two integrals, Eqs. (116) and (119), are used in the expression for R_{∞} , Eq. (114), one obtains

$$R_{\infty} = (1/2) (b' - 1) (s + 1) (s + 2) (b' + 1)^{-1} \quad (120)$$

Finally, Adams took $b' = s$ and obtained the approximation

$$\begin{aligned} R_{\infty} &= (1/2) (s - 1) (s + 2) \\ &= (1/2) [(a/\tau_{\infty}) - 1] [(a/\tau_{\infty}) + 2] \end{aligned} \quad (121)$$

Wilde improved on the Adams treatment by pointing out that there is no need to approximate $F(0)$ since the integral may be evaluated in terms of the exponential integral go give

$$\begin{aligned} F(0) &= [2\tau_{\infty}^2 (1 - \theta_0^2)]^{-1} \{ \tau_{\infty} (1 + \tau_{\infty}) - \tau_{\infty} \theta_0 (1 + 2\tau_{\infty} - \tau_{\infty} \theta_0) \\ &\times \exp [-(1 - \theta_0) / \tau_{\infty} \theta_0] + (1 + 2\tau_{\infty}) \exp [(\tau_{\infty} \theta_0)^{-1}] [E_i(-\tau_{\infty}^{-1}) \\ &\quad - E_i(-(\tau_{\infty} \theta_0)^{-1})] \} \end{aligned} \quad (122)$$

Because of the small reaction rate at the lower temperatures, the second and fourth terms in this expression are usually negligible. Wilde then arbitrarily took $b' = s + 1$ and obtained the approximation

$$R_{\infty} = s/[2(s + 2)F(0)] = a/[2(a + 2\tau_{\infty})F(0)] \quad (123)$$

(4) *Hirschfelder Approximations*

Hirschfelder⁹ has recently pointed out that there is also no reason to estimate b' in an arbitrary manner. The constant b' may be fixed by the condition that the approximate form of G , Eq. (115), have the correct slope at the hot boundary. From Eqs. (89) and (115), this condition leads to

$$b' = b = (1/2)[1 + (1 + 4R_{\infty})^{\frac{1}{2}}] \quad (124)$$

or

$$R_{\infty} = b(b - 1) \quad (125)$$

From the exact expression for R_{∞} , Eq. (114), and the approximation to the integral of G , Eq. (116), we find that

$$R_{\infty} = (b - 1)/[2(b + 1)F(0)] \quad (126)$$

Equating the last two expressions for R_{∞} , one obtains a quadratic equation for b . The only physically acceptable solution of this quadratic is

$$b = -(1/2) + (1/2)[1 + (2/F(0))]^{\frac{1}{2}} \quad (127)$$

Thus we obtain as an approximation to R_{∞} ,

$$R_{\infty} = [1 + (2/F(0))] - [1 + (2/F(0))]^{\frac{1}{2}} \quad (128)$$

Hirschfelder has also suggested a slightly more complex approximation in which G is approximated by the form

$$G = 1 - (\theta')^b [1 - j(1 - \theta')^2] \quad (129)$$

and the two constants b and j are fixed by the condition that this form have the correct first and second temperature derivatives at the hot boundary. This approximation leads to results which are in good agreement with the results of numerical integration.

TABLE VI. Results of the Adams, Wilde, and Hirschfelder (H1) approximations and comparison with results of numerical integration. The values of b' should compare with b_{exact}

$1/\tau_{\infty}$	ϵ	s	b_{exact}	$(R_{\infty})_{\text{exact}}$	b'_{Adams}	$(R_{\infty})_{\text{Adams}}$	b'_{Wilde}	$(R_{\infty})_{\text{Wilde}}$	b'_{H1}	$(R_{\infty})_{\text{H1}}$
2	10.5864	1.81108	2.4285	3.4693	1.81108	1.5455	2.81108	3.5629	2.2834	2.9305
3	9.7304	2.69169	3.0860	6.4372	2.69169	3.9684	3.69169	6.7185	2.9584	5.7937
4	9.3466	3.57204	3.7320	10.196	3.57204	7.1658	4.57204	10.717	3.6191	9.4788
5	9.1482	4.45345	4.3714	14.738	4.45345	11.1433	5.45345	15.543	4.2721	13.9787
7	8.9839	6.22083	5.6390	26.160	6.22083	21.4598	7.22083	27.654	5.5659	25.4133
10	8.9589	8.8838	7.5257	49.111	8.8838	42.9029	9.8838	51.951	7.4936	48.6604
15	9.1033	13.35225	10.653	102.83	13.35225	94.8174	14.35225	108.89	10.7004	103.7982
20	9.3300	17.8564	13.771	175.87	17.8564	167.3537	18.8564	186.68	13.9165	179.7525

In Table VI values of R_∞ and of the limiting slope of $G(\theta)$, as obtained by the Adams, Wilde, and first Hirschfelder approximations, are compared with the results of numerical integration for a range of values of τ_∞ . In Table VII values of $G(\theta)$ for $1/\tau_\infty = 7$ and $\theta_0 = 0.11131$, computed by the Adams, Wilde, and two Hirschfelder approximations, are compared with the results of numerical integration. For these values of the parameters, the second Hirschfelder approximation gives $b = 5.6367$ as compared to the exact $b = 5.6390$. The approximate value of R_∞ is 26.137 as compared to the exact value of 26.159.

TABLE VII. Approximate Values of G , $1/\tau_\infty = 7$ and $\theta_0 = 0.1113$

θ	G_{Adams}	G_{Wilde}	G_{H1}	G_{H2}	G_{exact}
1.00	0.0000	0.0000	0.0000	0.0000	0.0000
0.98	0.1321	0.1517	0.1191	0.1199	0.1219
0.96	0.2491	0.2829	0.2261	0.2291	0.2333
0.92	0.4439	0.4940	0.4085	0.4175	0.4259
0.88	0.5944	0.6492	0.5540	0.5693	0.5817
0.84	0.7091	0.7615	0.6687	0.6889	0.7046
0.80	0.7953	0.8413	0.7581	0.7811	0.7990
0.76	0.8589	0.8970	0.8266	0.8503	0.8689
0.72	0.9050	0.9350	0.8783	0.9010	0.9188
0.68	0.9378	0.9602	0.9166	0.9369	0.9526
0.64	0.9605	0.9765	0.9445	0.9616	0.9743
0.60	0.9758	0.9867	0.9642	0.9778	0.9872
0.56	0.9858	0.9928	0.9777	0.9880	0.9943
0.52	0.9920	0.9963	0.9867	0.9940	0.9978

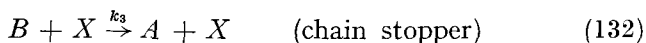
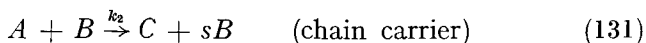
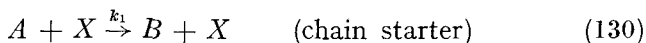
(5) The Klein Approximation

Klein¹⁷ developed an iterative procedure for determining the flame solutions accurate to within any desired precision. The Klein procedure is applicable to a wide variety of complex as well as simple flame systems. The Klein procedure corresponds to approximating R_∞ and the G on the right hand side of Eq. (112). Then Eq. (112) is used as a quadratic equation for an improved value of G at each temperature. This new approximation for G is then used in Eq. (114) to obtain an improved value for

R_∞ . The process is repeated until the desired precision is obtained. The potency of the Klein approach becomes apparent when it is applied to more complicated types of flame systems.

IV. FLAMES SUPPORTED BY COMPLEX SYSTEMS OF CHEMICAL REACTION CHAINS

The great majority of flames of practical interest involve a complicated set of reactions leading to the degradation of chemical energy.^{6,7} The outstanding feature of many of these flame systems is the presence of a reaction chain. A typical chain system contains three sorts of reactions: (1) a chain starter, (2) a chain carrier, and (3) a chain breaker. To illustrate the nature of chain reactions we might suppose that A is the fuel, C is the product, B is the free radical or chemically active species and X stands for a molecule of A , B , or C . Then a simple form of chain reaction might consist of the following reaction steps:



If s were greater than unity, the system would be termed a branched-chain. Detonations are particularly likely with branched-chain systems but steady-state flames can also occur. For illustrative simplicity we take $s = 1$ in the hypothetical example.

Flames and detonations occurring with systems involving complex sets of chemical reactions can be treated mathematically by solving the general equations of change, Eqs. (28) through (31), together with the boundary conditions in much the same manner as for the simple flame system which we considered in detail. The mathematical problem, however, is much more difficult since there is now more than one linearly independent G_i . If there are l linearly independent functions, G_i , the solution near the hot boundary has the asymptotic form:

$$T = T_\infty + \sum_{j=1}^l t_j \exp(-\alpha_j z) \quad (133)$$

$$G_i = G_{i\infty} + \sum_{j=1}^l t_j F_{ji} \exp(-\alpha_j z) \quad (134)$$

$$x_i = x_{i\infty} + \sum_{j=1}^l t_j J_{ji} \exp(-\alpha_j z) \quad (135)$$

Here all of the l roots, α_j , are positive and hence physically acceptable; the l constants, t_j , are eigenvalues to be adjusted so as to make the G_i agree with their specified values, G_{i0} , when $T = T_0$. Complex flame systems therefore lead to difficult multiple eigenvalue problems. If, however, the concentrations of the intermediate chemical species or free radicals are nearly equal to their pseudo-steady state values throughout the flame, then solutions of the flame equations can be obtained.

One would obtain the pseudo-stationary state concentrations for each of the intermediate chemical species from the thermodynamics of irreversible processes if it were supposed that the relaxation time for the production or destruction of each of these species is very small compared to the half-time for the overall chemical reaction of the fuel to go to the product molecules. In the pseudo-stationary states approximation, the net rate of formation, K_i , of each of the intermediate chemical species by chemical reactions is set equal to zero. This provides exactly the right number of simultaneous algebraic equations to express the concentration of each of the chemical intermediates in terms of powers of the concentrations of the fuel and product molecules. For example, in the hypothetical chain system given by Eqs. (130), (131), and (132), the pseudo-stationary mole fraction of B (which we shall designate as x_B^*) is the solution of the equation:

$$K_B = k_1 n^2 x_A - k_3 n^2 x_B^* = 0 \quad (136)$$

or

$$x_B^* = k_1 x_A / k_3 \quad (137)$$

Once the concentrations of the intermediates have been determined in this manner, the chemical kinetics for the overall reaction behaves like a single step chemical reaction in which the rate depends in a complex manner on the concentrations of the fuel and product molecules. For example, in our hypothetical example,

the net rate of production of the product molecules is

$$K_C = k_2 n^2 x_A x_B^* - k'_2 n^2 x_C x_B^* \quad (138)$$

The simplest approximation for treating a complex flame system corresponds to assuming the pseudo-stationary state concentration for each of the chemical intermediates in the expressions for the net rate of production of the fuel and product molecules, and setting the mole fractions and fractions of the mass rate of flow for each of these intermediates equal to zero in the diffusion, energy balance, and motion equations. The resulting equations correspond to a simple one step chemical reaction system with only a single linearly independent G_i , and the solution of these equations presents no difficult mathematical problems.

The qualitative nature of the departure from the pseudo-stationary state can be explained on the basis of very simple considerations.⁷ Let us treat our hypothetical chain system and simplify the multi-component diffusion equations by assuming that the free radical B diffuses through the mixture of other components (regarded as a single species) with an effective binary diffusion coefficient, \mathcal{D} . Then, combining the equation of continuity with the equation for diffusion of the free radical,

$$K_B = (M/m_B)(dx_B/dz) - (d/dz)(n\mathcal{D} dx_B/dz) \quad (139)$$

where

$$K_B = n^2[k_1 x_A - k_3 x_B] \quad (140)$$

If we ignore the small variations in $n\mathcal{D}$ and assume that x_B^* is almost equal to x_B , then Eq. (139) becomes

$$K_B = (M/m_B)(dx_B^*/dz) - n\mathcal{D}(d^2 x_B^*/dz^2) \quad (141)$$

If the right-hand side of Eq. (141) were zero, the concentration of B would agree with the pseudo-stationary state approximation. The two terms on the right-hand side of Eq. (141) would correspond to the two causes for deviations. The first term, $(M/m_B)(dx_B^*/dz)$, results from the mass flow of the gases or the fact that a molecule of B is born at one point and dies at another. The second term,

$-n\mathcal{D}(d^2x_B^*/dz^2)$, corresponds to the concentration profile of B being altered by virtue of diffusion.

Figure 6 shows a typical plot of x_B^* and x_B versus distance in

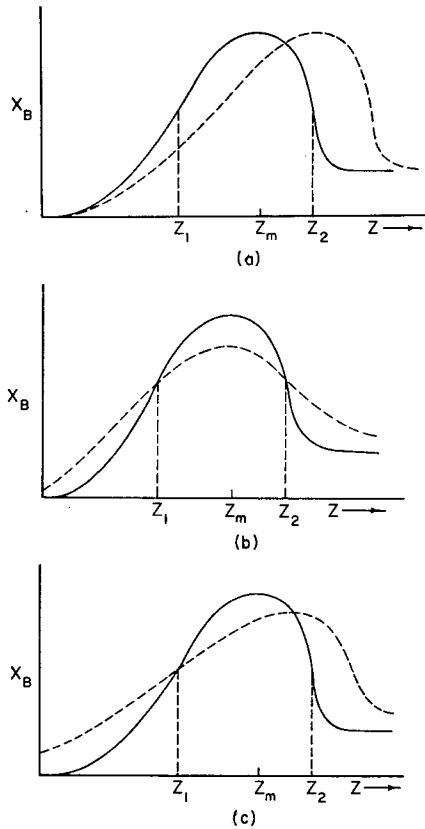


Fig. 6. The solid curves are x_B^* , and the dotted curves are (a) x_B^* corrected for the effect of mass flow; (b) x_B^* corrected for diffusion; and (c) x_B^* corrected for both mass flow and diffusion.

the flame zone. The value of x_B^* reaches a maximum for $z = z_m$. Between z_1 and z_2 , the curvature of x_B^* is negative, so that $d^2x_B^*/dz^2 < 0$. For z less than z_1 or greater than z_2 , the curvature is positive. The effect of mass flow is to shift the concentration curve towards the right without appreciably changing the height of the maximum. The effect of diffusion is to lower the con-

centration in the region between z_1 and z_2 and to increase it elsewhere. Between z_m and $z = \infty$ the diffusion velocity of the free radical is directed *away from* the flameholder; whereas, between $z = 0$ and z_m the diffusion velocity of the free radical is directed *towards* the flameholder. In most practical flames the largest fraction of the chemical changes take place between z_m and $z = \infty$. This argument tends to disprove the purely diffusional theories of flame propagation, such as that of Tanford and Pease,²³ which assume that for *all temperatures* or *all distances* the net flow of the free radicals is *towards* the flameholder.

In case the deviations of the free radical concentration from the pseudo-stationary state approximation are small, the flame equations can be solved by an iterative procedure in which the first approximation corresponds to setting $K_B = 0$ and determining the x_B^* . Then the second approximation corresponds to resolving the flame relations using Eq. (141) as an algebraic equation. Unfortunately, such an iterative procedure is only asymptotically convergent. It is excellent when the deviations from the pseudo-stationary state are small, but it fails completely to provide a solution when the deviations are large. Fortunately, most practical flame systems probably have small deviations. However, for the hydrogen-bromine flame the deviations are quite large.

The calculations of Klein,¹⁶ and Campbell, Hirschfelder, and Schalit² on the *ABC* flame provide an excellent example of the deviations from the pseudo-steady state. The reaction scheme for the *ABC* flame is that given in our hypothetical example, Eqs. (130), (131), and (132). To simplify the calculations the specific heats at constant pressure of *A*, *B*, and *C* are taken equal to $5R$ (where R is the gas constant); the three binary diffusion coefficients, \mathcal{D}_{ab} , \mathcal{D}_{bc} , and \mathcal{D}_{ac} are taken to be equal and have values such that the corresponding Lewis numbers δ_{ab} , δ_{bc} , δ_{ac} are each equal to unity. The rate constants are taken to be

$$\begin{aligned} k_3 &= 10^{13} \text{ cm}^3 \text{ mole}^{-1} \text{ sec}^{-1} \\ k_1 &= k_3 \exp(-15000/T) \\ k_2 &= \omega k_3 \\ k'_2 &= \omega k_1 \end{aligned}$$

Here ω is a parameter which is of considerable interest. When ω is small, the pseudo-stationary state is an excellent approximation. However, when ω becomes as large as 100 or 1000, the flame behaves quite differently from pseudo-stationary state expectations. It is easy to see that the variation of ω should have this effect. The characteristic time, t_A , for the duration of the over-all reaction can be defined as

$$t_A = -nx_A/K_A^* \quad (142)$$

where K_A^* is the net rate of formation of A when the free radicals are maintained in their pseudo-stationary state concentration. Neglecting the small effect of the back-reaction,

$$t_A = [k_2nx_B^*]^{-1} = [\omega k_3nx_B^*]^{-1} \quad (143)$$

TABLE VIII. Deviations from the Pseudo-Stationary State, $(x_B - x_B^*)/x_B^*$, as a Function of ω for the ABC Flame

T	$\omega = 1$	$\omega = 10$	$\omega = 100$	$\omega = 1000$
3270	0	0	0	0
3210	0.0002	0.0015	0.0159	0.2680
3150	0.0002	0.0022	0.0225	0.0453
3000	0.0001	0.0009	0.0006	-2.0650
2850	-0.0003	-0.0031	-0.0319	8.4480
2700	-0.0008	-0.0075	-0.0475	19.8620
2550	-0.0011	-0.0104	-0.0868	-24.1450
2400	-0.0011	-0.0106	-0.1248	-77.6870
2250	-0.0007	-0.0071	-0.0874	-55.1470
2100	0.0001	0.0008	0.0177	44.1510
1950	0.0015	0.0133	0.1792	181.9800
1800	0.0033	0.0306	0.2878	189.5900
1650	0.0055	0.0527	0.3223	-20.5970
1500	0.0080	0.0799	0.4372	-347.2700
1350	0.0109	0.1127	0.9152	-553.7200
1200	0.0143	0.1532	2.1490	-340.2300
1050	0.0182	0.2062	4.9721	858.0400
900	0.0230	0.2834	12.6580	5577.6000
600	0.0610	3.5800	1223.8000	1022000.
300	∞	∞	∞	∞

But the relaxation time for the destruction of B is

$$t_B = [nk_3]^{-1} \quad (144)$$

The ratio of these times is

$$t_B/t_A = \omega x_B^* \quad (145)$$

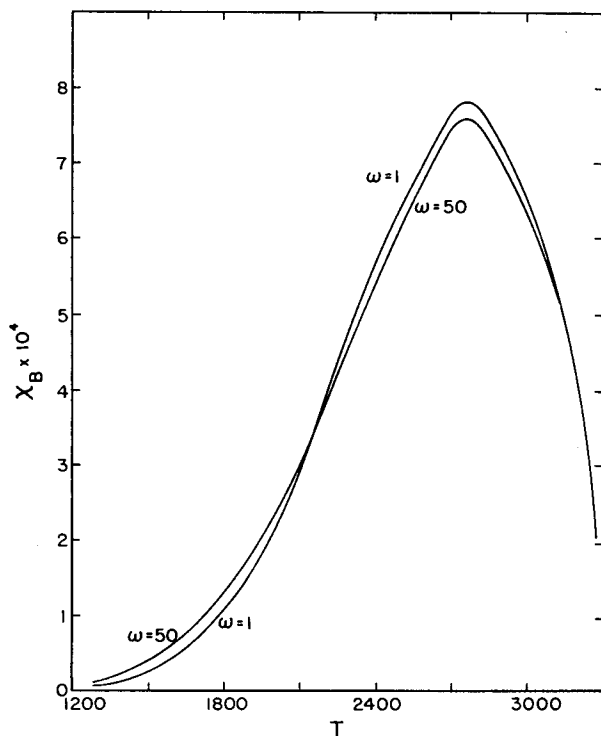


Fig. 7. Variation of x_B with ω in the ABC flame.

Since the maximum value of x_B^* is 0.00076, the ratio t_B/t_A is small compared to unity if ω is 1, 10, or even 100. However, if $\omega = 1000$ this ratio can exceed unity. Thus, the ratio of the relaxation time for the destruction of the free radicals to the characteristic time for the over-all reaction provides a good indication for the magnitude of the deviations from the pseudo-stationary state. Table VIII gives the ratio $(x_B - x_B^*)/x_B^*$

computed for different values of ω . At very low temperatures this ratio becomes large for even small values of ω . However, at such temperatures, the value of x_B^* is negligibly small.

Figure 7 shows how slight are the deviations of x_B from the

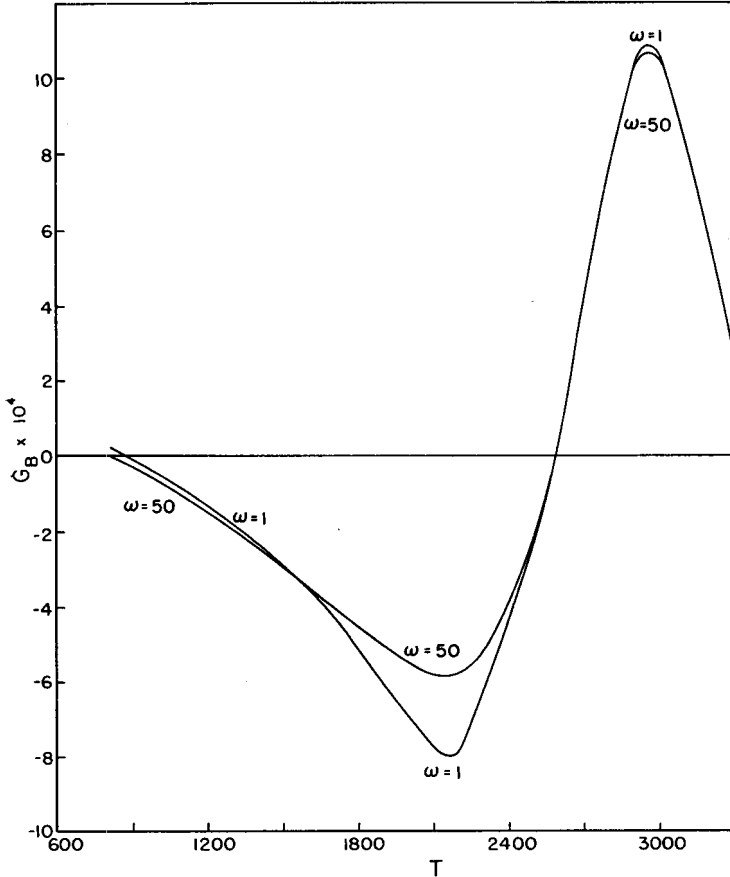


Fig. 8. Variation of G_B with ω in the *ABC* flame.

pseudo-stationary state even for $\omega = 50$. Figure 8 shows the variation of G_B with ω . Note that for $T > 2700^\circ\text{K}$, the value of G_B is positive indicating that the flux of *B* is *away* from the flameholder. For lower temperature G_B is negative corresponding to the flow of *B towards* the flameholder. Purely diffusional

theories of flame propagation lack the important region where G_B is positive.

V. SINGLE STEP, UNIMOLECULAR REACTION DETONATION^{10, 4}

A detonation is a wave in which an exothermal chemical reaction takes place and which moves with supersonic velocity with respect to the undetonated gas. This is in contrast to a flame, which moves with subsonic velocity. Flames and detonations are associated with qualitatively distinct types of solutions of the same set of hydrodynamic equations and boundary conditions.

In the theory of von Neumann,²⁰ Döring,⁵ and Zeldovitch,²⁷ the assumption is made that a detonation wave is a flame preceded by a shock-wave. The shock zone and the reaction zone are then considered separately. For a long time it had been known that the velocity of a steady-state plane detonation wave could be calculated from considerations of the conservation of mass, momentum, and energy across the detonation front and by assuming the Chapman-Jouguet condition that the velocity of the hot detonated gas is the velocity of sound. On the basis of their model, von Neumann, Döring, and Zeldovitch independently justified the Chapman-Jouguet condition on the basis of stability arguments. In these treatments it was shown that with the shock wave preceding the reaction zone, the Mach number of the detonated gases is necessarily less than unity and must approach unity under the influence of perturbations. However, they were not able to prove that detonation solutions cannot occur in which the detonated gases have Mach number greater than unity and the shock wave coalesces with, rather than precedes, the reaction zone.

There has been considerable question regarding the importance of transport phenomena in detonations. We have found that the transport phenomena lead to coupling between the shock and reaction zones and that any degree of coupling may occur in one-dimensional steady-state detonations in a simple gaseous system involving a simple unimolecular exothermic chemical reaction. In general, the coupling between the two zones becomes smaller as the ambient pressure becomes larger.

The boundary conditions which describe a steady state plane detonation wave in a coordinate system fixed with respect to the wave are illustrated in Fig. 9. The undetonated cold gas moves in the positive z direction with the velocity v_0 and the detonated hot gases move with the velocity v_∞ . Clearly, v_0 is the velocity with which the detonation wave would move into stationary undetonated cold gas.

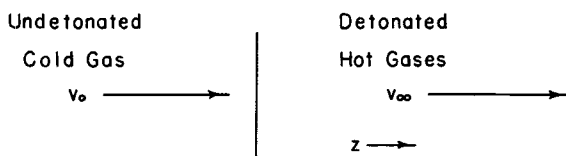


Fig. 9. Detonation in moving coordinate system.

Whereas bunsen burners provide a close approximation to our mathematical model of a steady-state flame system, there does not seem to be any practical way of realizing a true steady-state detonation. The practical ways of producing plane wave detonations may be idealized as initiation either at a fixed wall or at a free surface. In addition, after a sufficiently long time, the diverging spherical detonation waves of a homogeneous explosive, initiated at a point, approximate plane waves. In all three of these practical systems, the boundary conditions are quite different from those discussed above. However, G. I. Taylor* has shown that (after a long time) if the Mach number immediately behind the detonation wave is equal to or greater than unity, the gas flow behind the detonation wave is the same as for the true steady state. Thus, for a Mach number greater than or equal to unity, we might, in principle, compare our theoretical steady-state results with experimental detonations produced by initiation at a point, at a fixed wall, or at a free

* Reference 24. Taylor did not consider a detonation initiated at a free surface, but it is easy to show that the conditions immediately behind the detonation front must be the same for the free surface as for the fixed wall initiation. One of the authors (J. O. H.) recalls a proof of R. E. Peierls to this effect.

surface. However, we know of no way of comparing with experimental data the theoretical and steady-state solutions which we generate for Mach number less than unity.

Let us now examine the gross hydrodynamic behavior of a gas in the region behind a detonation wave initiated at a fixed wall. It is assumed that, except in the neighborhood of the detonation front, the velocity and temperature gradients are sufficiently small so that the method of Riemann characteristics may be used to solve the hydrodynamic equations, (MTGL, reference 9, p. 736). In order to study this gross behavior, the detonation front is idealized as a line of discontinuity in the space-time plane.

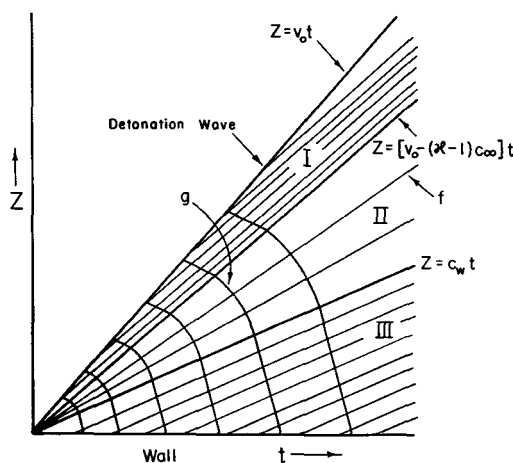


Fig. 10. Detonation initiated from a fixed wall, $\kappa > 1$.

The solution is illustrated in Fig. 10 in which the time, t , is the abscissa and the distance from the fixed wall, Z , is the ordinate. Along the fixed wall, $Z = 0$, the particle velocity, V , is zero. It is assumed that the detonation front moves with the constant velocity v_0 , and that the gases behind the front move away from the front with the constant velocity

$$v_\infty = \kappa c_\infty \quad (146)$$

where

$$c_\infty = (\gamma p_\infty / \rho_\infty)^{\frac{1}{2}} \quad (147)$$

is the velocity of sound and κ is the Mach number of the hot gases immediately behind the detonation front relative to the front. In the fixed wall coordinate system, this particle velocity is then $V_D = v_0 - v_\infty$. The subscript D or ∞ is used to designate conditions immediately after the detonation wave has passed, and W to designate the conditions at the fixed wall.

The method of Riemann characteristics states that the characteristic $f = V + \sigma$ remains unchanged in the neighborhood of a point moving with the velocity $V + c$, and the characteristic $g = V - \sigma$ remains unchanged in the neighborhood of a point moving with the velocity $V - c$. In these expressions, σ is the Riemann characteristic which, for a perfect gas having a specific heat ratio of γ and velocity of sound c , is

$$\sigma = 2c/(\gamma - 1) \quad (148)$$

The lines of constant g are curves, originating at the detonation front and extending to the fixed wall. Thus, since the conditions behind the detonation are constant, the value of g is everywhere constant and equal to its value at either the front or the fixed wall, i.e.,

$$g = g_D = V_D - \sigma_D = -\sigma_W = v_0 - [\kappa + (2/(\gamma - 1))]c_\infty \quad (149)$$

The other set of characteristics, $f = V + \sigma$, also emanate from the detonation front. Since these characteristics always have the slope $V + c$, in the neighborhood of the front, their slope is

$$dZ/dt = v_0 + (1 - \kappa)c_\infty \quad (150)$$

Since the g characteristics are everywhere constant, the f characteristics are necessarily straight lines. If κ is less than unity, we have an impossible situation. For κ less than unity, all of the f characteristics would extend from the detonation front to the fixed wall and all of the gas properties would be constant in the whole region between the front and the wall. This is clearly impossible since the particle velocity behind the front, V_D , is not zero as it is at the wall. Thus, for a detonation initiated at a fixed wall, the Mach number, κ , must be equal to or greater than unity.

For a detonation initiated at a fixed wall, if κ is greater than unity, we have the situation illustrated in Fig. 10. There are

three regions. In region I, bounded by the lines $Z = v_0 t$ and $Z = [v_0 - (\kappa - 1)c_\infty]t$, the f characteristics originate at the front and therefore f is constant throughout this region. Thus all of the gas properties, such as temperature and particle velocity, are the same as immediately behind the front.

In region II, bounded by the lines $Z = [v_0 - (\kappa - 1)c_\infty]t$ and $Z = c_W t$, the f characteristics originate at the origin and a Prandtl-Meyer expansion takes place. In this region the f characteristics have the slope

$$[(3 - \gamma)g_D + (\gamma + 1)f]/4$$

so that

$$f = [4/(\gamma + 1)] Z/t - [(3 - \gamma)/(\gamma + 1)]g_D \quad (151)$$

and since $c = (\gamma - 1)(f - g_D)/4$ and $V = (g_D + f)/2$ it follows that

$$c = [(\gamma - 1)/(\gamma + 1)] (Z/t - g_D) \quad (152)$$

$$V = [2/(\gamma + 1)] Z/t + [(\gamma - 1)/(\gamma + 1)]g_D \quad (153)$$

Since the gas flow is adiabatic between the detonation front and the wall, the density, pressure, and temperature at any point are given by the relations

$$\rho = \rho_\infty (c/c_\infty)^{2/(\gamma-1)} \quad (154)$$

$$p = p_\infty (c/c_\infty)^{2\gamma/(\gamma-1)} \quad (155)$$

$$T = T_\infty (c/c_\infty)^2 \quad (156)$$

In region III, the f characteristics originate at the fixed wall and have the value $f = \sigma_W$. Since both f and g are constant throughout this region, all of the gas properties are constant and equal to their values at the wall. Thus the particle velocity is zero and the velocity of sound is

$$c_W = \{1 - \kappa [\frac{1}{2}(\gamma - 1)] (v_0/v_\infty - 1)\} c_\infty \quad (157)$$

For a detonation initiated at a fixed wall, the Chapman-Jouguet condition of κ equal unity represents a limiting case of κ greater than unity. In this limit, the detonation front itself is an f characteristic and region I disappears.

The conditions behind a detonation initiated at a free surface are similar to those behind a detonation initiated at a fixed wall. This is illustrated in Fig. 11. Here the Prandtl-Meyer region II extends up to the free surface which itself is an f characteristic. At the free surface, it is supposed that the temperature is zero so that both c and σ are zero. The particle velocity, the value of the f characteristic,

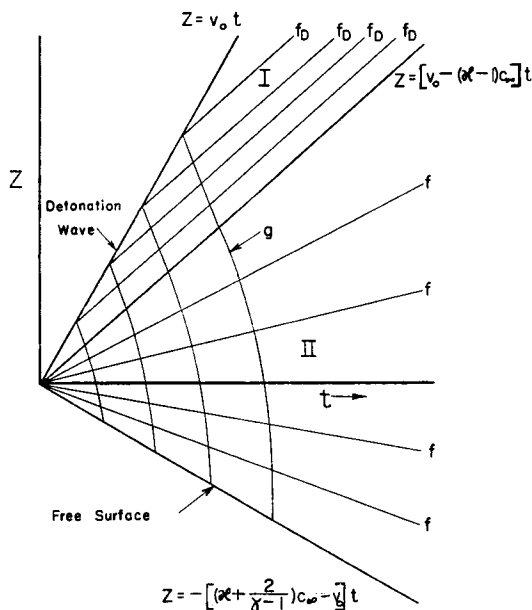


Fig. 11. Detonation initiated at a free surface, $\kappa > 1$.

and the velocity of the free surface are all equal to g_D . The impossibility of κ less than unity can be shown in the same manner as for the detonation initiated at a fixed wall.

Thus from these macroscopic considerations, we find that in a detonation initiated at a wall or a free surface $\kappa \geq 1$. It is shown below from detailed considerations of the structure of the detonation wave that a steady state solution of the equations exists only if $\kappa \leq 1$. We are thus lead to the Chapman-Jouguet condition that in a free detonation $\kappa = 1$. In principle, however, other steady state detonations are possible. These are "piston

driven" detonations in which the steady state is maintained by introducing cold gas at the velocity v_0 . It is the structure of such detonations which is considered in detail in the following discussion.

A. The Detonation Equations

Let us consider the application of the hydrodynamic equations of section II to a simple detonation system. As in the discussion of a simple flame, we consider a detonation supported by a single step unimolecular reaction,



As discussed earlier, the same equations and boundary conditions describe the structure of both flames and detonations. Unlike a flame, however, the pressure change through a detonation is generally large, and it is not possible to neglect the equation of motion.

The detonation equations may be written in terms of dimensionless variables and groups in a manner quite similar to that used in the treatment of the flame equations. It is convenient to introduce a dimensionless velocity variable

$$u = v/v_\infty \quad (158)$$

and a modified Prandtl number

$$P'_r = (\eta + \frac{3}{4}\kappa') \hat{C}_p / \lambda \quad (159)$$

Here, of course, κ' is the coefficient of bulk viscosity not to be confused with κ , the Mach number of the gas at the hot boundary. In terms of these dimensionless quantities and those defined in section III, the detonation equations are quite similar to the flame equations, Eqs. (51) to (54):

1. The equation of continuity of species A is unchanged,

$$dG/d\xi = -Rx \quad (160)$$

where

$$R = nm\lambda k(T)/M^2 \hat{C}_p = R_\infty k(T)/k(T_\infty) \quad (161)$$

2. The equation of motion is (see Eq. (29))

$$\frac{4}{3} P'_r du/d\xi = h = (u - 1) + (\theta - u)/\gamma\kappa^2 u \quad (162)$$

3. The energy balance equation is modified by the addition of the kinetic energy terms and the pV work terms (see Eq. (30)),

$$d\theta/d\xi = g = aG - (1 - \theta) - [(\gamma - 1)/\gamma] (\theta - u) - \frac{1}{2} (\gamma - 1) \kappa^2 (u - 1)^2 \quad (163)$$

4. The diffusion equation is unchanged,

$$\delta (dx/d\xi) = x - G \quad (164)$$

The boundary conditions on the equations are those discussed in section III in the study of flames. If the fuel is pure A , then the value of G at the cold boundary is

$$G_0 = 1 \quad (165)$$

As discussed above in the treatment of flames, if the reaction rate expression is identically zero at the cold boundary temperature, the cold boundary can be taken to be at $\xi = -\infty$. Then

$$x_0 = 1 \quad (166)$$

and the initial values of θ and u are determined by Eqs. (162) and (163), by noting that in this limit the derivatives on the left of these equations are zero. Thus

$$\theta_0 = u_0 - \gamma \kappa^2 u_0 (u_0 - 1) \quad (167)$$

$$a - (1 - \theta_0) + [(\gamma - 1)/\gamma] (\theta_0 - u_0) - \frac{1}{2} (\gamma - 1) \kappa^2 (u_0 - 1)^2 = 0 \quad (168)$$

This pair of equations may be solved to obtain u_0 and θ_0 as functions of κ , γ , and $\varepsilon = 1 + (a/\theta_0)$. The result is

$$1/u_0 = \{(\gamma \kappa^2 + 1)/[(\gamma - 1) \kappa^2 + 2]\} \times \{\varepsilon \pm [\varepsilon^2 - \kappa^2(\gamma - 1) \kappa^2 + 2](\gamma \kappa^2 + 1)^{-2}(2\gamma \varepsilon - \gamma + 1)]^{\frac{1}{2}}\} \quad (169)$$

and θ_0 is given in terms of u_0 by Eq. (167). The positive sign in the last equation is used in the study of flames and the negative sign is associated with detonations. In this section we are concerned primarily with the latter case. The detonation velocity v_0 is also the relative velocity of the undetonated gas at the cold boundary. It can be expressed in the form

$$v_0 = c_0 u_0 \kappa / \theta_0^{\frac{1}{2}} \quad (170)$$

where $c_0 = (\gamma k T_0 / m)^{\frac{1}{2}}$ is the velocity of sound at the cold boundary.

Since ε is usually a large number, it often is useful to expand in powers of $1/\varepsilon$. Thus neglecting terms in $1/\varepsilon$ and higher orders,

$$v_0 = c_0 \left\{ [2(\gamma\kappa^2 + 1)^2 / (2\gamma\kappa^2 - \gamma + 1)] [\varepsilon - (\gamma - 1)/\gamma] - 2/\gamma + \dots \right\}^{\frac{1}{2}} \quad (171)$$

Since $M = \rho v$ is a constant, it follows directly from the definition of u , Eq. (158), that $u_0 = \rho_\infty/\rho_0$ and from the perfect gas equation of state that $p_0/p_\infty = \theta_0/u_0$. Thus we find on simple rearrangement that Eq. (167) becomes

$$\gamma\kappa^2 = [1 - (p_0/p_\infty)] / [(\rho_\infty/\rho_0) - 1] \quad (172)$$

It may easily be shown that $M^2 = \gamma\kappa^2 p_\infty/\rho_\infty$. Thus the last equation leads directly to the familiar relation

$$M^2 = \rho_0^2 v_0^2 = -p_0 \rho_0 [(p_\infty/p_0) - 1] / [(\rho_0/\rho_\infty) - 1] \quad (173)$$

We may also eliminate κ from Eqs. (167) and (169) to obtain a relation between θ_0 and u_0 , which depends in addition on γ and ε ,

$$\theta_0 = [(\gamma + 1)/(\gamma - 1) - u_0] / [2\gamma(\varepsilon - 1)/(\gamma - 1) + (\gamma + 1)/(\gamma - 1) - 1/u_0] \quad (174)$$

This result, when written in terms of p_∞/p_0 and ρ_0/ρ_∞ , is the usual detonation Hugoniot,

$$p_\infty/p_0 = [2\gamma(\varepsilon - 1)/(\gamma - 1) + (\gamma + 1)/(\gamma - 1) - \rho_0/\rho_\infty] / \{ [(\gamma + 1)/(\gamma - 1)] \rho_0/\rho_\infty - 1 \} \quad (175)$$

Thus, the detonation Hugoniot corresponds to $h = g = 0$.

The curve of intersection of the $g = 0$ surface with the $G = 1$ plane is of particular significance since it is closely related to the "shock Hugoniot." If there were no chemical reaction, the final condition of the gas after the passage of a shock wave would be a point on this curve. In the von Neumann-Döring-Zeldovitch theory, a detonation is idealized as consisting of a shock wave followed by a flame. The conditions in the gas after the passage of the shock wave and before the passage of the flame are assumed to be those corresponding to the point on the intersection of the $g = 0$ and $h = 0$ surfaces at $G = 1$. This point then specifies the

strength of the shock. The conditions at this point, which is referred to as the "von Neumann spike" and designated by a subscript N , are

$$u_N = 1 + (1 - \kappa^2)/(\gamma + 1)\kappa^2 - [1/(\gamma + 1)\kappa^2][2a(\gamma + 1)\kappa^2 + (1 - \kappa^2)^2]^{\frac{1}{2}} \quad (176)$$

$$\theta_N = u_N(1 + \gamma\kappa^2) - \gamma\kappa^2 u_N^2 \quad (177)$$

$$x_N = 1 \quad (178)$$

In the present treatment, in which we solve the set of differential equations, some of the solutions are shown to come close to, but not pass through, the von Neumann spike.

One integral of the differential equations, Eqs. (160), (162), (163), and (164), may be obtained in simple form in the special case in which $\delta = 1$ and $P'_r = 3/4$. Since these are physically reasonable values of the dimensionless groups, we restrict the present discussion to this special case. As a result of this choice of unity for the Lewis number and of three-fourths for the Prandtl number, it follows that the enthalpy of the gas (relative to the detonation wave) remains constant throughout the wave. The specific enthalpy including kinetic energy is

$$\hat{H}^* = \hat{Q}x + \hat{C}_p T + v^2/2 \quad (179)$$

In terms of the parameters and reduced variables defined above,

$$\hat{H}^* - \hat{H}_\infty^* = \hat{C}_p T_\infty [ax - (1 - \theta) + (1/2)(\gamma - 1)\kappa^2(u^2 - 1)] \quad (180)$$

It follows from Eqs. (162), (163), and (164) that

$$d(\hat{H}^* - \hat{H}_\infty^*)/d\xi = \hat{H}^* - \hat{H}_\infty^* \quad (181)$$

so that direct integration leads to the result

$$(\hat{H}^* - \hat{H}_\infty^*) = (\text{const}) \exp(\xi) \quad (182)$$

But since $(\hat{H}^* - \hat{H}_\infty^*) = 0$ in the limit that ξ approaches infinity, it follows that the integration constant of Eq. (182) must be zero, so that, for all values of ξ ,

$$\hat{H}^* - \hat{H}_\infty^* = 0 \quad (183)$$

From Eqs. (180) and (183), an algebraic relation can be obtained for x as a function of θ and u ,

$$ax = 1 - \theta - (1/2)(\gamma - 1)\kappa^2(u^2 - 1) \quad (184)$$

This last result may be used in the detonation equations to express θ in terms of x and u . Thus the momentum equation, Eq. (162), becomes

$$\gamma\kappa^2 u (du/d\xi) = -ax + (1/2)(\gamma + 1)\kappa^2(u - 1)(u - f) \quad (185)$$

where

$$f = 1 + [2(1 - \kappa^2)/(\gamma + 1)\kappa^2] \quad (186)$$

These equations may be transformed into an equation relating u and x , by use of Eq. (164),

$$du/d\xi = (dx/d\xi)(du/dx) = -(G - x)(du/dx) \quad (187)$$

Thus

$$\gamma\kappa^2 u (G - x)(du/dx) = ax - (1/2)(\gamma + 1)\kappa^2(u - 1)(u - f) \quad (188)$$

Hugoniot diagrams, such as Fig. 12, are very useful in visualizing the course of a detonation. The detonation Hugoniot gives the locus of all values of p_∞/p_0 , as a function of ρ_0/ρ_∞ , which are consistent with the conservation principles. The shock Hugoniot gives the locus of all values of p_{shock}/p_0 , as a function of $\rho_0/\rho_{\text{shock}}$, which would be consistent with the conservation equations if there were no chemical reactions. According to Eq. (173), the square of the detonation velocity is proportional to the negative of the slope of the line joining a point on the detonation Hugoniot with the initial point, 0. This line is called the "Rayleigh line". The von Neumann spike is the point of crossing of the Rayleigh line with the shock Hugoniot. If the coefficients of heat conductivity, viscosity, and diffusion were zero, the condition of the gas at all points within the detonation wave would be constrained to lie on the Rayleigh line. However, because these transport coefficients are not sufficiently small, the detailed progress of the detonation may deviate considerably.

The Rayleigh line can cross the detonation Hugoniot at two points. The upper crossing point, 1, corresponds to $\kappa^2 < 1$, whereas the lower crossing point, f , corresponds to $\kappa^2 > 1$. The lowest

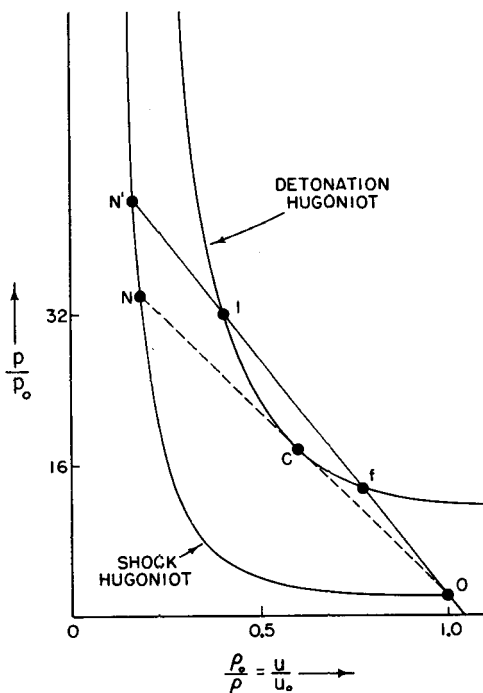


Fig. 12. Hugoniot diagram.

possible detonation velocity is obtained by drawing the Rayleigh line tangent to the detonation Hugoniot. The point of tangency, C, is the Chapman-Jouguet point corresponding to $\kappa^2 = 1$.

B. Ignition Temperature Model

As in the study of flames, it is convenient to consider first an overly simplified model of the kinetics, in which the specific rate constant is taken to be identically zero for T less than an ignition temperature, T_i , and a constant for $T > T_i$.

With this model the equations for G and x are uncoupled from the remaining equations. The most general solution (which satisfies the hot boundary conditions) of these equations in the region $\theta > \theta_i$ is then given by Eqs. (60) and (61), and the solution

in the region $\theta < \theta_i$ is given by Eqs. (66) and (67). In the treatment of detonations it is convenient to take $\xi = 0$ at the point where $\theta = \theta_i$. The solution which satisfies the hot and cold boundary conditions is then, in the high temperature region,

$$G = \exp(-\alpha\xi), \quad \theta > \theta_i \quad (189)$$

$$x = (1/b) \exp(-\alpha\xi), \quad \theta > \theta_i \quad (190)$$

where

$$\alpha = -(1/2) + (1/2)(1 + 4R_\infty)^{\frac{1}{2}} \quad (191)$$

and

$$b = \alpha + 1 \quad (192)$$

The solution in the low temperature region is

$$G = 1, \quad \theta < \theta_i \quad (193)$$

$$x = 1 - [(b - 1)/b] \exp \xi, \quad \theta < \theta_i \quad (194)$$

It then follows from Eq. (188) that

$$dx/du = -\alpha x/h, \quad \theta > \theta_i \quad (195)$$

$$dx/du = -(1 - x)/h, \quad \theta < \theta_i \quad (196)$$

where

$$h = [-ax + (1/2)(\gamma + 1)\kappa^2(u - 1)(u - f)]/\gamma\kappa^2u \quad (197)$$

As shown in either Figs. 13 or 14, $h = 0$ is a parabola in the x - u plane opening toward positive values of x . Inside the parabola h is negative, and outside h is positive. If a solution curve crosses the curve $h = 0$ at any point except the four singular points (1, f , N and O), the slope at this point is infinite. Within the parabola and below the line $x = 1$, the slope dx/du is positive. Thus solution curves are repelled by and cannot cross the right-hand branch of the $h = 0$ parabola.

The curve corresponding to $\theta = \theta_i$ is also a parabola in the x - u plane. The high temperature region lies below and the low temperature region lies above the $\theta = \theta_i$ curve. In the low temperature region, a solution cannot cross the line $x = 1$ since its slope dx/du would be zero along this line. Thus any solution curve which enters the low temperature region within the $h = 0$

parabola, and below the line $x = 1$, is trapped and must pass through the point O .

If θ_i is greater than θ_N , there is a lower limit of R_∞ which corresponds to a flame having the von Neumann spike as its initial conditions. If, on the other hand, θ_i is less than θ_N , the curve $\theta = \theta_i$ cuts the line $x = 1$ within the $h = 0$ parabola. The point of intersection corresponds to $R_\infty = 0$. The solution curve for

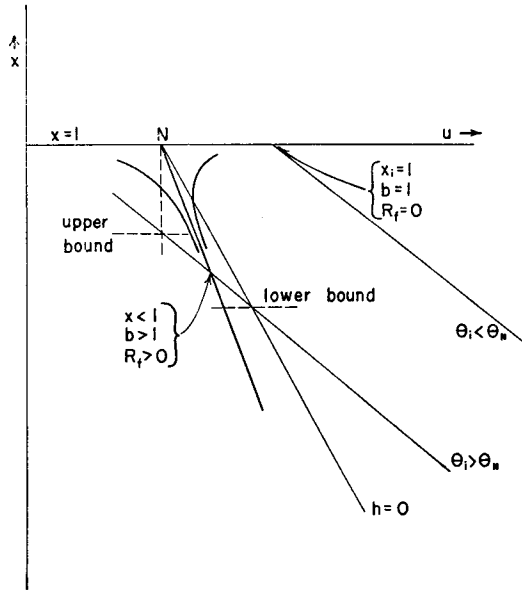


Fig. 13a. A schematic illustration of the behavior of the solutions near the von Neumann spike.

$R_\infty = 0$ would then extend from O to N along the line $x = 1$ and then follow the parabola $h = 0$ from N to 1 . This would correspond to the von Neumann-Döring-Zeldovitch picture of a detonation being a shock wave followed by a flame or reaction zone. For small values of R_∞ , the shock and reaction zones are essentially uncoupled. However, for large values of R_∞ the von Neumann-Döring-Zeldovich mechanism is no longer followed.

Figure 13a shows the behavior of the solutions near the von Neumann spike. If $\theta_i > \theta_N$, there is one solution with $R_\infty = R_i$,

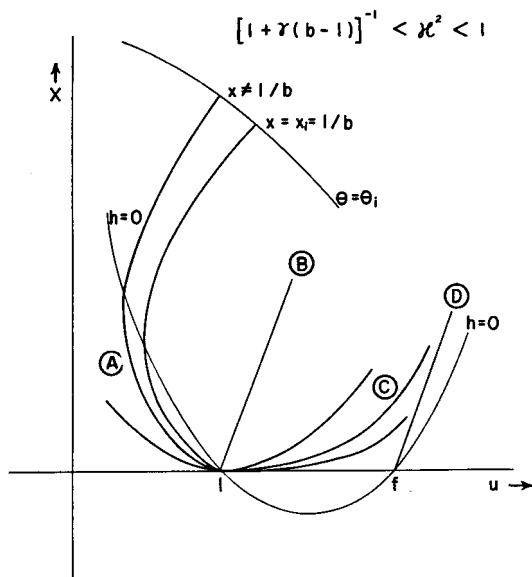


Fig. 13b. A schematic illustration of the behavior of the solutions near the hot boundary for $[1 + \gamma(b-1)]^{-1} < \kappa^2 < 1$.

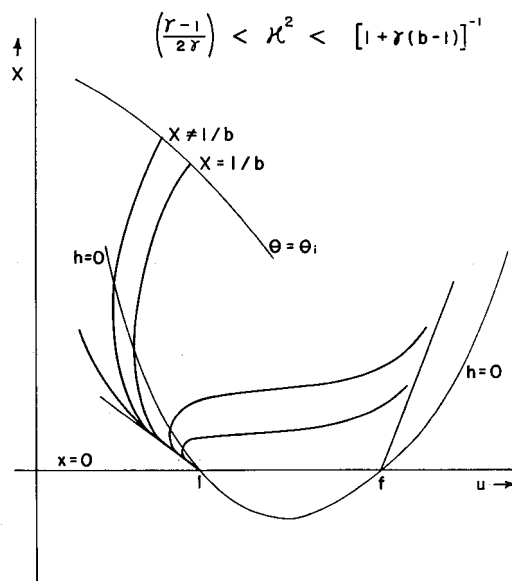


Fig. 13c. A schematic illustration of the behavior of the solutions near the hot boundary for $(\gamma-1)/2\gamma < \kappa^2 < [1 + \gamma(b-1)]^{-1}$.

which terminates at the von Neumann spike. This solution corresponds to a flame with initial conditions corresponding to the von Neumann spike. If R_∞ is less than R_f , no detonation solution is possible; whereas if R_∞ is greater than R_f , the solution curves cross $h = 0$ before reaching the von Neumann spike and are constrained to terminate at the initial point $x = 1$, $u = u_0$. Thus, R_f forms a lower limit for the values of R_∞ which will support

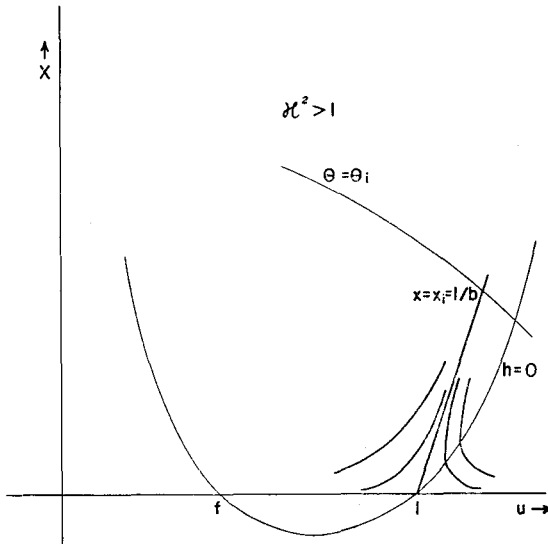


Fig. 13d. A schematic illustration of the behavior of the solutions near the hot boundary for $\kappa^2 > 1$.

the detonation. If, however, $\theta_i < \theta_N$, there is no solution which reaches the von Neumann spike and hence there is no lower limit for the R_∞ which will support a detonation.

Figure 13b shows the behavior of the solutions near the hot boundary when κ^2 lies between unity and $(1 + \gamma(b - 1))^{-1}$. Here the curve (A) is typical of the solutions having small values of R_∞ in starting out along the u -axis before heading upwards. Then a critical value of R_∞ is reached for which the solution behaves like curve (B) starting inside the $h = 0$ parabola. For larger values of R_∞ , the solutions look like curve (C). Finally an upper limit

for R_∞ is reached. The solution corresponding to this upper limit starts out along the u -axis from 1 to f (corresponding to a shock wave) and continues as the curve (D).

Figure 13c shows the behavior of the solutions for κ^2 less than $(1 + \gamma(b-1))^{-1}$. Here again there is a manifold of solutions with an upper limit for R_∞ corresponding to a shock wave from 1 to f and a special solution emanating from f .

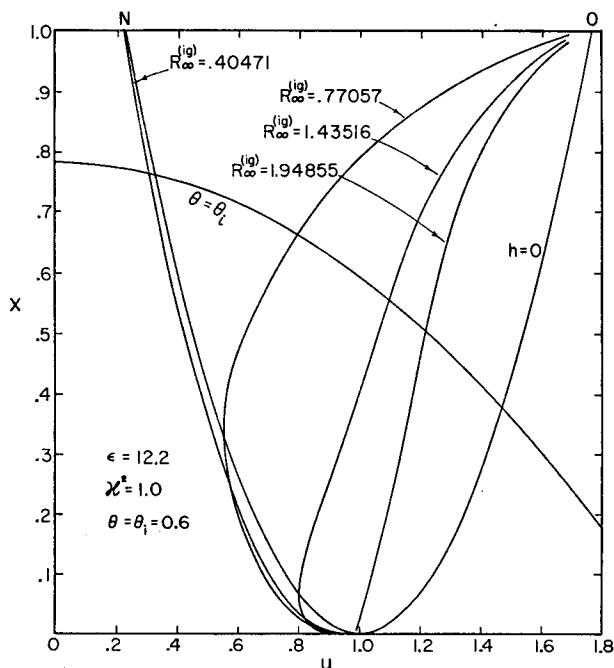


Fig. 14a. Curves of x as a function of u for $\kappa^2 = 1$ and various values of $R_\infty^{(ig)}$ as based on the ignition temperature model.

Figure 13d shows only a single solution for $\kappa^2 > 1$.

The manifold of possible values for R_∞ which will support a steady state detonation are shown in Fig. 15 as a function of κ^2 . For $\kappa^2 > 1$ there is only a single allowed value of R_∞ which seems to correspond to an extension of the curve R_u , the upper limit of R_∞ . If θ_i were less than θ_N , the lower limit for R_∞ would be zero when $\kappa^2 < 1$.

Figures 14a, b, and c show typical solution curves which were obtained assuming that $\gamma = 1.25$.

Figure 16 shows a set of solution curves plotted upon a Hugoniot diagram. Here $\theta_i > \theta_N$, so that there is a lower limit to R_∞ . This lower limit corresponds to a shock wave with $x = 1$ followed by the reaction zone starting at the von Neumann spike, N . The

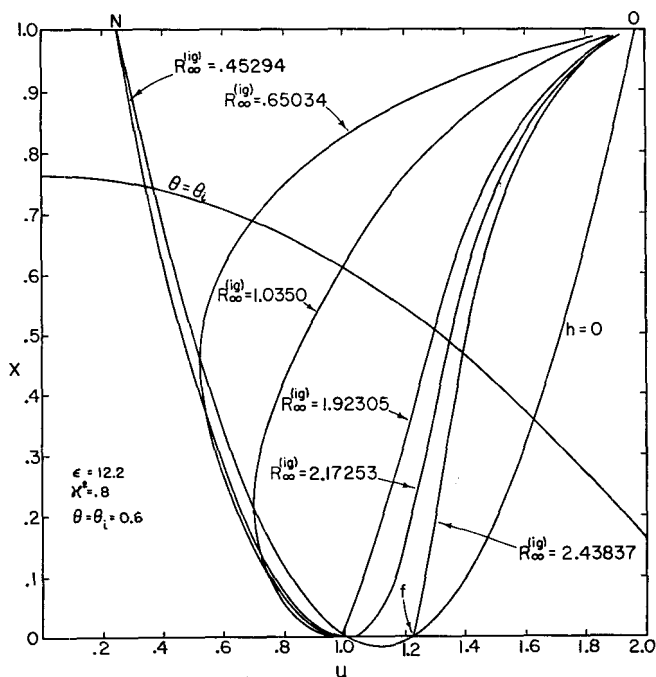


Fig. 14b. Curves of x as a function of u for $\kappa^2 = 0.8$ and various values of $R_\infty^{(ig)}$ as based on the ignition temperature model.

curve with $R_\infty = 0.6116$ corresponds to an intermediate value of the reaction rate. Then finally the curve $R_u = 1.7125$, corresponding to the largest possible value of R_∞ , proceeds directly from the initial conditions to the Chapman-Jouguet point, C , without any initial shock.

C. Arrhenius Kinetics and Detonations in Real Gases

The detonation equations can also be integrated using the Arrhenius temperature dependence of the reaction rate. The

details of the mathematics and the numerical procedures are somewhat more difficult than for the ignition temperature model, but the results are very similar.

Solutions for several values of the various parameters are illustrated in Figs. 17 and 18. In Fig. 17, x is given as a function

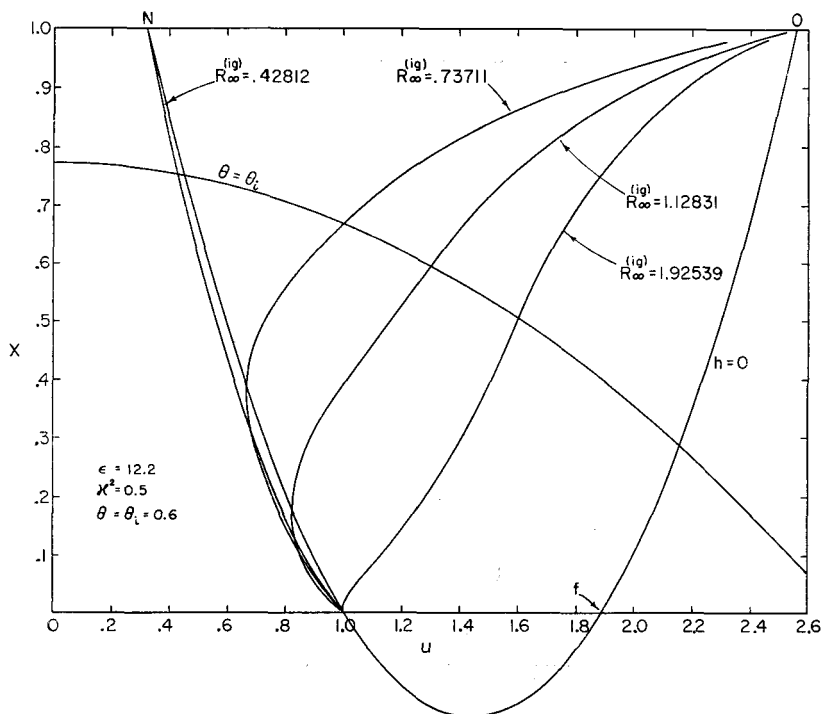


Fig. 14c. Curves of x as a function of u for $\kappa^2 = 0.5$ and various values of $R_{\infty}^{(ig)}$ as based on the ignition temperature model.

of u . The figures may be compared with Figs. 14, which illustrate similar results using the ignition temperature model. In Fig. 18, various variables are plotted as functions of the reduced distance variable ξ .

It is to be noted that in the solutions illustrated in Fig. 17, R_{∞} is of the order of unity. It is interesting to express R_{∞} in terms of the mean time between collisions, t_0 , and the characteristic

time of the first order reaction, t_r . The mean time between collisions of molecules in the hot gas is approximately

$$t_c = (4n_\infty \sigma^2)^{-1} (m/\pi RT_\infty)^{\frac{1}{2}} \quad (198)$$

where σ is the effective rigid sphere diameter of the molecules.

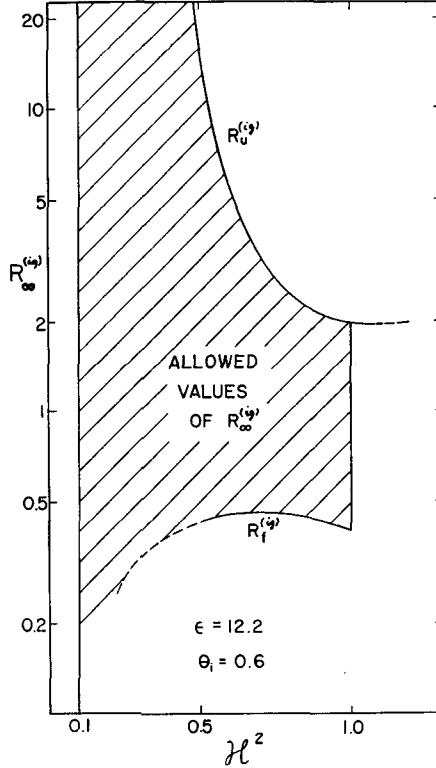


Fig. 15. The limiting values of R_∞ , that is, R_u and R_l , as functions of κ^2 . Steady-state detonation solutions exist inside the shaded area, and for κ^2 greater than unity along the line R_u .

The characteristic time of the first order reaction at the hot boundary temperature is

$$t_r = 1/k(T_\infty) \quad (199)$$

For the rigid sphere model, the coefficient of thermal conductivity is

$$\lambda_\infty = (25/8) \hat{C}_v p_\infty t_c \quad (200)$$

With these expressions, R_∞ , as given by Eq. (161) can be rewritten in the form*

$$R_\infty = (25/8) (\gamma\kappa)^{-2} (t_c/t_r) \quad (201)$$

Since both γ and κ are of the order of unity, it follows from the last equation that R_∞ is approximately the ratio of t_c to t_r . However,

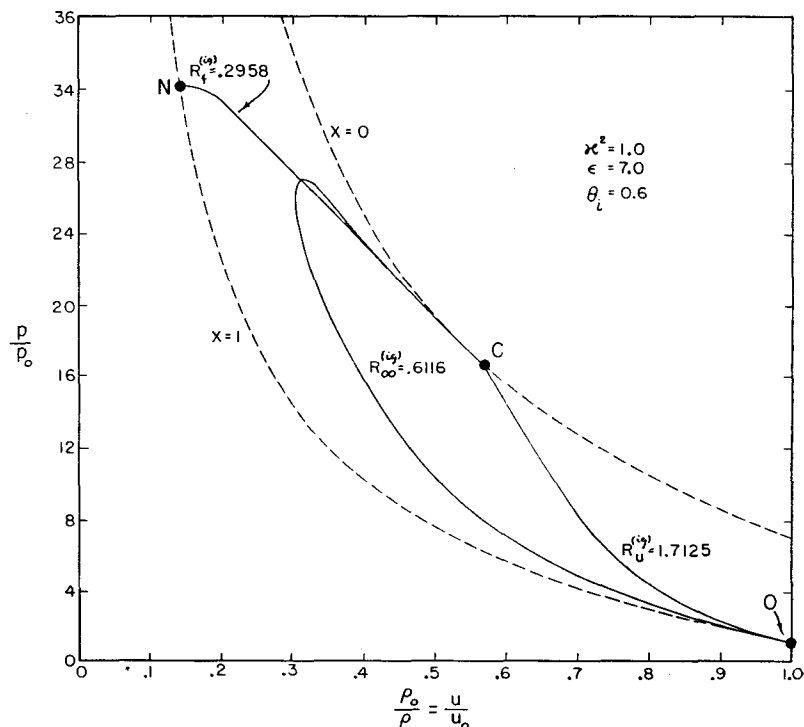


Fig. 16. The Hugoniot description of detonations. A family of detonation solutions are found for values of R_∞ varying between the limits, R_f and R_u . If the transport properties were unimportant, these solutions would all lie on the straight line joining O , C , and N .

if a reaction is to be first order, the ratio t_c/t_r must be small compared to unity. For larger values of the ratio t_c/t_r , a unimolecular reaction would become second order. Thus, only values of R_∞ which are small compared to unity can be physically significant.

* The authors want to thank W. W. Wood for pointing out this relation.

A similar conclusion is obtained by comparing the thickness of the detonation wave to the mean free path of the molecules in the hot gas,

$$l_{\infty} = (2^{\frac{1}{2}} n_{\infty} \pi \sigma^2)^{-1} \quad (202)$$

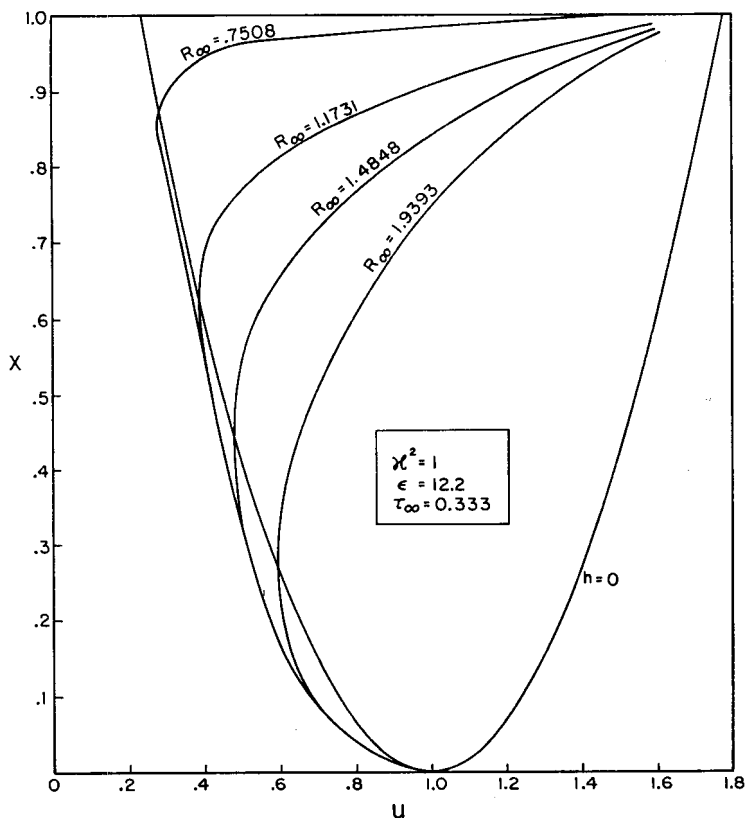


Fig. 17a. Curves of x as a function of u for $\kappa^2 = 1$ and various values of R_{∞} , based on Arrhenius kinetics.

The actual distance in the detonation is then related to the reduced distance by

$$z = [(3/8) (1/\kappa) (2\pi\theta_0/\gamma)^{\frac{1}{2}}] l_{\infty} \xi \quad (203)$$

The factor multiplying $l_{\infty} \xi$ is of the order of unity. W. W. Wood has recently shown that the reduced thickness of the detonation

wave, ξ_θ (defined as the distance between $\theta = \theta_0 + 0.1$ and $\theta = 0.9$), is of the order of $1/R_\infty$. Here again we see that in order for the thickness of the detonation wave to be of the order of one hundred mean free paths, R_∞ must be of the order of 0.01. Clearly

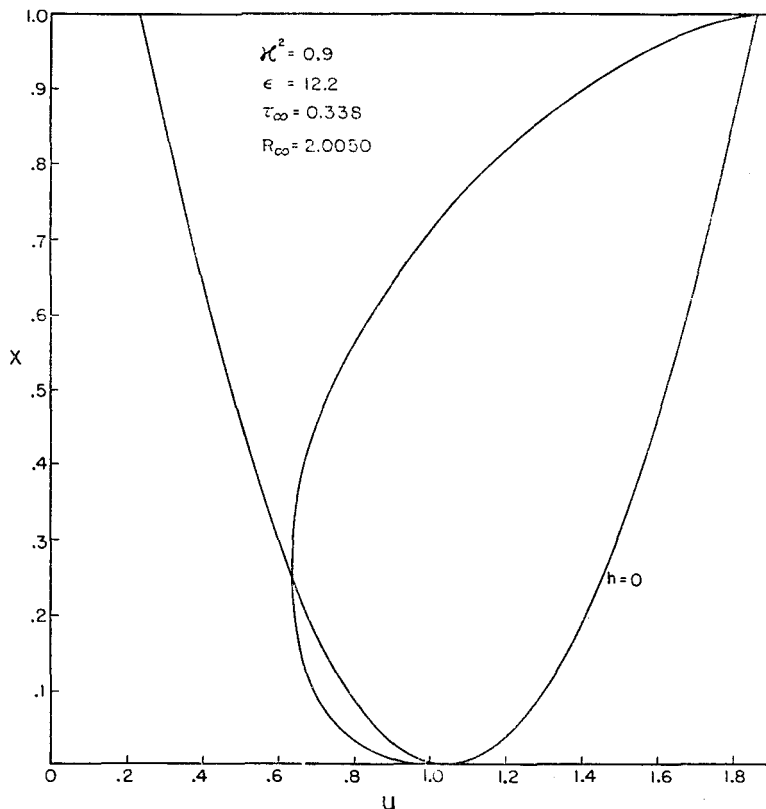


Fig. 17b. Curve of x as a function u for $\kappa^2 = 0.9$ and $R_\infty = 2.0050$, based on Arrhenius kinetics.

the detonation wave cannot be as thin as one mean free path, which would be required if R_∞ were of the order of unity.

We find that for ethylene oxide and for hydrazine, under conditions where they might reasonably be expected to detonate by a unimolecular mechanism, R_∞ is of the order of 0.01. For such small values of R_∞ , the transport properties have very little effect

and the detonation proceeds very much in accordance with the von Neumann-Döring-Zeldovitch mechanism of a shock wave followed by a set of adiabatic chemical reactions. With such a mathematical model it is possible, for any assumed value of κ , to determine the von Neumann spike conditions and to integrate the reaction rate equations together with the equation of motion, $h = 0$, and the equation of energy balance, $g = 0$.

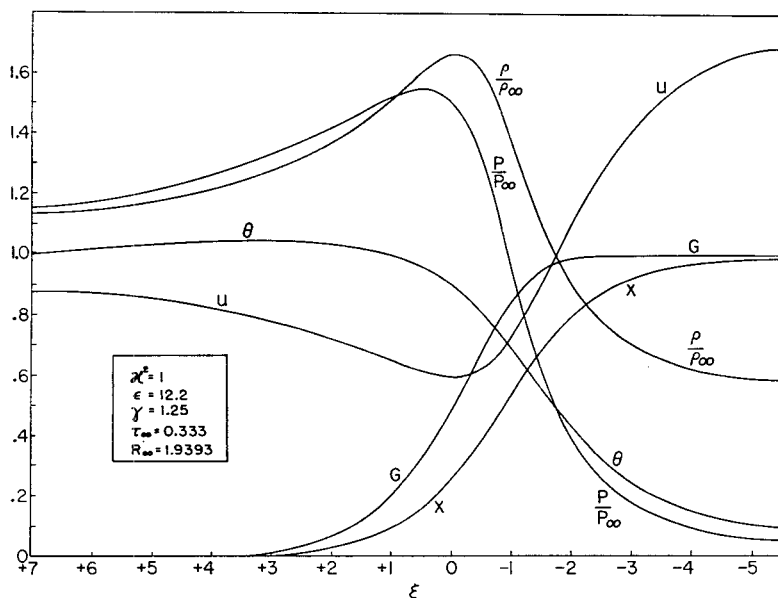


Fig. 18. Curves of various quantities as functions of the reduced distance ξ based on Arrhenius kinetics.

With systems of chemical kinetics involving more than one chemical reaction, there is some ambiguity as to the definition of the Chapman-Jouguet point. At first, Kirkwood and Wood¹⁵ thought that the Chapman-Jouguet point should correspond to complete chemical equilibrium, but the velocity of sound at the Chapman-Jouguet point should correspond to frozen chemical reactions. Subsequently, Wood and Kirkwood²⁶ decided that the velocity of sound at the Chapman-Jouguet point should correspond to the chemical reactions remaining in equilibrium.

This view was substantiated by calculations of Linder, Curtiss, and Hirschfelder¹⁸ for the reversible $A \rightleftharpoons B$ reaction, and more recently by Salsburg and Wood²¹ for the case of completely general systems of chemical reactions. However, at the present time there is no case where the experimental detonation velocity corresponds to a detonation ending precisely at the Chapman-Jouguet point. Perhaps a one dimensional idealization of detonations is not truly realistic.

References

1. Adams, Jr., E. N., *Univ. of Wisconsin Naval Research Lab. Report CF-957*, Part V, (1948).
2. Campbell, E. S., Hirschfelder, J. O., and Schalit, L. M., "Deviation from the Kinetic Steady-State Approximation in a Free-Radical Flame," *Seventh International Symposium on Combustion*, Butterworth, 1958, p. 332.
3. Corner, J., *Proc. Roy. Soc. (London)* **A198**, 388 (1949).
4. Curtiss, C. F., Hirschfelder, J. O., and Barnett, M. P., *J. Chem. Phys.* **30**, 470 (1959).
5. Döring, W., *Ann. Physik* **43**, 421 (1943).
6. Giddings, J. C., and Hirschfelder, J. O., "Property of Flames Supported by Chain-Branching Reactions," *J. Phys. Chem.* **61**, 738 (1957).
7. Giddings, J. C., and Hirschfelder, J. O., "Flame Properties and the Kinetics of Chain-Branching Reactions," *Sixth International Symposium on Combustion*, Reinhold, New York, 1957, p. 199.
8. Henkel, J., Spaulding, W. P., and Hirschfelder, J. O., *Third International Symposium on Combustion*, Williams and Wilkins, Baltimore, 1949, p. 127.
9. Hirschfelder, J. O., *Phys. of Fluids* **2**, 565 (1959).
10. Hirschfelder, J. O., and Curtiss, C. F., *J. Chem. Phys.* **28**, 1130 (1958).
11. Hirschfelder, J. O., Curtiss, C. F., and Bird, R. B., *Molecular Theory of Gases and Liquids*, Wiley, New York, 1954.
12. Hirschfelder, J. O., Curtiss, C. F., and Campbell, D. E., *Fourth International Symposium on Combustion*, Williams and Wilkins, Baltimore, 1953.
13. Hirschfelder, J. O., and McCone, A., Jr., *Phys. of Fluids* **2**, 551 (1959).
14. Hirschfelder, J. O., McCone, A., Jr., and Odell, T., *Univ. of Wisconsin Naval Research Lab. Report CM-934* (1958).
15. Kirkwood, J. G., and Wood, W. W., *J. Chem. Phys.* **22**, 1915 (1954).
16. Klein, G., *Univ. of Wisconsin Naval Research Lab. Reports Squid-1*, 2 (1955).
17. Klein, G., *Phil. Trans. Roy. Soc. (London) Ser. A*, **249**, 389 (1957).

18. Linder, B., Curtiss, C. F., and Hirschfelder, J. O., *J. Chem. Phys.* **28**, 1147 (1958).
19. *Natl. Advisory Comm. Aeronautics Tech. Mem.* 1261 (1950).
20. Neumann, J. von, *O. S. R. D. Report* 549 (1942); *Ballistics Research Lab. File No.* X-122.
21. Salsburg, Z., and Wood, W. W., Los Alamos, unpublished (1959).
22. Spalding, D. B., *Proc. Roy. Soc. (London)* **A240**, 83 (1957).
23. Tanford, B. C., and Pease, R. N., *J. Chem. Phys.* **15**, 861 (1947).
24. Taylor, G. I., *Proc. Roy. Soc. (London)* **A200**, 235 (1950).
25. Wilde, K. A., *J. Chem. Phys.* **22**, 1788 (1954).
26. Wood, W. W., and Kirkwood, J., *J. Chem. Phys.* **25**, 1276 (1956).
27. Zeldovitch, Y. B., *J. Exptl. Theoret. Phys. (U.S.S.R.)* **10**, 542 (1940).

LARGE TUNNELLING CORRECTIONS IN CHEMICAL REACTION RATES

HAROLD S. JOHNSTON, *Department of Chemistry,
University of California*

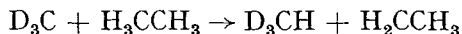
CONTENTS

I. Introduction	131
II. Number of Essential Coordinates	132
III. New Method of Expressing Molecular Partition Functions	134
IV. Parameters Needed from the Potential Energy Surface	139
V. Tunnelling Factors	148
VI. Applications to Experimental Data	151
VII. Summary and Conclusions	164
VIII. Evaluation of Index p from Symmetrical Activated Complex	167
IX. Acknowledgement	169
References	169

I. INTRODUCTION

Recently, R. P. Bell² published a solution to the problem of quantum mechanical penetration or "tunnelling" through a one-dimensional parabolic barrier, and his work is an invitation to consider problems in reaction rates for which large degrees of tunnelling are expected. We wish to explore this prospect using as examples the abstraction of hydrogen or deuterium from various substances by methyl or deuteromethyl radicals. These reactions are useful for this purpose because the chemical mechanisms have been very thoroughly studied and a large body of results is available.^{32,33} Aside from the methyl radicals, reactants vary from the relatively simple H₂, HD, and D₂ to large hydrocarbons and other organic molecules. It is usual to treat atom-transfer reactions as if a three-atom reaction; the potential energy surface is displayed as contour lines in a plane defined by the lengths of the bond broken and the bond formed. We shall discuss the problem of the minimum number of coordinates demanded

to describe the essence of a reaction such as

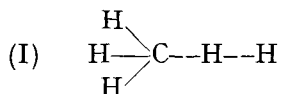


This discussion is presented in the general framework of the activated complex theory.¹²

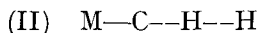
For many years Pitzer²⁵ has pointed out the conceptual and the computational advantages of expressing the partition function for molecules and activated complexes as the classical phase integral with quantum correction factors. For a number of molecular structures, Pitzer and co-workers^{25,31} have evaluated the classical phase integral. Recently the classical phase integral has been given a general solution¹⁵ for any molecular structure; with the aid of a simple table of geometrical factors one can write down the classical partition function of any molecule or activated complex by inspection; to apply the quantum corrections a vibrational analysis must be carried out, at least for the high frequencies of vibration. This method will be reviewed briefly and set up sufficiently to be used in the methyl radical reactions, and it will be seen that the tunnelling factor appears as a natural part of this formalism.

II. NUMBER OF ESSENTIAL COORDINATES

For the reaction $\text{H}_3\text{C} + \text{H}_2 \rightarrow \text{CH}_4 + \text{H}$, there are 6 atoms and 18 degrees of freedom. One bond is broken and one bond is formed, upon the transfer of the hydrogen atom. The activated complex

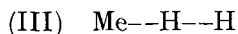


is sufficiently simple and symmetric that a normal mode analysis of its 12 vibrations is readily carried out, after assignment of force constants and molecular geometry. A linear four-atom substitute for the complex can be constructed as



where M is treated as an atom with three times the mass of hydrogen and the MC bond treated as rigid. A linear three-atom

complex can also be considered



where Me is an atom with the mass of the methyl group. The frequencies of these three complexes are given in Table I, where distances and force constants are evaluated as described in a

TABLE I. Models and Frequencies of Activated Complexes for Methyl Radical Reactions with Hydrogen

Normal mode	Multiplicity	Vibration frequencies in cm ⁻¹	
		Tetrahedral methyl	Planar methyl

A. Full Model

$$\begin{array}{c}
 \text{H} \\
 \diagup \\
 \text{H} \rightarrow \text{C} - \text{H} - \text{H} \\
 \diagdown \\
 \text{H}
 \end{array}$$

(1) Complex			
Me str	1	2959	2913
sym str	1	2290	2290
Me bend	1	1155	676
reaction coord.	1	(computed separately as 1778 <i>i</i>)	
anti Me str	2	3076	3094
anti Me bend	2	1424	1578
bend	2	1218	1215
wag	2	573	574
(2) Radical			
Me str	1	2954	2913
Me bend	1	953	681
anti Me str	2	3074	3097
anti Me bend	2	1415	1570
(3) Hydrogen str	1	4277.2	

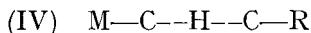
B. Four-atom substitute model for complex H₃—C—H—H

str	1	2334
reaction	1	1778 <i>i</i>
bend	2	1158
wag	2	459

C. Three-atom substitute model for complex Me—H—H

str	1	2334
reaction	1	1778 <i>i</i>
bend	2	1021

later section. The rates of reaction based on these three sets of frequencies were computed. At 500°K model II gives a rate which is 1.15 times that given by model I, but model III gives a rate 6.2 times that of model I. In the real reaction four components of classical rotation of reactants go over to the four wagging vibrations of the complex; models I and II recognize this change of degrees of freedom; whereas, model III does not. Thus, use of the three-atom substitute complex leads to an error of almost a factor of ten in computed A -factor or rate constant. In this study all calculations are based on model II for hydrogen reactants. For more complicated reactants a linear five-atom model is used,



where MC and CR bonds are treated as rigid. Here again, a negligible error is introduced by this simplification of the model, but very serious errors are caused by further simplification.

By virtue of the linearity of these models and the rigidity of the bonds which do not change during reaction, the stretching vibrations, symmetric and antisymmetric, can be treated as if the complex contained only three atoms, and the orthogonal bending and wagging vibrations treated as a four or five-atom molecule. Thus, so far as bond changes are concerned, we can express the problem by means of the familiar diagrams of potential energy contours in an $R_1 - R_2$ plane.

III. NEW METHOD OF EXPRESSING MOLECULAR PARTITION FUNCTIONS

If the energy of a molecule can be expressed as the sum of separate classes of energy

$$E = E_{tr} + E_{rot} + E_{vib} + E_{el} + E_{nuc} + \dots \quad (1)$$

then and only then the partition function is the product of independent partition functions

$$Q = Q_{tr} Q_{rot} Q_{vib} Q_{el} Q_{nuc} \dots \quad (2)$$

and to this approximation the usual simple formulas¹² follow for reaction rates according to activated complex theory. Specifically, rotation-vibration interactions, anharmonicity, and gas imperfections are neglected. To exactly the same level of approximation

TABLE I (Continued)

D. Dimensions in A of models

$$\begin{array}{c} \text{H} \\ \diagup \\ \text{H}-\text{C} \cdots \text{H} \cdots \text{H} \\ \diagdown \\ \text{H} \end{array}$$

1.09 1.27 0.92
1.09
1.09

$$\begin{array}{c} \text{H} \\ \diagup \\ \text{H}-\text{C} \\ \diagdown \\ \text{H} \end{array}$$

1.09
1.09
1.09

$$\text{H}_3-\text{C}-\text{H}-\text{H}$$

1.09 1.27 0.92

$$\text{Me}-\text{H}-\text{H}$$

1.27 0.92

E. Force constants

Stretch in 10^5 dyne/cm

Bend in 10^{-11} erg/radian²

C—H(Me) 5.00^a

H—C—H(Me) 0.52^a

C—H($\frac{1}{2}$) 2.50

H—C—H($\frac{1}{2}$) 0.26

H—H 2.87

C—H—H 0.13

Interaction constant between C—H— and —H—H

3.53

$(1 - F_{12}^2/F_1 F_2)^{\frac{1}{2}} = 0.858i$

F. Full set of frequencies in cm^{-1} for all isotopic variations of the reaction of methyl with hydrogen, based on the four-atom linear model

Reaction	ω^*/i	ω str	ω bend	ω wag	ω reactant
H ₃ CHH	1778	2334	1158	459	4277
H ₃ CHD	1759	1716	1117	417	3722
H ₃ CDH	1299	2324	904	459	3722
H ₃ CDD	1282	1711	852	414	3054
D ₃ CHH	1772	2319	1151	405	4277
D ₃ CHD	1754	1697	1109	361	3722
D ₃ CDH	1289	2309	895	404	3722
D ₃ CDD	1274	1691	840	360	3054


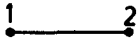
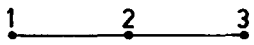
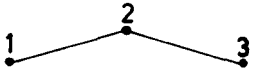
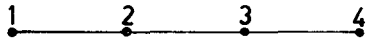

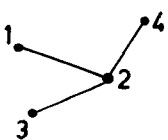
^a These are rigid in the four-atom model, and the force constants may be taken as infinite.

the partition function for a nonlinear molecule of N atoms may be expressed as¹⁵

$$Q = (Q_e/\sigma) \prod^N \Lambda^{-3} (2\pi kT)^{\frac{1}{2}(3N-6)} |\mathbf{F}|_{3N-6}^{-\frac{1}{2}} \prod^N J_\alpha \prod^{3N-6} \Gamma_i \quad (3)$$

where Λ is the atomic de Broglie wavelength $h/(2\pi mkT)^{\frac{1}{2}}$, $|\mathbf{F}|_{3N-6}$ is the determinant for the force constant matrix³⁸ in internal (bond and angle) coordinates, the quantum correction factor Γ_i is $(u_i/2)/\sinh(u_i/2)$ where $u_i = \hbar\nu_i/kT$, and a J is a geometrical factor for each atom in the molecule (a short list of J 's is given in Table II). For linear molecules $3N - 6$ is replaced by $3N - 5$.

TABLE II. A Short Table of J_α Functions for Simple Molecular Structures (For longer list see ref. 15)

α atoms	Configuration	J_α
1		V
2		$4\pi R_{12}^2$
3		R_{23}^2
		$2\pi R_{23}^2 \sin \phi_{123}$
4		R_{34}^2
		$R_{34}^2 \sin \phi_{234}$
		$\frac{R_{24}^2}{\sin \psi_{341}}$

For a nonlinear activated complex of N atoms the product of the complete partition function times the average rate to cross the barrier is

$$Q \langle 1/\tau \rangle = (Q_e/\sigma) \prod^N \Lambda^{-3} (2\pi kT)^{\frac{1}{2}(3N-6)} |\mathbf{F}|_{3N-6}^{-\frac{1}{2}} \prod^N J_\alpha \prod^{3N-7} \Gamma_i \Gamma_* \nu^* \quad (4)$$

where new terms are ν^* the imaginary frequency in sec^{-1} of the activated complex, $|\mathbf{F}|$ is the complete force constant determinant including cross product terms which lead to the imaginary frequency, and Γ_* is Bell's tunnelling correction factor, $(u/2)/\sin(u/2)$, for small values of u , or Γ_* may be an even larger tunnelling factor based on graphical integration of an Eckart barrier potential.⁹ For diagonal \mathbf{F} -matrices in molecules, the term $[(2\pi kT)^{3N-6}/|\mathbf{F}|]^{\frac{1}{2}}$ becomes $\prod^{3N-6} l_i$ where l_i is the classical vibrational amplitude $(2\pi kT/F_i)^{\frac{1}{2}}$. For atom transfer reactions the F -determinant has a block

$$\begin{vmatrix} F_1 & F_{12} \\ F_{12} & F_2 \end{vmatrix}$$

which can be expressed as $w^2 F_1 F_2$ where

$$w = (1 - F_{12}^2/F_1 F_2)^{\frac{1}{2}}$$

In this way the imaginary term w can be associated with the imaginary ν^* to give a real ratio; and the rest of the force constant terms give, $\prod^{3N-6} l_i$, the product of vibrational amplitudes as before. In any chemical reaction the de Broglie wavelengths cancel between reactants and activated complex. Unchanging bond lengths or bond angles between reactants and complex lead to cancellation of J_α factors, unchanging force constants lead to cancellation of vibrational amplitudes $(2\pi kT/F)^{\frac{1}{2}}$, and unchanging group frequencies lead to cancellation of quantum correction factors Γ_i . The computational advantage of this form of the partition function is that all terms appear as products, so cancellation of unchanging terms and evaluation of ratios for terms which change are at once apparent. Changes in geometry between reactants and complex give ratios of J factors, and changes in force field give ratios of $F^{\frac{1}{2}}$. The proper power of $(2\pi kT)^{\frac{1}{2}}$ appears automatically. In forming an activated complex, a new bond is formed giving a new J_α and new F factors. The factors Γ are such that they approach unity as the frequency becomes low, and they approach $ue^{-u/2}$ for high frequencies (the zero of energy is at the bottom of the potential curve in this formalism, so that proper zero point energies are always accounted for).

The ratio of two rate-constant expressions for two different isotopic species leads to cancellation of all J factors and $|\mathbf{F}|$ and directly to Bigeleisen's³ formulation of the kinetic isotope effect ratio. (The converse, of course, is not true; from the expressions for the ratio of k'/k , one cannot recover the factors J_α or F .)

In terms of a potential energy surface, we need bond distances and angles in order to evaluate the factors J_α ; we also need force constants, or the second derivatives of the potential energy surface with respect to internal coordinates, d^2V/dS^2 . For the reactants the structure and force constants can be found experimentally by spectroscopic and other means. For the activated complex we do not need the entire potential energy surface but only the location of the point of maximum energy along the reaction path and the various curvatures through that point. From these distances and force constants all real frequencies of the reactants can be evaluated by the usual $\mathbf{F} - \mathbf{G}$ matrix method;³⁸ for the activated complex all frequencies, including the imaginary one, can be evaluated in the same way as for the reactant. This formalism does not omit the "reaction coordinate," but rather it treats the whole activated complex as a vibrational problem in $3N - 6$ degrees of freedom. From these frequencies the quantum correction factors I_i are found, and the tunnelling factor is the I for the reaction coordinate.

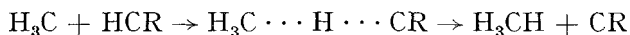
In this section we have reviewed and set up the general activated complex theory, emphasizing that additivity of energies and separability of coordinates is a necessary feature of the general theory as it is used. It is well known that coordinates of a dynamical system are separable over a region near an extremum where the potential energy is adequately represented by quadratic terms of a Taylor series. The reactants are represented by separable coordinates defined with respect to the independent, stable molecules. The activated complex is represented by a largely different set of coordinates, separable only in the immediate vicinity of the saddlepoint extremum. In between these two relatively simple states, the internal coordinates of the interacting reactants are not all separable. In particular, there is no separable coordinate connecting reactants and activated complex; the line

of minimum potential energy, let us call it the "reaction path," is not a separable coordinate, but represents strong, nonseparable interactions between two or more degrees of freedom. A central question in the problem of large degrees of tunnelling is the magnitude of configuration space over which the potential energy is quadratic; a one-dimensional tunnelling theory cannot be expected to work outside such a region.

IV. PARAMETERS NEEDED FROM THE POTENTIAL ENERGY SURFACE

To calculate a reaction rate in the usual manner according to activated complex theory, we do not need an entire potential energy surface, but only the saddlepoint and its curvatures there. At present we know of no adequate theoretical method for obtaining these parameters. Unfortunately, Eyring's^{12, 26} semi-empirical method of constructing a potential energy surface breaks down very badly just in this critically important region, as Kassel¹⁷ pointed out. Sato's²⁹ method is but a formal extension of Eyring's method; one still uses simple London theory to correlate empirical Morse functions. Thus we reject use of these semi-empirical methods, and turn to strictly empirical methods. Our ideal is to fix the needed parameters by means of 100 per cent empiricism from the fields of molecular structure and molecular spectroscopy, that is, fields outside of kinetics itself. This goal is not yet reached, although we are very close to it. In this section we review^{14, 16, 39} our current methods of using the correlations and rules of molecular structure and spectroscopy in fixing the properties of activated complexes. These rules will be stated only with respect to methyl radical reactions, since we do not wish to let this tedious but necessary side discussion overshadow the main topic.

For the reaction of methyl radicals with a hydrocarbon to remove a hydrogen atom



the number of bonds is the same for reactants and products. A

single bond H—C in the hydrocarbon disappears, but a single bond C—H in methane appears. Since bond dissociation energies here are about 100 kcal and since the activation energy is only about 10 kcal, it is obvious that the loss of one bond must at

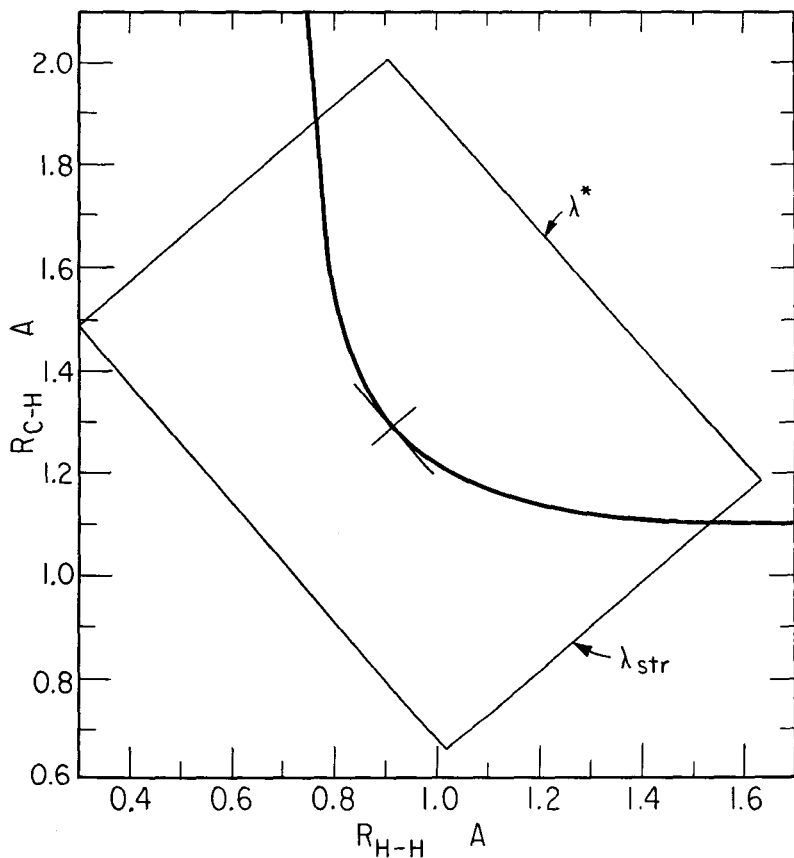


Fig. 1. Reaction path for the reaction $\text{H}_3\text{C} + \text{H}_2 \rightarrow \text{CH}_4 + \text{H}$. The point of maximum energy is indicated by the crossed lines, and the de Broglie wavelengths λ for motion along and normal to the reaction path are indicated.

all times be strongly offset by the formation of the other. We then assume *conservation of bond order* for the process; as in all assumptions in this section, we feel that the assumption cannot

be purely correct, but it cannot be totally wrong either, and it provides a definite starting point for the discussion.

For a bond of any order Pauling²⁴ has proposed a simple relation between the bond length and the length of the cor-

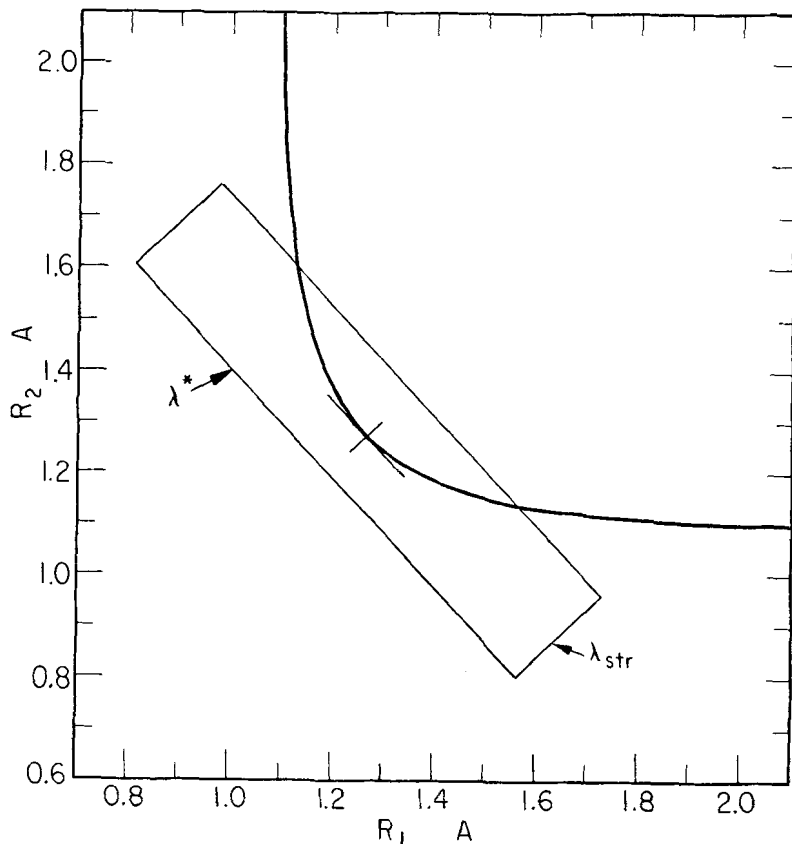


Fig. 2. Reaction path for the reaction $\text{H}_3\text{C} + \text{C}_3\text{H}_6$.

responding single order bond

$$R = R_s - 0.6 \log_{10} n \quad (5)$$

in Angstrom units, where R is the bond length, R_s is the single bond length, and n is the order. We let R_1 be the length of the bond to be broken and R_2 be the length of the bond to be formed.

Conservation of bond order gives $n_2 = 1 - n_1$, and this assumption plus Pauling's rule immediately determines the reaction path. The reaction path of methyl radical plus hydrogen is given by the curved line in Fig. 1, and the reaction path for methyl radical plus ethane or acetone, for example, is given in Fig. 2.

There are many empirical relations between bond length and stretching force constant, for example, Badger's rule.¹ A simpler rule which appears slightly better for excited states of H_2 is simply that the stretching force constant is proportional to order for a given bond. Thus we assume

$$F = F_s n \quad (6)$$

where F is the stretching force constant, F_s is that for a single bond, and n is the order.

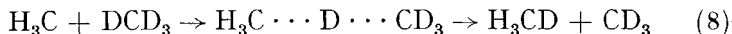
The empirical situation with respect to bending force constants is not so simple as that for stretching force constants. To evaluate bending force constants for fractional bonds, we simply use Eyring's semi-empirical method.¹² It is easy to derive a closed, cumbersome expression for the bending force constant in terms of bond distances and parameters of the Morse function between end atoms. For half-bond bending about a hydrogen atom, we find 0.13×10^{-11} ergs radian⁻². Although the semi-empirical method is not good enough to give the bond length and bond energy changes, we feel it is the best available method for estimating half-bond bending force constants.

It has been stated that almost anything is linear in a log-log plot, and bond energy versus bond order is no exception, for carbon-carbon bonds, among others. Thus we assume that bond dissociation energy is proportional to bond order raised to some power, p

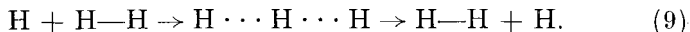
$$V = V_s n^p \quad (7)$$

where V is the potential energy (not including zero point energy). If we had some theoretical or empirical rate (from molecular structure or spectroscopy) for estimating p for C—H and H—H bonds, our goal would be reached of fitting all required potential energy properties for an activated complex to data 100 % external to kinetics itself. Unfortunately, at present we are forced to

evaluate p for C—H bonds from the activation energy of the symmetrical reaction (9) (ref. 9).



and we evaluate p for H—H bonds from the activation energy for the symmetrical ortho-, para-hydrogen reaction¹¹



The details of this procedure are given in Section VIII. The values found are $p_{\text{CH}} = 1.195$ and $p_{\text{HH}} = 1.086$.

All other features of this article are purely deductive from the stated assumption. The algebra for these deductions will be given here. For the reaction $\text{H}_3\text{C} + \text{H—H}$ the simplified model is:

Reactants			
Bond length	R_3	R'_2	R'_1
Force constant	∞	0	F'_1
Order		0	1
Complex			
Bond length	R_3	R_2	R_1
Force constant	∞	F_2	F_1
Bending force constant		Φ_b	Φ_a
Order		$(1-n)$	n

The potential energy relative to zero for reactants is

$$\begin{aligned} V &= V_1 - V_1 n_1^{p_1} - V_2 n_2^{p_2} \\ &= V_1(1 - n^{p_1}) - V_2(1 - n)^{p_2} \end{aligned} \quad (10)$$

The derivative of V with respect to order n is zero at the saddle-point or the maximum along the reaction path of Fig. 1:

$$dV/dn = 0 = -p_1 V_1 n^{p_1-1} + p_2 V_2 (1 - n)^{p_2-1} \quad (11)$$

By successive approximations this equation is readily solved for the order at the maximum, n^* , which when substituted into Eq. (10) gives the change in potential energy for activation; subtraction of zero point energies and correction for the temperature derivative of the partition functions gives the observed

activation energy. The second derivative of V with respect to n , multiplied by $(dn/ds)^2$, where s is the distance along the reaction path, gives the negative force constant at the saddlepoint:

$$d^2V/dn^2 = -p_1(p_1 - 1)V_1 n^{p_1-2} - p_2(p_2 - 1)V_2(1 - n)^{p_2-2} \quad (12)$$

$$(ds/dn)^2 = (0.6/2.303)^2 [1/n^2 + 1/(1 - n)^2] \quad (13)$$

$$-F^* = (d^2V/dn^2) (dn/ds)^2 \quad (14)$$

where Eq. (13) follows from Pauling's rule, Eq. (5). In terms of the general quadratic potential energy function

$$2V = F_1(dR_1)^2 + F_2(dR_2)^2 + 2F_{12}dR_1dR_2$$

but for the special case of along the reaction path

$$2V = -F^*(ds)^2 = -F^*[(dR_1)^2 + (dR_2)^2]$$

From Pauling's rule we get $dR_1/dR_2 = -n_2/n_1 = C$, and

$$F_{12} = [F_1C^2 + F_2 + (1 + C^2)F^*]/2C \quad (15)$$

It is F_{12} , not F^* , which is directly needed in $|\mathbf{F}|$ in (4).

The geometrical factors needed to set up Wilson's³⁸ \mathbf{G} -matrix have already been prescribed. With F_{12} as found above and the bending and stretching force constants derived above, the \mathbf{F} -matrix is also complete. The straightforward solution of $|\mathbf{FG} - \mathbf{E}\lambda| = 0$ gives the imaginary frequency ν^* as well as the real frequencies ν_i . From these frequencies the terms F_i in Eq. (4) can easily be evaluated.

From the bond lengths of this linear model, the J factors are just the volume of the container V for atom 1, $4\pi R_1^2$ for atom 2, R_2^2 for atom 3, and R_3^2 for atom 4. Thus all factors are found for Eq. (4), and we may compute activation energy, A factors, rate constants, or hydrogen-deuterium isotope effect for all isotopic variations of $\text{H}_3\text{C} + \text{H}-\text{H}$.

First, we shall summarize the numerical aspects of the above derivation. Correction of the H_2 dissociation energy at absolute zero for the zero point energy gives 109.4 kcal as the depth of the potential energy well, V_1 . Similarly, the depth of the well in the $\text{C}-\text{H}$ bond of methane, V_2 , is 108.5 kcal.¹⁸ The bond orders in the activated complex are $n_1 = 0.517$ and $n_2 = 0.483$.

The difference in potential energy between complex and reactants is 10.5 kcal. The potential energy along the reaction path is given in Fig. 3. The negative force constant is 0.82×10^5 dynes/cm, and the portion of the potential energy curve fit by the quadratic approximation is shown by dotted lines in Fig. 3. Stretching

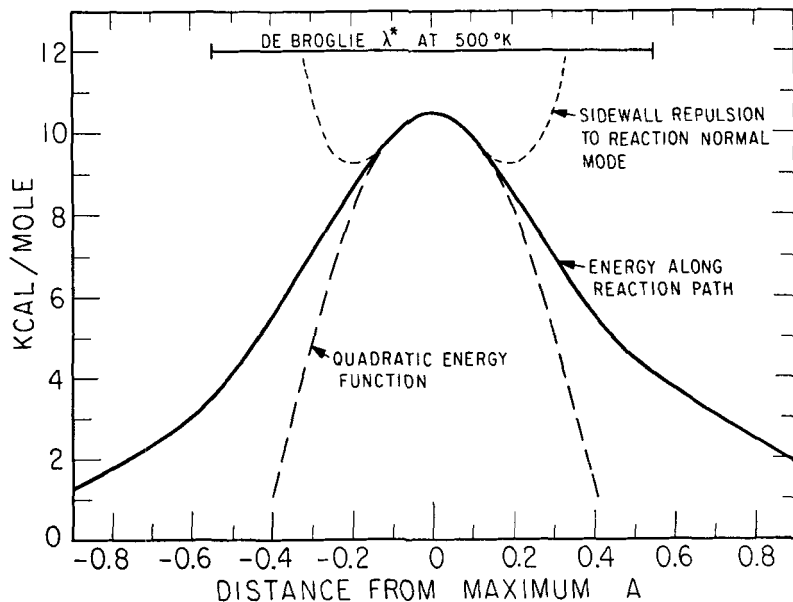
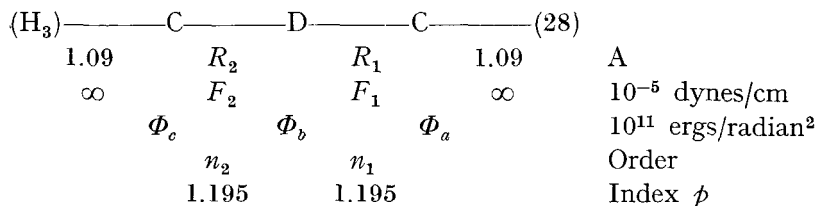


Fig. 3. Potential energy profile of reaction path for $\text{H}_3\text{C} + \text{H}_2$. The region described by the quadratic potential energy is indicated by the inner dotted-line curve. The upturned dotted-line curve is an intuitive estimate of the side-wall repulsions encountered by the extension of the tangent to the reaction path as shown in Fig. 1.

force constants were taken to be $F_1 = 2.87 \times 10^5$, $F_2 = 2.50 \times 10^5$ dynes/cm. Bending force constants were 0.13×10^{-11} ergs radian $^{-2}$ for $\text{C} \cdots \text{H} \cdots \text{H}$ and 0.26×10^{-11} for $\text{H}-\text{C} \cdots \text{H}$. The frequencies of vibration derived from this model have been given in Table I.

For the family of reactions of methyl radical attack on hydrocarbons, a single simplified model is used with one parameter V_1 to be varied from one reactant to another



A variation in the independently measured bond potential energy V_1 for bond 1 leads, as outlined above, to a predicted variation in R_1 , R_2 , F_1 , F_2 , n_1 , n_2 the Φ 's, and F^* . A list of these parameters for various values of V_1 is given in Table III together with properties of the reactant

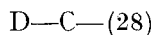


TABLE III. Variation of Properties of Activated Complex for $\text{H}_3\text{C---D---CR}$ Reaction as a Function of D---CR Bond Energy (Depth of Potential Well) where $\text{H}_3\text{C---D}$ Energy is 108.5 kcal

Depth of potential well, kcal	108.5	103	97.6	86.8	76	65
n_1	0.500	0.566	0.631	0.760	0.860	0.931
n_2	0.500	0.434	0.369	0.240	0.140	0.069
ΔV_{act} , kcal	13.7	10.8	8.40	4.51	2.20	0.93
R_1 , Angstroms	1.27		1.21	1.16	1.14	1.11
R_2	1.27		1.35	1.46	1.60	1.79
$F_1 \times 10^{-5}$ dynes/cm	2.50		3.16	3.80	4.30	4.65
F_2	2.50		1.84	1.20	0.70	0.35
F^*	1.13		0.93	0.56	0.28	0.11
$\Phi_b \times 10^{11}$ ergs/radian ²	0.13		0.122	0.095	0.063	0.033
Φ_a	0.26		0.328	0.395	0.447	0.484
Φ_c	0.26		0.192	0.125	0.073	0.036
ω^* cm ⁻¹	1412i		1412i	1382i	1365i	
ω str	668		668	715	763	
ω bend	852			789		
ω wag sym	419			332		
ω wag antisym	154			139		
ω str reactant	2124					
ω bend reactant	807					

With symmetrical bond energies and indices p , the bond orders are symmetrical, the activation energy is a maximum for the series, and the curvature F^* is the greatest. As the reaction becomes more exothermic, the activated complex more nearly corresponds to reactants: the order of the bond to be broken increases, it is less extended, the activation energy decreases, and the negative force constant F^* decreases. These deductions are consistent with Polanyi's²⁶ conclusions, which were based largely on a one-dimensional analysis of intersecting Morse functions. For the activation energy trend Polanyi proposed the relation $E_{\text{act}} = E_0 - \alpha q$, where q is the heat of reaction and E_0 and α are two parameters to be determined from kinetic data; Polanyi's relation suffers from the logical disadvantage of predicting a negative activation energy for a sufficiently exothermic reaction. The present formalism requires only one parameter from kinetics, either p or any one activation energy; also it asymptotically approaches zero for highly exothermic reactions. The relation is more cumbersome than the Polanyi relation, being

$$V_{\text{act}}/V_2 = (1 - q/V_2) \{1 - [1 + (1 - q/V_2)^{1/(p-1)}]^{1-p}\} \quad (16)$$

where $-q$ is $V_2 - V_1$. This, of course, gives the change in potential energy for activation; a vibrational analysis is required to convert this to the observed activation energy.

The reaction coordinate is the normal mode associated with the imaginary frequency, as found by a normal coordinate analysis of the quadratic region near the saddlepoint. Even though F^* decreases fairly rapidly as the reaction becomes exothermic, the imaginary frequencies change relatively slowly, as we see from the entries in Table III. This feature is a qualitative illustration of what we see definitely when the normal coordinates are worked out: the reaction coordinate is not, in general, along or tangent to the reaction path, (except for symmetrical activated complexes) but it is a straight line crossing it at some angle. The reaction coordinate, which is essentially the antisymmetric stretching vibration, remains almost purely a hydrogen atom motion even for large asymmetries of bond order. Similarly, the stretching vibration is largely the reduced-mass

motion of the end groups, and the bending and wagging vibrations change but slowly with changing bond order.

We feel that the properties of the activated complexes as given in Table III cannot be quantitatively precise; on the other hand we believe no gross qualitative errors are introduced, such as the spurious well in the top of the pass as given by Eyring's semi-empirical method or the excessively sharp curvature at the top of the pass as given by Sato's semi-empirical method. For future use in this article, we now want to point out two features which limit the extent of the quadratic region: In Fig. 3 the energy along the reaction path is adequately fitted by a parabola for only about $\pm 0.15A$; from Figs. 1 or 2 we see that the curvature along the reaction path is such that the straight-line reaction normal mode can at most extend $\pm 0.15 A$ without encountering serious repulsions against the rising potential energy on the sides of the reaction path.

V. TUNNELLING FACTORS

For a particle encountering a one-dimensional parabolic barrier, jointly characterized by an imaginary frequency ω^* cm^{-1} , the parameter which determines the degree of tunnelling is $u^* = \hbar c \omega^* / kT$. R. P. Bell² has shown that for $u^* \ll 2\pi$, the tunnelling factor is

$$I^* = (u^*/2) / \sin (u^*/2) \quad (17)$$

and its change with temperature is given by

$$(1/T)(d \ln I^* / d 1/T) = 1 - (u^*/2) \operatorname{ctn} (u^*/2) = -\theta^* \quad (18)$$

For comparison it will be recalled that for real vibrations

$$I = (u/2) / \sinh (u/2) \quad (19)$$

$$(1/T)(d \ln I / d 1/T) = 1 - (u/2) \operatorname{ctnh} (u/2) = -\theta \quad (20)$$

The relation between the change in potential energy for activation and the observed activation energy for methyl radical reactions is

$$E_{\text{act}} = \Delta V_{\text{act}} + RT \left[5/2 + \sum_{\text{complex}} \theta + \theta^* - \sum_{\text{reactants}} \theta \right] \quad (21)$$

Mr. Donald Rapp²⁷ of this laboratory has solved for the distribution function for molecules which react, according to Bell's tunnelling formula. For hydrogen atom transfer with activation energies such as are found for methyl radical reactions, he finds there is extensive tunnelling below the region where the parabola fits the reaction path energy as given by Fig. 3, if $u^*/2$ exceeds about 1.8. Thus we set an upper limit of 1.8 on the validity of Eqs. (17) and (18) for the methyl radical reactions. (The range of validity of Wigner's¹³ correction of $1 + u^2/24$ is at most $u/2 = 1.0$). For hydrogen atom transfer to methyl radicals, the condition of $u/2$ less than 1.8 is valid only above about 750°K, and virtually all experimental data falls in the excluded range.

To permit us to apply large tunnelling corrections, Rapp carried out a graphical integration of the tunnelling factor for an Eckart⁹ potential. For a single energy the tunnelling factor for this potential is a known simple expression;¹⁰ for a Boltzmann distribution of incident particles, a graphical integration was required. A symmetrical Eckart potential was used with curvature at the top fitted to that of Fig. 3 and with the flat portion at infinity fitted to the energy of the reactants; thus ΔV_{act} and F^* are fitted to the real problem. Above $u^*/2 = 1.8$, Bell's correction greatly overestimates the degree of tunnelling; and above some as yet undetermined value the Eckart potential surely overestimates it also. The reaction normal mode is a straight line in Fig. 1 through the saddlepoint. The reaction coordinate and the reaction path are not the same thing. The Eckart-potential correction is computed as if the reaction normal coordinate continued all the way to reactants, and this is grossly not true. Outside the quadratic region near the saddlepoint, the coordinates are mixed; any one is not conservative. Every change in direction along the curved reaction path corresponds to a changed effective mass. Skewing the coordinates to make the mass constant¹² and thus diagonalizing the kinetic energy leaves the potential energy function mixed up and non-diagonal; it by no means generates a reaction normal coordinate which is separable outside the quadratic region. Our method of picking certain features of the potential energy surface from strictly empirical considerations does not give an estimate

of the rise of potential energy on each side of the reaction path. Thus we have no basis for predicting the potential energy actually encountered by an extension of the reaction normal coordinate beyond its separable region; a purely qualitative guess as to this energy is given by the upturned dotted lines in Fig. 3. Even if we knew the potential encountered by the extended reaction normal mode, it would not solve the problem, because the quantum mechanical tunnelling from one non-separable region to another need not occur along or even parallel to the classical mechanical normal mode. Apparently the problem is one in two-dimensional nonseparable time-dependent quantum mechanics, and we see no rigorous method of reducing it to two separate one-dimensional problems.

From these considerations we see quite clearly that below 750°K for methyl radical reactions, tunnelling is very important, but Bell's correction for a parabolic barrier greatly overestimates the effect, and the Eckart potential along the artificially straightened reaction path also overestimates the tunnelling, though in this case it is difficult to set limits *a priori*. We turn, therefore, to the experimental data to see if a comparison of calculated and observed rate features gives any further information as to the magnitude of tunnelling for methyl radical reactions. The tunnelling factor which we use is derived as follows: for Eckart potentials the ratio $2\pi V^*/\hbar\nu^*$ is an important index, and different curves for I_* are obtained for each value of this ratio. For methyl radical reactions this index is about 10 or 12, and for this value the fourth power expansion of Bell's correction

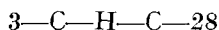
$$(u/2)/\sin(u/2) \approx 1 + (u/2)^2/3! + 7(u/2)^4/(3 \times 5!) + \dots \quad (22)$$

is an excellent approximation out to $u/2 = 2.5$, and it falls somewhat below the Eckart function for higher values of $u/2$. Thus we are daring to use Eq. (22) out to $u/2 = 3.1$, and all actual tunnelling corrections are based on this relation. (This decision was made before any actual application to data was carried out. The advantage of this choice is that the temperature coefficient θ is a simple function; use of the Eckart function would require graphical differentiation for θ .)

VI. APPLICATION TO EXPERIMENTAL DATA

A failure of these calculations to fit experimental data could be ascribed to either of two sources: (1) The failure of the empirical rules about conservation of bond order, Pauling's bond order and bond length relation, the relation between bond order and bond energy, etc; or (2) the failure of the assumption of separability if large degrees of quantum mechanical tunnelling override the classical mechanical theorems about small vibrations and separable normal modes. In an effort to evaluate the first item above, we should focus attention on rate constants at high temperature, especially for deuterium atom transfer. The kinetic isotope effect, k_H/k_D , then provides a fairly sharply differentiated test of item (2) above, especially at low temperatures, although in all cases there is considerable overlap of the contributions of the two factors.

The reaction of methyl radicals with acetone is perhaps the most extensively and carefully studied reaction in the chemical literature. For the vibration frequencies which change upon forming an activated complex, we believe the substitute model of five linear atoms



constitutes an adequate approximation to the activated complex. For acetone or ethane¹⁸ as reactant the ratio V_1/V_2 is taken to be 0.97; the bond orders then are $n_1 = 0.539$ and $n_2 = 0.461$; and the change in potential energy upon activation is 12.0 kcal. We have noticed that the frequencies change very slowly between $n_1 = 0.45$ to $n_1 = 0.55$ and the imaginary frequency not at all. Consequently we use the frequencies from Table III for the symmetrical complex for this problem. For $CH_3 + D - CR$ the calculated activation energy is 12.4 kcal at 600°K and the Arrhenius A -factor at 600°K is 2.7×10^{11} cc mole⁻¹ sec⁻¹ per reaction site. Literature values for A -factors and E vary somewhat from one author to another, but these values are definitely within the range claimed.³³ A more stringent and interesting test of the theory is to calculate actual rate constants over a wide range of temperature and compare them with experimental data.

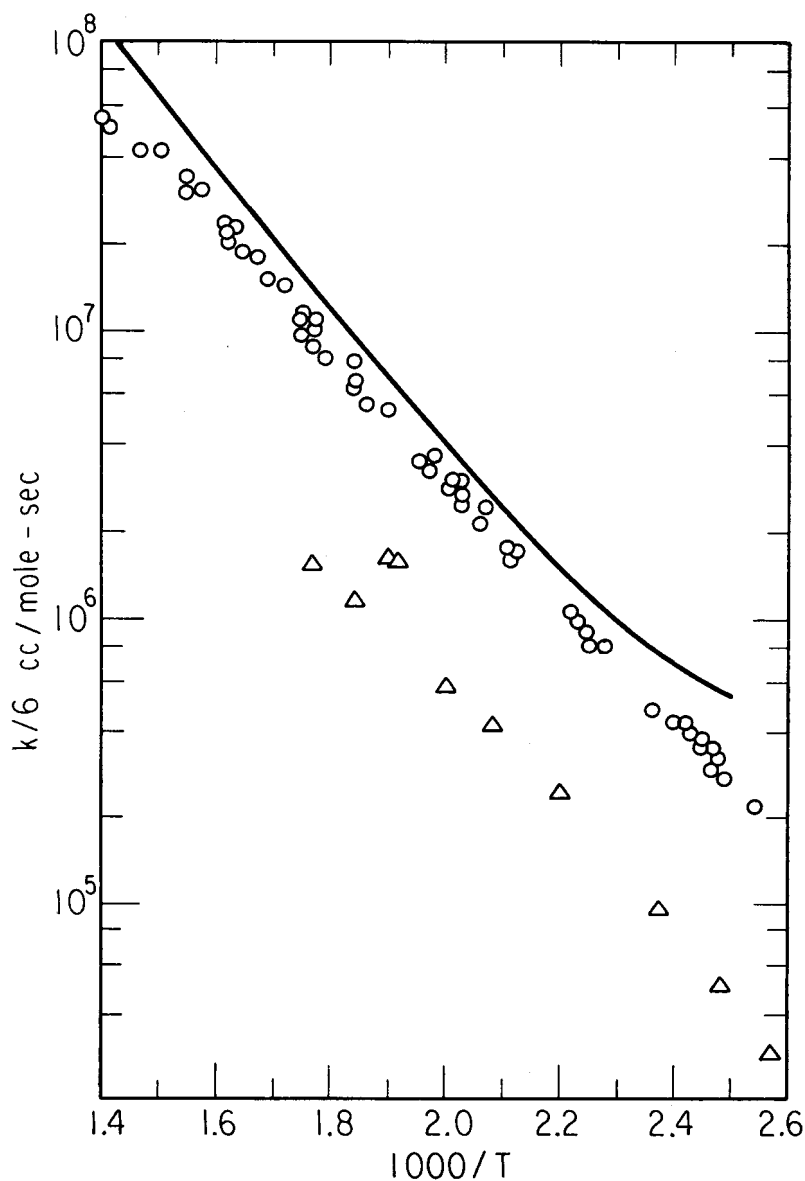


Fig. 4. Calculated and observed rate constants per reaction site for the reaction of methyl radicals with primary hydrogen atoms in ethane or acetone. \circ , $\text{CH}_3 + \text{CH}_3\text{COCH}_3$; \triangle , $\text{CD}_3 + \text{CH}_3\text{CH}_3$.

In Fig. 4 a curve is given for calculated rate constants for $\text{CH}_3 + \text{CH}_3\text{COCH}_3$ at different temperatures. Within the limits of our assumed model this calculated curve also applies to $\text{CD}_3 + \text{CH}_3\text{CH}_3$. Experimental points from many different workers in Steacie's laboratory^{20, 21, 23, 34, 35} are plotted on the same scale as are the data for deuteromethyl radicals with ethane.³⁴ Either of these sets of data confirm that this method, which is absolute so far as these reactions are concerned, gives the right order of magnitude of the rate constant, especially at high temperatures. This model is not fine enough to pick up the difference between ethane and acetone, but so far no gross failure of the model is indicated.

The calculated curve in Fig. 4 shows a sharp bending of the Arrhenius plot around 400°K; this feature is introduced by the tunnelling function. The experimental data do not show this bending around 400°K, but the data do show just such an anomaly about 100 degrees lower.^{8, 22} This anomaly has been ascribed to hot radical reactions, although we believe it to indicate extensive tunnelling. The occurrence of this curvature at a lower temperature indicates that tunnelling is less than we calculate, but still highly important. If this explanation is correct, the interesting experiment would be to study $\text{CD}_3 + \text{CD}_3\text{COCD}_3$ between 27°C and 100°C. The break in the curve should be very much less pronounced for the deuterium case, and the kinetic isotope effect should become large, a factor of 20 or so.

The kinetic isotope effect is independent of small errors in calculated activation energy, and it is a sharp test of the vibrational analysis and tunnelling correction. Steacie and coworkers have thoroughly studied $\text{CH}_3 + \text{CH}_3\text{COCH}_3$ and $\text{CD}_3 + \text{CD}_3\text{COCD}_3$ in separate experiments, and rate ratios at three typical temperatures³⁷ are computed from the separate sets of data and presented in Fig. 5. McNesby and Gordon¹⁹ have studied mixtures of CH_3COCH_3 and CD_3COCD_3 , and obtained directly the ratio of rates for $\text{H}_3\text{D}-\text{H}-\text{CH}_2\text{COCH}_3$ and $\text{H}_3\text{C}-\text{D}-\text{CD}_2\text{COCD}_3$; these studies include low temperature photolyses and high temperature pyrolyses. Rice and Vanderslice²⁸ thermally decomposed a trace (1 per cent) of $\text{CH}_3\text{N}_2\text{CH}_3$ in the presence of CH_3CD_3

to obtain directly k_H/k_D . These three sets of data are plotted on Fig. 5, together with a calculated curve with tunnelling correction and a calculated curve omitting the tunnelling correction. Here, quite clearly, we see that some tunnelling correction is required, but that the function we use overestimates it. This conclusion is

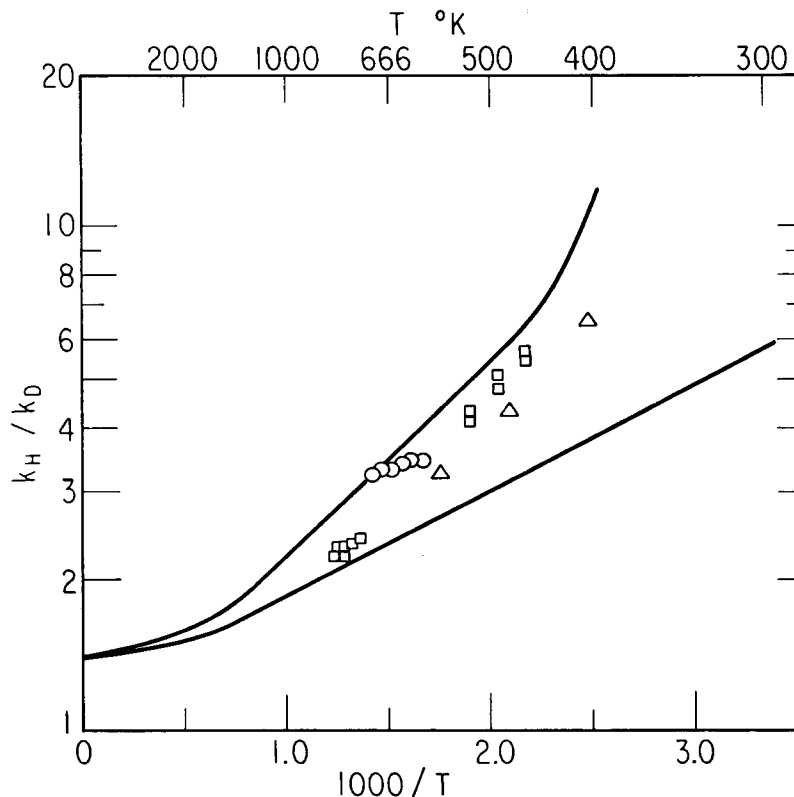


Fig. 5. Kinetic isotope effect for reactions of methyl radicals with primary hydrogen atoms in ethane or acetone, for $(H_3C + H-CR)/(H_3C + D-CR)$.

○, ethane, ref. 28; △, acetone, ref. 37; □, acetone, ref. 19.

much firmer than the similar one reached relative to absolute rates and Fig. 4.

For the calculations above with acetone and ethane as reactants, we suffer from some disadvantage in not knowing

precisely the properties, especially bond dissociation energies, of the reactants. Many dissociation energy methods are kinetic in nature,⁶ we find tunnelling to be very important in hydrogen atom reactions, tunnelling acts to lower the activation energy below the classical value, and thus bond dissociation energies themselves are perturbed by tunnelling and uncertain by a kilocalorie or more. This disadvantage is absent when we consider hydrogen or deuterium as the reactant. Thus our main emphasis in the test of these methods is on the family of reactions $\text{H}_3\text{C} + \text{H}_2$, where various deuterium substitutions are made. The properties of reactants and activated complexes are given in Table I. From these bond distances, force constants, and frequencies, one can immediately calculate rate constants or rate constant ratios at any temperature. By evaluating the θ 's of Eqs. (18, 20) we can evaluate Arrhenius A -factors and activation energies.

TABLE IV. Calculated and Observed Arrhenius Rate Factors at 563°K for Reactions of Methyl Radicals with Hydrogen ^a

Reaction	ΔV_{act}		log A -factor		E_{act}
	Obs.	Calc.	Obs.	Calc.	Obs.
H_3CHH	10.8	10.5	11.1	11.3	10.0
H_3CHD	11.0	10.5	11.0	11.2	10.0
H_3CDH	10.5	10.5	11.4	11.5	11.3
H_3CDD	11.0	10.5	11.5	11.4	11.8
D_3CHH	12.0	10.5	11.7	11.3	11.1
D_3CHD	11.7	10.5	11.2	11.2	10.7
D_3CDH	9.9	10.5	11.2	11.5	10.7
D_3CDD	10.2	10.5	11.1	11.4	10.9

^a Energies are kcal/mole and A -factors are cc/mole-sec.

Marjury and Steacie²¹ and Whittle and Steacie³⁷ have studied in detail the kinetics of the eight reactions whose activated complexes are given in Table I. For all eight of these reactions the observed activation energies corrected for zero-point energy and for thermal excitation energy, by way of θ of Eqs. (18, 20), should give the same value for ΔV_{act} . Our method of estimating

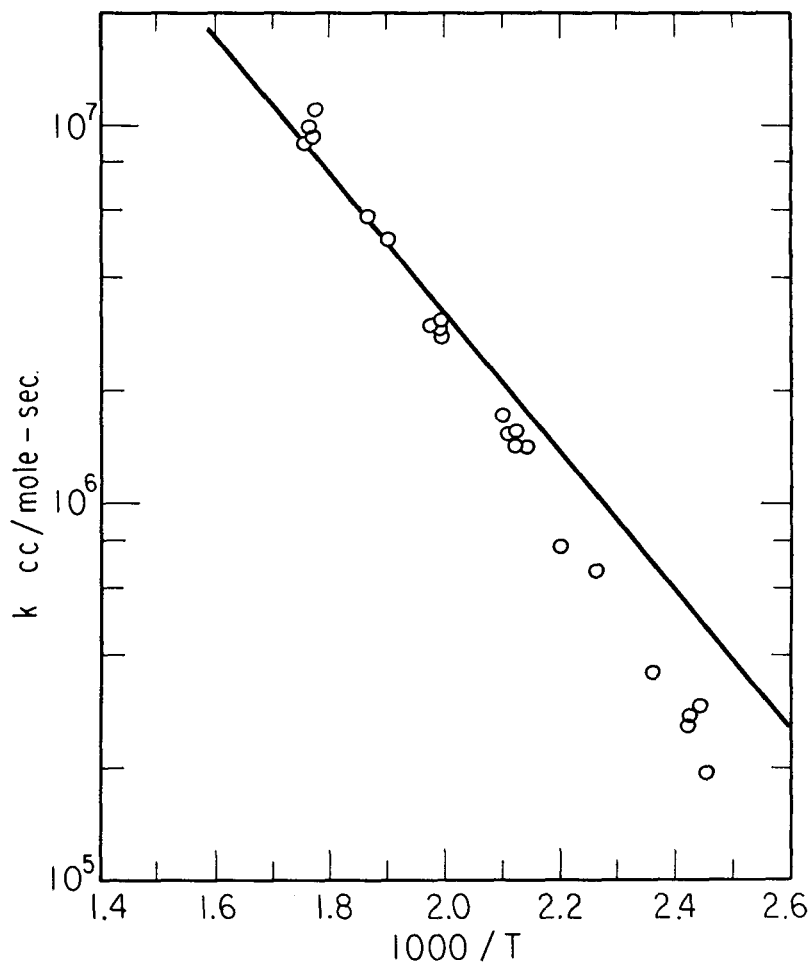


Fig. 6. Calculated and observed rate constants per reaction site for $\text{H}_3\text{C}-\text{D}-\text{H}$.

ΔV_{act} gives 10.5 kcal. This value is compared with the eight values deduced from experiment in Table IV; the average of these is 10.9 kcal. For the four reactions involving CH_3 radicals, the ΔV_{act} are as nearly constant as one could expect, but the values for the CD_3 radicals are badly scattered. We believe there are some spurious temperature-dependent trends in these data. The

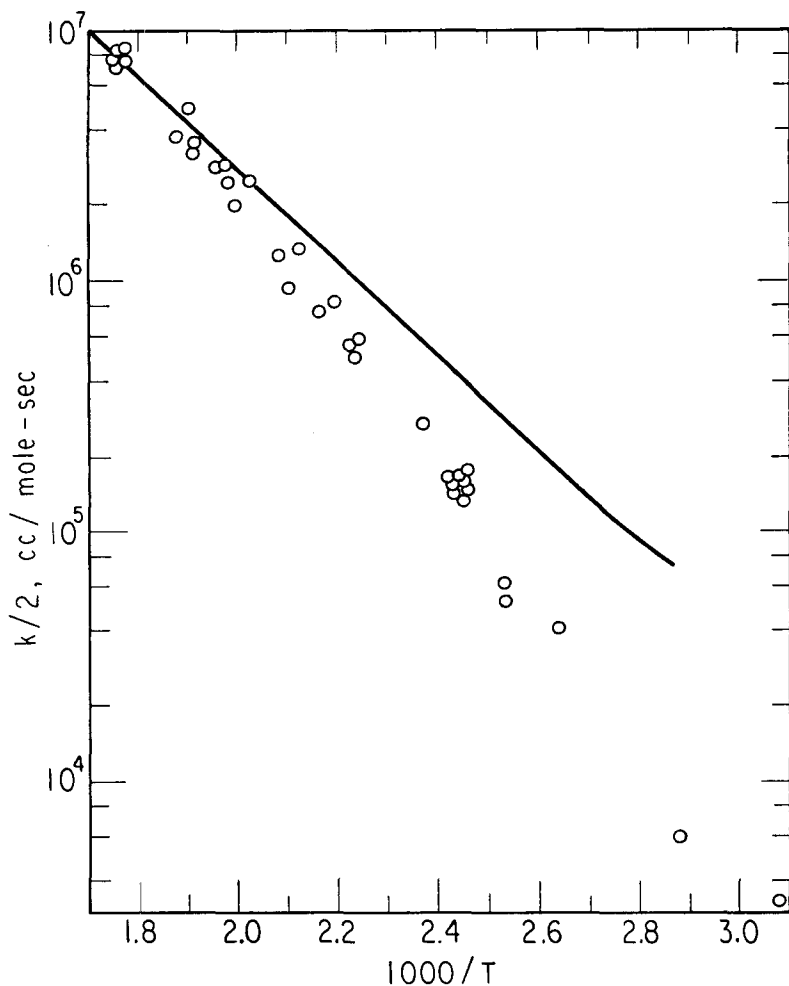


Fig. 7. Calculated and observed rate constants per reaction site for $\text{H}_3\text{C}-\text{D}-\text{D}$.

eight A -factors are also listed in Table IV, together with calculated values. In general the calculated A -factors agree with experiment; the average absolute deviation is 0.20 log units or a factor of 1.6; and the average net deviation is that calculated values are higher by 0.14 log units or a factor of 1.4. As noted

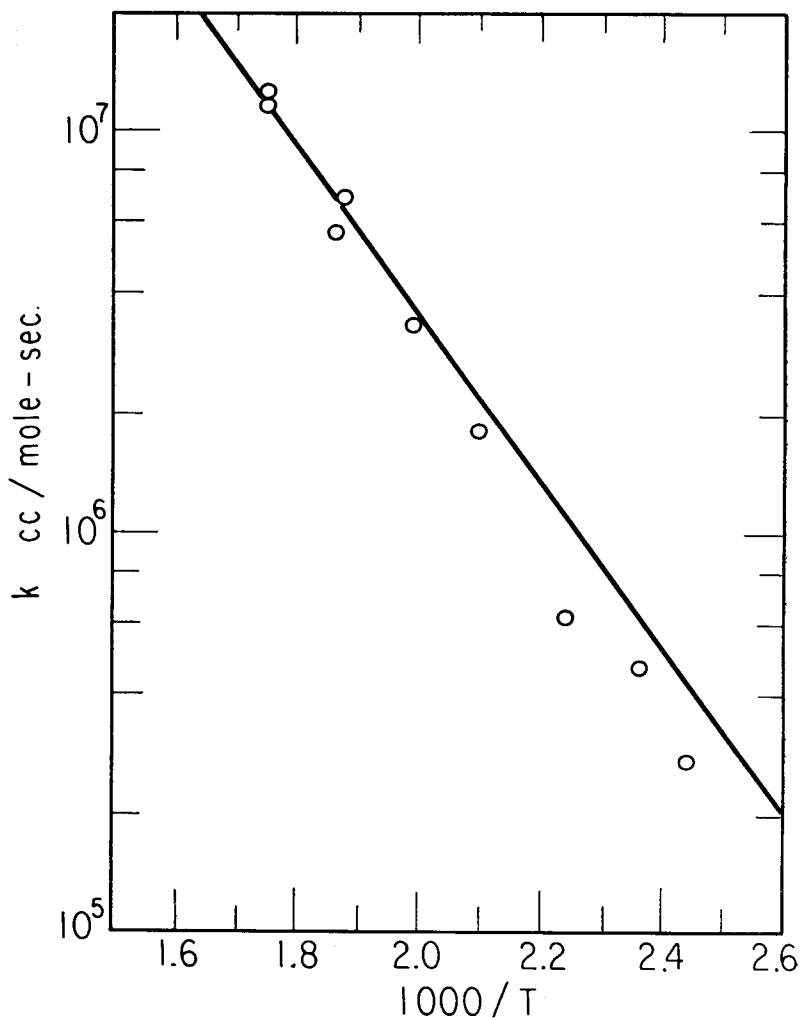


Fig. 8. Calculated and observed rate constants per reaction site for D_3C-D-H .

before, A -factors are relatively insensitive tests of theory; absolute values of the rate constant or k_H/k_D ratios are much more sensitive.

In Figs. 6, 7, 8, and 9 we plot calculated rate constant curves

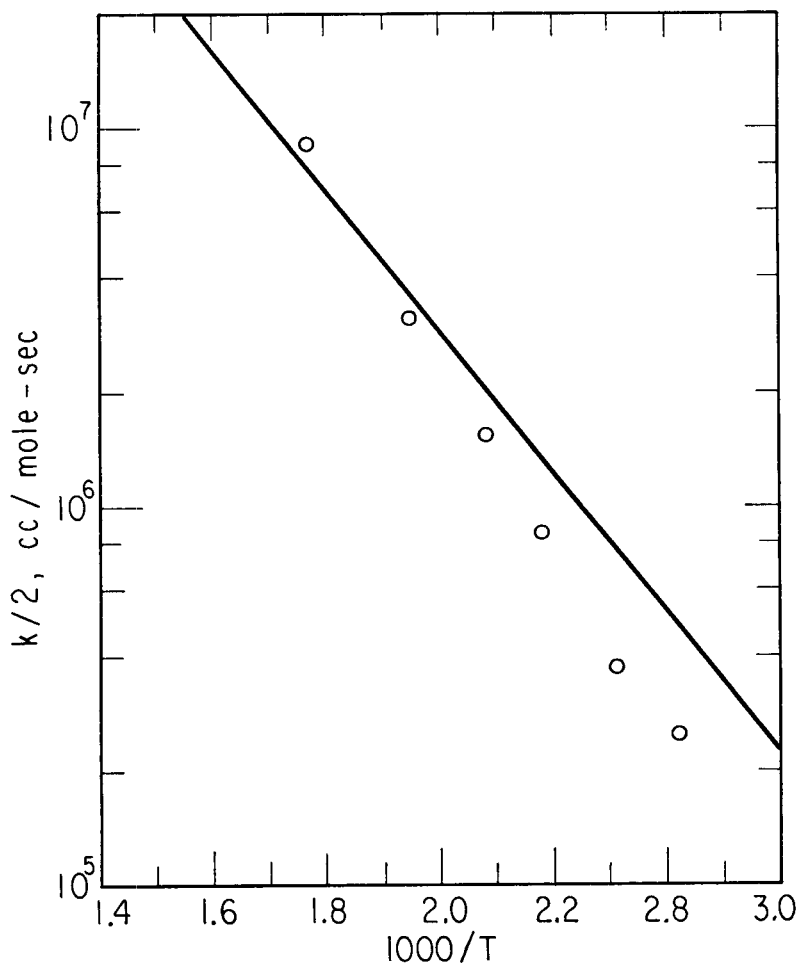


Fig. 9. Calculated and observed rate constants per reaction site for $\text{D}_3\text{C}-\text{D}-\text{D}$.

and observed rate constants per reaction site against temperature for all reactions in which deuterium is the atom transferred. The reactions, especially at high temperature, are only very slightly affected by tunnelling corrections. All of these plots show amazing agreement of calculated rate constants at high temperatures. At low temperatures the calculated curves, with their heavy tun-

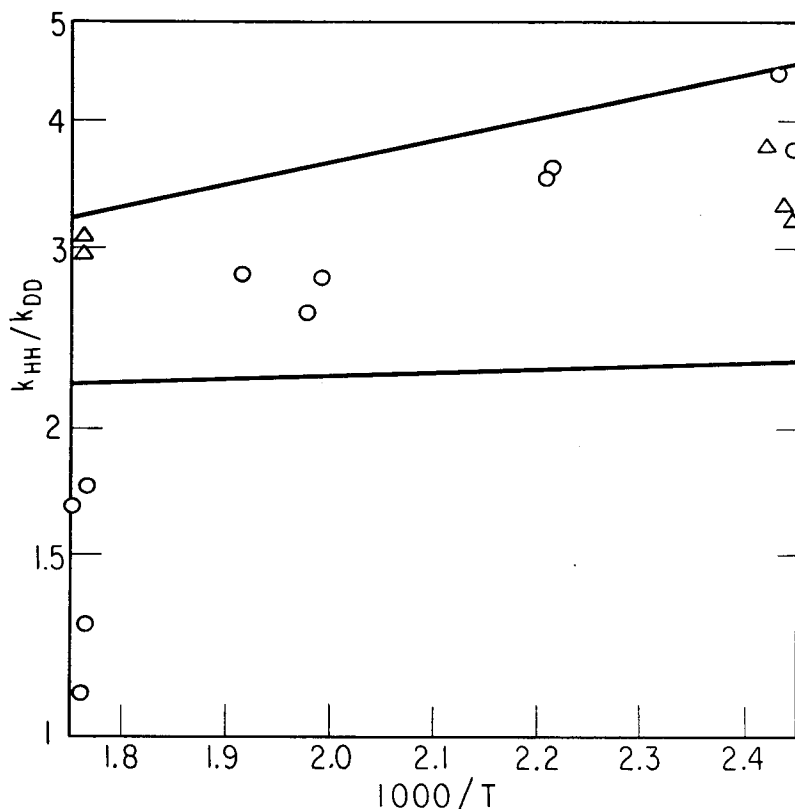


Fig. 10. Calculated and observed kinetic isotope effect per reaction site for reaction of methyl radicals with hydrogen species. Upper line is calculated rate ratio including ratio of tunnelling factors; lower curve is calculated with omission of ratio of tunnelling factors. ○, $(\text{H}_3\text{C}-\text{H}-\text{H})/(\text{H}_3\text{C}-\text{D}-\text{D})$; Δ, $(\text{D}_3\text{C}-\text{H}-\text{H})/(\text{D}_3\text{C}-\text{D}-\text{D})$.

nelling corrections, overestimate the rate.* These figures give us considerable confidence that the empirical rules from other fields with the p factors other reactions are not totally wrong, and we can turn to isotope effects at low temperatures for a relatively unambiguous answer to the contribution from tunnelling.

* The first effect of large tunnelling corrections is to lower the activation energy while preserving the form of the Arrhenius equation; it requires extremely large tunnelling factors to give a significant curvature on an Arrhenius plot.

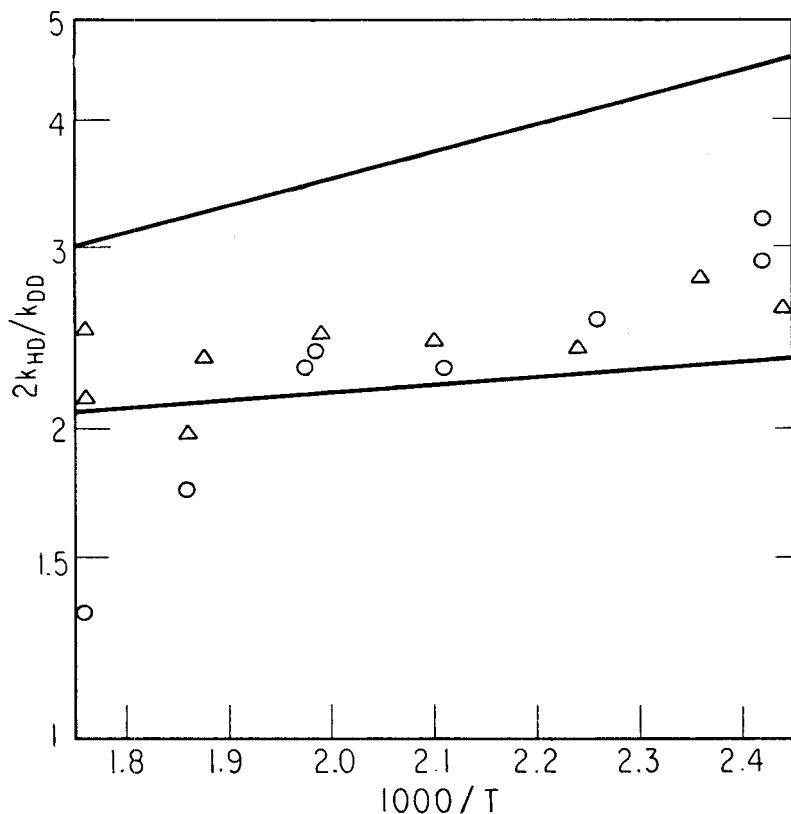


Fig. 11. Calculated and observed kinetic isotope effect per reaction site for reaction of methyl radicals with hydrogen species. Upper line is calculated rate ratio including ratio of tunnelling factors; lower curve is calculated with omission of ratio of tunnelling factors,

O, $(\text{H}_3\text{C}-\text{H}-\text{D})/(\text{H}_3\text{C}-\text{D}-\text{D})$; Δ , $(\text{D}_3\text{C}-\text{H}-\text{D})/(\text{D}_3\text{C}-\text{D}-\text{D})$.

Except for the $\text{Me}-\text{H}-\text{D}/\text{Me}-\text{D}-\text{H}$ reactions, these studies were carried out on separate systems with one hydrogen species at a time. The experiments were never run at identical temperatures for two different isotopes, and so direct presentation of experimental rate ratios is difficult. If all sets of data are fit to the Arrhenius equation by least squares, we can then pick off points at definite temperatures, but then we lose all feeling for the magnitude of experimental error. We have taken the least

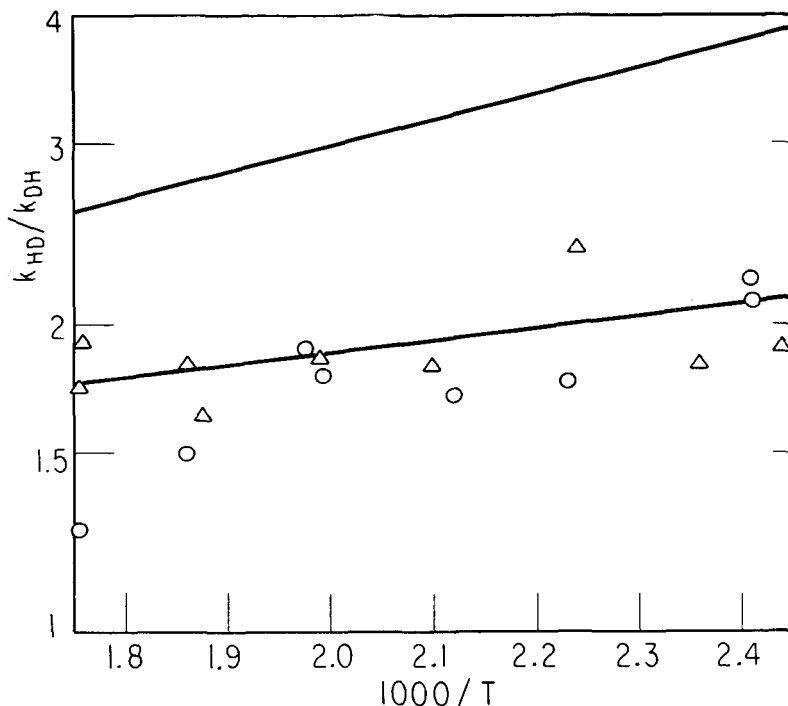


Fig. 12. Calculated and observed kinetic isotope effect per reaction site for reaction of methyl radicals with hydrogen species. Upper line is calculated rate ratio including ratio of tunnelling factors; lower curve is calculated with omission of ratio of tunnelling factors.

O, $(H_3C-H-D)/(H_3C-D-H)$; Δ , $(D_3C-H-D)/(D_3C-D-H)$.

squares parameters for the reactions H_3CDD and D_3CDD and from them constructed curves for these reactions over the full temperature range. To get the experimental point for the kinetic isotope effect of H_3CHH/H_3CDD , for example, we read off the curve for H_3CDD the rate constant it would have at the temperature at which a run on H_3CHH was made. Then we take the experimental point for H_3CHH and divide it by the interpolated point for H_3CDD to get an "observed" k_H/k_D . The experimental points in Fig. 10 were found in this way, and similar treatment produced Figs. 11, 12, and 13. This method smooths out some experimental scatter, but it still leaves enough to provide some

feeling for its magnitude. Reactions of CD_3 radicals are computed to be about 3 to 8 per cent faster than CH_3 radicals; these small effects are ignored in Figs. 10–13, and data for CD_3 and CH_3 radicals are pooled on each graph.

The theoretical curves for the kinetic isotope effect are presented in Figs. 10–13 with the tunnelling correction as described above. Also in each case a curve is given in which the tunnelling factor has been omitted entirely. The ratios of rates for $\text{H}_3\text{CHH}/\text{H}_3\text{CDD}$

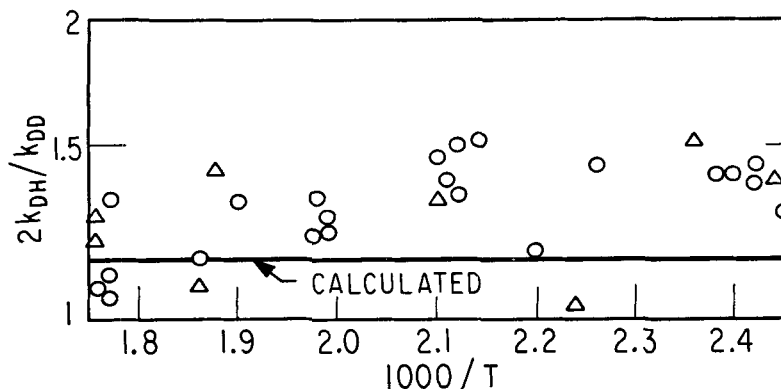


Fig. 13. Calculated and observed kinetic isotope effect per reaction site for reaction of methyl radicals with hydrogen species. The theoretical ratio of tunnelling factors is essentially unity for these cases, so that there is only one calculated curve. O, $(\text{H}_3\text{C}-\text{D}-\text{H})/(\text{H}_3\text{C}-\text{D}-\text{D})$; Δ , $(\text{D}_3\text{C}-\text{D}-\text{H})/(\text{D}_3\text{C}-\text{D}-\text{D})$.

and $\text{D}_3\text{CHH}/\text{D}_3\text{CDD}$, as given in Fig. 10, scatter rather badly but in general lie between the tunnelling and nontunnelling curves. As a whole, this figure seems to indicate that some tunnelling is surely occurring, but our method substantially overestimates the effect. The reactions in Fig. 11 have the same end atom, and isotopic change occurs at the center only: $\text{H}_3\text{CHD}/\text{H}_3\text{CDD}$ and $\text{D}_3\text{CHD}/\text{D}_3\text{CDD}$. In this case the points lie above the curve for no tunnelling. Probably some tunnelling is indicated, but it is far less than expected by our method. The best data of any should be the competitive reactions with HD. In Fig. 12 we see the direct experimental ratios for $\text{H}_3\text{CHD}/\text{H}_3\text{CDH}$

and D_3CHD/D_3CDH . Here the answer is quite clear-cut: the curve with no tunnelling correction describes the data fully. Either no tunnelling at all occurs here or *equal amounts* occur for $Me-H-D$ and $Me-D-H$, contrary to the dictates of the classical mechanical normal modes based on small displacement theory. This matter will be discussed again later. Meanwhile we look at Fig. 13 where the transferred atoms are the same and no difference in rate is expected except for a small correction, 1.15, for differences in the wagging vibrations as the end mass changes. The reactions are H_3CDH/H_3CDD and D_3CDH/D_3CDD . Here we seem to have tunnelling, comparable to Fig. 11, certainly, when the end atom is H instead of D. This fact leads us to postulate that, speaking loosely, the end atom if light can "tunnel away" as well as the center atom "tunnel across". This conclusion is completely contrary to classical small vibration theory and roughly symmetrical bond orders. Apparently we are, indeed, facing a situation of two dimensional nonseparable quantum mechanical tunnelling.

Without going into detail, we may point out another case where a similar explanation may be needed for the anomaly at hand. Bigeleisen and co-workers⁴ reviewed the literature and added new experimental results for the reaction of chlorine atoms with hydrogen species, H_2 , HD , D_2 , and HT . These data were interpreted according to activated complex theory and for several potential energy surfaces, including Sato's.²⁹ Large tunnelling corrections were made by means of Bell's² parabolic relation. Although many features of the results could be explained very satisfactorily, no model (using, it may be noted, quadratic potential energy parameters) was adequate to account for all the data of all the isotopes. We believe this case, also, is an example of large scale quantum mechanical leakage, and nonclassical behavior by the light end atom as well as the atom transferred.

VII. SUMMARY AND CONCLUSIONS

The experimental data seem to be telling a clear-cut but unusual story. At high temperatures with deuterium atom transfer the observed rate constants agree extremely well with

calculated rate constant, so that we feel fairly confident about the broad aspects of the method and model.

The kinetic isotope effect at low temperatures shows large degrees of tunnelling for $\text{H}_3\text{CHCR}/\text{H}_3\text{CDCR}$, but substantially less than we predict from a one-dimensional correction when the reaction normal coordinate is extended along the reaction path, ignoring the curvature of the reaction path. It may be recalled that previous calculations of A -factors,³⁹ with no correction for barrier penetration for hydrogen-atom transfer, agreed fairly well with experiment. When the end groups are heavy and the transferred atom is light, the curvature along the reaction path plus the rising potential energy along each side force the system to behave more nearly classically than indicated by the extended one-dimensional model.

For the family of reactions involving methyl and hydrogen, the kinetic isotope effect shows substantial degrees of tunnelling, in general, but the relative amount from one reactant species to another is quite surprising. The displacement of the observed rate constant ratios $k_{\text{H}}/k_{\text{D}}$ from the curve calculated for no tunnelling in Figs. 10–13 is interpreted as the logarithmic *difference* in tunnelling for the two species involved. Figure 10 shows that H_3CHH tunnels substantially more than H_3CDD , not a surprising finding. Figure 13 demonstrates that H_3CDH tunnels more than H_3CDD ; this finding is inconsistent with the usual assumption that rate problems can be treated in terms of separable coordinates. A comparison of Figs. 11 and 13 reveals that the difference in tunnelling for $\text{H}_3\text{CDH}/\text{H}_3\text{CDD}$ is every bit as big as for $\text{H}_3\text{CHD}/\text{H}_3\text{CDD}$; this, too, is quite contrary to the assumption that quantum mechanical barrier penetration occurs along classical mechanical normal mode paths. Figures 11 and 13 provide the explanation for the anomaly of Fig. 12; it is not that no tunnelling occurs for $\text{H}_3\text{CHD}/\text{H}_3\text{CDH}$ but that the same amount occurs for each. It is as if we have a reduced mass tunnelling of both hydrogens, instead of the normal coordinate motion which is a simple transfer of the central one.

The inevitability of these conclusions is brought in Figs. 1, 2, and 3, by certain features upon which no previous comment has

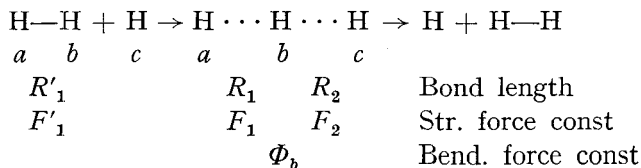
been made. The relation of the de Broglie wavelength of the motion of interest to the curvatures of the reaction path and energy profile is shown in the first three figures. The mass in the reaction coordinate for an atom transfer complex with symmetrical force constants is half the reduced mass of the atom transferred and the sum of the end groups. If the end groups are heavy, this mass is simply half the mass of the atom transferred. Thus it is easy to calculate the de Broglie wavelength for motion along the reaction normal mode, $\lambda = h/(2\pi m^* kT)^{1/2}$. If hydrogen is the atom transferred at 500°K, the de Broglie wavelength is 1.1 Angstrom units! For symmetrical force constants, the mass of the real symmetric stretch vibration is simply the reduced mass of the two end groups. For $\text{H}_3\text{C}-\text{H}-\text{C}-28$, the de Broglie wavelength for the symmetrical stretching vibration is about 0.25 Å; for $\text{H}_3\text{C}-\text{H}-\text{H}$ it is about 0.8 Å. The area enclosed by these wavelengths is given in Fig. 1 and Fig. 2. The de Broglie wavelengths along the reaction coordinate clearly overlaps enormous curvature along the reaction path. As seen in Fig. 3 it extends far beyond the quadratic potential, that is, far outside the region of separability. Inside the area given, more or less, by the de Broglie wavelengths in Figs. 1 and 2, we may not use classical mechanics. Even if the translations of the reactants are effectively classical over far distant regions, inside an area about the size of that shown in the figures we must use a proper quantum mechanical treatment throughout. Since this area spreads out over non-quadratic potential energy regions, the normal mode coordinates are not separable. In our treatment (following Bell and others) we applied quantum mechanics to the reaction coordinate but only after separating out classical normal coordinates and extending them far beyond their valid range. For heavy end groups the principal effect is to encounter the steep side-wall repulsions, arbitrarily sketched in Fig. 3; thus tunnelling is simply overestimated since there is really only one direction in which it can occur. If the height of the minimum of the upturned dotted lines in Fig. 3 could be found from a potential energy surface, one might try data fitting with an Eckart potential based on this minimum instead of taking the reactant energy as zero. This

would be a desperate last attempt to save simple, quadratic, separable theory for a special case, but it might work. For the complexes with light end groups, we can see no way to extend the separable-dimension treatment. There must be many tunnelling paths with almost equal potential energy area under the curve; different isotopic species may well choose different paths and all with no concern for where classical mechanics places its normal modes.

In this chapter we have accepted Bell's invitation to consider large degrees of barrier penetration by chemically reacting systems. It appears that Bell's function for penetration of a parabolic barrier is limited to $hc\omega^*/2kT < 1.8$ for hydrogen atom transfer. Once ω^* is greater than this, we expect and seem to find a mixing of coordinates such that one-dimensional tunnelling corrections are not adequate. This conclusion calls for more information about the potential energy surface than its saddlepoint and its curvatures there. The detailed structure of the rest of the saddle becomes essential to the problem. The amount of this structure needed, how to obtain this information from nonkinetic considerations, and how to treat a two-dimensional tunnelling problem become interesting topics for the further development of activated complex theory.

VIII. EVALUATION OF INDEX p FROM SYMMETRICAL ACTIVATED COMPLEX

For the ortho-, para-hydrogen conversion



the rate constant is

$$\begin{aligned}
 k = & \left\{ (Q_{\text{el}}^\ddagger / Q_\sigma) (\nu^* / w) \left[\left(\prod_{\alpha}^3 J_{\alpha}^\ddagger \right) / \left(\prod_{\alpha}^2 J_{\alpha} J_{\text{H}} \right) \left[F_1'^{\frac{1}{2}} / (F_1 F_2 \phi_b^2)^{\frac{1}{2}} \right] \right\} \\
 & \times \left\{ [F_{\text{str}} \Gamma_* \Gamma_b^2 (2\pi kT)^{\frac{3}{2}} / \Gamma_{\text{str}}'] \exp(-V/kT) \right\} \quad (24)
 \end{aligned}$$

where terms in the first braces are temperature independent and terms in the second braces depend on temperature; the terms w is $(1 - F_{12}^2/F_1 F_2)^{\frac{1}{2}}$. The observed activation energy is

$$E_{\text{act}} = V_{\text{act}} + RT \left[\frac{3}{2} - (1 - \frac{1}{2}u \operatorname{ctnh} \frac{1}{2}u)_{\text{str}}^{\ddagger} - 2(1 - \frac{1}{2}u \operatorname{ctnh} \frac{1}{2}u)_b^{\ddagger} - (1 - \frac{1}{2}u^* \operatorname{ctn} \frac{1}{2}u^*)_{\text{r.c.}} + (1 - \frac{1}{2}u \operatorname{ctnh} \frac{1}{2}u)_{\text{str}}' \right]. \quad (25)$$

The θ term for the reaction coordinate as evaluated from Eq. (18) is valid only if $0.5u^* < 1.8$, as turns out to be the case for hydrogen at 1000°K . The value of u^* and $u_{\text{str}}^{\ddagger}$ depend on the barrier height V_0 , according to this method, and we can determine the barrier height only by correcting the activation energy for θ^* and θ_{str} . Thus a method of successive approximation is called for. The barrier height is taken to be the activation energy as a first approximation, the orders of the bonds are 0.5 and 0.5, F^* is evaluated from Eqs. (12, 13, 14) where great simplification results from symmetry, and F_{12} is $F_1 + F^*$. From these values of force constants, the frequencies ν_{str} and ν_* are found, and a revised estimate of V_0 is made from Eq. (25). New values of F^* and ν^* are found until the method converges—about three repetitions are sufficient. The activation energy for the reaction was taken to be 7.8 kcal.^{5,11,36} The potential energy of activation was found to be 6.3 kcal, the index p is 1.086, the negative force constant is $F^* = 0.52 \times 10^5$ dynes/cm, and Φ_b was 0.13×10^{-11} ergs/radian². The imaginary frequency is $1629i$, the real vibration frequency 3258 cm^{-1} , and the bending vibrations 1250 cm^{-1} .

For the methyl radical attack on hydrocarbons, the most nearly symmetrical case is $\text{H}_3\text{C}-\text{D}-\text{CD}_3$; this reaction was carefully and thoroughly investigated by Dainton⁷ who found $E_{\text{act}} = 12.9 \pm 0.6$ kcal. The substitute model chosen here is



with half-bonds about the atom transferred. The method of successive approximations gave $V_0 = 13.7$ kcal, $F^* = 1.13 \times 10^5$ dynes/cm, and $p = 1.195$. The frequencies for the complex are $1410i$, 834 str, 849 bend, 449 antiwag, 218 wag, and the frequencies for the reactant $\text{D}-\text{C}-6$ are 2202 str and 861 bend.

IX. ACKNOWLEDGEMENT

To the Alfred P. Sloan Foundation we are grateful for a Fellowship in support of this study. We wish to express our great appreciation to Mr. Terry Sharp for computing the vibration frequencies given in Table I and to Mr. Donald Rapp and Professor Dudley Herschbach for discussions of these problems. Finally, we want to commend Dr. E. W. R. Steacie and co-workers for presenting their kinetic data in detailed tabular form with consistent units and notation from year to year, and we thank the referees and editors who let these beautiful data be presented in both tabular and graphical form.

References

1. Badger, R. M., *J. Chem. Phys.* **2**, 128 (1933); **3**, 710 (1934).
2. Bell, R. P., *Trans. Faraday Soc.* **55**, 1 (1959).
3. Bigeleisen, J. and Wolfsberg, M., *Advances in Chemical Physics*, Vol. I, Interscience, New York, 1958, and references cited therein.
4. Bigeleisen, J., Klein, F. S., Weston, R. E., Jr., and Wolfsberg, M., *J. Chem. Phys.* **30**, 1340 (1959).
5. Boato, G., Careri, G., Cimino, A., Molinari, E., and Volpi, G. G., *J. Chem. Phys.* **24**, 783 (1956).
6. Cottrell, T. L., *Strengths of Chemical Bonds*, Academic Press, New York, 1954.
7. Dainton, F. S. and McElcheran, D. E., *Trans. Faraday Soc.* **51**, 657 (1955).
8. Dorfman, L. M. and Noyes, W. A., Jr., *J. Chem. Phys.* **16**, 557 (1948).
9. Eckart, C., *Phys. Rev.* **35**, 1303 (1930).
10. Eyring, H., Walter, J. and Kimball, G. E., *Quantum Chemistry*, Wiley, New York, 1944.
11. Farkas, A. and Farkas, L., *Proc. Roy. Soc. (London)*, **A152**, 124 (1935).
12. Glasstone, S., Laidler, K. J. and Eyring H., *Theory of Rate Processes*, McGraw-Hill, New York, 1941.
13. *Ibid.*, p. 191.
14. Herschbach, D. R., Johnston, H. S., Pitzer, K. S., and Powell, R. E., *J. Chem. Phys.* **25**, 736 (1956).
15. Herschbach, D. R., Johnston, H. S., and Rapp, D., *J. Chem. Phys.* **31**, 1652 (1959).
16. Johnston, H. S., Bonner, W. A., and Wilson, D. J. *J. Chem. Phys.* **26**, 1002 (1957).
17. Kassel, L. S., *Kinetics of Homogeneous Gas Reactions*, Chemical Catalog Co., New York, 1932, p. 57.

18. Kistiakowsky, G. B. and Van Artsdalen, E. R., *J. Chem. Phys.* **12**, 479 (1944).
19. McNesby, J. R. and Gordon, A. S., *J. Am. Chem. Soc.* **76**, 1416 (1954); McNesby, J. R., Davis, T. W., and Gordon, A. S., *J. Am. Chem. Soc.* **76**, 823 (1954).
20. Mandelcorn, L. and Steacie, E. W. R., *Can. J. Chem.* **32**, 331 (1954).
21. Marjury, T. G. and Steacie, E. W. R., *Can. J. Chem.* **30**, 800 (1952).
22. Nicholson, A. J. C., *J. Am. Chem. Soc.* **73**, 3981 (1951).
23. Oswin, H. G., Rebbert, R., and Steacie, E. W. R., *Can. J. Chem.* **33**, 472 (1955).
24. Pauling, L., *J. Am. Chem. Soc.* **69**, 542 (1947).
25. Pitzer, K. S., *J. Chem. Phys.* **8**, 711 (1940); *J. Am. Chem. Soc.* **79**, 1804 (1957).
26. Polanyi, J. C., *J. Chem. Phys.* **23**, 1505 (1955).
27. Rapp, D., *Dissertation*, University of California, Berkeley, 1960.
28. Rice, F. O. and Vanderslice, T. A., *J. Am. Chem. Soc.* **80**, 291 (1958).
29. Sato, S., *J. Chem. Phys.* **23**, 592, 2465 (1955).
30. Semenov, N. N., *Some Problems in Chemical Kinetics and Reactivity*, Princeton University Press, Princeton, New Jersey, 1958, pp. 29–33.
31. Sinanoglu, O. and Pitzer, K. S., *J. Chem. Phys.* **30**, 422 (1959).
32. Steacie, E. W. R., *Atomic and Free Radical Reactions*, 2nd Ed., Reinhold, New York, 1954.
33. Trotman-Dickenson, A. F., *Gas Kinetics*, Academic Press, New York, 1955, pp. 199–202.
34. Trotman-Dickenson, A. F., Birchard, J. R., and Steacie, E. W. R., *J. Chem. Phys.* **19**, 163 (1951).
35. Trotman-Dickenson, A. F. and Steacie, E. W. R., *J. Chem. Phys.* **18**, 1097 (1950).
36. Van Meersche, M., *Bull. soc. chim. Belg.* **60**, 99 (1951).
37. Whittle, E. and Steacie, E. W. R., *J. Chem. Phys.* **21**, 993 (1953).
38. Wilson, E. B., Jr., Decius, J. C., and Cross, P., *Molecular Vibrations*, McGraw-Hill, New York, 1955.
39. Wilson, D. J. and Johnston, H. S., *J. Am. Chem. Soc.* **79**, 29 (1957).

ASPECTS RÉCENTS DU DIAMAGNÉTISME

A. PACAULT, J. HOARAU, et A. MARCHAND, *Laboratoire de Chimie Physique, Université de Bordeaux*

TABLE DES MATIÈRES

I.	Introduction	172
II.	Mesures des Susceptibilités Diamagnétiques	172
	A. Appareil de Broersma	173
	B. Appareil de Pacault, Lemanceau, et Jousset-Dubien	174
	(1) Méthode employée. Ses exigences	175
	(2) Schéma de Principe	176
III.	Théorie des Susceptibilités Diamagnétiques	178
	A. Introduction	178
	B. Méthode de Van Vleck	181
	C. Méthode de Tillieu et Guy	187
	D. Anisotropie Diamagnétique des Molécules Aromatiques. Méthode de London	190
	(1) Comparaison avec les Résultats Expérimentaux.	194
IV.	Les Systématiques Magnétochimiques	199
	A. Systématique Théorique	199
	B. Systématiques Expérimentales	202
	(1) Loi d'Additivité	202
	(2) Établissement des Systématiques	204
	(a) Susceptibilité du Groupe CH ₂	204
	(b) Détermination des Susceptibilités Atomiques	204
	(c) Introduction des Incréments de Structure	208
	(3) Applications des Systématiques Expérimentales.	211
	C. Comparaison des Systématiques Expérimentales et Théoriques avec l'expérience	213
V.	Diamagnétisme des Électrons Quasi Libres	214
	A. Susceptibilité Magnétique d'un Cristal Métallique	215
	(1) Théorie	215
	(2) Résultats Expérimentaux et Interprétation	220
	(a) Éléments de Transition	220
	(b) Alcalins et Alcalino-Terreux	220
	(c) Autres Métaux	221

B. Magnétisme du Graphite Mono et Polycristallin.	222
(1) Résultats Expérimentaux.	222
(2) Études Théoriques.	224
(a) Graphite. Interprétation de Ganguli et Krishnan	225
(b) Graphite Polycristallin et Noirs de Carbone . .	226
(c) Discussion	229
C. Détermination des Masses Effectives par Voie Magnétique	234
Références	235

I. INTRODUCTION

Il n'est pas question dans cet article de résumer tous les travaux fait jusqu'à ce jour sur le diamagnétisme. Ceux-ci sont décrits dans un certain nombre de livres ou d'articles généraux.^{5, 52, 72, 91}

Nous nous contenterons de signaler quelques progrès récents faits dans ce domaine, en insistant plus particulièrement sur les travaux faits à l'Institut de magnétochimie, non pas parce qu'ils sont nécessairement les plus intéressants, mais parce que nous avons l'avantage de les mieux connaître.

Après avoir indiqué rapidement les perfectionnements récents apportés dans l'appareillage (Ch. II), nous ferons le point sur les théories du diamagnétisme (Ch. III), ce qui conduit à leur utilisation dans l'établissement d'une systématique magnétochimique théorique qui est comparée aux systématiques expérimentales (Ch. IV). Enfin, dans le chapitre V, nous développerons la question du diamagnétisme des liaisons complètement délocalisées que l'on rencontre dans les métaux et en particulier dans le graphite.

Cet exposé nous permettra de passer en revue les propriétés magnétiques des liaisons localisées, puis celles des liaisons partiellement délocalisées existant dans les composés aromatiques, pour arriver enfin à celles des liaisons métalliques dont l'étude apporte des renseignements intéressants en ce qui concerne les masses effectives et les porteurs de charge.

II. MESURES DES SUSCEPTIBILITÉS DIAMAGNÉTIQUES

Les mesures des susceptibilités diamagnétiques se ramènent le plus souvent à une mesure de force, que ce soit dans la méthode de Gouy ou dans celle de Faraday. Ces méthodes de mesure

sont bien connues et les appareils fondés sur celles-ci sont décrits dans tous les ouvrages classiques.

Les innovations seront difficiles dans ce domaine.

En revanche, les appareils fondés sur une variation d'inductance utilisés depuis longtemps pour mesurer le ferromagnétisme n'avaient pu être adaptés à la mesure du diamagnétisme.

En 1947, Broersma²⁰ proposa un appareil de mesure des susceptibilités diamagnétiques en basse fréquence et en 1953, Pacault, Lemanceau et Jousset-Dubien⁷⁵ construisirent un appareil de mesure en haute fréquence.

A. Appareil de Broersma

Cet appareil comprend essentiellement deux bobines de self S_+ et S_- (fig. 1) de surface S_s bobinées en sens inverse avec N

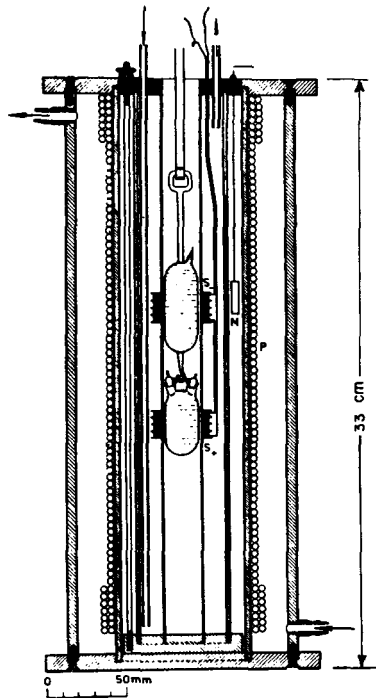


Fig. 1. Appareil de Broersma.

tours de fil et placées dans un solénoïde P constitué de n tours de fil par mètre.

Le solénoïde P parcouru par un courant I_{eff} de pulsation $\omega = 1000$ induit dans chaque bobine du secondaire S_+ et S_- une différence de potentiel alternative donné dans le système de Giorgi par l'expression

$$V_{\text{eff}} = -n NS_s I_{\text{eff}} \omega \mu_0$$

où μ_0 = perméabilité du vide.

Si les deux bobines étaient rigoureusement identiques, la différence de potentiel induite aux bornes du secondaire devrait être nulle. L'introduction d'une substance de susceptibilité volumique κ dans l'une des bobines S_+ crée une dissymétrie et la différence de potentiel aux bornes du secondaire devient

$$\Delta V_{\text{eff}} = I_{\text{eff}} \omega n NS_s \mu_0 \eta \kappa$$

η étant un coefficient de remplissage qui tient compte du fait que la substance n'emplit pas tout l'espace dans lequel l'induction du primaire exerce son action ($\eta \approx 0,5$).

Il en résulte que

$$\Delta V/V = |\eta \kappa| \approx 3 \times 10^{-6}$$

Une mesure de κ à 1/1000 près suppose donc la mesure d'une différence de potentiel à 3×10^{-9} près.

Comme on peut mesurer convenablement 3×10^{-8} volts la différence de potentiel à mesurer doit être de 10 volts au moins

On double l'effet précédemment décrit en déplaçant la substance dont on veut mesurer la susceptibilité de la bobine S_+ à la bobine S_- et toute la difficulté se ramène alors à mesurer avec une bonne précision la différence de potentiel induite.

Ce problème technologique a été convenablement résolu par Broersma qui mit ainsi au point un appareil de mesure des susceptibilités diamagnétiques. La précision des mesures est supérieure au $\frac{1}{2}$ %.

B. Appareil de Pacault, Lemanceau, et Jousset-Dubien

Lorsqu'une substance de perméabilité μ est introduite dans une bobine, le coefficient de self de celle-ci varie et on peut déterminer

sa perméabilité si on connaît la variation d'inductance. Cette constatation très ancienne n'a pu être exploitée que lorsque les progrès de l'électronique furent suffisants. Il existe actuellement un appareil, le χ -mètre qui fonctionne sur ce principe.

(1) *Méthode employée. Ses exigences*

L'inductance d'un solénoïde devient, lorsqu'on y introduit une substance de susceptibilité κ

$$L = L_0(1 + \kappa)$$

d'où

$$(L - L_0)/L_0 = \Delta L/L_0 = \kappa$$

(L_0 = coefficient de self par rapport au vide), dans le cas pratiquement irréalisable où la substance occupe tout le volume v soumis au champ magnétique de la self. La variation de self est donc toujours inférieure à sa valeur théorique, on peut écrire

$$\Delta L/L_0 = \kappa\eta$$

($\eta < 1$: coefficient de remplissage tenant compte de ce que la substance n'occupe qu'une partie du volume v).

La mesure d'une susceptibilité magnétique se ramène à celle de la variation d'un coefficient de self, qui peut se ramener elle-même à celle d'une variation de fréquence d'un circuit oscillant self-capacité, dont la fréquence ν est donnée par l'équation: $LC\omega^2 = 1$. (C = capacité totale du circuit, ω = pulsation = $2\pi\nu$). Par conséquent, à la variation de self ΔL due à l'introduction d'une substance correspond une variation de fréquence

$$\Delta\nu/\nu = -\frac{1}{2}\Delta L/L = -\eta\kappa/2$$

$$\Delta\nu/\nu \approx \kappa/10$$

car l'expérience montre que η est de l'ordre de 0,2 d'où $\Delta\nu/\nu \approx 10^{-6}$, puisque $\kappa \approx 10^{-5}$.

La variation de fréquence $\Delta\nu$ n'est mesurable que si la stabilité des oscillations électriques est excellente pendant le temps nécessaire à une mesure et si la sensibilité du dispositif de mesure de cette variation de fréquence est suffisante.

Le choix de la fréquence résulte d'un compromis entre la

stabilité de l'oscillateur en fonction de la fréquence d'une part et de la sensibilité du détecteur d'autre part. La fréquence ν a été choisie égal à 1 Megahertz; dans ces conditions $\Delta\nu$ est de l'ordre de 1 Hertz.

Pour obtenir la précision de 1% environ donnée par les appareils classiques à champ magnétique statique, la fréquence doit être mesurée à 0,01 Hertz près. Ceci limite les fluctuations de l'oscillateur à des valeurs inférieures à 0,01 Hertz autrement dit impose une stabilité relative

$$\Delta\nu/\nu = 0,01/10^6 = 10^{-8}$$

pendant le temps évidemment court (quelques dizaines de secondes) nécessaire à la mesure. Des conditions aussi strictes sont délicates à réaliser.

(2). *Schéma de principe*

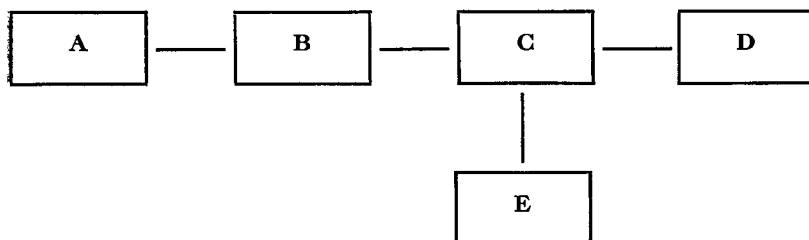


Fig. 2. Schéma de principe de l'appareil de Pacault, Lemenceau, et Jousset-Dubien.

L'appareil (figure 2) comprend essentiellement: A, l'oscillateur d'essai—oscillateur self capacité— dans la self duquel on introduit la substance dont on veut mesurer la susceptibilité. B, Plusieurs étages électroniques—tampon, amplificateur. C, Mélangeur fournissant entre les deux oscillateurs un battement de quelques centaines de Hertz. D, L'oscillateur de référence—oscillateur à quartz

de fréquence 1 Megahertz. E, Le dispositif de mesure dont l'organe essentiel est un tube cathodique.

La variation de self résultant de l'introduction dans la bobine de la substance dont on veut mesurer la susceptibilité est mesurée par une méthode de double battement.

On fait battre l'oscillateur d'essai avec l'oscillateur de référence piloté par un quartz. La tension d'oscillation de ce battement dont la fréquence est de l'ordre de quelques centaines de hertz est mise aux bornes du Wehnelt du tube cathodique du détecteur. On forme sur l'écran du tube un cercle, en portant sur les plaques horizontales la tension du secteur et sur les plaques verticales la même tension déphasée de 90° . Lorsque la fréquence du battement est un multiple entier de la fréquence du secteur on observe sur l'écran un nombre d'arcs de cercles égal à ce multiple et ces arcs de cercle sont immobiles.

La self est garnie d'un écran spécial qui élimine les effets du champ électrique nuisibles parce que largement supérieurs à ceux recherchés.

Cet appareil, permet d'effectuer des mesures relatives par une méthode de zéro. La mesure relative s'impose parce que le calcul du coefficient de remplissage η est moins précis que sa détermination grâce à un corps de référence.

La manipulation est simple. La substance est introduite dans la self par un dispositif mécanique convenable. Un bouton gradué agissant sur un condensateur qui fait varier légèrement la fréquence de l'oscillateur de référence, permet d'arrêter les spots sur l'écran. Le tube de mesure étant hors de la self, les spots sont arrêtés grâce au bouton gradué et on lit la division m ; on introduit mécaniquement le tube dans la self, il s'y trouve dans une position bien déterminée fixée par construction, les spots se mettent à tourner, on les arrête grâce au même bouton et on lit la division m' .

L'introduction du tube vide dans la self provoque donc une variation de fréquence proportionnelle à $(m - m') = n_a$ (La proportionnalité est obtenue par construction du condensateur).

On répète très exactement la même opération en remplissant successivement le tube d'un même volume, 3 cm³ environ, de la

substance dont on veut mesurer la susceptibilité et d'un corps dont la susceptibilité est prise pour référence. On mesure n et n_R .

L'équation

$$\bar{\chi} = (\lambda/\rho_{ap})(\bar{\chi}_R \cdot \rho_R - \bar{\kappa}_a) + \bar{\kappa}_a/\rho$$

$\bar{\chi}$ = susceptibilité massique cherchée; ρ_{ap} = quotient de la masse de substance par le volume qu'elle occupe; $\bar{\chi}_R$ = susceptibilité massique du corps de référence; ρ_R = masse spécifique du corps de référence; $\bar{\kappa}_a$ = susceptibilité volumique de l'air = $0,029 \times 10^{-6}$; ρ = masse spécifique de la substance; donne la susceptibilité recherchée à condition de poser:

$$\lambda = (n - n_a)/(n_R - n_a)$$

Cet appareil est d'un usage commode et rapide. Il permet de mesurer à mieux de 1% les susceptibilités magnétiques des quantités de substances diamagnétiques de l'ordre du gramme, et paramagnétiques de l'ordre du centigramme (la quantité de matière à utiliser dépend de la valeur de la susceptibilité).

Un dispositif convenable permet de mesurer les susceptibilités entre la température ordinaire et les basses températures.

III. THÉORIE DES SUSCEPTIBILITÉS DIAMAGNÉTIQUE

A. Introduction

Le présent article étant consacré au diamagnétisme, on admettra que le moment cinétique orbital, de même que le moment résultant de spin, est nul en l'absence de champ magnétique.

On définit le moment magnétique d'un système constitué par un atome ou une molécule isolée par la relation suivante (si l'on néglige les dimensions des électrons et des noyaux)

$$\mathbf{m} = (1/2c) \sum_i e_i(\mathbf{r}_i \times \mathbf{v}_i) = \sum_i (e_i/2m_i c) \cdot \mathbf{L}_i$$

où c est la vitesse de la lumière, et e_i , \mathbf{r}_i , \mathbf{v}_i , m_i , et \mathbf{L}_i sont respectivement la charge, le vecteur position, la vitesse, la masse, et le moment cinétique de la $i^{\text{ème}}$ particule.

On montre alors en mécanique classique que le moment magnétique m_H en présence du champ magnétique H est égal à

$$m_H = -\partial \mathcal{H} / \partial H \quad (\text{III.1})$$

où \mathcal{H} est la fonction de Hamilton dy système

$$\mathcal{H} = \sum_i (1/2m_i) [(p_{x_i} - (e_i/c)A_{x_i})^2 + (p_{y_i} - (e_i/c)A_{y_i})^2 + (p_{z_i} - (e_i/c)A_{z_i})^2] + V \quad (\text{III.2})$$

établie en tenant compte du fait qu'en présence de champ magnétique les composantes du moment d'impulsion sont données par des expressions de la forme

$$p_{x_i} = m_i dx_i/dt + (e_i/c)A_{x_i}$$

A_{x_i} étant la composante suivant l'axe Ox du potentiel vecteur A_i définissant le champ magnétique au point où est localisée la $i^{\text{ème}}$ particule. V est le potentiel électrostatique (de la forme $\sum_{j>i} e_i e_j / r_{ij}$).

En mécanique quantique, la valeur moyenne de ce moment est donnée par l'expression

$$m_H = -\partial W / \partial H$$

où W est l'énergie du système en présence de champ magnétique. Le moment induit M_H d'un ensemble d'atomes ou de molécules est généralement proportionnel au champ H et l'on définit la susceptibilité magnétique par la relation

$$\chi = M_H / H$$

Si M_H est le moment correspondant à une mole, χ est la susceptibilité moléculaire.

Les susceptibilités magnétiques doivent être en réalité représentées par des tenseurs du second ordre. Afin de simplifier les calculs, nous supposons que, dans tous les cas, le champ magnétique sera dirigé suivant un axe principal d'aimantation de l'atome, de la molécule ou de la liaison étudiée, l'axe Oz par exemple. Le calcul fournit alors la susceptibilité principale χ_z . En plaçant ensuite le champ H suivant les deux autres directions principales (Ox et Oy) on obtient les deux autres susceptibilités principales χ_x et χ_y .

La susceptibilité moyenne est alors donnée par l'expression

$$\bar{\chi} = \frac{1}{3} (\chi_x + \chi_y + \chi_z)$$

Le problème du calcul des susceptibilités magnétiques consiste

donc en premier lieu à déterminer les états d'énergie d'un système en présence de champ magnétique. Ceux-ci sont donnés par l'équation de Schrödinger

$$\mathcal{H}\psi_n = W_n\psi_n \quad (\text{III.3})$$

où ψ_n est la fonction d'onde du système correspondant à l'état d'énergie, W_n et \mathcal{H} l'opérateur hamiltonien en présence de champ magnétique. Ce dernier est obtenu à partir de la fonction III.2 grâce aux correspondances habituelles.

$$\mathcal{H} = \sum_i (1/2m_i) \left((h/2\pi i) \text{grad} - (e_i/c)\mathbf{A}_i \right)^2 + V$$

En développant et en tenant compte du fait que $\text{div } \mathbf{A} = 0$ pour le champ magnétique, on obtient

$$\mathcal{H} = \sum_i \left[- (h^2/8\pi^2 m_i) \Delta_i - (e_i h/4\pi m_i c) \mathbf{A}_i \cdot \text{grad } \mathbf{A}_i + (e_i^2/2m_i c^2) |\mathbf{A}_i|^2 \right] + V$$

Le plus souvent, le potentiel vecteur est pris sous la forme comode

$$\mathbf{A}_i = \frac{1}{2} \mathbf{H} \times \mathbf{r}_i$$

Dans ces conditions, si le champ \mathbf{H} est dirigé suivant la direction Oz d'un trièdre de référence $Oxyz$, on a

$$A_{x_i} = -\frac{1}{2} H y_i, \quad A_{y_i} = \frac{1}{2} H x_i, \quad A_{z_i} = 0$$

et l'opérateur \mathcal{H} prend la forme

$$\mathcal{H} = \sum_i \left[- (h^2/8\pi^2 m_i) \Delta_i - (e_i h/4\pi m_i c) (x_i \partial/\partial y_i - y_i \partial/\partial x_i) H + (e_i^2/8m_i c^2) (x_i^2 + y_i^2) H^2 \right] + V$$

ce que l'on peut écrire en mettant en évidence l'opérateur hamiltonien \mathcal{H}^0 du système en l'absence de champ magnétique

$$\mathcal{H} = \mathcal{H}^0 - M_z^0 H + P_z H^2 \quad (\text{III.4})$$

M_z^0 est l'opérateur correspondant au moment magnétique

$$M_z^0 = \sum_i (e_i h/4\pi m_i c) (x_i \partial/\partial y_i - y_i \partial/\partial x_i)$$

P_z est l'opérateur

$$P_z = \sum_i (e_i^2/8m_i c^2) (x_i^2 + y_i^2)$$

Bien entendu, la résolution rigoureuse de l'équation III.3 est

généralement impossible et l'on est conduit à utiliser des méthodes d'approximation.

Jusqu'à ces dernières années, les calculs de susceptibilité magnétique se ramenaient à une méthode due à Van Vleck fondée sur la théorie des perturbations. Récemment, Guy et Tillieu ont développé une méthode utilisant la théorie des variations. Bien que cette dernière soit moins rigoureuse dans son principe, elle conduit à des formules dont le calcul est beaucoup plus aisé et, en fin de compte, les résultats obtenus sont comme nous le verrons bien meilleurs.

Ces deux méthodes ont été utilisées principalement pour le calcul des susceptibilités des molécules à liaisons localisées; dans le cas des composés aromatiques, une méthode ingénieuse due à London est spécialement adaptée au calcul de la contribution des électrons π à l'anisotropie diamagnétique.

La théorie du calcul des susceptibilités diamagnétiques des composés à liaison métallique est reportée au chapitre V.

B. Méthode de Van Vleck¹⁰⁷

Van Vleck caractérise un état quantique par trois indices, n , j , et m . L'indice n est tel que la transition d'un état représenté par l'indice n à un état représenté par un autre indice n' correspond à une énergie bien supérieure à kT , k étant la constante de Boltzmann et T la température absolue.

Les indices j et m au contraire correspondent à des transitions énergétiques comparables ou inférieures à kT , m représentant plus particulièrement le nombre quantique magnétique.

Dans ces conditions, si l'on néglige les termes contenant les puissances de H supérieures à 2, l'énergie d'un état non dégénéré correspondant aux trois indices n , j , m est donné par la théorie des perturbations.

$$W_{njm} = W_{njm}^0 - H(njm|M_z^0|njm) \\ - H^2 \sum_{n'j'm' \neq njm} |(njm|M_z^0|n'j'm')|^2 / (W_{n'j'm'} - W_{njm}) + H^2(njm|P_z|njm)$$

Elle fait apparaître quatre termes qui sont successivement: l'énergie du système non perturbé (en l'absence de champ magné-

tique) les perturbations du premier ordre et du second ordre correspondant au terme $M_z^0 H$ de III.4, et la perturbation du premier ordre du terme $P_z H^2$ de III.4.

Le moment magnétique est alors égal à

$$\begin{aligned} m_{z_{njm}} &= -\partial W_{njm} / \partial H \\ &= \langle njm | M_z^0 | njm \rangle + 2H \sum_{n'j'm' \neq njm} |\langle njm | M_z^0 | n'j'm' \rangle|^2 / (W_{n'j'm'} - W_{njm}) \\ &\quad - 2H \langle njm | P_z | njm \rangle \end{aligned}$$

Le moment magnétique moyen \bar{M}_z pour un ensemble de N molécules soumises au champ H (toujours dirigé suivant Oz), à la température T est égal à

$$\bar{M}_z = N \sum_{jm} M_{z_{njm}} \exp(-W_{njm}/kT) / \sum_{jm} \exp(-W_{njm}/kT)$$

Van Vleck a montré que les termes provenant de la perturbation du second ordre du terme $M_z^0 H$ peuvent être séparés en deux parties: les termes dits de „basse fréquence” pour lesquels $n = n'$ et les termes dits „haute fréquence” pour lesquels $n \neq n'$. Dans le cas de molécules ne contenant pas de moment magnétique permanent, seuls ces derniers ont une contribution non nulle au moment \bar{M}_z et celui-ci, après quelques simplifications peut s'écrire:

$$\bar{M}_z = 2NH \sum_{n'(\neq n)} |\langle n | M_z^0 | n' \rangle|^2 / (W_{n'} - W_n) - 2NH \langle n | P_z | n \rangle$$

La susceptibilité magnétique s'écrit dans ces conditions:

$$\chi_z = \bar{M}_z / H = 2N \sum_{n'(\neq n)} |\langle n | M_z^0 | n' \rangle|^2 / (W_{n'} - W_n) - 2N \langle n | P_z | n \rangle \quad (\text{III.5})$$

Le dernier terme correspond dans le formalisme de la mécanique quantique au résultat obtenu par Langevin en mécanique classique:

$$\chi_z = -N \sum_i (e_i^2 / 4m_i c^2) \overline{(x_i^2 + y_i^2)}$$

il est négatif et il correspond à un diamagnétisme. Son calcul ne présente pas de difficulté majeure, car il ne nécessite que la connaissance de la fonction d'onde du système dans l'état fondamental.

L'autre terme, appelé souvent terme de „haute fréquence,” par contre, n'a pas d'équivalent en mécanique classique et son évaluation est impossible sans approximations très grossières, car elle fait intervenir les fonctions d'onde et les énergies de tous les états excités, qui presque toujours sont inconnues. Or ce terme ne doit pas être négligé car c'est la somme des deux termes de III.5 qui est indépendante de l'origine choisie pour le potentiel vecteur. Il ne peut s'annuler que dans le cas où la fonction d'onde présente un axe de révolution parallèle au champ magnétique, à la condition de prendre cette origine sur cet axe (on a en effet en coordonnées polaires

$$M_z^0 = \sum_i (e_i \hbar / 4\pi i m_i c) \cdot (\partial / \partial \varphi_i)$$

φ étant l'angle de rotation autour de Oz).

On ne pourra donc calculer aisément par cette méthode que la susceptibilité des atomes ou des ions simples dans l'état 1S , car le terme de haute fréquence sera nul. Au contraire, dans le cas des molécules, il ne pourra s'annuler à la fois pour les trois directions principales suivant lesquelles on placera successivement le champ magnétique.

Les calculs qui ont été faits par cette méthode négligent souvent purement et simplement ce terme de haute fréquence. Les résultats sont alors relativement satisfaisants dans le cas de molécules très simples telles que la molécule d'hydrogène, car ce terme est faible, mais le désaccord devient très grand pour des molécules plus complexes.

Van Vleck et Miss Franck¹⁰⁸ ont utilisé l'approximation suivante dans le cas de la molécule d'hydrogène: Si l'on remplace les dénominateurs $W_{n'} - W_n$ par un dénominateur commun ΔW , il est facile de montrer que

$$\sum_{n'(\neq n)} |(n|M_z^0|n')|^2 / \Delta W = (n|M_z^{02}|n) / \Delta W$$

(car $(n|M_z^0|n) = 0$ en l'absence de moment permanent).

L'intégrale du numérateur est alors facile à calculer, car elle ne fait intervenir que la fonction d'onde de l'état fondamental, quant à ΔW on peut en calculer un ordre de grandeur à partir de l'indice de réfraction.

TABLEAU III.1

Composé	Auteur	Fonction d'onde	$-\chi_d \times 10^6$	$\chi_s \times 10^6$	$-\chi \times 10^6$
H_2	Van Vleck et Franck ¹⁰⁸	Fonction de Wang ¹¹²	4,71	0,51	4,20
	Wick ¹¹⁴	$e^{-\chi(r_1+r_2+\rho_1+\rho_2)}$	4,02	0,06	3,96
	Mrowka ⁶⁶	Fonction de Kemble et Zener ⁵⁰	4,50	0,296	4,20
	Hirschfelder ⁴²	Fonction de Rosen ⁸⁷		0,51	3,4
		Fonction de Wang ¹¹²		0,51	3,6
	Witmer ¹¹⁷	Fonction de James et Coolidge à 11 termes pour le calcul de χ_s	4,198	0,285	3,91
	Steensholt ⁹⁸	$\psi = e^{-\delta\lambda} (1 + a\mu^2)$	4,8	0	4,8
		$\psi = e^{-\delta\lambda} (1 + a\mu^2 + b\lambda)$	3,8	0	3,8
		$\psi = e^{-\delta\lambda} (1 + a\mu^2 + b\lambda + c\lambda^2 + d\lambda\mu^2)$	3,8	0	3,8
	Weltner ¹¹³	Newell ⁶⁹ Orbitales moléculaires		0,209 0,052	
N_2	Wills et Hector ¹¹⁵	Valeurs expérimentales			3,94
	Soné ⁹⁶				3,99
	Bonet et Bushkovitch ¹⁸	Fonction de distribution de Hund (méthode de Thomas-Fermi)	33,7	9,1	24,6
	Morrow ⁶⁵	Fonction de distribution de Brinkman (méthode de Thomas-Fermi)	22,0	1,9	20,1

TABLEAU III.1 (*A suite*)

Composé	Auteur	Fonction d'onde	$-\chi_d \times 10^6$	$\chi_p \times 10^6$	$-\chi \times 10^6$
	Hector, ⁴¹ Vaidyanathan, ¹⁰⁵ Bitter ¹⁶	Valeurs expérimentales			11-14
CH ₄	Buckingham, Massey et Tibbs ²²	Champ self consistant	33,2	0	33,2
	Coulson ²⁵	Orbitales moléculaires	26,6	0	26,6
		Méthode de Heitler et London $\beta = 1,0$	31,0	0	31,0
		$\beta = 1,1$	27,7	0	27,7
		$\beta = 1,2$	25,3	0	25,3
Venkatachalam et Kabadi ¹⁰⁹		Fonction utilisée par Coulson + formes ioniques	21,11	0	21,11
Hartmann ⁴⁰		„Pseudo-néon”	27,4	0	27,4
Bitter ¹⁵					12,2
Systématique de Pascal, Pacault, Hoarau ⁷⁸		Valeurs expérimentales			15,4
NH ₄ ⁺	Hartmann ⁴⁰	„Pseudo-néon”	17,9	0	17,9
	Venkatachalam et Kabadi ¹⁰⁹	Fonction de Heitler et London	24,89	0	24,89
		<i>Id.</i> + formes ioniques	13,4	0	13,4
Trew ¹⁰²		Valeur expérimentale			13,3

De tels calculs n'ont été effectués que sur des molécules ou des ions relativement simples: les molécules d'hydrogène, d'azote, de méthane et l'ion ammonium NH_4^+ .

Le tableau III.1 rassemble quelques uns de ces résultats théoriques on a noté successivement: le nom du composé, le nom des auteurs, la fonction d'onde utilisée, le terme de Langevin diamagnétique χ_d , le terme correctif paramagnétique χ_p , et enfin la susceptibilité moléculaire calculée χ .

On remarque que le terme paramagnétique de „haute fréquence” n'a été évalué théoriquement que pour les molécules d'hydrogène et d'azote.

Pour la molécule d'hydrogène, Van Vleck et Miss Franck¹⁰⁸ ont estimé le dénominateur moyen ΔW à 16,6 ev (valeur qui a été reprise par la majorité des auteurs (Wick,¹¹⁴ Mrowka,⁶⁶ Witmer,¹¹⁷) ce qui les a conduit à un terme correctif χ_p égal à $0,51 \times 10^{-6}$ (valeur utilisée également par Hirschfelder.⁴²) Voir également Witmer.¹¹⁸

Il semble que ce résultat soit trop élevé, en effet, il est possible de déterminer expérimentalement le terme de „haute fréquence” à partir des moments magnétiques rotationnels des molécules obtenues par effet Zeemann en micro-ondes ou à partir des rayons moléculaires (Wick,¹¹⁴ Ramsey⁸⁵.) (L'origine doit alors être prise obligatoirement au centre de gravité des molécules.) De telles mesures conduisent en effet à la valeur $\chi_p = 0,0846 \times 10^{-6}$ (Espe²⁸).

On trouvera une discussion intéressante sur les déterminations théoriques et expérimentales de ce terme dans un article de Weltner.¹¹³

Quoiqu'il en soit, il est facile de voir que même pour ces molécules simples, son évaluation théorique dépend dans une large mesure de la fonction d'onde utilisée et pour des molécules telles que le méthane, l'écart entre les susceptibilités théoriques et expérimentales montre qu'il ne peut pas être négligé, même quand la molécule possède une symétrie élevée.

L'inconvénient majeur de cette méthode tient donc à la difficulté, voire l'impossibilité du calcul du terme de „haute fréquence.”

La méthode suivante permet au contraire un calcul relativement aisé et donnant des résultats en accord avec l'expérience.

REMARQUE. La présence du terme paramagnétique de haute fréquence avait été invoquée par un certain nombre d'auteurs, à la suite de Van Vleck, pour expliquer l'existence dans certaines molécules d'un faible paramagnétisme indépendant de la température, mais Guy, Tillieu, et Baudet³⁷ ont montré que l'on devait toujours avoir $|\chi_d| < \chi_p$.

C. Méthode de Tillieu et Guy^{100, 101} *

Ces auteurs utilisent la méthode des variations qui consiste à choisir une fonction d'onde variationnelle Φ convenable et à calculer l'intégrale

$$W = \int \Phi^* \mathcal{H} \Phi d\tau \quad (\text{III.6})$$

où \mathcal{H} est l'opérateur hamiltonien III.4 du système. On sait en effet que cette intégrale est toujours supérieure à la valeur de l'énergie réelle du système dans l'état fondamental. Il suffit donc de faire varier les paramètres contenus dans la fonction Φ de façon à rendre W minimum pour avoir une valeur approchée par excès de l'énergie.

Guy et Tillieu mettent Φ sous la forme

$$\Phi = \Phi^0(1 + iG_z \cdot H)$$

(si on suppose que H est appliqué suivant la direction d'aimantation principale Oz), Φ^0 étant la fonction d'onde du système en l'absence de champ magnétique.

Ils ont montré en effet que le terme perturbateur devait être imaginaire pur dans le cas de substances dont le moment orbital est nul, ce que laisse d'ailleurs prévoir la forme de la fonction d'onde obtenue à partir de la théorie des perturbations.

Dans ces conditions on a, pour un électron:

$$W = W^0 + (e^2 H^2 / 8mc^2) (\phi^0 | x^2 + y^2 | \phi^0) - 4i(\phi^0 | G_z M_z^0 | \phi^0) H^2 \\ - (\hbar^2 H^2 / 4\pi^2 m) (\phi^0 | \text{grad } G_z | \phi^0)$$

La minimisation de W conduit à l'équation d'Euler:

$$(8\pi^2 m i / \hbar^2) \phi^0 M_z^0 \phi^0 - \phi^0 \Delta G_z \phi^0 - 2\phi^0 \text{grad } G_z \cdot \text{grad } \phi^0 = 0$$

* Voir également Gans et Mrowka.³⁴

qui devrait permettre de déterminer la fonction G_z . En réalité, on ne peut résoudre cette équation, mais elle permet de discuter la forme analytique de cette fonction.

Les fonctions d'onde Φ^0 utilisées sont celles de la méthode des orbitales moléculaires non antisymétrisées et se présentent sous la forme d'un produit d'orbitales monoélectroniques. On peut alors montrer que, dans ces conditions, la susceptibilité du système est égale à la somme des susceptibilités des diverses orbitales monoélectroniques.

Il suffit par conséquent de calculer pour les molécules ne comportant pas de doubles liaisons conjuguées: (a) la susceptibilité des électrons internes des atomes; (b) la susceptibilité des doublets libres des atomes; (c) la susceptibilité des liaisons. (Pour ces deux dernières susceptibilités, il y a lieu de tenir compte des angles de valence en utilisant une hybridation convenable).

Cette remarque constitue une justification des systématiques magnétochimiques et il a été possible d'établir une systématique théorique dont les résultats seront donnés dans les sections IV.A et IV.C.

Cette systématique a été établie en utilisant les fonctions d'onde de Slater (ou celle de Coulson pour le carbone) et les distances interatomiques déterminées expérimentalement par les méthodes classiques (Rayons X, diffraction électronique ou spectrographie).

Si l'on veut déterminer par exemple, la susceptibilité d'un électron d'une liaison σ AB , on pose

$$\Phi^0 = N(\Phi_A^0 + \Phi_B^0)$$

La susceptibilité principale suivant l'axe de la liaison est facile à calculer car, par suite de la symétrie de révolution de la liaison σ , le terme de haute fréquence est nul et elle se réduit au terme de Langevin.

Pour les susceptibilités perpendiculaires à l'axe de la liaison, on montre que, par suite des conditions de symétrie, la fonction G_z est de la forme

$$G_z = ax + bxy + \dots$$

Le calcul de l'intégrale W (eq. III.6) est alors facile et il suffit

TABLEAU III.2

Composé	Auteur	Fonction d'onde	$-\chi_a \times 10^6$	$\chi_p \times 10^6$	$-\chi \times 10^6$
H ₂	Tillieu et Guy ^{100, 101}	Orbitales moléculaires	4,03	0,09	3,94
		Fonction de Heitler et London	4,22	0,11	4,11
		Fonction de Weimbaum	5,55	0,26	5,29
		Fonction de James et Coolidge à 3 paramètres	3,92	0,07	3,85
	Wills et Hector ¹¹⁶ Sone ⁹⁵	Valeurs expérimentales			3,94
					3,99
N ₂	Baudet, Tillieu et Guy ⁷	Fonction d'Abbott et Bolton ¹			13,71
		Fonction de Scherr ⁸⁸			13,73
	Hector, ⁴¹ Bitter ¹⁶ Vaidyanathan ¹⁰⁵	Valeurs expérimentales			11-14
CH ₄	Tillieu et Guy ^{100, 101}	Orbitales moléculaires avec différents coefficients			17,56
					17,11
					16,35
					16,23
	Bitter ¹⁶ Systématique de Pascal, Pacault, Hoarau ⁷⁸	Valeurs expérimentales			12,2
					15,4

de la rendre minimum en écrivant

$$\partial W/\partial a = 0 \quad \partial W/\partial b = 0$$

On en déduit les valeurs de a et b correspondantes: a est nul si l'origine est prise au centre de gravité électronique de la liaison et

$$b = (\pi e/\hbar c) (\Phi^0|x^2 - y^2|\Phi^0)/(\Phi^0|x^2 + y^2|\Phi^0)$$

on en déduit facilement

$$\begin{aligned} \chi_z = & -(e^2/4mc^2) (\Phi^0|x^2 + y^2|\Phi^0) \\ & + (e^2/2mc^2) (\Phi^0|x^2 - y^2|\Phi^0)^2/(\Phi^0|x^2 + y^2|\Phi^0) \end{aligned} \quad (\text{III.7})$$

on retrouve donc 2 termes, le premier n'est pas différent du terme de Langevin, le second est positif et correspond au terme de haute fréquence de Van Vleck. Mais il ne fait plus intervenir que la fonction d'onde de l'état fondamental Φ^0 et, par conséquent, son calcul ne présente pas de difficultés.

Le détail des résultats obtenus à partir de la théorie de Guy et Tillieu sera donné dans la section IV. Nous nous bornerons ici à donner la susceptibilité des molécules les plus simples (tableau III.2) que l'on pourra comparer aux valeurs données au paragraphe précédent.

Il n'est pas possible ici de donner les valeurs χ_p et χ_d sauf pour la molécule d'hydrogène car les termes correspondant aux différents électrons ont été évalués à partir d'origines différentes. (alors que dans la méthode de Van Vleck l'origine était toujours prise au centre de gravité des molécules).

Dans l'ensemble, les résultats sont plus satisfaisants que ceux obtenus à partir de la théorie des perturbations.

Comme nous le verrons section IV.3, l'accord avec l'expérience est également excellent pour les molécules plus complexes.

D. Anisotropie Diamagnétique des Molécules Aromatiques. Méthode de London

L'importante exaltation du diamagnétisme suivant l'axe perpendiculaire au plan de ces molécules a été expliquée qualitativement par Hückel⁴⁶ et par Ubbelohde.¹⁰³ Un premier essai de calcul quantitatif a été effectué un peu plus tard par Pauling,⁷⁹ mais

c'est à London⁵⁴ que revient le mérite d'avoir donné une théorie quantitative satisfaisante.

Ce procédé de calcul s'inspire de la théorie des métaux de Bloch et utilise la méthode classique des Orbitales Moléculaires (L.C.A.O.)

Nous rappellerons que, dans cette méthode, une molécule organique conjuguée est considérée comme étant formée d'un squelette rigide réalisé par les liaisons σ et d'électrons mobiles π . On n'étudie que le comportement de ces électrons π et on néglige de plus leurs interactions.

Soit une molécule plane constituée par n atomes semblables auxquels correspondent les fonctions d'ondes atomiques $\varphi_1^0 \dots, \varphi_k^0 \dots, \varphi_n^0$ (fonctions d'onde que l'on supposera réelles et approximativement orthogonales).

London pose qu'en première approximation on doit écrire ces fonctions d'onde en présence de champ magnétique sous la forme

$$\varphi_k = \varphi_k^0 \exp [(2\pi i e / hc) \mathbf{A}_k \cdot \mathbf{r}]$$

\mathbf{A}_k désignant le potentiel vecteur du champ magnétique au centre de l'atome k et \mathbf{r} le vecteur position de l'électron.

L'énergie correspondant à ces fonctions d'ondes atomiques en présence de champ magnétique est de la forme

$$E_k = E_k^0 - \frac{1}{2} \cdot \chi_k \cdot H^2$$

χ_k est la susceptibilité magnétique correspondant à l'orbitale φ_k , elle est donnée par une expression analogue à l'équation III.5.

On utilise alors la fonction de variation linéaire

$$\psi = \sum_k c_k \varphi_k = \sum_k c_k \varphi_k^0 \exp [(2\pi i e / hc) \mathbf{A}_k \cdot \mathbf{r}]$$

La perturbation E^1 de l'énergie due à l'interaction des atomes conduit suivant la méthode classique des Orbitales moléculaires au déterminant

$$|V_{kl} - E^1 \delta_{kl}| = 0 \quad (\text{III.8})$$

dans lequel

$$\delta_{kl} \begin{cases} = 0 & \text{si } k \neq l \\ = 1 & \text{si } k = l \end{cases} \quad (\text{symbole de Kronecker})$$

et

$$\begin{aligned}
 V_{kl} &= \int \varphi_l^* (V - V_k) \varphi_k d\tau \\
 &= \int \exp [(2\pi i e / hc) (\mathbf{A}_l - \mathbf{A}_k) \cdot \mathbf{r}] \cdot \varphi_l^0 (V - V_k) \varphi_k^0 d\tau
 \end{aligned}$$

$V - V_k$ = potentiel total duquel on a ôté la part qui revient à l'atome k . On voit que, dans ces conditions, les éléments diagonaux tels que $V_{kk} = \varepsilon_k^0$ seront indépendants du champ magnétique.

Pour calculer les éléments V_{kl} correspondant à deux atomes k et l voisins (on suppose que les autres sont nuls), London considère que r s'éloigne peu de la valeur qu'il prend à mi-distance des atomes k et l dans le domaine où la fonction placée sous l'intégrale a une valeur notable.

Ses composantes sont alors:

$$r_x = \frac{1}{2}(x_k + x_l) \quad r_y = \frac{1}{2}(y_k + y_l)$$

Si le champ magnétique est dirigé suivant l'axe Oz perpendiculaire au plan de la molécule, on peut prendre pour composante de A_k

$$A_{k_x} = -\frac{1}{2}H_{y_k} \quad A_{k_y} = \frac{1}{2}H_{x_k} \quad A_{k_z} = 0$$

il vient finalement

$$(2\pi i e / hc) (\mathbf{A}_l - \mathbf{A}_k) \cdot \mathbf{r}_k = (\pi i e / hc) (x_l y_k - x_k y_l) H = 2\pi i f_{kl}$$

(f_{kl} désignant le flux magnétique traversant le triangle formé par l'origine et les centres des atomes k et l , multiplié par la quantité e/hc).

Cette approximation permet de faire sortir l'exponentielle de l'intégrale et d'écrire

$$V_{kl} = \exp (2\pi i f_{kl}) \cdot \beta_{kl}^0$$

avec

$$\beta_{kl}^0 = \int \varphi_l^0 (V - V_k) \varphi_k^0 d\tau$$

(intégrale de résonance en l'absence de champ magnétique). Si l'on suppose en outre que les éléments ε_k^0 et β_{kl}^0 ont les mêmes valeurs ε^0 et β^0 quels que soient les atomes considérés, avec le changement de variable

$$g = (\varepsilon^0 - E) / \beta$$

le déterminant III.8 prend la forme

$$\eta_{kl} \exp (2\pi i f_{kl}) + g \delta_{kl} = 0$$

avec

$$\eta_{kl} \begin{cases} = 0 & \text{si } k \text{ et } l \text{ ne sont pas voisins} \\ = 1 & \text{si } k \text{ et } l \text{ sont voisins} \end{cases}$$

Pour les chaînes aliphatiques, l'équation séculaire obtenue en développant ce déterminant ne dépend pas du champ magnétique, d'où une contribution à la susceptibilité magnétique due à la conjugaison nulle.

Au contraire, dès qu'il existe un cycle, par exemple, dans la molécule, l'équation séculaire peut se mettre sous la forme

$$F_0(g) + F_2(g) \cdot \omega^2 + F_4(g) \cdot \omega^4 + \dots = 0 \quad (\text{III.9})$$

$F_0(g)$ est un polynôme en g identique à celui obtenu en l'absence de champ magnétique; $F_2(g)$, $F_4(g)$... sont des polynômes en g ,

$$\omega = (2\pi e / hc) SH$$

(S = surface du cycle).

Il est intéressant de noter que les termes tels que f_{kl} dépendent de l'origine choisie pour effectuer le calcul, mais qu'il n'en est plus de même pour l'équation III.9 qui ne dépend que de la surface du cycle.

Il est alors facile de calculer la variation d'une racine simple g_i solution de l'équation séculaire en l'absence de champ magnétique.

En posant:

$$g_{iH} = g_i + \mu_i \omega^2$$

on obtient

$$\mu_i = -F_2(g_i) / F'_0(g_i)$$

$F_2(g_i)$ = valeur de polynôme $F_2(g)$ pour $g = g_i$; $F'_0(g_i)$ = valeur de la dérivée du polynôme $F_0(g)$ pour $g = g_i$.

Dans le cas d'une racine multiple (niveaux dégénérés), il se produit une séparation des racines proportionnelles au champ, mais la somme des racines subit encore une variation proportionnelle à ω^2 , qu'il est facile de calculer.⁶³

E^1 se mettra donc finalement sous la forme

$$E^1 = n\varepsilon^0 - \sum_i n_i(g_i + \mu_i\omega^2)\beta^0 \quad (\text{III.10})$$

n_i étant le nombre d'électrons occupant le niveau i .

Il est facile de voir que si l'on avait considéré le champ magnétique H parallèle au plan de la molécule, le terme ω^2 qui est proportionnel au carré du flux traversant la surface du cycle serait nul. La contribution à la susceptibilité K_3 perpendiculaire au plan d'une molécule que l'on peut calculer à partir de l'équation III.10 en utilisant la relation

$$\chi = -(1/H) \cdot (\partial E^1 / \partial H)$$

correspond donc bien à une anisotropie. On aura, puisque ω^2 est proportionnel à H^2 :

$$\Delta K_{\text{London}} = 2 \sum_i n_i \mu_i (\omega^2 / H^2) \beta^0$$

La présence de champ magnétique ne laisse subsister que les symétries centrales; celles-ci peuvent d'ailleurs être mises à profit pour simplifier les calculs.¹¹

Brooks²¹ a montré, en outre, que si au lieu de négliger les intégrales de recouvrement telles que

$$S_{kl}^0 = \int \varphi_k^0 \varphi_l^0 d\tau$$

on suppose qu'elles sont proportionnelles aux intégrales de résonance β_{kl}^0 , on peut en tenir compte en modifiant simplement les termes μ_i correspondant à chaque niveau. Ce perfectionnement ne modifie d'ailleurs en général que très peu les résultats.

Actuellement un grand nombre d'anisotropies ont été calculées grâce à cette méthode, notamment par London,⁵⁴ Mayot, Berthier, et Pullman^{10, 11, 63} et McWeeny.⁵⁷ Il est théoriquement possible d'effectuer le calcul pour des composés contenant des hétéroatomes mais on se heurte à la difficulté du choix des paramètres; on peut citer cependant le travail de Evans, de Heer, et Gergely²⁹ sur la quinone.

(1) Comparaison avec les Résultats Expérimentaux

Expérimentalement, on peut déterminer les trois susceptibilités principales χ_1 , χ_2 , χ_3 , d'un cristal. La connaissance de la position

des molécules dans la maille cristalline (généralement donnée par l'étude aux Rayons X) permet alors de calculer les susceptibilités principales K_1 , K_2 et K_3 de la molécule elle même. Dans le cas d'une molécule aromatique on appelle K_3 la susceptibilité principale perpendiculaire au plan de la molécule et K_1 et K_2 les deux autres susceptibilités principales qui sont situées dans ce plan. L'anisotropie magnétique est alors définie généralement par la relation

$$\Delta K = K_3 - \frac{1}{2}(K_1 + K_2)$$

Les anisotropies théoriques obtenues par la méthode de London classique sont proportionnelles au paramètre β^0 , aussi présente-t-on ces résultats sous la forme du rapport ρ de l'anisotropie du composé étudié à celle du benzène. La comparaison est donnée dans le tableau III.3.

TABLEAU III.3

Composé	$\rho_{\text{expérimental}}^a$	ρ_{London}
Naphtalène	1,91	2,185
Anthracène	3,06	3,448
Chrysène	3,76	4,439
Biphényle	1,98	1,868
<i>p</i> -Diphénylbenzène	2,99	2,729

^a Calculé à partir des anisotropies données par K. Lonsdale⁵⁵ et rapporté^{43'} à $\Delta K_{\text{benzène}} = -59,7 \times 10^{-6}$.

On remarque que l'accord n'est pas toujours très satisfaisant, ceci peut être expliqué simplement par le fait que la théorie précédente néglige une partie de l'anisotropie: d'une part, l'anisotropie due aux liaisons σ (qui peut prendre des valeurs relativement importantes par suite de la planéité de la molécule),⁴³ d'autre part, l'anisotropie des électrons π localisés autour d'un atome de carbone.^{9, 43}

C'est ainsi qu'elle ne prévoit aucune anisotropie dans le cas des doubles liaisons éthyléniques, alors que leur présence paraît indispensable pour expliquer l'anisotropie de la quinone (cf. section IV.B(3)).

Dans le cas de la quinone, on trouve en effet une anisotropie expérimentale⁵⁵ égale à $-40,6 \times 10^{-6}$ alors que les calculs théoriques faits par Evans, de Heer, et Gergely²⁹ conduisent à un rapport ρ négatif, c'est-à-dire à une anisotropie positive.

Il semble que l'accord devrait être meilleur si l'on utilise comme mesure expérimentale l'exaltation diamagnétique Δ définie comme étant égale à la différence entre la susceptibilité moléculaire moyenne mesurée $\bar{\chi}_M$ et la susceptibilité calculé par la systématique χ_{calc} en utilisant un schéma fictif dans lequel les doubles liaisons ne seraient pas conjuguées.^{9,43}

$$\Delta = \bar{\chi}_M - \chi_{\text{calc}}$$

En effet, si l'on suppose que cette exaltation Δ provient uniquement de la variation de la susceptibilité K_3 représentée par l'anisotropie théorique ΔK_{London} , on doit avoir:

$$\Delta = \frac{1}{3} \Delta K_{\text{London}}$$

car, dans ce cas, il n'y a pas à tenir compte des anisotropies parasites précédentes qui s'éliminent dans le calcul de Δ .

Effectivement, l'accord est meilleur qu'avec les anisotropies expérimentales.

Un autre avantage purement pratique réside dans le fait que la détermination de l'exaltation Δ ne nécessite que la connaissance de la susceptibilité moyenne du composé étudié; il n'est donc pas utile de préparer de beaux monocristaux, ni de connaître la position des molécules dans le cristal, ce qui permet d'étendre la comparaison à un beaucoup plus grand nombre de corps: composés liquides ou composés solides dont l'étude complète aux Rayons X n'a pas été faite, c'est-à-dire la grande majorité.

Dans le tableau III.4 sont rassemblés pour quelques composés organiques conjugués le rapport ρ_{London} calculé à partir de la méthode de London et le rapport

$$r_{\text{exp}} = \Delta / \Delta_{\text{C}_6\text{H}_6}$$

(l'exaltation diamagnétique du benzène étant prise égale à $\Delta_{\text{C}_6\text{H}_6} = -15,1 \times 10^{-6}$).

On constate cependant certaines divergences systématiques.⁴³

TABLEAU III.4

Composé	ρ_{London}	$\chi_{\text{expérimental}}$	$\chi_{\text{théorique}}$
Benzène	1	1	1
Naphtalène	2,185	2,06	2,09
Anthracène	3,448	3,25	3,24
Naphtacène	4,747	4,35	4,41
Biphényle	1,868	2,00	1,95
<i>p</i> -Diphényl benzène	2,729	2,93	2,90
<i>p</i> -Diphényl biphényle	3,589	3,80	3,85
Stilbène	1,794	1,65	1,97
Diphényl-1, 4 butadiène	1,760	1,89	2,00
Diphényl-1,8 octatétraène	1,71	2,28	2,10
Diméthyl dibenzopentalène	-0,750	0,87	0,30

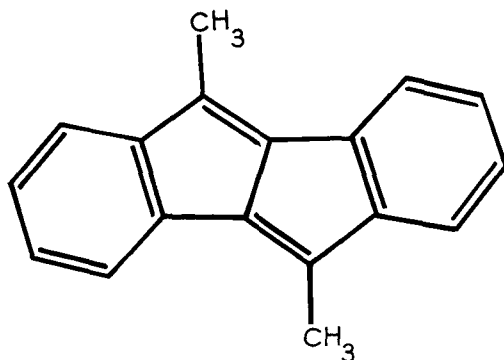


Fig. 3. Diméthyl dibenzopentalène.

(a) pour les hydrocarbures aromatiques contenant un grand nombre de noyaux accolés, la valeur théorique est systématiquement supérieure à la valeur expérimentale. (b) La théorie de London ne permet pas d'expliquer l'exaltation diamagnétique observée expérimentalement pour les molécules contenant une chaîne de doubles liaisons conjuguées (diphényl polyènes).

(c) Pour certains composés non benzénoïdes, la théorie conduit à une dépréciation du diamagnétisme due à la conjugaison (Δ positif) en contradiction avec les résultats expérimentaux.

L'un de nous a montré⁴³ que les résultats théoriques étaient meilleurs si l'on écrivait

$$\nu_{\text{théorique}} = \frac{1}{3}\Delta K_{\text{London}} + k \cdot R$$

Le terme supplémentaire ajouté est proportionnel à l'énergie de résonance R calculée de la molécule, le coefficient de proportionnalité k devant être voisin de $0,776 \times 10^{-18}$ pour donner un accord satisfaisant avec l'expérience.

Un calcul plus complet portant sur le calcul des éléments V_{kl} en présence de champ magnétique et sur le choix des fonctions d'ondes atomiques perturbées donne une justification théorique de l'introduction d'un tel terme proportionnel aux énergies de résonance, bien qu'il ne soit pas possible d'en préciser la valeur théoriquement.

Nous avons porté dans la dernière colonne du tableau précédent la valeur $\Delta_{\text{théorique}}$ rapportée à la valeur correspondante calculée pour le benzène que nous avons appelée $\nu_{\text{théorique}}$.

On remarquera le meilleur accord obtenu après cette correction, avec les valeurs expérimentales dans les différentes séries. En particulier celle-ci permet de retrouver pour le diméthyl dibenzopentalène, une valeur de $\nu_{\text{théorique}}$ positive.

Tous ces résultats sont fonction du paramètre β^0 que l'on élimine comme nous l'avons vu, en présentant les résultats sous la forme du rapport ρ de l'anisotropie calculée pour la molécule considéré à l'anisotropie calculée pour le benzène. Certains auteurs K. Kambe,⁴⁹ Fujii et Shida,³¹ Itoh, Ohno, et Yoshizumi⁴⁷ ont cherché à calculer d'une manière absolue l'anisotropie du benzène lui-même en utilisant la méthode des orbitales moléculaires anti-symétrisées (méthode de Goeppert-Mayer et Sklar). Ces calculs conduisent à une anisotropie de l'ordre de 50 % de l'anisotropie réelle du benzène.

Cet écart provient sans doute du fait que la méthode de London néglige, comme nous l'avons dit, une partie importante de l'anisotropie.

IV. LES SYSTÉMATIQUES MAGNÉTOCHIMIQUES

Une systématique magnétochimique est un ensemble de nombres généralement caractéristiques d'atomes ou de liaisons, qui permettent de calculer à priori la susceptibilité diamagnétique d'une molécule. On décrira successivement une systématique théorique et les systématiques magnétochimiques expérimentales.

A. Systématique Théorique

Nous avons vu, paragraphe III.3, que Tillieu et Guy^{100, 101} ont proposé une théorie satisfaisante pour le calcul des susceptibilités diamagnétiques dont nous avons donné le principe.

Les résultats ont été étendus par Baudet⁶ aux atomes et aux liaisons les plus couramment rencontrées en chimie organique. Les tableaux suivants rassemblent les résultats de ces calculs et forment une véritable systématique théorique à l'aide de laquelle on peut calculer la susceptibilité magnétique d'un grand nombre de molécules à liaisons localisées.

On rappelle que ces valeurs ont été établies à l'aide des fonctions d'onde de la méthode des orbitales moléculaires, en utilisant les fonctions atomiques hydrogénoïdes de Slater (ou de Coulson dans le cas du carbone).

On donnera successivement la susceptibilité des électrons internes des atomes (tableau IV.1), la susceptibilité des doublets

TABLEAU IV.1. Susceptibilités Magnétiques des Couches Électroniques Internes des Atomes — $\chi \times 10^6$.

Atomes	1s ²	2s ²	2p ⁶	3s ²	3p ⁶	3d ¹⁰	4s ²	4p ⁶	4d ¹⁰	χ total
C	0,15*									0,15*
N	0,105									0,105
O	0,08									0,08
F	0,06									0,06
Si	0,025	0,49	0,78							1,30
S	0,019	0,34	0,53							0,89
Cl	0,017	0,29	0,46							0,77
Br	0,004	0,05	0,08	0,36	0,54	3,07				4,10
I	0,002	0,01	0,03	0,11	0,17	0,92	0,77	1,13	6,43	9,57

libres (tableau IV.2), la susceptibilité des liaisons σ (tableau IV.3) et la susceptibilité des paires d'électrons π de quelques liaisons multiples (tableau IV.4).

TABLEAU IV.2. Susceptibilité Magnétique des Doublets Libres

Atomes	μ_A	$-\chi \times 10^6$	Atomes	μ_A	$-\chi \times 10^6$
N	1	2,22	Cl	0	5,37
	1,732	2,43		1,732	4,13
O				∞	2,58
	1,414	1,73	Br	0	8,45
	1,732	1,78		1,732	7,46
F				∞	3,85
	0	1,76	I	0	14,49
	1,732	1,37		1,732	11,03
S	∞	0,91		∞	6,34
	1,732	5,14			

Les résultats obtenus par Tillieu et Guy^{100, 101} ont été signalés par un astérisque,* les autres ont été calculés par Baudet⁶ (voir également les références 7 et 8).

Dans le cas des doublets libres et des liaisons σ , il y a lieu de tenir compte des états d'hybridation des différents atomes, les fonctions d'onde atomiques ont donc été prises sous la forme d'une combinaison linéaire des fonctions d'ondes φ_s et φ_p . Pour un atome A , on aura donc

$$\varphi_A = N(\varphi_{s_A} + \mu_A \varphi_{p_A})$$

Ce qui correspond, suivant les valeurs du coefficient μ_A à:

- une orbitale p pure pour $\mu_A = \infty$
- une hybridation sp^3 pour $\mu_A = 1,732$
- une hybridation sp^2 pour $\mu_A = 1,414$
- une hybridation sp pour $\mu_A = 1$
- une orbitale s pure pour $\mu_A = \infty$

Ces coefficients d'hybridation doivent être choisis pour rendre compte des angles de liaisons; c'est ainsi que les angles C—C—O, C—O—C ou C—N—C sont voisins de 109°, il faudra donc prendre

* Certaines de ces valeurs ont été légèrement corrigés par Baudet.

pour l'atome central un coefficient d'hybridation μ égal à 1,732 (correspondant à une hybridation sp^3).

TABLEAU IV.3. Susceptibilités des Liaisons

Liaisons $A-B$	μ_A	μ_B	$-\chi \times 10^6$
H—H	0	0	3,94*
C—H	1	0	3,33*
	1,414	0	3,74*
	1,732	0	4,05*
C—C	1	1	2,38*
	1,414	1	2,47*
	1,414	1,414	2,60*
	1,732	1	2,91*
	1,732	1,414	3,01*
	1,732	1,732	3,10*
C—N	1	1	2,37
	1,732	1,732	3,15
C—O	1,414	1,414	2,55
	1,414	1,732	2,51
	1,732	1,732	2,73
C—F	1,732	1,732	2,51
	1,732	∞	2,44
C—Si	1,732	1,732	6,00
C—S	1,732	1,732	4,83
C—Cl	1,732	1,732	4,28
	1,732	∞	4,24
C—Br	1,732	1,732	7,41
	1,732	∞	7,69
C—I	1,732	1,732	7,88
	1,732	∞	7,63
N—H	1,732	0	3,63
N—N	1	1	2,18
O—H	1,732	0	3,34
Si—H	1,732	0	7,00
Si—O	1,732	1,732	5,03
S—H	1,797	0	5,28
S—S	1,797	1,797	5,29

On calcule par exemple à partir de ces tableaux la susceptibilité de l'hexène-1, C_6H_{12} , de la manière suivante.

TABLEAU IV.4. Susceptibilité d'une Paire d'Électrons π

Liaisons	$-\chi \times 10^6$	Liaisons	$-\chi \times 10^6$
C=C	3,42*	N \equiv N	2,35
C \equiv C	4,94*	C=O	3,05
C \equiv N	3,44		

Électrons internes de 6 atomes de Carbone:

$$-0,15 \times 10^{-6} \times 6 = -0,90 \times 10^{-6}$$

Susceptibilités des liaisons:

$$3 \text{ liaisons C } (sp^3) - \text{C } (sp^3) \quad -3,10 \times 10^{-6} \times 3 = -9,30 \times 10^{-6}$$

$$1 \text{ liaison C } (sp^3) - \text{C } (sp^2) \quad -3,01 \times 10^{-6} \times 1 = -3,01 \times 10^{-6}$$

$$1 \text{ liaison C } (sp^2) - \text{C } (sp^2) \quad -2,60 \times 10^{-6} \times 1 = -2,60 \times 10^{-6}$$

$$9 \text{ liaisons C } (sp^3) - \text{H} \quad -4,05 \times 10^{-6} \times 9 = -36,45 \times 10^{-6}$$

$$3 \text{ liaisons C } (sp^2) - \text{H} \quad -3,74 \times 10^{-6} \times 3 = -11,22 \times 10^{-6}$$

$$\text{Susceptibilité de la liaison } \pi \quad -3,42 \times 10^{-6} \times 1 = -3,42 \times 10^{-6}$$

$$\chi_{\text{C}_6\text{H}_{12}} = -66,90 \times 10^{-6}$$

$$\chi_{\text{expérimental}} = -66,71 \times 10^{-5}$$

Le détail des calculs montre, d'une manière générale, que, d'une part la valeur absolue de la susceptibilité des liaisons augmente avec la distance interatomique et décroît avec l'augmentation de la charge nucléaire effective, et que d'autre part le terme correctif paramagnétique est généralement faible pour les doublets libres et les liaisons alors que les anisotropies correspondantes sont souvent de l'ordre de 30%.

Cette systématique théorique permet de calculer avec une approximation de l'ordre de 2% les susceptibilités des molécules à liaisons localisées, comme on le constatera dans le tableau IV.14. Le précision est cependant moins bonne pour les atomes.

Malheureusement, les susceptibilités des composés aromatiques échappent pour l'instant à ce mode de calcul.

B. Systématiques expérimentales

(1) Loi d'Additivité

L'établissement d'une systématique est lié directement à l'existence d'une loi d'additivité.

Etant donné les corps A, B, C, D, \dots jouissant de la propriété P (masse chaleur spécifique, susceptibilité magnétique, etc. . . .), $P_A, P_B, P_C, P_D, \dots$ les nombres qui caractérisent la propriété de chacun des corps; et P_M , celle du mélange ou de la combinaison des corps considérés, on dit que la propriété obéit à une loi d'additivité, si:

$$P_M = \alpha P_A + \beta P_B + \gamma P_C + \delta P_D + \dots,$$

$\alpha, \beta, \gamma, \delta, \dots$ étant les proportions relatives de A, B, C, D, \dots dans la masse unité du mélange ou de la combinaison.

S'il est logique que la loi d'additivité soit rigoureuse dans le cas des mélanges, lorsque les constituants de celui-ci sont en interaction faible, que devient-elle dans le cas des combinaisons? Les atomes n'y sont plus juxtaposés, mais liés de façon intime; leur action réciproque n'est pas favorable au maintien de l'intégrité des propriétés atomiques. Et pourtant, contre cette évidence, les physicochimistes ont cherché des propriétés additives moléculaires. De fait ils n'en ont point trouvé.

La loi de Woestyn, relative à l'additivité des chaleurs spécifiques, ne se vérifie pas mieux que celle relative au parachor; et les rotativités magnétiques n'obéissent pas mieux à la loi que les réfractivités. Même l'additivité des masses a été infirmée par la théorie de la relativité.

Il n'y a, dans ces faits, rien qui doive troubler; car, dans l'évolution d'une loi d'additivité, il y a toujours deux phases successives: „Tout d'abord les relations numériques généralement fournies par les séries homologues de la chimie organique permettent d'affecter chaque élément d'un coefficient atomique constant, et les coefficients moléculaires correspondants s'obtiennent, pour chaque composé, en faisant la somme des coefficients atomiques des éléments constituants. Puis vient une période de malaise dont on sort en attachant à chaque particularité de structure un coefficient propre, l'incrément, destiné à entrer comme terme correctif dans le calcul des constantes moléculaires. On voit alors le principe d'additivité perdre peu à peu sa simplicité initiale, trop heureux lorsque de nouvelles déterminations n'en détruisent pas définitivement l'utilité pratique" (Pascal). La loi d'additivité,

ainsi modifiée, prend alors, pour une combinaison, la forme:

$$P_M = \alpha P_A + \beta P_B + \gamma P_C + \delta P_D + \dots + \Sigma \lambda$$

($\Sigma \lambda$ = somme des termes correctifs caractéristiques de la structure appelés incréments) et c'est alors qu'elle devient féconde.

L'additivité des propriétés magnétiques n'a pas fait exception à la règle générale. On peut la résumer par l'expression suivante:

$$\chi_M = \Sigma \chi_A + \Sigma \lambda$$

indiquant que la susceptibilité moléculaire d'un composé est égale à la somme des susceptibilités des atomes qui la constituent et des incréments de structure.

Après les tentatives de Henrichsen qui datent de 1888, c'est Pascal qui, le premier, en 1910, établit une systématique magnétochimique cohérente. Construite à partir des composés organiques, cette systématique a été étendue par la suite à la chimie minérale; mais les difficultés rencontrées dans ce domaine ont été plus nombreuses.

(2) *Établissement des Systématiques*

(a) *Susceptibilité du Groupe CH₂*. Le premier résultat que Pascal dégagait nettement de ses recherches est la variation régulière des susceptibilités moléculaires dans toutes les séries homologues. Cette variation se fait suivant une progression arithmétique, et, lorsque l'on passe du terme en C_n au terme en C_{n+1} la susceptibilité moléculaire varie d'une quantité sensiblement constante.

Cette susceptibilité du groupe CH₂ est sensiblement indifférente à la présence, dans une molécule, d'un ou plusieurs atomes d'azote d'oxygène, de soufre, etc.

Depuis, la susceptibilité du groupe CH₂ a fait l'objet de nombreuses recherches résumées dans le tableau IV.5, d'après lequel il semble bien que la valeur $\chi_{CH_2} = -11,36 \times 10^{-6}$ puisse être désormais retenue. Cette détermination est le point de départ des différentes systématiques proposées.

(b) *Détermination des Susceptibilités Atomiques*. Les différents auteurs ont opéré de manière différente: Pascal⁷⁷ a constaté que le remplacement d'un atome d'halogène par un atome d'hydrogène

TABLEAU IV.5. Susceptibilité Magnétique du Groupe CH₂

Années	Auteurs	$-\chi_{\text{CH}_2} \times 10^6$	Valeurs extrêmes	Erreurs en %	Composés	Nombre de composés
1910	Pascal ¹⁷	11,86	11,5 -12,5	1,5	11 Séries	35
1927	Vaidyanathan ¹⁰⁶	11,2			Vapeurs et liquides organiques	
1929	Bitter ¹⁵	14,5	13,2 -16,9	7,3	Hydrocarbures gazeux	5
1934	Cabrera et Fahlenbrach ²⁴	11,48	11,08-12,13	2,3	Alcools, esters, acides	6
1934	Bhatnagar, Mitra, et Tuli ¹⁴	11,36	11,23-11,55	0,9	Carbures, nitrates, nitrites, composés nitrés	20
1935	Gray et Cruickshank ³⁵	11,86				
1935	Woodbridge ¹¹⁹	11,67	11,25-12,06	2,1	Esters	4
1936	Bhatnagar et Mitra ¹³	11,68	10,6 -12,5	2,1	11 Séries	82
1937	Farquharson et Sastri ³⁰	11,64	11,39-11,86	1,6	Acides	5
1943	Augus et Hill ⁴	11,68	10,96-11,99	1,4	Carbures, acides, esters	27
1947	Broersma ²⁰	11,37			Carbures	48
1951	Pascal, Pacault et Hoarau ⁷⁸	11,36			Hydrocarbures, alcools, acides	36

ou par un autre atome d'halogène dans une molécule faisait varier régulièrement la susceptibilité moléculaire, comme on peut le constater dans le tableau IV.6, où sont rassemblées les susceptibilités moléculaires χ_M de quelques composés et les différences Δ correspondantes.

TABLEAU IV.6

Composé	$-\chi_M \times 10^6$	$\Delta \times 10^6$	$\Delta_1 \times 10^6$
C_6H_6	55,1		
C_6H_5Cl	71,9	16,8	16,97
$CH_3CO_2C_2H_5$	55,2		
$CH_2ClCO_2C_2H_5$	72,3	17,1	16,97
C_6H_6	55,1		
$C_6H_6Cl_3$	106,5	$3 \times 17,1$	$3 \times 16,97$
C_6H_5Cl	71,9		
C_6H_5Br	82,2	10,3	10,5
C_6H_5I	96,0	13,8	14,6
$CH_2ClCO_2C_2H_5$	72,3		
$CH_2BrCO_2C_2H_5$	83,0	10,7	10,5
$CH_2ICO_2C_2H_5$	97,8	14,8	14,6

De plus, il est facile de voir que ces différences Δ sont sensiblement égales aux différences Δ_1 des susceptibilités atomiques des éléments correspondants à l'état pur (H_2 , Cl_2 , Br_2 , I_2).

Pascal en a déduit que la susceptibilité atomique des halogènes étaient les mêmes à l'état pur et en combinaison et que l'on pouvait prendre en particulier pour susceptibilité atomique du chlore en combinaison:

$$\chi_{Cl} = -20,1 \times 10^{-6}$$

valeur déterminée sur le chlore liquide et à partir de laquelle il a calculé les autres susceptibilités atomiques en choisissant successivement des familles de composés ne possédant qu'un atome de susceptibilité encore inconnue. Bhatnagar, Mitra, et Tuli¹⁴ ont proposé pour base la susceptibilité du carbone-diamant ($-6,0 \times 10^{-6}$).

Cabrera et Fahlerbach²⁴ ont déterminé les susceptibilités atomiques de l'hydrogène ($-2,545 \times 10^{-6}$) et de l'oxygène en

comparant les susceptibilités d'un alcool C_nH_{2n+1} et de l'hydrocarbure correspondant C_nH_{2n+2} . On a en effet

$$\chi_{C_nH_{2n+1}OH} - n\chi_{CH_2} = 2\chi_H + \chi_O$$

$$\chi_{C_nH_{2n+1}OH} - \chi_{C_nH_{2n+2}} = \chi_O$$

Pascal, Pacault et Hoarau⁷⁸ ont cherché à déduire la susceptibilité χ_H de celle des hydrocarbures saturés. On devrait avoir en effet:

$$\chi_{C_nH_{2n+2}} - n\chi_{CH_2} = 2\chi_H$$

Cependant, on a observé expérimentalement que les composés organiques ramifiés présentent systématiquement un excès de diamagnétisme par rapport aux composés normaux.^{4, 20, 78} Le tableau IV.7 donne pour quelques isomères les susceptibilités moléculaires χ_M et les différences λ correspondantes.

TABLEAU IV.7

Composé	$-\chi_M \times 10^6$	$\lambda \times 10^6$
<i>n</i> -Hexane	74,0	$2 \times 0,9$
Diméthyl-2,3 butane	75,8	
Méthyl-2 hexanol-3	92,3	0,7
Diméthyl-2,4 pentanol-3	93,0	
<i>n</i> -Octane	96,5	1,5
Méthyl-3 heptane	98,0	0,8
Diméthyl-2,3 hexane	98,8	1,2
Triméthyl-2,2,4 pentane	100,0	

Ils ont attribué ces différences à l'existence des groupes CH_3 auxquels ils font correspondre un incrément λ_{CH_3} égal à $-0,85 \times 10^{-6}$.

Dans ces conditions, la susceptibilité atomique de l'hydrogène est donnée par une expression de la forme suivante, pour un hydrocarbure linéaire:

$$\chi_{C_nH_{2n+2}} - n\chi_{CH_2} - 2\lambda_{CH_3} = 2\chi_H$$

La moyenne des valeurs ainsi obtenues conduit à prendre

$$\chi_H = -2,0 \times 10^{-6}$$

Il est facile de déterminer alors la susceptibilité atomique du

carbone:

$$\chi_{\text{C}} = \chi_{\text{CH}_2} - 2\chi_{\text{H}} = -7,4 \times 10^{-6}$$

La susceptibilité atomique de l'oxygène sera déterminée par exemple à partir des susceptibilités expérimentales des alcools, pour un alcool primaire normal de formule $\text{C}_n\text{H}_{2n+1}\text{OH}$, on a en effet:

$$\chi_{\text{O}} = \chi_{\text{C}_n\text{H}_{2n+1}\text{OH}} - n\chi_{\text{CH}_2} - 2\chi_{\text{H}} - \lambda_{\text{CH}_3}$$

et ainsi de suite.

(c) *Introduction des Incréments de Structure.* Nous venons de voir comment Pascal, Pacault, et Hoarau⁷⁸ ont du introduire un incrément de structure λ_{CH_3} pour déterminer les principales susceptibilités atomiques.

Ce fait est général: lorsque les molécules présentent des accidents structuraux (liaisons éthyléniques, liaisons acétyléniques, noyaux aromatiques etc.), ceux-ci se manifestent le plus souvent par une différence entre les susceptibilités mesurées et calculées. Il est alors indispensable de faire intervenir de nombreux incréments, qui mettent en évidence les limites d'une construction trop simpliste.

Le nombre de ces incréments n'est naturellement pas limité puisque pour chaque structure particulière, il faudrait en faire intervenir un, mais nous pensons qu'il faut se garder de les multiplier à l'excès, ce qui ramènerait finalement les systématiques magnétochimiques à des tables de constantes: une systématique doit s'appliquer au plus grand nombre de composés possibles avec le minimum d'incrément.

Dans ces conditions, il y a lieu de faire une distinction entre les composés à liaisons localisées et les composés à liaisons délocalisées. Dans le premier cas, on peut s'attendre en effet à retrouver une systématique satisfaisante, après l'introduction de quelques incréments et c'est effectivement ce que l'on constate. Au contraire, il est normal que les composés à liaisons délocalisées présentent une individualité qui nécessiterait l'introduction d'un incrément pour chaque molécule.

Pascal, Pacault, et Hoarau⁷⁸ ont préféré limiter leur systéma-

tique aux molécules à liaisons localisées. Dans ces conditions, si l'on veut étudier la susceptibilité magnétique d'une molécule à liaisons délocalisées, il est encore possible de calculer grâce à cette systématique une susceptibilité χ_{calc} pour la molécule hypothétique correspondante qui ne serait pas conjuguée. Cette valeur est bien entendu différente de la susceptibilité moléculaire expérimentale χ_M et la différence, que l'on peut appeler incrément de délocalisation,

$$\Delta = \chi_M - \chi_{\text{calc}}$$

représente la modification du diamagnétisme due à la conjugaison et peut alors être interprétée en termes de structure. Les tableaux IV.10 et IV.11 rassemblent les valeurs de la systématique de Pascal, Pacault, et Hoarau.⁷⁸

On notera que certaines de ces valeurs sont légèrement différentes de celles données dans les publications initiales, car nous avons tenu compte de valeur plus récentes en ce qui concerne l'azote d'une part (François et Hoarau,⁷⁸) les halogènes et le soufre d'autre part. (Communications personnelles de H. François et R. Perceau, en cours de publication).

TABLEAU IV.8 Susceptibilités Atomiques

Élément	Composé	$-\chi \times 10^6$	Élément	$-\chi \times 10^6$
H		2.0	F	5.8
C		7.36	Cl	18.0
N	amines primaires	6.4	Br	27.6
N	amines secondaires	4.55	I	43.2
O	alcools, éthers	5.3	S	19.0

TABLEAU IV.9

Structure	Incrément $\lambda \times 10^6$
C=C	5,5
C=O	6,4
CH ₃	-0,85

Il est cependant encore possible d'étendre la systématique aux cas des molécules conjuguées. C'est ainsi que la susceptibilité du groupe CO_2 dans les acides reste égale à $-15,15 \times 10^{-6}$. Dans le cas des molécules aromatiques, il est facile de voir (tableau IV.12) que la susceptibilité peut encore être calculée à priori par la formule

$$\chi'_{\text{calc}} = \chi_{\text{calc}} + nA_{\text{C}_6\text{H}_6}$$

TABLEAU IV.10

Composé	$-\chi_{\text{exp}} \times 10^6$	$-\chi'_{\text{calc}} \times 10^6$
Benzène	55,0	55,0
Naphtalène	93,6	92,7
Anthracène	134,2	130,4
Biphényle	106,0	106,0
<i>p</i> -Diphénylbenzène	156,0	157,0

où χ_{calc} est la susceptibilité calculée pour le composé supposé non conjugué, n le nombre de noyaux benzéniques accolés ou non du composé, $A_{\text{C}_6\text{H}_6} = -15,1 \times 10^{-6}$ incrément de délocalisation du benzène. (Cette dernière formule revient à écrire que l'incrément de délocalisation d'une molécule contenant n noyaux aromatiques est égal à n fois l'incrément correspondant du benzène.) Mais il est bien certain qu'un tel calcul conduira à un résultat moins précis que dans la cas des composés à liaisons localisées.

D'autres découpages plus complexes ont été proposés d'une part par Tan Yuan Yang⁹⁹ et d'autre part par Gray et Cruickshank³⁵ dont on trouvera d'ailleurs une critique dans la référence.⁷² Peu importe en définitive le découpage adopté pour définir les susceptibilités des atomes en combinaison, le plus simple sera le meilleur à condition qu'il permette de calculer à priori une susceptibilité moléculaire; ce qui est essentiel, c'est la validité des mesures expérimentales utilisées qui ont servi de base à ces constructions.

Nous venons de décrire dans ce paragraphe les travaux récents faits sur les systématiques magnétochimiques en chimie organique; rappelons qu'il existe également une systématique des susceptibilités

ioniques en chimie minérale, dont l'initiateur fut également Pascal, mais qui a fait l'objet de peu de travaux depuis les mises au point de Pacault.⁷²

(3) *Applications des Systématiques Expérimentales*

Les systématiques magnétochimiques permettent donc de calculer à priori les susceptibilités des différentes molécules. De tels calculs sont très utiles pour déterminer la partie diamagnétique de la susceptibilité des composés paramagnétiques tels que les radiaux libres. Dans le cas des molécules conjuguées, l'étude des incréments de délocalisation est souvent très intéressante et ceux-ci peuvent être comparés, en particulier, aux calculs théoriques, comme on l'a vu section III.E.

Nous détaillons ci-dessous une application récente relative à l'évaluation de l'anisotropie magnétique des molécules aromatiques.

Comme nous l'avons déjà dit, la détermination expérimentale de l'anisotropie magnétique des molécules ne peut se faire que si l'on peut fabriquer des monocristaux de dimensions convenables et si l'étude complète de la position des molécules dans la maille cristalline a été faite aux rayons X. Ces deux impératifs diminuent singulièrement le champ d'investigations, puisqu'il n'est pas possible de déterminer l'anisotropie d'un composé liquide et que le nombre de cristaux organiques dont l'étude complète aux rayons X a été faite est limité.

Cependant la connaissance de l'anisotropie d'une molécule est intéressante. Elle peut constituer, par exemple, une aide pour les cristallographes en permettant de déterminer approximativement la position des molécules dans un cristal.

L'utilisation des systématiques magnétochimiques à la détermination des anisotropies avait été envisagée par Pacault,⁷⁴ Shiba en Hazato⁹² et précisée par Hoarau.⁴³ On peut en effet poser en première approximation que les écarts à la loi d'additivité pour les molécules aromatiques provient uniquement des variations de la susceptibilité principale K_3 perpendiculaire au plan des molécules. Dans ces conditions, il doit être possible de calculer à l'aide de la systématique la moyenne des susceptibilités dans le plan de la molécule $\frac{1}{2}(K_1 + K_2)$.

A partir des susceptibilités principales expérimentales, on peut établir une systématique permettant de calculer $\frac{1}{2}(K_1 + K_2)$; on trouve

$$\frac{1}{2}(K_1 + K_2) \approx \Sigma\chi_A + 2nl \quad (\text{IV.1})$$

$\Sigma\chi_A$ = somme des susceptibilités atomiques dans la systématique de Pascal, Pacault, et Hoarau; $2n$ = nombre de doubles liaisons éthyléniques; $l = +3,75 \times 10^{-6}$. On constate en effet (tableau IV.13) que l'écart entre les valeurs ainsi calculées et les valeurs expérimentales ne dépasse pas 5%.

TABLEAU IV.11

Composé	$\frac{1}{2}(K_1 + K_2)_{\text{exp}}$	$\frac{1}{2}(K_1 + K_2)_{\text{calc}}$	ΔK_{exp}	ΔK_{calc}
Naphtalène	55,0	52,5	114,0	121,5
Anthracène	69,2	71,1	182,6	176,7
Phénanthrène	74,0	71,1	166,0	174,6
Chrysène	85,7	89,7	225,2	213,0
Dibenzo- 1, 2, 5, 6 anthracène	110,0	108,3	248,0	252,9
Pyrène	80,6	78,4	232,9	239,4
Biphényle	63,4	63,8	118,6	117,3
<i>p</i> -Diphénylbenzène	92,5	93,7	178,9	174,9

Si $\bar{\chi}_M$ est la susceptibilité moléculaire moyenne, on a les relations:

$$\bar{\chi}_M = \frac{1}{3}(K_1 + K_2 + K_3)$$

et

$$\Delta K = K_3 - \frac{1}{2}(K_1 + K_2)$$

d'où

$$\Delta K = 3[\bar{\chi}_M - \frac{1}{2}(K_1 + K_2)]$$

Si on prend comme valeur de $\frac{1}{2}(K_1 + K_2)$ celle calculée à l'aide de la formule IV.1, on pourra déterminer l'anisotropie ΔK d'une molécule à partir d'une seule mesure de susceptibilité moyenne. La comparaison entre de tels calculs et les valeurs expérimentales

est donnée dans le tableau IV.13 pour quelques hydrocarbures.

Une conséquence de ces calculs est que la double liaison éthylénique doit avoir une anisotropie magnétique propre, voisine de

$$\Delta K = -6 \times 10^{-6}$$

Celle-ci n'a pas encore été mise en évidence expérimentalement de manière directe, mais elle permet d'expliquer l'anisotropie de la quinone et le fait que les calculs théoriques basés sur la théorie de London donnent toujours un résultat inférieur (en valeur absolue) à l'anisotropie réelle pour le benzène.

C. Comparaison des Systématiques Expérimentales et Théoriques avec l'Expérience

Les diverses systématiques expérimentales et théoriques ne procédant pas selon le même découpage, ne sont comparables que par leur application à des molécules dont on connaît la valeur numérique de la susceptibilité. Le tableau IV.14 rassemble la susceptibilité moyenne expérimentale, et les susceptibilités calculées à l'aide de la systématique théorique et la systématique

TABLEAU IV.12

Composé	$-\chi \times 10^6$		
	Expérience	Systématique théorique	Systématique expérimentale
<i>n</i> -Hexane	74,0	73,10	74,1
<i>n</i> -Heptane	85,5	84,45	85,5
<i>n</i> -Octane	97,0	95,80	96,9
Méthyl-2 heptène-4	88,0	89,6	88,2
<i>n</i> -Butylamine	58,9	59,09	58,85
<i>n</i> -Amylamine	69,4	70,44	70,25
Pentanol	66,8	67,41	67,1
Heptanol	89,0	90,11	89,9
Chlorure de <i>n</i> -butyle	66,4	63,79	66,35
Bromure de <i>n</i> -butyle	75,5	74,49	76,05
Iodure de <i>n</i> -butyle	91,8	90,74	91,65

expérimentale et de Pascal, Pacault, et Hoarau. On constatera

que la systématique expérimentale permet de calculer les susceptibilités moléculaires avec une erreur généralement inférieure à 1%. La systématique théorique conduit à une précision du même ordre de grandeur.

V. DIAMAGNÉTISME DES ÉLECTRONS QUASI LIBRES

L'anisotropie diamagnétique de London étant, dans les carbures aromatiques, sensiblement proportionnelle au nombre de noyaux benzéniques, que se passe-t-il lorsque ce nombre tend vers l'infini? En d'autres termes, que devient la susceptibilité de la liaison π quand les électrons qui assurent cette liaison ne sont plus délocalisés seulement à l'intérieur de cycle benzénique, mais dans un plan graphitique tout entier? Ainsi se trouve tout naturellement posé, à partir de la magnétochimie des composés organiques, le problème du magnétisme de la liaison métallique totalement délocalisée. C'est ce problème que nous allons donc examiner d'abord dans ses grandes lignes avant d'aborder le cas du graphite.

A. Susceptibilité Magnétique d'un Cristal Métallique

(1) *Théorie*

Le réseau d'ions constituant un cristal métallique forme un édifice dont la cohésion est assurée par un gaz d'électrons de valence complètement délocalisés.

La susceptibilité magnétique totale χ d'un cristal métallique peut donc être écrite comme la somme de quatre termes:

$$\chi = \chi_D^i + \chi_P^i + \chi_D^c + \chi_P^c$$

où χ_D^i est la susceptibilité diamagnétique correspondant aux électrons qui restent liés aux ions; χ_P^i est la susceptibilité paramagnétique de spin correspondant éventuellement aux sous-couches incomplètement remplies des ions; χ_D^c et χ_P^c sont les composantes diamagnétique et paramagnétique de la susceptibilité du gaz électronique (électrons de conduction). Les termes χ_D^i et χ_P^i sont fournis par les méthodes habituelles de la magnétochimie. Ils correspondent à des électrons „localisés,” et nous nous bornerons

donc ici à les mentionner: χ_D^i est indépendant de la température et χ_P^i varie en principe suivant la loi de Curie-Weiss des corps paramagnétiques. Les électrons de conduction sont, de leur côté, libres de se déplacer n'importe où, pourvu qu'ils restent à l'intérieur du cristal, et leurs mouvements sont soumis au potentiel périodique créé par les ions du réseau cristallin.

La manière la plus simple de calculer théoriquement la susceptibilité $\chi_D^e + \chi_P^e$ de ce gaz électronique consiste à étudier d'abord le cas où le potentiel périodique est nul en tout point intérieur au cristal, et infini à l'extérieur: on obtient ainsi le magnétisme du gaz d'électrons libres dans une boîte.

Alors que la mécanique classique laissait prévoir pour un tel gaz un diamagnétisme nul, Landau⁵³ a montré en 1930 que le gaz d'électrons libres possède, outre son paramagnétisme de spin, un diamagnétisme important. Le calcul quantique de Landau fut repris et précisé par Stoner.⁹⁸ On part de l'expression générale du moment magnétique:

$$M = -(\partial F / \partial H)_{v, T} \quad (V.1)$$

où H est le champ magnétique, v le volume, et F l'énergie libre du gaz. En désignant par N le nombre d'électrons par unité de volume, par μ le magnéton de Bohr, et par ζ l'énergie libre électronique partielle, on obtient pour le gaz d'électrons libres (en négligeant les termes dépendant du champ) une susceptibilité diamagnétique par unité de volume:

$$K_D = -N\mu^2 F'(\eta) / 3kT F(\eta) \quad (V.2)$$

avec

$$\eta = \zeta / kT$$

$$F(\eta) = \int_0^\infty x^{\frac{1}{2}} dx / [1 + \exp(x - \eta)]$$

et

$$F'(\eta) = \partial F(\eta) / \partial \eta$$

La susceptibilité paramagnétique est d'autre part:

$$K_p = (N\mu^2 / kT) F'(\eta) / F(\eta) \quad (V.3)$$

et par conséquent

$$K_p = -3K_D$$

Comme la théorie permet de calculer η en fonction de T , on connaît donc à toute température la susceptibilité du gaz.

A haute température, les susceptibilités dia et paramagnétique se réduisent à

$$K_D = -N\mu^2/3kT \text{ et } K_p = N\mu^2/kT \quad (\text{V.4})$$

tandis qu'à basse température ($T \ll T_0$) (gaz dégénéré):

$$K_D = -N\mu^2/2kT_0 \text{ et } K_p = 3N\mu^2/2kT_0 \quad (\text{V.5})$$

où

$$T_0 = (h^2/2mk)(3N/8\pi)^{\frac{2}{3}} \quad (\text{V.6})$$

est la „température de dégénérescence” du gaz, $\varepsilon_0 = kT_0$ étant le „niveau de Fermi.”

Pour passer du gaz d'électrons libres aux électrons de conduction dans un cristal réel, il faut introduire d'une façon ou d'une autre le potentiel périodique créé par les ions du réseau métallique dans lequel se meuvent les électrons. On sait que l'existence de ce potentiel détermine la formation de bandes d'énergie interdites ou permises. La plupart des bandes permises ont leurs niveaux entièrement occupés par des électrons, les bandes supérieures pouvant seules être partiellement „remplies” par les électrons de valence du métal.

La formule V.1 est toujours utilisable, mais il est extrêmement difficile de déterminer les niveaux d'énergie électronique en présence du champ magnétique en tenant compte du potentiel périodique. Peierls ⁸⁰ a néanmoins réussi à obtenir, pour la susceptibilité diamagnétique χ_D^e d'un gaz d'électrons incomplètement libres et dégénéré (c'est-à-dire à très basse température), l'expression

$$\chi_D^c = -(e^2/24\pi^2\hbar^2c^2) \iint [(\delta^2 E/\delta k_x^2) (\delta^2 E/\delta k_y^2) - (\delta^2 E/\delta k_x \delta k_y)^2] dS/|\text{grad}_k E| \quad (\text{V.7})$$

où $E(\mathbf{k})$ est l'énergie des électrons, supposée connue, en l'absence de champ magnétique, en fonction de leur vecteur „nombre d'onde” \mathbf{k} , et où l'intégration s'étend sur la surface de Fermi S , le champ magnétique étant dirigé suivant Oz .

Cette expression présente l'avantage de ne pas nécessiter la connaissance des niveaux d'énergie en présence du champ. Il n'est même pas nécessaire de connaître en détail l'énergie en l'absence de champ, puisqu'on n'utilise que les niveaux voisins de la surface de Fermi.

Wilson¹¹⁶ a d'ailleurs donné une expression plus générale de χ_D^c , valable même pour un gaz non dégénéré:

$$\chi_D^c = (e^2/24\pi^2\hbar^2c^2) \iiint [(\delta^2 E/\delta k_x^2) (\delta^2 E/\delta k_y^2) - (\delta^2 E/\delta k_x \delta k_y)^2] (\delta f_0/\delta E) dk_x dk_y dk_z \quad (\text{V.8})$$

où $f_0(E)$ est la fonction de distribution de Fermi-Dirac

$$f_0(E) = [1 + \exp(E/kT - \eta)]^{-1}$$

et où l'intégration s'effectue cette fois dans tout l'espace des vecteurs \mathbf{k} . Il est aisé de montrer que la formule de Wilson conduit, à très basse température, à celle de Peierls.

On peut encore observer que ces formules font intervenir explicitement les composantes

$$m_{ij}^* = \hbar^2/(\delta^2 E/\delta k_i \delta k_j)$$

du tenseur de la „masse effective” des électrons dans le cristal, ce qui suggère une appréciable simplification des calculs.

On peut en effet supposer que cette masse effective est constante et indépendante de l'énergie de l'électron dans la bande considérée. Cela revient, avec un choix d'axes convenables, à écrire l'équation des surfaces d'énergie constante dans l'espace k sous la forme:

$$\begin{aligned}
 E &= (\hbar^2/2) [k_x^2/m_x^* + k_y^2/m_y^* + k_z^2/m_z^*] \\
 &= (\hbar^2/2m) [\alpha_x k_x^2 + \alpha_y k_y^2 + \alpha_z k_z^2]
 \end{aligned}
 \tag{V.9}$$

où m est la masse électronique réelle, et

$$m_x^* = m/\alpha_x, \quad m_y^* = m/\alpha_y, \quad m_z^* = m/\alpha_z$$

sont les masses effectives correspondant aux mouvements de l'électron suivant les axes Ox , Oy , et Oz .

En d'autres termes, cette approximation (qui est fréquemment utilisée) consiste à traiter les électrons comme s'ils étaient complètement libres, à ceci près que leur masse réelle est remplacée par une „masse effective” qui permet de tenir compte du potentiel du réseau.

Les formules de Peierls et Wilson sont alors remplacées par une expression plus simple, valable quels que soient la température et le degré de dégénérescence du gaz électronique, et très semblable à la formule V.2 de Landau-Stoner:

$$\chi_D^c = -(N\mu^2\alpha_x\alpha_y/3kT) F'(\eta)/F(\eta) \tag{V.10}$$

(le champ magnétique étant dirigé suivant Oz) avec

$$F(\eta) = \frac{2}{3}(\varepsilon_0/kT)^{\frac{3}{2}} \tag{V.11}$$

et

$$\varepsilon_0 = (\hbar^2/2m)(\alpha_x\alpha_y\alpha_z)^{\frac{1}{3}}(3N/8\pi)^{\frac{2}{3}}$$

Quant au terme paramagnétique χ_p^c , il est encore donné par la formule V.3, de sorte que

$$\chi_D^c/\chi_p^c = -\alpha_x\alpha_y/3 \tag{V.12}$$

Malheureusement l'approximation sur laquelle repose la formule de Peierls est souvent inapplicable aux cristaux métalliques réels. Les formules simplifiées, à masse effective constante, sont à fortiori encore plus rarement utilisables.

Des travaux récents ont cependant amorcé une étude plus rigoureuse du problème du diamagnétisme des électrons de liaison

métallique. Wilson¹¹⁶ d'une part, et Adams² d'autre part, ont trouvé pour χ_D^e des expressions où figurent, outre le terme de Peierls, un certain nombre d'autres contributions, dont certaines ne sont d'ailleurs pas évaluées explicitement. Mais tandis que Wilson pense, avec quelques réserves, que le terme de Peierls est le plus important de tous, Adams a montré que, dans certains cas importants, certaines des autres contributions sont d'un ordre de grandeur comparable à celui du terme de Peierls. Malheureusement la complexité des méthodes de Wilson et d'Adams rend très difficile leur application aux métaux réels. Enfin une étude très récente de Kjeldaas et Kohn⁵¹ donne, pour un gaz dégénéré dans un réseau cubique, une expression de χ_D^e qui paraît effectivement applicable aux métaux alcalins.

Il convient d'autre part de mentionner les travaux de Dingle,²⁶ Ham,³⁹ et Osborne et Steele⁷¹ sur la valeur de χ_D^e pour des systèmes contenant un nombre très grand mais fini d'électrons.

En ce qui concerne le terme χ_p^e du au spin des électrons de conduction, l'expression initiale V.3 de Landau-Stoner a été peu à peu améliorée pour le cas des cristaux réels: parmi les travaux récents, mentionnons ceux de March et Donovan⁵⁸ et de Pines.⁸¹ Ce terme est généralement du même ordre de grandeur que les contributions diamagnétiques, et beaucoup plus petit que le terme χ_p^i (quand ce dernier n'est pas nul) parce que seuls y interviennent les spins des électrons de conduction voisins du niveau de Fermi, c'est-à-dire en général une très petite fraction du nombre total d'électrons de conduction.

(2) *Résultats Expérimentaux et Interprétation*

Du point de vue expérimental, on peut mesurer bien entendu la susceptibilité spécifique totale moyenne χ du cristal. La systématique magnétochimique fournit d'autre part les valeurs des termes χ_D^i et χ_p^i correspondant aux ions du réseau. Mais il est généralement impossible d'obtenir séparément les termes χ_p^e et χ_D^e : Schumacher, Carver, et Slichter⁸⁹ ont, il est vrai, mis au point une intéressante méthode de résonance paramagnétique qui permet la mesure précise de χ_p^e , mais cette méthode n'a pu jusqu'ici

être appliquée qu'au lithium et au sodium.^{90*} Dans tous les autres cas, l'expérience fournit seulement $(\chi_p^e + \chi_D^e)$ par différence entre χ et $(\chi_D^i + \chi_p^i)$.

(a) *Éléments de Transition*. Tous ces éléments ayant une sous-couche d incomplète, le terme χ_p^i existe, et c'est généralement de beaucoup le plus important. On a donc des cristaux paramagnétiques dont la susceptibilité varie le plus souvent de façon appréciable en fonction de la température. Cette variation ne suit d'ailleurs qu'exceptionnellement la loi de Curie-Weiss en raison des interactions entre les sous-couches d des ions voisins.

(b) *Alcalins et Alcalino-Terreux*. Pour les éléments qui n'appartiennent pas aux séries de transition, la sous-couche d interne est complète et le terme χ_p^i est nul. Les trois autres termes étant tous sensiblement du même ordre de grandeur, la susceptibilité spécifique totale est para ou diamagnétique suivant les cas, mais toujours de l'ordre de 10^{-6} cgs.

Dans le cas des métaux alcalins (Li, Na, K, Rb, Cs) et alcalino-terreux (Ca, Sr, Ba), c'est le terme χ_p^e qui est prépondérant. Comme ces métaux ont dans leur bande de conduction un très grand nombre d'électrons (un par atome pour les alcalins et deux pour les alcalino-terreux), le gaz électronique du cristal est fortement dégénéré à toutes les températures accessibles à l'expérience ($T \ll T_0$; cf. formule V.6 par exemple), et χ_p^e est pratiquement indépendant de la température.

On a effectivement constaté que les métaux alcalins et alcalino-terreux ont une susceptibilité χ paramagnétique sensiblement indépendante de la température.

Le cas des alcalins a été plus spécialement approfondi. Le tableau V.1 donne pour χ_p^e les valeurs théoriques de Pines⁸¹ et expérimentales^{89, 90} ramenées à l'unité de masse. On y a aussi réuni les plus récentes valeurs expérimentales de χ et les valeurs

* On étudie, sur un même échantillon, la résonance paramagnétique électronique et la résonance nucléaire, en ne faisant varier que la valeur du champ magnétique statique. Cela permet d'obtenir, pour la courbe de résonance électronique, un étalonnage suffisamment précis pour permettre la détermination de χ_p^e .

les plus vraisemblables de χ_D^i ,⁷² ce qui permet d'obtenir pour χ_D^e des valeurs „expérimentales” ($\chi_D^e = \chi - \chi_p^e - \chi_D^i$) que l'on peut comparer (pour Li et Na) aux valeurs théoriques de Kjeldaas et Kohn.⁵¹ On voit que, compte tenu de la précision des mesures et de l'évaluation de χ_D^i , l'accord n'est pas trop mauvais entre théorie et expérience, mais qu'on est encore loin de pouvoir confronter de façon décisive les calculs théoriques avec les résultats expérimentaux.

TABLEAU V.1

Métal	$\chi_p^e \times 10^6$		$\chi \times 10^6$		$\chi_D^i \times 10^6$ ⁷²	$\chi_D^e \times 10^6$	
	Théor. ⁵¹	Exp. ^{89, 90}	Exp. ^a	Réf.		Théor. ⁵¹	Exp.
Li	3.51	3.9 ± 0.2	3.54 ± 0.09	84	-0.1	-0.14	-0.26 ± 0.3
Na	0.875	0.98 ± 0.1	0.70 ± 0.03	19	-0.22	-0.27	-0.06 ± 0.13
	0.875	0.98 ± 0.1	0.575	110	-0.22	-0.27	-0.185
K	0.71		0.45	110			
Rb	0.35		0.196	111			

^a A température ordinaire.

(c) *Autres Métaux.* Tous les autres métaux non ferromagnétiques à l'exception de l'aluminium, du magnésium, de l'étain blanc, et aussi peut-être du béryllium, sont diamagnétiques. C'est-à-dire que la somme $\chi_D^i + \chi_D^e$ est en valeur absolue supérieure au terme paramagnétique χ_p^e . Ce diamagnétisme dépend généralement de la température, sauf si le gaz des électrons de conduction est complètement dégénéré, ou lorsqu'il advient que les termes χ_p^e et χ_D^e s'annulent réciproquement.

B. Magnétisme du Graphite Mono et Polycristallin

Abordant maintenant le problème du magnétisme des électrons π totalement délocalisés et de sa variation lors du passage des carbures aromatiques au graphite, nous allons voir que, dans l'état présent de la théorie, la confrontation avec l'expérience peut ici être poussée beaucoup plus loin que dans l'étude des

métaux proprement dits. Cela tient en particulier à ce que la structure pratiquement bidimensionnelle du graphite simplifie considérablement les calculs.

(1) *Résultats Expérimentaux*

Jusqu'en 1950, peu de chercheurs s'étaient intéressés, du point de vue magnétique, au processus de la transition entre les carbures à noyaux accolés et le graphite. Les résultats de quelques auteurs^{76, 86, 104} semblaient indiquer pour le graphite pulvérisé ou colloïdal un diamagnétisme inférieur à celui du graphite monocristallin. Miwa seul avait en 1934⁶⁴ tenté de relier avec précision la susceptibilité aux dimensions des cristallites graphitiques, mais la pureté des charbons étudiés laissait sans doute à désirer.

Le graphite monocristallin lui-même est assez bien connu du point de vue magnétique depuis les travaux de Ganguli et Krishnan.³³ et ceux de Poquet et al.⁸³ si χ_{\parallel} et χ_{\perp} sont les susceptibilités spécifiques mesurées parallèlement et perpendiculairement à l'axe hexagonal du cristal, l'anisotropie $\Delta\chi = \chi_{\parallel} - \chi_{\perp}$ vaut $-20,7 \times 10^{-6}$ à température ordinaire et sa variation entre 80 et 1200° K a été déterminée avec précision.

On trouve, en effet, $-10^6 \Delta\chi = 1,3 + 28,5(1 - e^{-\frac{330}{T}})$. La susceptibilité χ_{\perp} est indépendante de la température et égale à $-0,3 \cdot 10^{-6}$.

Les noirs de carbone et les charbons plus ou moins graphitisés par traitement thermique au dessus de 1000° C présentent tous des structures analogues, constituées par l'agglomération généralement désordonnée de petits „cristallites” graphitiques. Ces cristallites sont formés d'éléments de plans graphitiques, dont la largeur est désignée par L_a , disposés à peu près parallèlement les uns aux autres, la hauteur totale de la pile ainsi réalisée étant L_c . Le rapport L_c/L_a est en général de l'ordre de 2/3, et les valeurs de L_a varient suivant les cas d'une vingtaine à quelques centaines d'Angströms. Pour un type de noir ou de carbone donné, la valeur de L_a ne dépend pratiquement que de la température à laquelle l'échantillon a été traité. Il est donc clair que ces substances

constituent un matériau de choix pour l'étude de la variation du magnétisme lorsqu'on passe des carbures aromatiques au graphite.

La susceptibilité de ces produits a été largement étudiée depuis quelques années. Citons, outre nos propres travaux,⁵⁹ ceux de Blayden et de ses collaborateurs,^{17,120} ceux de Pinnick,⁸² et Kiive,⁸³ et ceux des chercheurs japonais groupés autour d'Akamatu et Honda.^{3,44} On sait maintenant que la susceptibilité moyenne reste voisine de celle des aromatiques tant que le diamètre L_a des plans graphitiques ne dépasse pas 40 Å environ. Entre 40

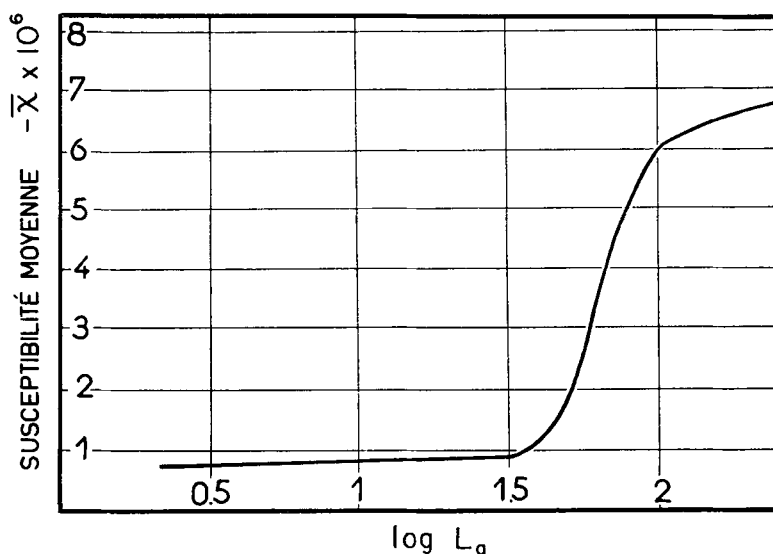


Fig. 4. La susceptibilité moyenne en fonction de L_a à température ordinaire.

et 200 Å se produit une très rapide croissance du diamagnétisme, qui atteint à partir de 200 Å des valeurs très proches de celles du graphite. Simultanément, alors qu'au dessous de 40 Å, la susceptibilité reste indépendante de la température, il apparaît entre 40 et 200 Å une variation thermique, qualitativement analogue à celle du graphite, et d'autant plus importante en valeur relative que L_a est grand.

Les figures 4 et 5 donnent une idée de la variation de la sus-

ceptibilité moyenne en fonction de L_a , à température ordinaire, et de sa variation thermique pour diverses valeurs de L_a .

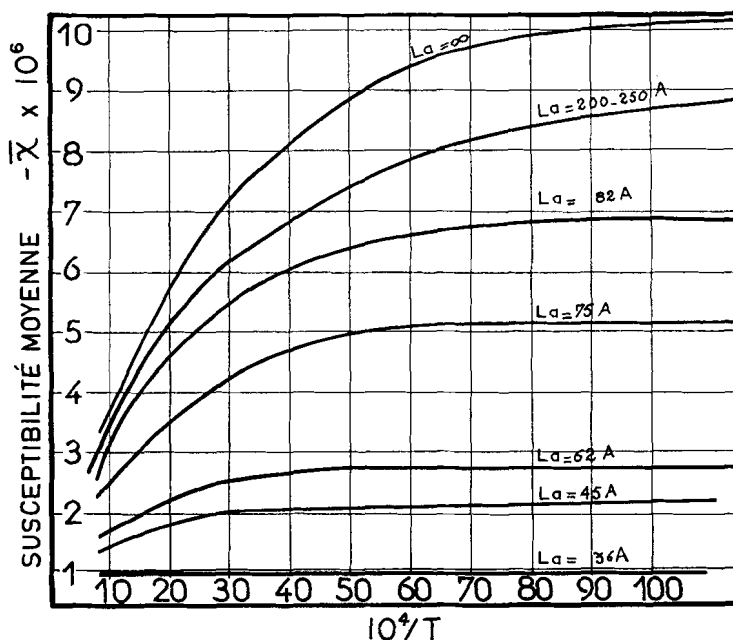


Fig. 5. La variation thermique de la susceptibilité moyenne pour diverses valeurs de L_a .

(2) Études Théoriques

Le réseau du graphite étant formé d'un „pavage” de noyaux benzéniques édifiés conjointement au moyen de liaisons σ localisées et de liaisons π totalement délocalisées, sa susceptibilité magnétique doit être la superposition (1) de la susceptibilité (isotrope) des atomes du réseau et de celle (pratiquement isotrope) des liaisons σ : ensemble que nous désignerons par χ_D^i ; et (2) de la susceptibilité des électrons π , c'est-à-dire des termes χ_D^e et χ_p^e : susceptibilité de la liaison métallique, à laquelle ne contribue qu'un seul électron par atome de carbone.

Nous négligeons ici la susceptibilité dite „de London” des électrons π , qui se manifeste dans les carbures aromatiques: elle est anisotrope et indépendante de la température. Il est en effet logique de penser que cette susceptibilité χ_L se transforme, lorsque le nombre de noyaux benzéniques devient très grand, en susceptibilité de la liaison métallique $\chi_p^e + \chi_D^e$. S'il n'en est pas ainsi d'ailleurs, on pourra admettre que ce terme χ_L est inclus dans χ_D^i : il n'y aura alors rien à changer dans les considérations qui suivent.

Comme, pour des valeurs de L_a inférieures à 40 Å environ, la susceptibilité moyenne $\bar{\chi}$ diffère fort peu de la susceptibilité $\bar{\chi}_0$ des carbures aromatiques, il est raisonnable de considérer que les termes χ_D^e et χ_p^e sont encore de faible importance dans ce domaine, c'est-à-dire que le caractère métallique des électrons π (encore très incomplètement délocalisés) reste peu marqué. Ce point de vue est confirmé par le fait que $\bar{\chi}$ est indépendant de la température pour ces valeurs de L_a , alors que les contributions χ_p^e et χ_D^e présentent en général une variation thermique notable et caractéristique.

Quand L_a dépasse 40Å, et que $\bar{\chi}$ devient nettement différente de $\bar{\chi}_0$, on est donc amené à écrire:

$$\chi_p^e + \chi_D^e = \bar{\chi} - \bar{\chi}_0 = \bar{\chi} + 0,85 \times 10^{-6} \quad (\text{V.13})$$

en donnant à $\bar{\chi}_0$ la valeur $-0,85 \times 10^{-6}$ vers laquelle elle paraît tendre, pour les carbures aromatiques, lorsque le nombre de noyaux y devient grand.

Cette égalité V.13 nous permet d'obtenir, pour la susceptibilité $\chi_p^e + \chi_D^e$ des électrons π métalliques, des valeurs expérimentales que nous pourrions comparer à celles que fournira la théorie.

(a) *Graphite. Interprétation de Ganguli et Krishnan.* La première interprétation du magnétisme du graphite fut celle de Ganguli et Krishnan.³³ Ces auteurs ont utilisé les formules V.10, V.11 et V.12 du modèle de gaz électronique à masse effective constante pour rendre compte de la susceptibilité du gaz d'électrons π du graphite et de sa variation thermique. L'accord avec leurs résultats expérimentaux est remarquable: malgré les approximations faites, leur interprétation rend compte de la susceptibilité du graphite

aussi bien sinon mieux que des théories plus élaborées et plus rigoureuses comme celles de Hove⁴⁵ ou de Wallace et Haering.³⁸ Mrozowski⁶⁷ a d'ailleurs suggéré quelques légères modifications de leurs hypothèses qui rendent beaucoup plus acceptables leurs conclusions quant au nombre et à la masse effective des électrons π responsables de cette susceptibilité. De toutes façons, la valeur élevée que l'on trouve pour le rapport $\alpha_x \alpha_y / \alpha_z^2$ (Oxy étant le plan graphitique) confirme la quasi-impossibilité des mouvements électroniques hors du plan Oxy . Il est dès lors raisonnable de traiter le graphite comme un cristal bidimensionnel.

(b) *Graphite Polycristallin et Noirs de Carbone*. A la suite des travaux de Mrozowski et de ses collaborateurs,^{67, 68} il paraît aujourd'hui vraisemblable que dans ces substances les électrons

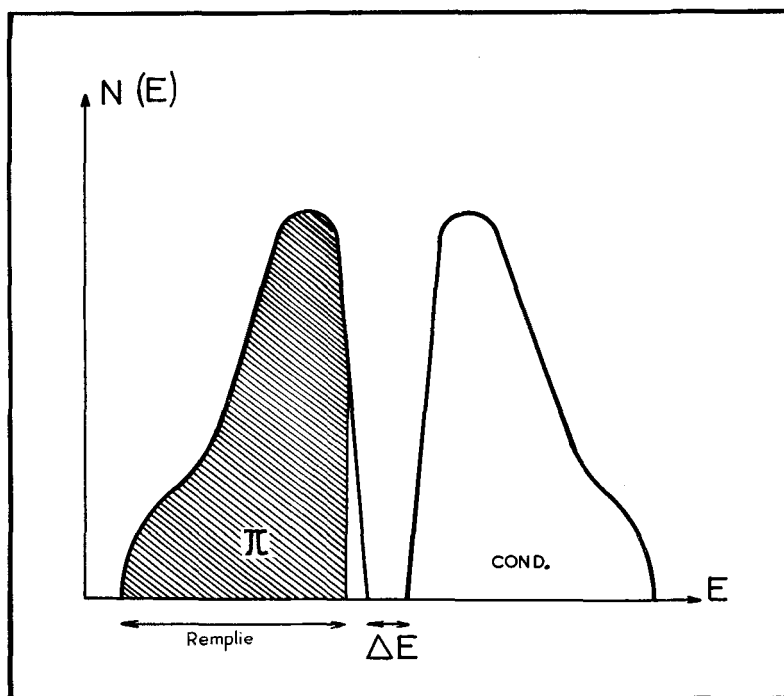


Fig. 6. La densité de niveaux $N(E)$ en fonction de l'énergie électronique E . La bande π et la bande de conduction sont représentées schématiquement.

π occupent presque totalement une bande d'énergie, qui n'est séparée d'une bande de conduction complètement vide que par une faible énergie d'activation ΔE . Ces deux bandes sont représentées schématiquement sur la figure 6, où l'on a porté la densité de niveaux $N(E)$ en fonction de l'énergie électronique E .

Dans le cas du graphite, considéré comme un cristal bidimensionnel, ΔE est nulle. Mais Slonczewski et Weiss⁹⁴ ont montré que la prise en considération de la troisième dimension conduit à $\Delta E < 0$, c'est-à-dire à un recouvrement de la bande π et de la bande de conduction. La valeur de ΔE croît quand diminue la largeur L_a des cristallites, et atteindrait 0,2 à 0,3 ev quand L_a est de l'ordre de 30 Å. La bande π est d'autre part d'autant plus remplie que L_a est grand. A 0°K, la partie vide de la bande π représenterait, d'après Mrozowski, 1/1000 de la bande totale pour le graphite, et 1/100 quand L_a est de l'ordre de 30 Å.

Il est parfaitement possible que le magnétisme du graphite ne puisse complètement s'interpréter qu'en tenant compte de la troisième dimension, et en particulier de la structure assez complexe trouvée pour les bandes d'énergie par Slonczewski et Weiss. Il semble néanmoins que des résultats satisfaisants puissent déjà être obtenus au moyen de modèles plus simples, valables aussi bien pour le graphite que pour les carbones à microcristallites graphitiques. C'est donc à partir d'un modèle bidimensionnel que nous avons tenté de fournir une interprétation générale du magnétisme des électrons π métalliques dans les carbones à structure graphitique.

Etant donné que les trous en excès dans la bande π aussi bien que les électrons thermiquement excités dans la bande de conduction n'occupent qu'une très faible partie de ces bandes, on peut se contenter de supposer une certaine forme pour la partie supérieure de la bande π et pour la partie inférieure de la bande de conduction, et raisonner comme si ces bandes se prolongeaient indéfiniment vers les énergies négatives et positives respectivement.

Une hypothèse simple consiste en particulier à admettre que l'énergie des électrons est, dans la partie des bandes qui nous intéresse, de la forme $E = A |\hbar|^n$, A étant une constante quel-

conque (positive pour la bande de conduction, négative pour la bande π) et n un exposant quelconque positif, inférieur ou égal à 2 (cette dernière restriction provenant de ce que, pour $n > 2$, $N(E)$ deviendrait infini pour $E = 0$), l'origine des énergies, ainsi que celle des vecteurs \mathbf{k} , étant prises au sommet de la bande π (ou au bas de la bande de conduction).

Poussant encore plus loin les hypothèses simplificatrices, nous avons supposé constante, pour une substance donnée, la masse effective des porteurs de charges responsables du magnétisme (ce qui revient à prendre $n = 2$), et nous avons admis que (pour une raison ou une autre) l'activation thermique des électrons passant de la bande π dans la bande de conduction pouvait être négligée. Les seuls porteurs de charges „magnétiquement actifs” sont alors les trous de la bande π dont le nombre est constant en vertu de nos hypothèses.

Si N est le nombre total des électrons π , et si ν est la fraction (très faible) de la bande π qui n'est pas remplie, nous avons alors affaire à un gaz bidimensionnel de νN porteurs de charges, dont la masse effective $m^* = m/\alpha$ (correspondant aux mouvements dans le plan graphitique) est isotrope et constante. Le calcul du magnétisme d'un tel gaz électronique nous a conduits, en se limitant aux termes indépendants du champ magnétique, aux résultats suivants,⁶¹ les susceptibilités étant relatives à l'unité de surface de plan graphitique, contenant N atomes de carbone:

$$K_D = -(\nu N \mu^2 \alpha^2 / 3kT_0) (1 - \exp -T_0/T) \quad (\text{V.14})$$

terme diamagnétique anisotrope correspondant à la direction normale au plan graphitique.

$$K_p = (\nu N \mu^2 / kT_0) (1 - \exp -T_0/T) \quad (\text{V.15})$$

terme paramagnétique isotrope, où μ est le magnéton de Bohr et

$$T_0 = \nu N \hbar^2 \alpha / 4\pi m k \quad (\text{V.16})$$

la température de dégénérescence du gaz.

Les contributions χ_D^c et χ_p^c à la susceptibilité moyenne sont, par suite

$$\begin{aligned} \chi_D^c &= \frac{1}{3} K_0 (1 - \exp -T_0/T) \\ \chi_p^c &= (-3/\alpha^2) K_0 (1 - \exp -T_0/T) \end{aligned} \quad (\text{V.17})$$

où

$$K_0 = -\nu N \mu^2 \alpha^2 / 3kT_0 \quad (\text{V.18})$$

Or nous allons voir que la comparaison avec les résultats expérimentaux conduit à des valeurs si grandes de α que le terme paramagnétique χ_p^e est parfaitement négligeable devant le terme diamagnétique χ_D^e .

L'expression théorique de $\chi_p^e + \chi_D^e$ devient donc

$$\chi_p^e + \chi_D^e = \frac{1}{3} K_0 (1 - \exp -T_0/T) \quad (\text{V.19})$$

Après conversion de ces susceptibilités par unité de surface en susceptibilités spécifiques, on constate qu'il est facile de trouver pour les paramètres K_0 et T_0 des valeurs telles que les susceptibilités théoriques tirées de V.19 soient à toute température en excellent accord avec les susceptibilités expérimentales fournies par V.13.

TABLEAU V.2

Substance	$L_a(\text{\AA})$	$T_0(^{\circ}\text{K})$	$-10^{13} \times K_0$	$10^5 \times \nu^\dagger$	$\alpha = m/m^* \dagger$
Graphite	∞	330	21,7	4,3	145
Thermax traité à 3100°C	250	375	18,35	5,76	123
Spheron 6 traité à 2700°C	82	460	14,05	9,2	94
Spheron 6 traité à 2000°C	75	490	9,94	13,88	67
P 33 traité à 1500°C	62	660	4,27	43,6	28

A titre d'exemple, nous donnons dans le tableau V.2 les valeurs de K_0 et T_0 correspondant à quelques noirs de carbone,⁶¹ ainsi que celles que les résultats expérimentaux permettent de calculer pour le graphite.⁸³

On peut alors, en se servant de V.16 et V.18, obtenir les valeurs correspondantes de α (c'est-à-dire de m^*) et de ν pour le gaz de porteurs de charges responsable du magnétisme. Ces valeurs ont été aussi réunies dans le tableau V.2.

(c) *Discussion.* Nous arrivons ainsi à la conclusion que le modèle de gaz bidimensionnel de porteurs de charges que nous

† Ces valeurs sont calculées à partir des formules V.16 et V.18 en considérant que les porteurs du graphite forment deux gaz bidimensionnels 75¹.

avons proposé permet d'interpréter de manière satisfaisante le magnétisme des électrons π métalliques, non seulement dans le graphite ou les noirs de carbone, mais dans tous les charbons (constitués de cristallites graphitiques de dimensions finies) qui forment la transition entre les carbures aromatiques et le graphite. Blayden et Adamson ont en effet montré¹⁷ que l'équation V.19 donne une représentation correcte du comportement des charbons des types les plus divers. Il reste cependant à vérifier que les valeurs déterminées pour K_0 et T_0 sont raisonnables, ou, ce qui revient au même, que les valeurs trouvées pour ν et $m^* = m/\alpha$ sont admissibles, en admettant que les porteurs de charges soient les „trous” de la bande π .

Il apparaît effectivement que la décroissance de la masse effective m^* et du nombre ν de trous par atome de carbone, quand L_a augmente, est exactement ce à quoi l'on doit s'attendre à priori. De même l'ordre de grandeur trouvé pour T_0 est vraisemblable. Enfin les grandes valeurs de α expliquent que le graphite soit diamagnétique et non paramagnétique; nous avons d'ailleurs admis à priori que α est assez grand pour que l'on puisse négliger χ_p^e devant χ_D^e : cette hypothèse se trouve justifiée.

Les valeurs obtenues pour m^* (et aussi pour ν) sont même un peu trop faibles, notablement plus petites en fait que celles que prévoit Mrozowski⁶⁷ à partir des propriétés électriques des carbones et du graphite. D'autre part notre interprétation a l'inconvénient grave de supposer le nombre νN de porteurs de charges indépendant de la température, alors qu'en réalité le nombre des trous de la bande π (comme celui des électrons de la bande de conduction), paraît devoir augmenter de façon appréciable avec la température, du fait de l'excitation thermique.

Ces difficultés pourraient cependant être surmontées en admettant qu'il y a en réalité plusieurs types de porteurs de charges dans les solides considérés: les uns, peu nombreux, mais dotés d'une très faible masse effective, seraient „magnétiquement actifs”, tandis que les autres, bien que beaucoup plus nombreux, ne contribueraient que de façon négligeable à la susceptibilité magnétique en raison de leur plus grande masse effective. Cela expliquerait les faibles valeurs de ν et m^* , ainsi que la non variation

de ν avec la température. A ce point de vue on peut remarquer que, dans l'étude de l'effet De Haas-Van Alphen du graphite, Shoenberg⁹³ a aussi trouvé des valeurs de ν de l'ordre de 10^{-5} .

Du point de vue théorique, une telle idée rejoindrait les conclusions d'une étude de Nozieres⁷⁰ qui, analysant les résultats expérimentaux de Galt, Yager, et Dail,³² sur la résonance cyclotronique du graphite, à partir du modèle de Slonczewski et Weiss,⁹⁴ montre que le graphite doit contenir des porteurs de charges libres dont les masses effectives s'échelonnent de manière continue entre 0 et 0,06 m . Mais le modèle de Slonczewski et Weiss est, rappelons-le, un modèle tridimensionnel, ce qui nous écarte beaucoup des hypothèses simplificatrices dont nous sommes partis.

On pourrait toutefois envisager d'interpréter le magnétisme des carbones à structure graphitique par un modèle bidimensionnel simple où la masse effective des porteurs soit variable de façon continue: il suffirait de supposer encore que l'énergie soit de la forme $E = A |k|^n$, mais en prenant cette fois $n \neq 2$. Dans ce cas la masse effective des porteurs varie comme $E^{(2-n)/n}$. Mais le calcul montre⁶² qu'un tel modèle conduit à une susceptibilité dépendant du champ magnétique, ce qui est en contradiction avec les données expérimentales actuelles.

On pourrait aussi prendre l'énergie électronique sous la forme $E = \pm A |k|^n$, relation qui a l'avantage de représenter à la fois la bande π et la bande de conduction du graphite ($\Delta E = 0$), et par suite de tenir compte du passage des électrons π d'une bande à l'autre par excitation thermique, mais qui, par contre, présente l'inconvénient de ne pas s'appliquer aux cas où $\Delta E \neq 0$, ce qui rend douteuse sa validité pour les carbones à microcristallites. Malheureusement, là encore, le calcul aboutit⁶² à une susceptibilité dépendant du champ, sauf si $n = 1$.

Ce cas $n = 1$ correspond précisément au modèle de McClure⁵⁶, perfectionné par Wallace et Haering.³⁸ La comparaison des expressions théoriques de McClure, Wallace et Haering avec la susceptibilité expérimentale du graphite fait apparaître un accord satisfaisant (si l'on excepte l'effet de Haas-Van Alphen) pour une valeur du niveau de Fermi de l'ordre de 0,06 eV ($T_0 = 700^\circ\text{K}$ environ).

Nous parvenons donc à la conclusion que les seuls modèles simples qui puissent rendre compte de façon satisfaisante de la susceptibilité magnétique des carbones à structure graphitique sont celui de McClure-Wallace-Haering et le nôtre. Le nôtre est plus simple, mais serre sans doute de moins près la réalité, tout au moins pour le graphite lui-même. Pour les carbones à petits cristallites (ΔE grand), notre modèle, qui implique l'absence d'excitation thermique des électrons, représente peut-être mieux les phénomènes réels, puisque les grandes valeurs de ΔE doivent rendre cette excitation thermique très faible.

Il faut au surplus remarquer que le modèle de McClure ne donne de résultats satisfaisants que si l'on suppose que les porteurs de charges sont des électrons, tandis que notre modèle conduit à des formules identiques pour des trous en excès dans la bande π ou pour des électrons supplémentaires dans la bande de conduction. Or, si l'hypothèse d'électrons en excès est assez vraisemblable dans le cas du graphite (en particulier si l'on se réfère au modèle de Slonczewski et Weiss), elle l'est beaucoup moins dans le cas des carbones à petits cristallites.

On en arrive ainsi à une situation assez paradoxale: d'une part le modèle que nous avons proposé ne semble constituer une représentation acceptable de la réalité que pour les carbones à microcristallites; et d'autre part ce même modèle conduit à des formules dont l'excellent accord avec l'expérience (pour toutes les catégories de carbones, graphite compris), ne peut être fortuit. Le paradoxe peut même être poussé plus loin, car il est facile de montrer⁶² que, à très basse température, la susceptibilité calculée pour le graphite à partir de notre modèle, et celle qui résulte des travaux de McClure, Wallace, et Haering, peuvent être mises toutes deux sous une forme absolument identique:

$$K_0 = -\frac{4}{3}(e^2/c^2 h^2) (\epsilon_0/\nu N)$$

si νN représente le nombre de porteurs de charges libres (pour notre modèle) et le nombre d'électrons en excès dans la bande de conduction (pour le modèle de McClure).

Notre conclusion sera que ces paradoxes s'expliquent sans doute par le fait que les modèles simples utilisés sont des modèles trop

simples pour être acceptables, sinon comme de grossières approximations: une étude rigoureuse exigerait, dans chaque cas particulier de carbone, l'utilisation d'un modèle bien plus complexe. Elle conduirait d'ailleurs probablement très vite à des calculs fort délicats. Au reste notre connaissance actuelle de la structure des bandes d'énergie dans les carbones est encore beaucoup trop schématique (sauf peut-être dans le cas du graphite lui-même) pour que cette étude rigoureuse puisse être menée avec succès.

L'important est donc pour le moment de s'efforcer de préciser cette structure des bandes d'énergie par une étude systématique de l'ensemble des propriétés électroniques des carbones (susceptibilité, conductivité, effet Hall, magnétorésistance, résonance paramagnétique, etc.). Toutes ces mesures doivent bien entendu être effectuées sur les mêmes échantillons, l'expérience ayant bien souvent montré que les résultats ne sont pas toujours exactement reproductibles pour des échantillons apparemment semblables. Il est également nécessaire d'étudier la variation de ces propriétés dans des séries homogènes de carbones: par exemple ceux que l'on obtient en traitant un même produit de départ à des températures progressivement croissantes. Mais les modèles simples que nous venons de décrire ont, pour le moment, un grand mérite: Ils conduisent, par des calculs simples, à des formules simples qui représentent fidèlement, au moyen de deux paramètres (ν et T_0 , ou α et T_0 , ou encore K_0 et T_0 , au choix), la susceptibilité magnétique de *toutes* les catégories de carbones à structure graphitique, et la variation thermique de cette susceptibilité.

La signification physique de ces paramètres n'est d'ailleurs sans doute pas très éloignée de celle que nous leur avons attribuée dans notre modèle.

On peut d'autre part se demander si deux paramètres sont toujours réellement nécessaires pour représenter le magnétisme des électrons π métalliques, et sa variation thermique. Il n'est pas exclu que l'on puisse par exemple mettre en évidence, pour certaines catégories de carbones, une relation empirique entre K_0 et T_0 ,⁶⁰ ce qui réduirait à un seul le nombre des paramètres et pourrait éventuellement permettre la détermination de la densité

$N(E)$ des niveaux en fonction de l'énergie E pour les porteurs „magnétiquement actifs”.

C. Détermination des Masses Effectives par Voie Magnétique

L'exemple du graphite mono et polycristallin nous a permis d'illustrer l'influence déterminante de la masse effective des porteurs de charges sur leur magnétisme. Nous avons vu que la mesure de la susceptibilité et la connaissance de sa variation thermique peuvent permettre à elles seules la détermination de la masse effective. Cette méthode de détermination repose sur la formule V.7 de Peierls (modifiée, comme nous l'avons précédemment indiqué, de façon à obtenir l'équation V.10), et implique évidemment la validité de cette formule, mais elle a pu tout de même être utilisée dans un certain nombre de cas, essentiellement dans l'étude d'éléments semi-conducteurs de la Colonne IV de la classification périodique. Ces éléments ont en effet le réseau cristallin du diamant, ce qui permet de supposer que la masse effective y est isotrope, et introduit une simplification appréciable dans les calculs.

La première étude dans ce domaine a été celle de Busch et Mooser²³ sur l'étain gris, mais le silicium et le germanium ont également fait l'objet de mesures précises et détaillées au cours des dernières années. Lorsque la comparaison était possible, un accord satisfaisant a généralement été observé entre les valeurs de m^* trouvées par voie magnétique et celles obtenues par d'autres méthodes (résonance cyclotronique en particulier).

Le procédé a même été étendu à des semi-conducteurs de même structure cristalline, formés par la combinaison d'éléments des Colonnes III et V. C'est ainsi que la susceptibilité d'échantillons d'antimoniure d'indium (InSb) a été mesurée, à diverses températures, par Stevens et Crawford⁹⁷ et par Marchand.⁶¹ Les masses effectives trouvées pour les électrons de conduction ($0,03 m$) sont notablement supérieures à celles que fournit la résonance cyclotronique ($0,014 m$), mais les valeurs obtenues pour les trous de la bande de valence ($0,12 m$) sont au contraire en bon accord avec les valeurs fournies par d'autres méthodes.

Le champ d'application de ce procédé magnétique de détermination des faibles masses effectives n'est donc sans doute pas totalement exploré. Cette perspective fait encore ressortir l'intérêt des techniques d'étude du diamagnétisme en fonction de la température, tant dans le domaine de la physique des solides que dans celui de la chimie structurale.

Références

1. Abott, J. A. et H. C. Bolton, *Proc. Roy. Soc. (London)* **A216**, 477 (1953).
2. Adams, E. N., *Phys. Rev.* **89**, 633 (1953).
3. Akamatsu, H., Inokuchi, H., Takahashi, H. et Matsunaga, Y., *Bull. Chem. Soc. Japan* **29**, 574 (1956).
4. Angus, W. R. et Hill, W. H., *Trans. Faraday Soc.* **31**, 1491 (1935).
5. Bates, L. F., *Modern Magnetism*, Cambridge Univ. Press, 3rd. ed., 1951.
6. Baudet, J., Communication personnelle.
7. Baudet, J., Tillieu, J. et Guy, J., *Compt. rend.* **244**, 1756 (1957).
8. Baudet, J., Tillieu, J. et Guy, J., *Compt. rend.* **244**, 2920 (1957).
9. Bergmann, E. D., Hoarau, J., Pacault, A. et Pullman, B., *J. chim. Phys.* **49**, 474 (1952).
10. Berthier, G., Mayot, M. et Pullman, B., *J. phys. radium* **12**, 717 (1951).
11. Berthier, G., Mayot, M. et Pullman, B., *J. phys. radium* **13**, 15 (1952).
12. Bhatnagar, S. S., Mathur, R. N. et Nevgi, M. B. *Z. Physik* **69**, 373 (1931).
13. Bhatnagar, S. S. et Mitra, N. G., *J. Indian Chem. Soc.* **13**, 329 (1936).
14. Bhatnagar, S. S., Mitra, N. G. et Tuli, G. D., *Phil. Mag.* **18**, 449 (1934).
15. Bitter, F., *Phys. Rev.* **33**, 389 (1929).
16. Bitter, F., *Phys. Rev.* **35**, 1648 (1930).
17. Blayden, H. E. et Adamson, A. F., *Proc. 3rd Conf. on Carbon*, Bufalo (1957).
18. Bonet, J. V. et Bushkovitch, A. V., *Phys. Rev.* **85**, 707 (1952); *J. Chem. Phys.* **21**, 2199 (1953).
19. Bowers, R., *Phys. Rev.* **100**, 1141 (1955).
20. Broersma, S., Thèse, La Haye, 1947; *J. Chem. Phys.* **17**, 873 (1949).
21. Brooks, H., *J. Chem. Phys.* **9**, 463 (1941).
22. Buckingham, R. A., Massey, H. S. W., Tibbs, S. T., *Proc. Roy. Soc. (London)* **A178**, 119 (1941).
23. Busch, G. et Mooser, E., *Helv. Phys. Acta* **26**, 611 (1953).
24. Cabrera, B. et Fahlenbach, H., *Z. Physik* **85**, 568 (1933).
25. Coulson, C. A., *Proc. Phys. Soc. (London)* **A54**, 51 (1942).

26. Dingle, R. B., *Proc. Roy. Soc. (London)* **A211**, 500 (1952); **A216**, 118 (1953); **A219**, 463 (1953).
27. Donovan, B., Lidiard, A. B. et March, N. H. *Proc. Phys. Soc. (London)* **A68**, 644 (1955).
28. Espe, I., *Phys. Rev.* **103**, 1254 (1956).
29. Evans, M. G., de Heer, J. et Gergely, J., *Proc. Phys. Soc. (London)* **62**, 505 (1949).
30. Farquharson, J. et Sastri, M. V. C., *Trans. Faraday. Soc.* **33**, 1472 (1937).
31. Fujii, S. et Shida, S., *Bull. Chem. Soc. Japan* **24**, 242 (1951).
32. Galt, J. K., Yager, W. A. and Dail, H. W., *Phys. Rev.* **103**, 1586 (1956).
33. Ganguli, N. et Krishnan, K. S., *Proc. Roy. Soc. (London)* **A177**, 168 (1941).
34. Gans, R. et Mrowka, B., *Königsberger Gelehrte Ges. Nachr.* **12**, 1 (1935).
35. Gray, F. W. et Cruickshank, J. H., *Trans. Faraday. Soc.* **31**, 1491 (1935).
36. Guy, J. et Tillieu, J., *Compt. rend.* **241**, 382 (1955).
37. Guy, J., Tillieu, J. et Baudet, J., *Compt. rend.* **246**, 574 (1958).
38. Haering, R. R. et Wallace, P. R., *Phys. and Chem. Solids* **3**, 253 (1957).
39. Ham, F. S. *Phys. Rev.* **92**, 113 (1953).
40. Hartmann, H., *Z. Naturforsch.* **2a**, 489 (1947).
41. Hector, L. G., *Phys. Rev.* **24**, 418 (1924).
42. Hirschfelder, J. O., *J. Chem. Phys.* **3**, 555 (1935).
43. Hoarau, J., *Ann. chim. (Paris)* **1**, 544 (1956); Thèse, Paris, 1954.
- 43¹. Hoarau, J., Lumbroso, N. et Pacault, A., *Compt. rend.* **242**, 1702 (1956).
44. Honda, H. et Ouchi, K., *Sci. Repts. Tôhoku Univ.* **37**, 55 (1953).
45. Hove, J. E., *Phys. Rev.* **100**, 645 (1955).
46. Hückel, Z. *Physik* **83**, 632 (1933).
47. Itoh, T., Ohno, K. et Yoshizumi, H., *J. Chem. Phys.* **22**, 947 (1954); *J. Phys. Soc. Japan* **10**, 103 (1955).
48. Johnston, D. F., *Proc. Roy. Soc. (London)* **A227**, 349 (1955).
49. Kambe, K., *Rept. Univ. Electro-Communication* **1**, 143 (1951); cité dans Itoh, T., Ohno, K., and Yoshizumi, H., *loc. cit.*
50. Kemble, E. C. et C. Zener, *Phys. Rev.* **33**, 512 (1929).
51. Kjeldaas, T., Jr., et Kohn, W., *Phys. Rev.* **105**, 806 (1957).
52. Klemm, W., *Magnetochemie*, Akademische Verlagsges., Leipzig, 1936.
53. Landau, L., *Z. Physik* **64**, 629 (1930).
54. London, F. J. *Phys. radium* **8**, 397 (1937); *Compt. rend.* **205**, 28 (1937).
55. Lonsdale, K. *Repts. Progress in Phys.*, **4**, 368 (1938); Lonsdale, K., et Krishnan, K. S., *Proc. Roy. Soc. (London)* **156**, 597 (1936).
56. McClure, J. W., *Phys. Rev.* **104**, 666 (1956).
57. MacWeeny, R., *Proc. Phys. Soc. (London)* **64**, 261, 921 (1951); **65**, 839 (1952).

- March, N. H., et Donovan, B., *Proc. Phys. Soc. (London)* **A66**, 1104 58. (1953).
59. Marchand, A., *Compt. rend.* **238**, 460 (1954); **239**, 1609 (1954).
60. Marchand, A., *Compt. rend.* **245**, 1534 (1957).
61. Marchand, A., These, Paris, 1956; *Ann. chim. (Paris)* **2**, 469 (1957).
62. Marchand, A., *Proc. 4th Conf. on Carbon*, Buffalo (1959).
63. Mayot, M., Berthier, G., et Pullman, B., *J. Phys. radium* **12**, 652 (1951); *J. chim. Phys.* **50**, 176 (1953).
64. Miwa, M., *Sci. Repts. Tôhoku Univ.* **23**, 242 (1934).
65. Morrow, J. C., *J. Elisha Mitchell Sci. Soc.* **73**, 294 (1957).
66. Mrowka, B., *Z. Physik* **80**, 495 (1933).
67. Mrozowski, S., *Phys. Rev.* **85**, 609 (1952).
68. Mrozowski, S., et Chaberski, A., *Phys. Rev.* **104**, 74 (1956).
69. Newell, G. F., *Phys. Rev.* **78**, 711 (1950).
70. Nozières, P., *Phys. Rev.* **109**, 1510 (1958).
71. Osborne, M. F. M., et Steele, M. C., *Phys. Rev.* **86**, 247 (1952).
72. Pacault, A., *Rev. sci.* **465** (1944); 169 (1946); 38 (1948).
73. Pacault, A., Thèse, Paris, 1946; *Ann. chim. (Paris)* **1**, 527 (1946).
74. Pacault, A., *Bull. soc. chim. France* **16**, D371 (1949).
75. Pacault, A., Lemaître, B., et Jousset-Dubien, J., *Compt. rend.* **237**, 1156 (1953); *J. chim. Phys.* **54**, 198 (1956).
- 75¹. Pacault, A., Marchand, A., Bothorel, P., Zanchetta, J., Boy, F., Cher-ville, J., et Oberlin, M., 10^e Réunion de la Société de Chimie Physique, *J. chim. Phys.* (1960).
76. Paramasivan, S., *Indian J. Phys.* **4**, 139 (1929).
77. Pascal, P., *Ann. chim. et phys.* **19**, 5 (1910); **24**, 218 (1913); **25**, 289 (1912); *Compt. rend.* **147**, 56, 242, 742 (1928); **148**, 413 (1909); **150**, 1167 (1910); **152**, 862, 1010 (1911); **156**, 323 (1913); **158**, 37 (1914); **173**, 144 (1921); **176**, 1887 (1923); **177**, 765 (1923); **180**, 1596 (1925). Voir également réf. 72.
78. Pascal, P., Pacault, A., et Hoarau, J., *Compt. rend.* **233**, 1078 (1951). Voir également Pacault, A., Lumbroso, N., et Hoarau, J., *Cahiers de phys.* **43**, 54 (1953); et François, H., et Hoarau, J., *Compt. rend.* **240**, 1220 (1955).
79. Pauling, L., *J. Chem. Phys.* **4**, 673 (1936).
80. Peierls, R., *Z. Physik* **80**, 763, 786 (1933).
81. Pines, D., *Phys. Rev.* **95**, 1090 (1954).
82. Pinnick, H. T., *Phys. Rev.* **94**, 319 (1954).
83. Pinnick, H. T., et Kiive, P., *Phys. Rev.* **102**, 58 (1956).
- 83¹. Poquet, E., Lumbroso, N., Hoarau, J., Marchand, A., Pacault, A., et Soule, D. E., 10^e Réunion de la Société de Chimie Physique, *J. chim. Phys.* (1960).
84. Pugh, E. W., et Goldman, J. E., *Phys. Rev.* **99**, 1633, 1641 (1955).
85. Ramsey, N. F., *Phys. Rev.* **58**, 226 (1940); **87**, 1075 (1952).

86. Rao, S. R., *Indian J. Phys.* **6**, 241 (1931).
87. Rosen, N., *Phys. Rev.* **38**, 2099 (1931).
88. Scherr, G. W., *J. Chem. Phys.* **23**, 569 (1955).
89. Schumacher, R. T., Carver, T. R., et Slichter, C. P., *Phys. Rev.* **95**, 1089 (1954).
90. Schumacher, R. T., et Slichter, C. P., *Phys. Rev.* **101**, 58 (1956).
91. Selwood, P. W., *Magnetochemistry*, Interscience, New York, London, 2nd ed., 1956.
92. Shiba, H., et Hazato, G., *Bull. Chem. Soc. Japan* **22**, 92 (1949).
93. Shoenberg, D., *Phil. Trans. Roy. Soc. London* **A245**, 1 (1952).
94. Slonczewski, J. C., et Weiss, P. R., *Phys. Rev.* **109**, 272 (1958).
95. Sone, T., *Phil. Mag.* **39**, 305 (1920).
96. Steensholt, G., *Phil. Mag.* **38**, 748 (1947).
97. Stevens, D. K., et Crawford, J. H., *Phys. Rev.* **99**, 487 (1955).
98. Stoner, E. C., *Proc. Roy. Soc. (London)* **A152**, 672 (1935).
99. Tai Yuan Yang, *J. Chem. Phys.* **19**, 647 (1951).
100. Tillieu, Thèse, Paris, 1956; *Ann. Phys.* **2**, 631 (1957).
101. Tillieu, J., et Guy, J., *Compt. rend.* **239**, 1203 (1954); **239**, 1283 (1954); **240**, 1402 (1955); **242**, 1279 (1956); **242**, 1436 (1956).
102. Trew, V. C. G., *Trans. Faraday Soc.* **37**, 476 (1941); **45**, 217 (1949).
103. Ubbelohde, A. R., *Nature* **132**, 1002 (1933).
104. Vaidyanathan, V. I., *Indian J. Phys.* **5**, 559 (1930).
105. Vaidyanathan, V. I., *Phil. Mag.* **5**, 380 (1928).
106. Vaidyanathan, V. I., *Phys. Rev.* **30**, 512 (1927); *Indian J. Phys.* **2**, 135 (1927).
107. Van Vleck, J. H., *The Theory of Electric and Magnetic Susceptibilities*, Oxford Univ. Press, 1932.
108. Van Vleck, J. H., et Franck, A., *Proc. Natl. Acad. Sci. U.S.* **15**, 539 (1929).
109. Venkatachalam, K. A., et Kabadi, M. B., *J. Phys. Chem.* **59**, 740 (1955).
110. Venkateswarlu, K., et Sriraman, S., *Current Sci.* **24**, 191 (1955).
111. Venkateswarlu, K., et Sriraman, S., *J. Sci. Ind. Research (India)* **14B**, 611 (1955).
112. Wang, S. C., *Phys. Rev.* **31**, 579 (1928).
113. Weltner, W., *J. Chem. Phys.* **28**, 476 (1958).
114. Wick, G. C., *Z. Physik* **85**, 25 (1933); *Nuovo cim.* **10**, 118 (1933).
115. Wills, A. P., et Hector, L. G., *Phys. Rev.* **23**, 209 (1924).
116. Wilson, A. H., *Proc. Cambridge Phil. Soc.* **49**, 292 (1953).
117. Witmer, E. E., *Phys. Rev.* **50**, 1094 (1936).
118. Witmer, E. E., *Phys. Rev.* **48**, 380 (1935); **51**, 383 (1937); **58**, 202 (1940); **61**, 387 (1942).
119. Woodbridge, D. B., *Phys. Rev.* **48**, 672 (1935).
120. Wynne-Jones, W. F. K., Blayden, H. E., et Iley, R., *Brennstoff-Chem.* **33**, 268 (1952).

POWDER ELECTRODES AND THEIR APPLICATIONS

WITOLD TOMASSI, *Warsaw Polytechnic*

CONTENTS

I. The Construction of a Powder Electrode	239
II. Powder Electrodes of the First Kind	241
III. Compound Powder Electrodes	246
IV. The Mechanism of Establishing the Potential of a Compound Powder Electrode	251
V. Investigation of Contact Substances by means of Powder Electrodes	253
VI. Investigations on Fe-Zn and Fe-C Systems	256
VII. Potentiometric Investigations of Adsorbents	258
VIII. Investigations of Dispersed-Crystal Organic Substances . .	261
IX. Powder Electrodes without a Powdered Substance . . .	263
References	264
Bibliography	264

I. THE CONSTRUCTION OF A POWDER ELECTRODE

A powder electrode is a half-cell which can be made in the two following ways:

Version 1. The powder and the leading-out electrodes, which are made of platinum wire fused into a surrounding glass tube, are placed in a testtube. The testtube is about 5 cm in length and from 3 to 5 mm in diameter. In the wall of the testtube is a hole through which the electrolytic solution passes from a bigger container in which the testtube is placed, wetting the powder and the leading-out electrode. The length of platinum wire is from 3 mm to 3 cm. The longer the wire the better is the reproduction of the potential value of this half-cell. Figure 1 shows the construction of this powder electrode, where 1 is the dispersed substance (the powder), 2, the platinum leading-out electrode, 3, the testtube, 4, the hole in the wall of the testtube, and 5, the container with a solution of electrolyte.

Version 2. Elaborated by H. Calus and A. Frackiewicz this is shown in Fig. 2. It is constructed on the same principles, as version 1 but its slightly different technical solution facilitates manipulation while assembling the half-cell and eliminates the majority of the experimental errors of measurement.

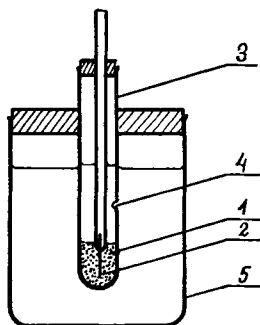


Fig. 1. Powder electrode, version 1.

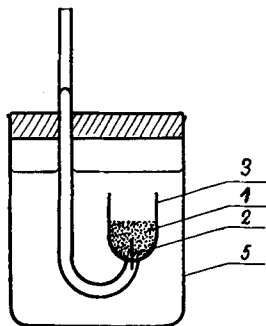


Fig. 2. Powder electrode, version 2.

The numbers in fig. 2 stand for the same things as in Fig. 1. The open top testtube, 3, is completely dipped in the solution which is in the container, 5.

The powder electrode half-cell is connected with another half-cell, e.g., with a saturated calomel electrode, and thus a cell is made. Measurements of electromotive force of such cells give information on the state of the surface of a substance in its dispersed solid phase.

Cells containing powders had already been constructed at the end of the last century. They were mainly modifications of electrodes of the first kind, the metal being introduced as a powder instead of in its homogeneous solid state to obtain better establishing and better reproduction of its potential in the solution of its own ions. By means of such electrodes the normal potentials of some metals were also determined. These electrodes were reversible to the cations present in the solution. In more recent times Hüttig and Herrman¹ sought some relation between catalytic properties of copper powders and the electromotive force of a cell containing such a half-cell, and they applied a half-cell made of a copper

leading-out electrode and a copper powder, the electrolyte being a copper sulfate solution. Minc and Oleszczyk⁴ enveloped the copper leading-out electrode with quartz powder, and dipped the electrode in the solution of copper sulfate. In both cases little influence of the powder on the potential of leading-out electrode was found and the electrode was reversible to cations of the solution. As we will prove further on, the condition for a considerable and characteristic potentiometric effect by the structure of the powder's surface, is for the leading-out electrode to reproduce its potential poorly in relation to the solution and not to be reversible to the solution's ions.

Systematic studies of the properties of powder electrodes and their application in the investigation on the state of the surface of substances in their dispersed solid phase were recently undertaken at the Institute of Physical Chemistry, Technical University of Warsaw, and in several other scientific institutions. In this paper we want to present some data obtained in our laboratory.

II. POWDER ELECTRODES OF THE FIRST KIND

Two types of powder electrodes can be distinguished and they have quite different characteristics. Electrodes belonging to one type are called powder electrodes of the first kind and electrodes belonging to the other types are called compound powder electrodes.

Powder electrodes of the first kind fulfill the following conditions: the powder in the electrode is a pure metal by which the platinum leading-out electrode is covered; the solution contains ions of that metal. Thus under such conditions both the leading-out electrode and the powder correspond to reversible electrodes of the first kind differing only in the dispersion of the metallic component. Powder electrodes not having this structure are compound powder electrodes.

We will give two examples of powder electrodes of the first kind to which this section is devoted:

1. The leading-out electrode is electroplated with nickel and

enveloped in nickel powder in an aqueous solution of nickel sulfate.

2. The leading-out electrode is copperplated and enveloped in copper powder in an aqueous solution of copper sulfate.

In our laboratory we have examined silver, nickel, and copper powder electrodes of the first kind, and the latter two especially have been examined in detail. As a rule, powder electrodes of the first kind correspond, as far as their properties are concerned, to ordinary electrodes of the first kind apart from some characteristics resulting from the dispersion of the metal. We have found experimentally the following properties. There is a marked, but not too big, influence of the metallic powder's preparation on the value of powder-electrode potential and on the value of its normal potential. These potentials are almost equal to the values for corresponding ordinary electrodes of the first kind but they are produced far better. The discrepancy of the measured values does not exceed 0.5 to 1 mv; the presence of oxygen has no influence and the size of the powder's grain is of no importance either.

Powders of metals were prepared in various chemical ways, by means of electrolysis, and by means of Raney's method with a different procedure in the process (different initial alloys, different temperatures of leeching, etc.). The amount by which the leading-out electrode is dipped in the powder has no influence on the measured potential value. The temperature coefficient of potential is almost equal to the values for ordinary electrodes of the first kind, in the examined temperatures from 15°C to 35°C. As for copper and nickel we have found too that powders prepared in various ways and differing in their catalytic properties change the potential values of powder electrodes which have the same-solutions. Such powders also differ in the values of their counted out normal potentials.

The formation of an adsorption layer on the metal powder, introduced later into the powder electrode, has little or no influence on the obtained potential value, or, in some cases, it has only a considerably insignificant influence. The facts can be easily explained when it is pointed out that, as far as the first kind of powder electrode is concerned, its potential in relation to

the solution is established through the medium of its own ions and that each element of the surface of the powder participates in the exchange of ions with the liquid. Covering a part of that surface by adsorbed particles will not alter the fundamental course of that process and will have little influence on the potential value of the phase boundary because, to establish that value, a very small number of ions must pass through the phase boundary. (The question of compound powders electrodes is different and will be dealt with in the next section.)

Powder electrodes of the first kind can be described in classical thermodynamic terms. Here it is to be considered that dispersion of the solid phase increases the molar thermodynamic potential of the metal, in relation to the value corresponding to its compact, homogeneous solid phase by raising the surface energy. Moreover, this potential is changed by the curvature of the surface of the crystal-solution phase boundary which leads to an increase of the surface pressure on that boundary. The dispersed material consists of irregular fragments of various sizes and surface shapes, e.g., concave, flat and convex. The more curved the surface of the solid phase, the bigger will be the molar thermodynamic potential of the substance at a given point, as can be deduced from the formula:

$$G_{(r)} - G_{(\infty)} = 2\sigma V/r \quad (1)$$

where $G_{(r)}$ and $G_{(\infty)}$ are the values of molar thermodynamic potential at the point of curve r and at the point of flat phase boundary with the surrounding remaining under constant pressure; σ is the surface tension and V the molar volume.

Different parts on the surface of the individual grains differ in the values of their thermodynamic molar potential, thermodynamic activity of metal, and electrical potential in connection with the solution. The powder in the electrode is therefore a system of local cells and, in consequence, its surface undergoes a gradual, rather slow change of structure. The changes of potential are rather fast and considerable (several millivolts) only in the initial period. In the course of time in this period the electrode's potential becomes more positive. Not later than a few days after the start, equilibrium is reached, the potential varying

by only tenths of millivolts even over a period of some months.

We have determined the normal potentials for nickel powder and copper powder electrodes. For nickel we obtained five preparations of Raney nickel applying various conditions of the first and second leachings of the initial alloy. Table I gives the differences in procedures during the preparation of the powders.

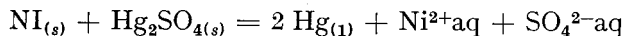
TABLE 1. Leaching Temperatures in the Preparation of Nickel Powders

Preparation	Temperature, °C	
	First leaching	Second leaching
1	0	30
2	0	50
3	0	70
4	0	90
5	15-70	50

All the five preparations served to construct powder electrodes connected with a reference electrode $\text{Hg}, \text{Hg}_2\text{SO}_4, \text{SO}_4^{2-}$, to make a cell:



Aqueous NiSO_4 solutions of concentration c , equal to 0.10, 0.15, 0.20, 0.30, 0.40, mole per liter were used. Next taking into account that in a cell itself the following reaction takes place:



the electromotive force can be expressed by the following formula:

$$E = E_{oc} - (RT/F) \ln a_{\pm} \quad (2)$$

where a_{\pm} is the activity of the NiSO_4 solution at concentration c .

Applying the formula of Debye-Hückel-Brønsted for the activity coefficient and the graphic extrapolation method, the basic values of the electromotive force of a cell for each nickel preparation were determined. Introducing, according to known data, the normal potential of a reference electrode, equal to 0.6151 v, the

values of normal potentials were obtained for the separate preparations of nickel powder. They are given in Table II.

As can be seen in Tables I and II, the temperature of the second leeching determines the value of the normal potential (the same π_{oc} values for preparations 2 and 5).

TABLE II. Values of Normal Potentials of Separate Preparations of Nickel Powders

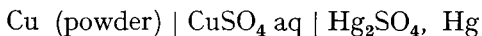
Preparation	π_{oc} , v
1	-0.247
2	-0.249
3	-0.244
4	-0.242
5	-0.249

Studies of kinetics of chemical reactions catalyzed with Raney nickel indicate that as a catalyst the nickel powder obtained from a second leeching at a temperature of 50°C is most active. Powder electrodes indicate that the most negative value of normal potential is obtained with such a powder.

Likewise we determined the values of the normal potential for Raney nickel obtained from alloys with different nickel content. The greater the nickel content in the initial alloy, the more negative was the normal potential. Subsequently, the Raney nickel was submitted to a complete or partial dehydrogenation, chemically or through an anodic polarization. The dehydrogenation resulted in more negative values of normal potential. With the cathodic polarization, which accounted for a marked saturation with hydrogen, the initial values of the potential of the active Raney nickel were reproduced. Measuring the potential of the powder electrode with partially dehydrogenated Raney nickel allowed us to investigate the process of hydrogen diffusion from the interior of powder granules to their surfaces. (This process was accompanied by an increase of electrode potential up to the value for the active, nondehydrogenated preparation.)

Neither copper nor nickel powder electrodes are sensitive to the presence of oxygen in the system. In a similar way as for the nickel electrode, we determined the normal potential of a copper powder electrode using deactivated copper powder, that is to say, a powder deprived of places of higher state of energy on its surface. Such a powder is, for example, the one obtained by means of electrolysis.

Investigating the cell



we determined the value of normal potential as 0.3401 v, approximate to the value of Müller and Reuther.⁵ The size of the powder grain has no influence on the potential value of the powder electrode in case of deactivated copper powder.

As we discovered the activity of metal ions in a solution is not changed in surrounding of a powder in spite of this system's capillarity.

III. COMPOUND POWDER ELECTRODES

Powder electrodes of the first kind as we have said, are a particular case of homogenous, compact electrodes of the first kind. They have some specific and valuable characteristics, are reversible to the positive ion of the electrode material, but are not very useful in apparatus for testing the surface of a powder.

Compound powder electrodes, however, are particularly valuable in the investigations of the state of the surface of a substance in its dispersed solid phase. We will review the principle of their construction. The leading-out electrode, most often made of platinum, is enveloped by the powder (of any composition) being investigated and both are dipped in a liquid electrolyte which has no common ions with either the leading-out electrode or the powder. Here an example will be platinum wire enveloped by powdered carbon dipped in a solution of potassium chloride. We have proved during a great number of investigations that the powder electrode potential is very sensitive to the state of the surface of the powder, the potential being a function of that state, and we have proved that measurements of potential can be applied

to determine the characteristics of the surface.

It was our task to work out theoretical principles of operation of a powder electrode, and of establishing its potential, and to solve in the best way, on the basis of reasonable theoretical interpretation, the question of how to construct powder electrodes according to the application intended. The aim was to obtain the potential value of a powder electrode which would be a characteristic of the state of the surface of the powder. The value should be sensitive to the state of that surface and fairly well approximated, experimentally.

For a well constructed compound powder electrode, the potential value is a parameter particularly important for investigations on contacts and absorbents because exist the connection between the potential and the state of the surface, the catalytic and adsorption properties of powders, and also the surface concentration of the substance adsorbed.

Principles of the Correct Construction of Compound Powder Electrodes

We have shown above the aims which we have in view while handling these compound powder electrodes. The construction of these electrodes must be adjusted to carrying out that task. Leaving out the glass parts which serve only as vessels, the powder electrode must contain these basic elements: the leading-out electrode, the powder, and the solution of electrolyte. The powder electrode potential as a measurable quantity is the sum of several potential differences at phase boundaries, viz., the conducting wire-leading-out electrode boundary, the leading-out electrode-solution boundary, the leading-out electrode-powder boundary, and the powder-solution boundary. Only the latter two differences (jumps) of potential will be connected with the formation of the surface of the powder. The selection of freely chosen elements of an electrode should be such as to give to these two potential differences, and in particular to the latter, a dominant significance in the measured magnitude of the electrode's potential.

We have shown by experimenting and proved theoretically that the leading-out electrode should not be a reversible electrode

in a given system, and that its own potential in relation to its solution should be poorly reproduced and established to have little influence on the general potential. A leading-out electrode made of platinum is here particularly convenient if the pH does not exceed 8-9. A platinum electrode has an oxide electrode character in aqueous and alcoholic solutions and is badly reversible in relation to ions of hydroxyl. The replacement of platinum by an electrode made of silver-silver chloride (Ag/AgCl) gives a better potential reproduction in a potassium chloride solution, but the values of the powder electrode potential are not too much shifted in relation to the potential value of the leading-out electrode itself in a given solution and the influence of the form of the surface of the powder is far less in this case. As an example we will quote some data obtained for various preparations of activated and nonactivated carbon in 0.5*N* aqueous solution of potassium chloride in regard to saturated calomel electrode (Table III).

TABEL III. Powder Electrode Potentials for Various Preparations of Carbon

Carbon	Leading-out electrode	
	Pt	Ag/AgCl
	<i>Powder electrode potential, mv</i>	
CF	+231	+28
CL	+197	+19
CS	+118	—
CA	+122	+4
CH	-339	-116
CR	+192	+5

It should be noted that platinum electrode prepared in a standard way and in aqueous 0.5*N* solution of potassium chloride gives the potential ranging from 150 to 350 mv, but most often about 230 to 280 mv (pH of solution approximately 6.65). The silver-silver chloride electrode's own potential in the same solution is 5 mv.

The liquid in which the leading-out electrode and the powder are dipped must contain ions of electrolyte in not too small a

quantity. Ions of electrolyte are to play a double part here, viz., to increase the conductivity of the electrical system in order to facilitate potentiometric measurement, and to help in creating a difference (jump) of potential on the boundary of the powder by forming a double electrical layer at the phase boundary.

We have found experimentally that potassium chloride is convenient to use here and gives better results than many other electrolytes. Thus standard solutions with which we experiment, in most cases, are those of 0.5 NKCl in water, and 0.5 g KCl per liter of rectified alcohol (95 per cent ethanol). Later experiments showed also the usefulness of potassium sulphate in aqueous solutions. Usually we use it in a 1N solution.

A solvent especially plays a great part in establishing the powder electrode potential. We are of the opinion that the properties most important here are the values of the dielectric constant of the liquid and of a stable dipole (electrical) momentum of its molecules.

In compound powder electrodes the potential on the powder-solution phase boundary is mostly of an adsorption potential character. The more molecules and ions adsorbed in the surface layer and the stronger they are bound there the better will be established and reproduced the potential value of phase boundary. Adsorption potential was the object of studies of Kamiński and his collaborators.^{2,3} To formulate briefly our conclusions from these studies as to powder half-cells, we will state that ion and dipole adsorption on the surface of the powder will be favored by a greater value of the ratio ϵ_s/ϵ_o , where ϵ_s is the value of dielectric constant of solid phase and ϵ_o of liquid phase. The ions being adsorbed in the cases we are discussing are the ions coming from the dissolved electrolyte and the solvent's dissociation, and the dipoles adsorbed are the solvent's molecules. The ions' solvation, which changes their size and geometrical shape, has an influence on the adsorption of ions. Thus the value of electrical momentum of the solvent's molecules as a magnitude determining the solvation energy and a product of the solvation process should be connected with the value and the reproductibility of the potential of the powder electrode.

We have carried out an experimental work aiming at checking these conclusions in our systems.

Independently, on all its other properties, the solvent was of no use in the case of a given powder if it reacted on it chemically involving an irreversible side reaction in addition to the in principle reversible process of establishing adsorption equilibrium. This was the case with water in relation to zinc oxide. At times potassium chloride must be substituted by another electrolyte for this reason. Investigating the copper powders we had to substitute potassium sulfate for the electrolyte. The course of any process irreversible between phases of a powder electrode (e.g., the solution of any component of the powder) gives rise to a permanent change of potential value of the half-cell being investigated. We will come back to the question of irreversible processes in powder electrodes further on.

The results of the measurements made have proved the suppositions formulated on the ground of Kamieński's studies. Generally they can be formulated thus: the dielectric constant of the liquid should not much exceed the dielectric constant of the solid phase; the electrical momentum of the solvent's particles should not be too great. In relation to metal powders water is a good solvent of electrolyte. For other powders we have achieved the best results by applying methanol and ethanol (adding 0.5 g of KCl to a litre of pure methanol or to a litre of rectified alcohol in case of ethanol). Water, ethanol, and methanol have stable dipole moments of their molecules rather near and less than 2.

For nonmetallic powders the methanol and ethanol solutions give the best reproduction and selectivity (discrimination of powders identical as far as quality is concerned, and different as far as the method of preparation and the surface structure are concerned).

From among the metallic powders, a dozen copper preparations in aqueous solution were investigated. An 0.1*N* potassium sulfate solution was used. The potential values of electrodes with the same preparations were different from several to twenty-odd millivolts. The value of electromotive force was being established for about two hours and remained more or less stable afterwards.

The material of the leading-out electrode (platinum or copper-plated platinum) gave here a shift of about 20 mv for the values measured, probably due to the change of potential value of the the contact point of the leading-out electrode with the powder and solution. Individual copper preparations were well distinguishable among themselves. Potassium chloride cannot be used in a copper compound powder electrode because of its reaction with the powdered copper. In the presence of potassium chloride the potential undergoes a constant change with time and a complete lack of regularity in its values.

The presence of molecules of great dipole momentum in a liquid solution prevents establishing a definite value of the powder electrode potential. These electrodes fail to characterize the preparation of the powder. It may be that high energy of solvation of ions in a solution hinders them in the process of desolvation and adsorption in the surface layer. The system becomes somehow deprived of its potentiometric factor and that always leads to the loss of a definite potential value by an electrode.

These generalizations do not include carbon when it forms the dispersed phase in a powder electrode. We have found that carbon acts here specifically, becoming either an oxygen electrode or a hydrogen electrode according to circumstances. Carbon also facilitates surface binding of free oxygen atoms and of the oxygen which is a part of different molecules.

Summarizing: to achieve good results in measurement a polar solvent of not too great dipole momentum of its molecules (CH_3OH , $\text{C}_2\text{H}_5\text{OH}$, H_2O) should be used. The concentration of electrolyte (KCl , K_2SO_4) cannot be too small. Water is, in general, a solvent of no advantage considering the large value of its dielectric constant and its great capacity of reaction with various substances. Water will however be a good solvent in an investigation on some dispersed metals and carbon.

IV. THE MECHANISM OF ESTABLISHING THE POTENTIAL OF A COMPOUND POWDER ELECTRODE

It seems that processes taking place between a powder and a liquid solution and those leading to a difference (jump) of potential

on the phase boundary can be divided into two groups. Adsorption processes of various kinds of particles (ions, molecules) from the liquid phase will constitute one group. These processes are reversible and they can, in principle, reach equilibrium. Surface reaction can be added to this group, e.g., the oxidation of a surface to an insoluble oxide, and these reactions can also reach equilibrium. The second group consists of various irreversible processes such as reactions of the whole or only a part of the solid phase with a solvent or other component of the liquid phase (producing soluble products). Further on, all solution processes of solid phase components (possibly even impurities) will belong here. The occurrence of these irreversible processes is easy to determine by means of the constant change of the electromotive force of a cell containing a given powder electrode.

The processes taking place on the surface of the solid are complicated and great in number. We measure a certain common resultant effect as the powder electrode potential. The full mastery of the subject would have to be based on the elaboration of a chemical and physicochemical model of all processes (i.e., giving the chemical equations of reactions in process, indicating the processes of solution, adsorption, desorption, and secondary reactions, etc.) as well as on the classical thermodynamic description, and possibly by thermodynamics of irreversible processes, and chemical and electrochemical kinetics.

The result of a qualitative and mathematical description should be the derivation of a magnitude for the powder electrode potential. It would have to be possible to indicate how the potentials of the individual phase boundaries in a powder electrode make up its resultant potential.

It seems that such a description is, at the present state of knowledge, impossible and very distant in general. The most that can be done at present seems to be the presentation of a chemical description of the phenomena, while the interpretation is tackled on the basis of investigations of changes of the powder electrode potential, of the pH and concentration of components of the solution at the time, of the influence of electrolyte concentration or other additional components of the system on the

electrode potential, of the influence of quality and degree of dipping of the leading-out electrode in the powder, etc. Recently, we made the first attempt at this interpretation in the case when carbon powders with an adsorption layer and silicon gel were used.^{8,9} Each interpretation, however contains, an optional attitude in treatment.

In Section VII we shall give an interpretation of processes for the carbon powder electrode with a chlorine adsorption layer; to this electrode we have devoted much experimental work.

As we have mentioned, a platinum electrode behaves as an oxide electrode in solutions containing hydroxyl ions, and as an oxide electrode it is reversible to these ions. The state of the surface of an electrode, the degree of its oxidation, has a great influence on the platinum potential in a given solution. In our experiments we have tried to standarize, as far as it is possible, the surface of the leading-out electrodes by means of their rather strong oxidation. For this purpose, before use and after cleaning, platinum electrodes were heated in concentrated nitrogen acid to boiling point, and afterwards they were washed with distilled water and kept for a day in the solution in which they were to be placed in the powder electrode. This procedure led to a decrease in the divergence of the potential values of these very same platinum electrodes in solutions.

V. INVESTIGATION OF CONTACT SUBSTANCES BY MEANS OF POWDER ELECTRODES

Because the contact properties of a substance result from the formation of its surface and, as we discussed, the values of the powder electrode potential for the same given parameters describing the powder electrode, are also a function of the surface state, then it seems to be true that there should be some relation between the value of the powder electrode potential and the catalytic properties of the powder contained in it. This relation must be based on the fact that certain catalytic properties of the dispersed substance being investigated (bad or passive contact, weak contact, active contact) as regards a given chemical reaction must

correspond in a given state of catalytic activity, to a characteristic, range of powder electrode potential.

We can see that powder electrodes can be applied to investigations of catalytic properties of powder since, by using experimentally derived tables together with known numerical data of powder electrode potential compared with catalytic activity, the nearly produced portions of contact can be assessed by an easy potentiometric measurement and the badly produced portions can be eliminated, without making any experiments with them in a reactor. Many experiments made in our laboratories and in those collaborating with us have completely proved that this can be done. The powder electrode was shown to be a sensitive, exact, and workable instrument. The extent of its application has been further extended because we have also shown the possibility of its use in tracing the using-up process of the working contact and the wearing-out process of unused contacts. Here only a compound powder electrode can be applied.

We will enumerate contact substances investigated potentiometrically (in all cases we have obtained positive results and we have not come across any negative results so far).

We have investigated copper preparations (Raney's and others), Raney nickel, zinc oxide, iron oxide, vanadium quin-toxide (V_2O_5), silica gel (SiO_2) and some varieties of silicon dioxide applied as carriers, zinc ferrocyanide pure, and with Fe^{3+} and Cu^{2+} ions, a cobalt-thorium contact for Fischer and Tropsch's synthesis, zinc hydroxide with Co^{2+} ions, and silica gel with nickel sulphate (II) fixed on it. We have investigated contact fixed on a carrier and without a carrier, with additions of an activator, etc. For example, Co^{2+} ions on $Zn(OH)_2$ could be clearly detected potentiometrically and still in the quantity of $3 \cdot 10^{-5}$ g Co^{2+} to a powder electrode.

As an example we will quote the results of our own potentiometric investigations on copper powders used in the catalytic investigations of Rienaecker and his collaborators.⁶ Eight different copper powder preparations obtained by heating electrolytically obtained copper powder in a hydrogen atmosphere for 30 minutes, at various temperatures, were used. The heating temperatures

applied were 150°C, 200°C, 300°C, 400°C, 500°C, 600°C, 700°C and 900°C. Copper powder was made a component of a compound powder electrode while the platinum leading-out electrode and on 0.1 m solution of potassium sulphate (K_2SO_4) in water were added. The reference electrode was the an electrode of the second kind, i.e., Hg , Hg_2SO_4 .

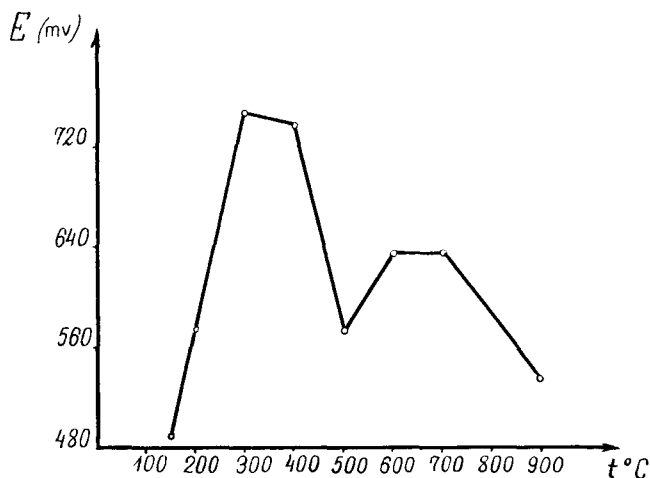
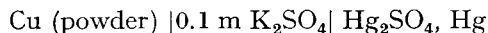


Fig. 3. Relation between the potential, E , of a cell and the heating temperature, t , of the powder.

Our own results are presented in Fig. 3, data quoted from Rienaecker's work in Fig. 4. Figure 3 gives the relation of the obtained electromotive force of a cell



and the heating temperature of powder.

Figure 4 gives the activation energy of the reaction of decomposition of formic acid as a function of the heating temperature of copper powder (used as a catalyst).

The greatest electromotive force values, i.e., the most negative values of powder electrode potential were obtained from powders heated at a temperature from 300°C to 400°C and from 600°C to 700°C. Figure 4 gives the lowest values of activation energy

for the same powders. Also the local minima of both diagrams fall to 500°C.

To close this section on potentiometric investigations of catalysts, we recall the work (mentioned in Section 2) on Raney nickel containing hydrogen and artificially deprived of it. The cycle of dehydrogenation and then of hydrogenation was successfully

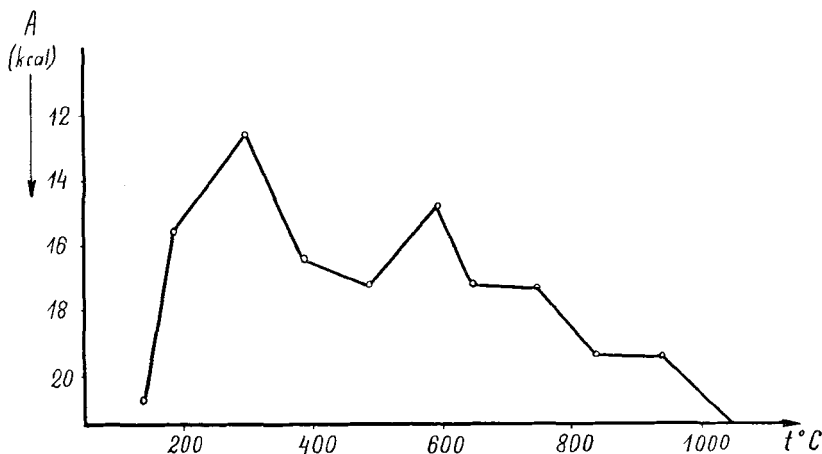


Fig. 4. Activation energy A , of the reaction of decomposition of formic acid as a function of the heating temperature, t , of copper powder used as a catalyst.

carried out for a given preparation which was investigated potentiometrically at each stage. From the values of the powder electrode potential, the individual stages of the cycle could be distinguished. The level of the hydrogenation of nickel can be connected with its catalytic activity.

VI. INVESTIGATIONS ON Fe-Zn AND Fe-C SYSTEMS

Interesting results were obtained by our collaborators, the Institute of General Chemistry* (the publication by E. Treszczanowicz *et al.*¹⁰). These were investigations on iron-zinc contact. It was found that the potential of the powder electrode containing

* Instytut Chemii Ogólnej, Warszawa.

a dispersed iron-zinc contact is a function of the quantitative composition of the alloy and its structure. We present these results in Fig. 5, which is taken from reference (10). (A water-calomel-saturated electrode was the reference electrode.)

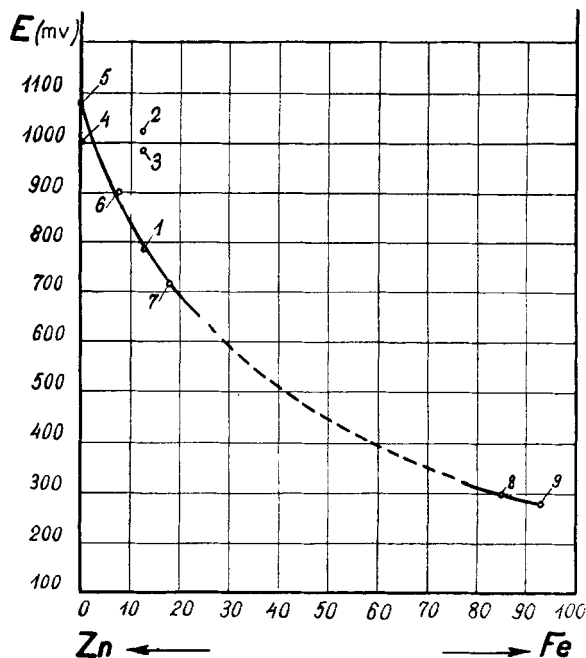


Fig. 5. Potential, E , of a powder electrode containing a dispersed iron-zinc contact as a function of the percentage of iron in the contact.

Points 1, 6, 7, 8, 9 are slowly-cooled alloys. Points 2, and 3 are quickly-cooled alloys; 4 is technical zinc; 5 is chemically pure zinc. As can be seen alloys prepared in the same way (slowly-cooled) have their points connected by one smooth curve.

Points 1, 2, and 3 have a common coordinate 12.5 per cent of iron. Metallographic investigations showed a varying structure of alloy 1 (eutectoid $\gamma + \sigma$) mainly of hexagonal crystals. Points 2 and 3 correspond to fixed states of equilibrium reached from a high temperature (phases: η of greater quantity of zinc, and γ of greater quantity of iron). Each of the alloys has a characteristic

catalytic activity and durability of activity. Potentiometric measurement enables us to define the structure and catalytic activity (as a solution, an ethanol solution of potassium chloride was used).

The occurrence of free zinc crystals or crystals of great zinc content in the powder investigated was indicated by a powder electrode with a much more negative potential.

The iron-carbon system has been investigated in our laboratory. The powders were subjected to thermal treatment and next they were investigated by the potentiometric method in powder electrodes, and by the metallographic method using grinds and corrosions of the powder in shellac. Both the carbon content and the structure of the system had an influence on the rates of change and the value of the powder electrode potential in aqueous solution of potassium sulphate. The potentiometric measurements enabled us to define the structure when the quantitative composition of an alloy was known.

VII. POTENTIOMETRIC INVESTIGATIONS OF ADSORBENTS

We have investigated different preparations of powdered activated and nonactivated carbon and silica gel. As the powder in a powder electrode we applied the adsorbent not covered with an adsorption layer and the one containing some amount of substance adsorbed on its surface.

We will recall here the data from Table III, which indicate that various carbon preparations differ considerably. The reproduction of results is good in general and the range of values amounts to several or a dozen millivolts at the most, but it depends on the preparation. The application of an 0.5 m aqueous solution of potassium chloride gives good results.

Next we carried out the adsorption of various substances from liquid solutions or from the gaseous state in different preparations of carbon powder. Acetic acid, hydrogen chloride, ammonia and chlorine were adsorbed from aqueous solutions. Ethyl acetate was adsorbed from an ethanol solution, and ammonia and chlorine were adsorbed from gaseous phases.

We have found out that the powder electrode potential is very sensitive to the presence of a substance adsorbed on the surface of the powder in the electrode. When the surface concentration is not too great there is a relation between the powder electrode potential Π , and the surface concentration of the substance adsorbed Γ :

$$\Pi = a\Gamma^b \quad (3)$$

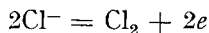
where a and b are constants which are characteristic of the system being investigated and of the temperature of the experiments.

During preliminary manipulations and in the potassium chloride solution there is a desorption of the adsorbed substance. Therefore it was necessary to adopt a standardized procedure for introducing the carbon into the powder electrode when experimenting with each preparation, and to adopt a standard time interval after which the measured potential was accepted as the correct experimental result. We generally used one hour, after initial establishing, as the period during which if there were no changes in the potential value then equilibrium was assumed to have been reached. The surface concentrations investigated by us were from hundredths to several millimoles to a gram of adsorbent.

According to given data⁷ we have proved that carbon in powder electrodes and at the atmosphere of air is positively charged in relation to a solution and acts as an oxygen electrode. It was negatively charged when saturated with hydrogen and then functioned as a hydrogen electrode. These carbon charges had an influence on the kinetics of the desorption process and on the direction of the potential changes of the powder electrode both in time and in relation to the surface concentration of a substance adsorbed.

Extensive researches, not yet finished, have been concerned with a powder carbon electrode with adsorbed chlorine. Investigations were carried out always using a solution of potassium chloride. Because of the presence of chlorine and chlorine ions we considered this as a chlorine electrode. The powder electrode potential always increased with the increase of the surface concentration of chlorine, and decreased with the increase of the

chlorine ions concentration in the solution. The observed changes in the electrode potential with time and the results of measurements of the potential of the powder carbon electrode during the process of chlorine adsorption on carbon (from the solution of Cl_2 in KCl_{aq}), suggest that the electrode process:



takes place without a stage relying on adsorption. It is a process near the face (as numerous catalytic processes) and not on the face of the adsorption layer, for we have observed a decrease in the electrode potential during the process of adsorption of chlorine from the solution of KCl . The surface concentration of adsorbed chlorine was then increasing; however, the concentration of solute chlorine was decreasing. According to our opinion, only the solute chlorine exchanges electrons with carbon at the surface of carbon, determining the electrode potential.

We have deduced theoretically and confirmed experimentally that for this system the following formula expresses the powder electrode potential:

$$\Pi = A + B \log F \quad (4)$$

Formula (3) is only empirical though well fulfilled by the experimental data. For low values of F the lines showing Π as a function of F according to formulas (3) and (4) are running quite near one another.

The investigations carried out on silica gel enabled us to state that by means of powder electrodes various preparations of the gel can be well distinguished; the wearing-out process can be observed, and adsorptive and carrier properties can be predicted. The adsorbed substances have a great influence on the potential of an electrode with powdered silica gel.

We have also investigated adsorption of Co^{2+} ions on $\text{Zn}(\text{OH})_2$ gel and Fe^{3+} and Cu^{2+} on $\text{Zn}_2\text{Fe}(\text{CN})_6$ (see Section V). We have found a great influence of sedimented ions on the powder electrode potential. The $\text{Zn}_2\text{Fe}(\text{CN})_6$ itself has hardly any influence on the potential of platinum wire twisted round it (in aqueous solution of KCl). After adsorbing Cu^{2+} and/or Fe^{3+} ions, the potential is

considerably changed and becomes a function of the concentration of these ions. In Fig. 6 we present a graph of the relation of the powder electrode potential (the electrode containing all the time the same quantity of $\text{Zn}_2\text{Fe}(\text{CN})_6$) to the number of Cu^{2+} and Fe^{3+} ions, the sum of which in gram equivalent was constant and amounted to 3.14×10^{-6} gram equivalent to one powder electrode.

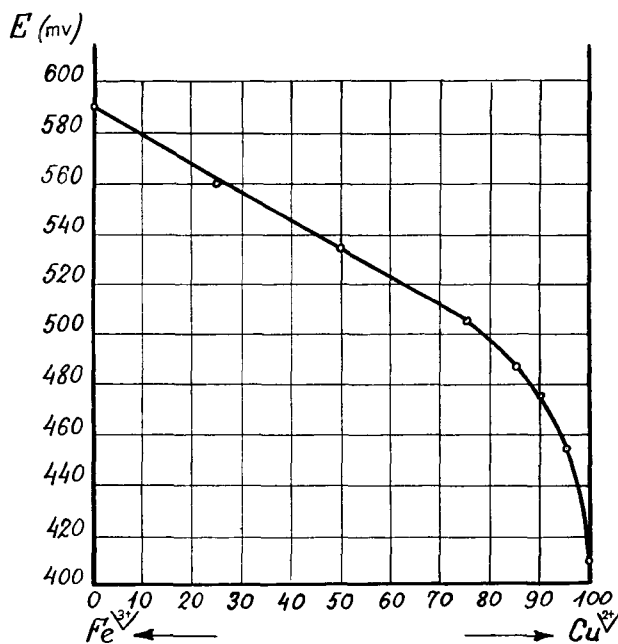


Fig. 6. Potential, E , of a powder electrode containing $\text{Zn}_2\text{Fe}(\text{CN})_6$ as a function of the concentration of Fe^{3+} and Cu^{2+} ions.

We point to the fact that iron as a less noble metal had a greater influence on the electrode's potential than copper, as it occurred in alloy electrodes.

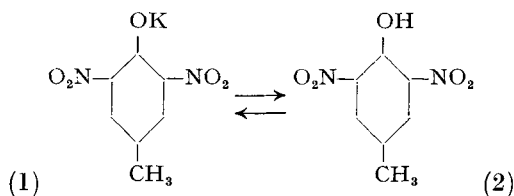
VIII. INVESTIGATIONS OF DISPERSED-CRYSTAL ORGANIC SUBSTANCES

Recently we tested the application of powder electrodes to investigations on organic compounds. We are of the opinion that if an organic substance poorly soluble in water is to be selected

(and if we intend to apply an aqueous solution of potassium chloride), if this substance is to be used as the powder in a powder electrode, and if a transformation in the structure of this substance is induced by some means, then the transformation will be recorded as a change of powder electrode potential, the difference surpassing the possible change of value of the potential caused by the means itself.

This change can be effected, for example, by an irradiation such as will cause an isomeric change, or by a change of concentration of the hydrogen ions.

Here are the results obtained for the transformation:



Both substances differ in color, 1 red, 2, yellow and in crystallographic nature. Each is stable in the other range of concentration of hydrogen ions. The aqueous solution of potassium chloride was saturated by both compounds, and by adding either hydrochloric acid (HCl) or an aqueous solution of potassium hydroxide (KOH) we obtained corresponding pH values of the solution. We dipped powder electrodes in solutions prepared in this way—one series with compound 1, the second series with compound 2 (in separate containers). The powder electrodes were specially constructed to facilitate measurement.

A distinct influence of the crystalline organic substance on the potential of the powder electrode was observed. This influence was different for each individual modification and was dependent on the initial solution. Also, it was different when the solution did not contain potassium chloride (0.5 m KCl aq. with KOH or HCl added to obtain the pH desired). The change in the electrode potential with time resulted from the change in the composition of the solution through the dissolving of the solid phase and through the eventual course of the chemical reaction between

solution and crystals. Potentiometric and pH measurements permit a full description and interpretation of the changes occurring under the influence of all the factors operating here. It was found that for $\text{pH} = 4.8$ the two solid phases reach the same point of equilibrium. The equilibrium conditions when reached correspond to a constant potential value. The pH is unchanged and remains at the initial value of 4.8. In the initial period the potential of the powder electrode changes because of the solubility of the crystals; this continues for about 24 hours. Outside the equilibrium state the two solid phases can be distinguished potentiometrically; also, with this method we can trace the transformation of one phase in to another for a given pH of the solution.

We are extending our investigations to compounds containing carboxyl and amine groups in a molecule.

IX. POWDER ELECTRODES WITHOUT A POWDERED SUBSTANCE

Continuing the process of dispersion of a solid substance one can reach colloidal dispersion. The question has arisen whether with that dispersion a system corresponding to a powder electrode can be formed. Apparently a test-tube containing the dispersed phase is unnecessary here because the sol is placed in the electrolyte solution. The system, therefore, is made of suitable sol and of a platinum leading-out electrode (of increased length) dipped in the sol, and it is connected with the reference electrode. From a statistical point of view, at any moment a number of colloidal particles contacts the platinum, reproducing the state of an ordinary powder electrode in a small test-tube. Comparing the results obtained from platinum wires dipped in a sol of silver chloride with the results obtained from wires dipped in a liquid (of composition exactly the same as the dispersing phase in the sol, we have found a distinct difference (over 100 mv) with a better reproduction of potential value in the case of the sol. In the course of time, after coagulation, the values obtained for the sol gradually approach these obtained for the liquid dispersing phase, becoming identical with them in the end.

We think that an investigation of albumen sol by this method may bring about many interesting results including ones important in certain biological problems.

References

1. Hüttig, G. F., and Herrman, E., *Z. anorg. u. allgem. Chem.* **247**, 235 (1941).
2. Kamiński, B., and Benis, L., *Roczniki Chem.* **16**, 81 (1936); **17**, 89 (1937).
3. Kamiński, B., and Karczewski, K., *Roczniki Chem.* **14**, 375, 394 (1934).
4. Minc, S., and Oleszczyk, Z., *Roczniki Chem.* **25**, 454 (1951).
5. Müller, F., and Reuther, H., *Z. Elektrochem.* **48**, 682 (1942).
6. Rienaecker, G., Breuzen, H., Unger, S., and Hansen, N., *Z. anorg. u. allgem. Chem.* **284**, 225 (1955).
7. Strazesko, D. M., *Doklady Akad. Nauk S.S.S.R.* **102**, 775 (1955).
8. Tomassi, W., Jankowska, H., and Prokopowicz, M., *Bull. classe sci. Acad. roy. belg.* **43**, 195 (1957); *Przemysl Chem.* **36**, 683 (1957).
9. Tomassi, W., and Wawrzyniak, I., *Przemysl Chem.* **37**, 157 (1958).
10. Treszczanowicz, E., Lipka, B., and Jurewicz, A., *Chem. Słosowana* **2**, 319 (1958).

Bibliography

This bibliography includes works published or sent for publication before the end of 1958. Beside each item numbers of sections connected with that item are given.

- W. Tomassi, *Roczniki Chem.* **27**, 304 (1953), I, V.
W. Tomassi, *Przemysl Chem.* **32**, 603 (1953), I, V.
W. Tomassi, and W. Palczewska, *Roczniki Chem.* **28**, 263 (1954), V.
W. Tomassi, A. Frackiewicz, and M. Sanchez, *Przemysl Chem.* **34**, 492 (1955), I, II, III.
B. Lipka, *Przemysl Chem.* **34**, 55 (1955), V.
W. Palczewska, *Roczniki Chem.* **29**, 594 (1955), II.
A. Frackiewicz, *Przemysl Chem.* **35**, 41 (1956), V, VII.
W. Tomassi, and Z. Libus, *Przemysl Chem.* **35**, 382 (1956), V.
W. Tomassi, and Z. Libus, *Przemysl Chem.* **35**, 386 (1956), V.
W. Tomassi, and M. Miazek, *Przemysl Chem.* **35**, 446 (1956), V, VII.
W. Tomassi, *Przemysl Chem.* **35**, 520 (1956), II, III, IV, V, VII.
W. Tomassi, *Termodynamika Chem.*, Vol. III, Warszawa, 1956, I, II, III, V.
W. Tomassi, and W. Lewicki, *Roczniki Chem.* **30**, 1003 (1956), VII.
W. Tomassi, and H. Wrobel, *Roczniki Chem.* **30**, 873 (1956), II, V.
W. Tomassi, and W. Lewicki, *Przemysl Chem.* **35**, 626 (1956), VII.

- W. Tomassi, and D. Kocot, *Przemysl Chem.* **35**, 670 (1956), VII.
- W. Sojecki, *Zeszyty Nauk. Politech. Warszaw. Chem.* No. **2**, 71 (1957), V.
- W. Tomassi, H. Jankowska, and M. Prokopowicz, *Bull. classe sci. Acad. roy. belg.* **43**, 195 (1957); *Przemysl Chem.* **36**, 683 (1957), III, IV, VII.
- W. Tomassi, and H. Wrobel, *Przemysl Chem.* **36**, 207 (1957), II, III, IV, V.
- W. Lewicki, *Przemysl Chem.* **36**, 268 (1957), VII.
- W. Tomassi, *Przemysl Chem.* **36**, 500 (1957), III, IV, VII.
- W. Tomassi, and H. Jankowska, *Ukrain. Khim. Zhur.* **24**, 162 (1958), VII.
- W. Tomassi, and S. Probulski, unpublished, VI.
- W. Tomassi, and A. Houwalt, *Bull. classe sci. Acad. roy. belg.* **44**, 244 (1958); *Przemysl Chem.* **37**, 77 (1958), III.
- E. Treszczanowicz, B. Lipka, and A. Jurewicz, *Chem. Stosowana* **2**, 319 (1958), V, VI.
- W. Tomassi, and I. Wawrzyniak, *Przemysl Chem.* **37**, 157 (1958), III, IV, VII.
- W. Tomassi, and M. Prokopowicz, *Przemysl Chem.* **37**, 465 (1958), VII.
- W. Tomassi, *Przemysl Chem.* **38**, 76 (1959), *Electrochim. Acta* **1**, 286 (1959), VII.
- W. Tomassi, *Przemysl Chem.* **38**, 285 (1959) VII.
- Z. Siedlecka, *Przemysl Chem.* **38**, 211 (1959), VII.
- W. Tomassi, and J. Bulawa, *Ukrain. Khim. Zhur.* **25**, 699 (1959), *Przemysl. Chem.* **38**, 544 (1959), V.

VARIATIONAL PRINCIPLES IN THERMO- DYNAMICS AND STATISTICAL MECHANICS OF IRREVERSIBLE PROCESSES

SYU ONO, *College of General Education, University of Tokyo*

CONTENTS

I.	Introduction	267
II.	General Remarks	269
III.	Principle of Least Dissipation of Energy	274
	A. Onsager's Reciprocity Relations	274
	B. Principle of Least Dissipation of Energy	277
IV.	Variational Principles in the Kinetic Theory of Gases	281
	A. Variational Principle for Mixtures of Dilute Gases	281
	B. Thermodynamic Interpretation	286
	C. Application to Dense Gases	289
V.	Principle of Minimum Production of Entropy	293
	A. Discontinuous Systems	293
	B. Minimum Production in Continuous Systems	298
	C. Nonlinear Irreversible Processes	304
VI.	Statistical Theory of the Minimum Entropy Production Prin- ciple.	307
	A. Microscopic Description of Entropy Production in an Ideal Gas	307
	B. Application to Magnetic Resonance	311
	C. Generalized Minimum Production Principle	316
	References	319

I. INTRODUCTION

In many branches of theoretical physics, various types of variational principles are known and play important roles. The second law of thermodynamics is an example of a law expressed in the form of a variational principle: the entropy tends to a minimum in an isolated system.

While the extremal property of the entropy concerns only

thermodynamic-equilibrium states, the variational principles concerning systems which deviate slightly from equilibrium are known, and play some important roles in the theory of irreversible processes. In the present article the variational principles for non-equilibrium, especially the nonequilibrium stationary state, will be treated and discussed from a thermodynamic and statistical-mechanical point of view. The reason why the variational principles are taken up here is as follows.

In the first place, the laws formulated as variational principles are themselves important, irrespective of their mathematical equivalence to those expressed in a set of differential equations, as seen from the importance of Hamilton's and Maupertuis' principles in theoretical mechanics. Physical insight into the behavior of rather complicated phenomena can be acquired much more easily from laws in this form than from those in the form of a complicated set of differential equations, and often more intuitive conceptions of the phenomena can be obtained.

Secondly, in the theory of irreversible processes, variation principles may be expected to help establish a general statistical method for a system which is not far from equilibrium, just as the extremal property of entropy is quite important for establishing the statistical mechanics of matter in equilibrium. The distribution functions are determined so as to make thermodynamic probability, the logarithm of which is the entropy, be a maximum under the imposed constraints. However, such methods for determining the statistical distribution of the system are confined to the case of a system in thermodynamic equilibrium. To deal with a system out of equilibrium, we must use a different device for each case, in contrast to the method of statistical thermodynamics, which is based on the general relation between the Helmholtz free energy and the partition function of the system.

On the other hand some of the thermodynamic variables are well defined for systems slightly deviating from equilibrium. It thus seems reasonable to make an attempt to find the relation between the transport coefficients and the distribution functions of a system on the basis of the variational principles in the theory of irreversible processes.

Finally, variational principles are convenient for estimating approximate solutions of problems. We can estimate the values of transport coefficients by using suitable trial functions and, at least, the lower or upper limit can be evaluated in this way. This is another great advantage of the variational formulation of laws and is often used in calculating the ground state in quantum mechanics.

Although many of the variational principles are known in the theory of irreversible processes, the relations between these principles are sometimes vague. They are confused in some papers where clear distinction between them may be very important: some of them may be independent of each other. However, the author wishes to emphasize throughout this article that entropy production always plays a central role in any principle, as we shall see later. Entropy production seems to play some role even when a system approaches thermodynamic equilibrium.

II. GENERAL REMARKS

It will be necessary to give a general description of the irreversible processes to be treated in this article. For convenience we shall divide the system considered into two classes: *discontinuous* and *continuous*. One of the examples of a discontinuous system is that consisting of two chambers, I and II, connected by a narrow capillary and maintained at uniform temperature T^I and T^{II} , respectively. The name "discontinuous" is given since we suppose that the physical properties are not continuous functions of the spatial coordinates, in contrast to the case of a continuous system.

In general the transfers of energy and matter are defined as the energy and matter transferred from I to II per unit time. Let us denote the transfer and the forces by J_1, \dots, J_f and X_1, \dots, X_f , respectively. Then the entropy production per unit time due to these flows is expressed by

$$\mathcal{P} = \sum_{i=1}^f X_i J_i \geq 0 \quad (1)$$

For the energy transfer and the transfer of matter of component

γ ($\gamma = 1, 2, \dots, s$), the conjugate forces, X_u and X_γ , are given, respectively, by

$$X_u = 1/T^{\text{I}} - 1/T^{\text{II}} \quad (2)$$

$$X_\gamma = \mu_\gamma^{\text{I}}/T^{\text{I}} - \mu_\gamma^{\text{II}}/T^{\text{II}} \quad (3)$$

where μ_γ^{I} and μ_γ^{II} are the chemical potentials of component γ in chambers I and II, respectively.

If the flows are linear functions of the forces, we call this irreversible process *linear*; and flows and forces are connected by the phenomenological relations

$$J_i = \sum_{j=1}^f L_{ij} X_j \quad (4)$$

where L_{ij} are called the *phenomenological coefficients*.

If we denote the element of the reciprocal matrix of L_{ij} by R_{ij} , then Eq. 4 can be expressed in an alternative form

$$X_i = \sum_{j=1}^f R_{ij} J_j \quad (5)$$

where

$$\sum_{j=1}^f L_{ij} R_{jk} = \delta_{ik} \quad (6)$$

δ_{ij} being Kronecker's delta.

Next we shall consider a homogeneous system with chemical reactions. Here the change in the mass of component γ during the time interval dt , dm_γ , and that in the mole number, dN_γ , are written as

$$\begin{aligned} dm_\gamma &= v_\gamma M_\gamma d\xi \\ dN_\gamma &= v_\gamma d\xi \end{aligned} \quad (7)$$

where M_γ is the molar mass of component γ , v_γ its stoichiometric coefficient, and ξ the degree of advancement of the reaction, first introduced by De Donder.⁸⁻¹¹ The stoichiometric coefficient is counted positive when it appears in the right-hand side of the reaction equation and negative when it appears in the left-hand side. The stoichiometric equation, which corresponds to the conservation of mass, is expressed as

$$\sum_\gamma v_\gamma M_\gamma = 0 \quad (8)$$

The above equation is generalized immediately to r simultaneous reactions. We shall designate the different reactions by subscript ρ ($\rho = 1, \dots, r$). The total changes in mass and mole number due to the chemical reactions, dm_γ and dN_γ , of component γ are, respectively,

$$\begin{aligned} dm_\gamma &= M_\gamma \sum_{\rho=1}^r v_{\gamma\rho} d\xi_\rho \\ dN_\gamma &= \sum_{\rho=1}^r v_{\gamma\rho} d\xi_\rho \end{aligned} \quad (9)$$

The reaction rate of the ρ th reaction is clearly

$$v_\rho = d\xi_\rho/dt \quad (10)$$

which is also a flow like the flow of matter from one chamber to another.

On the other hand, the chemical reaction rate depends generally on a set of chemical affinities given by

$$A_\rho = - \sum_\gamma \mu_\gamma v_{\gamma\rho} \quad (11)$$

where μ_γ is the chemical potential of one mole of component γ . The entropy production per unit time due to the r chemical reactions is

$$\mathcal{P} = \sum_{\rho=1}^r (A_\rho/T) v_\rho \quad (12)$$

which implies that the affinities A_ρ are the force conjugate to the flow v_ρ given by Eq. 10.

As the first approximation, we shall assume that the reaction rates are linear functions of the affinities A_ρ . This is the case in the immediate neighborhood of chemical equilibrium. Then the linear relations for the chemical reactions are written as

$$v_\rho = \sum_{\rho'=1}^r L_{\rho\rho'} A_{\rho'}/T \quad (13)$$

Since the Gibbs free energy is given by

$$G = \sum_{\gamma=1}^s N_\gamma \mu_\gamma$$

it is easily shown that

$$A_\rho = -(\partial G / \partial \xi_\rho)_{T, v, \xi_\rho} \quad (14)$$

Continuous systems are those in which the intensive variables are not only functions of time but also continuous functions of the spatial coordinates. In the usual thermal conduction and diffusion phenomena, we deal with such continuous systems. The forces \mathbf{X}_u and \mathbf{X}_γ in a continuous system are defined by

$$\mathbf{X}_u = \nabla(1/T) \quad (15)$$

$$\mathbf{X}_\gamma = \mathbf{F}_\gamma/T - \nabla(\mu_\gamma^+/T) \quad (16)$$

where \mathbf{F}_γ is the force acting on the unit mass of the component γ and

$$\mu_\gamma^+ = \mu_\gamma/M_\gamma$$

the chemical potential of the unit mass of γ . Then the local entropy production and the entropy flow at each point in the presence of the chemical reactions are given, respectively, by

$$\sigma = \mathbf{X}_u \cdot \mathbf{J}_u + \sum_{\gamma=1}^s \mathbf{X}_\gamma \cdot \mathbf{J}_\gamma + \sum_{\rho=1}^r (A_\rho/T) v_\rho \quad (17)$$

and

$$\mathbf{S} = (1/T)(\mathbf{J}_u - \sum_{\gamma=1}^s \mu_\gamma^+ \mathbf{J}_\gamma) \quad (18)$$

where \mathbf{J}_u is the energy flow and \mathbf{J}_γ is the flow of mass of component γ relative to the motion of the center of mass per unit time. The last summation of the right-hand side of Eq. 17 corresponds to the entropy source due to the chemical reactions, which has been given by Eq. 12. The integration of σ given by Eq. 17 over the volume of the system yields the total production of entropy per unit time.

We shall write the phenomenological relations for continuous systems in the form

$$\begin{aligned} \mathbf{J}_u &= L_{uu} \mathbf{X}_u + \sum_{\gamma=1}^s L_{u\gamma} \mathbf{X}_\gamma \\ \mathbf{J}_\gamma &= L_{\gamma u} \mathbf{X}_u + \sum_{\gamma'=1}^s L_{\gamma\gamma'} \mathbf{X}_{\gamma'} \end{aligned} \quad (19)$$

It should be noted here that the definition of the phenomenological coefficients is slightly different from customary ones such as the ordinary definition of thermal conductivity, which is different from L_{uu} by the factor T . This difference is not essential as long as the fluctuation of temperature in the system is not too large. However, this definition of the coefficient is essential in the derivation of the variational principle for continuous systems.

If we use the reciprocal matrix of L_{uu} , $L_{u\gamma}$, $L_{\gamma\gamma'}$, the linear relations are expressed in the form

$$\begin{aligned} \mathbf{X}_u &= R_{uu} \mathbf{J}_u + \sum_{\gamma=1}^s R_{u\gamma} \mathbf{J}_\gamma \\ \mathbf{X}_\gamma &= R_{\gamma u} \mathbf{J}_u + \sum_{\gamma'=1}^s R_{\gamma\gamma'} \mathbf{J}_{\gamma'} \end{aligned} \quad (20)$$

The interference between the flows of matter and energy on the one hand and the chemical reaction on the other are not taken up according to Curie's theorem.⁵

In the case of linear irreversible phenomena, it will be convenient to introduce Onsager's *dissipation function*³⁹

$$2\Phi(J, J) = \sum_{i,j} R_{ij} J_i J_j \quad (21)$$

where the R_{ij} 's are given as the coefficients of Eq. 5. This expression is the quadratic form of the flows and is a generalization of Lord Rayleigh's dissipation function.^{54,55} The corresponding function of the forces is

$$2\Psi(X, X) = \sum_{i,j} L_{ij} X_i X_j \quad (22)$$

which has a similar property. It is, however, noted that Eq. 22 is a function of state while the dissipation function given by Eq. 21 depends on the flows. By the linear relation given by either Eq. 4 or Eq. 5, the numerical values of Eqs. 21 and 22 are always equal to the entropy production, \mathcal{P} , given by Eq. 1.

Functions similar to Eqs. 21 and 22 may be defined for a continuous system.

III. PRINCIPLE OF LEAST DISSIPATION OF ENERGY

A. Onsager's Reciprocity Relations

Some of the variational principles which are to be described in the present article, are very closely connected with Onsager's *reciprocity relations*.^{39,40} Although there have been various methods of derivation of this theorem, we shall follow the traditional method of derivation by Onsager⁴⁰ and Casimir.² This is based on the consideration of fluctuations in an aged system, and this method is also connected with the derivation of Onsager's principle of least dissipation of energy.³⁹⁻⁴¹

Let us consider a set of macroscopic variables, A_1, \dots, A_f , with the equilibrium values A_1^0, \dots, A_f^0 , which will be sufficient to describe the macroscopic state of the system. Then this state can be represented by a set of deviations of the gross variables from their equilibrium values:

$$\alpha_i = A_i - A_i^0 \quad (i = 1, \dots, f) \quad (23)$$

Hereafter, a set of α_i 's is denoted by the boldface symbol α .

Since the entropy, S , of a system is a maximum for the equilibrium state, for which all α_i 's are zero, we have

$$S = S_0 - \frac{1}{2} \sum_{i,j} g_{ij} \alpha_i \alpha_j \quad (24)$$

where S_0 is the equilibrium value of the entropy and g_{ij} the positive definite symmetric tensor. In an isolated system, the time derivative of the macroscopic variable generally corresponds to the flow J_i , and hence we may write

$$J_i = d\alpha_i/dt \equiv \dot{\alpha}_i \quad (25)$$

The entropy production in an isolated system is equal to the time derivative of the entropy given by Eq. 24, and therefore we have, using the symmetry of g_{ij} ,

$$\mathcal{P} = \dot{S} \equiv dS/dt = - \sum_{i,j} g_{ij} \alpha_i \dot{\alpha}_j \quad (26)$$

From Eqs. 24, 25, and 26, we immediately obtain

$$\mathcal{P} = \sum_{i=1}^f X_i J_i \quad (27)$$

where

$$X_i = \partial S / \partial \alpha_i = - \sum_{j=1}^f g_{ij} \alpha_j \quad (28)$$

Comparing Eq. 27 with Eq. 1 for the entropy production, we can immediately see that X_i , defined by Eq. 28, is the force conjugate to the flow defined by Eq. 25.

We shall now introduce the probability distribution, function $F(\alpha)$ in the α -space. According to Boltzmann's principle this function is given by

$$F(\alpha) = c \exp (S - S_0) / k \quad (29)$$

where c is a normalization constant to be determined by

$$\int \cdots \int F(\alpha) d\alpha_1 \dots d\alpha_f = 1 \quad (30)$$

Thus the average of α_i , denoted by $\langle \alpha_i \rangle$, is given by

$$\langle \alpha_i \rangle = \int \cdots \int \alpha_i F(\alpha) d\alpha_1 \dots d\alpha_f \quad (31)$$

Now we shall calculate the following average of $\alpha_i X_j$:

$$\langle \alpha_i X_j \rangle = \int \cdots \int \alpha_i X_j F(\alpha) d\alpha_1 \dots d\alpha_f \quad (32)$$

With Eqs. 28 and 29, we obtain

$$\begin{aligned} \langle \alpha_i X_j \rangle &= k \int \cdots \int \alpha_i [\partial \log F(\alpha) / \partial \alpha_j] F(\alpha) d\alpha_1 \dots d\alpha_f \\ &= k \int \cdots \int d\alpha_1 \dots d\alpha_f \int \alpha_i [\partial F(\alpha) / \partial \alpha_j] d\alpha_j \\ &= -k \int \cdots \int d\alpha_1 \dots d\alpha_f \int F(\alpha) \delta_{ij} d\alpha_j \end{aligned} \quad (33)$$

where the last expression is obtained by partial integration. Thus,

$$\langle \alpha_i X_j \rangle = -k \delta_{ij} \quad (34)$$

Using Eq. 28, we immediately obtain

$$\langle X_i X_j \rangle = k g_{ij} \quad (35)$$

$$\langle \alpha_i \alpha_j \rangle = k g_{ij}^{-1} \quad (36)$$

where g_{ij}^{-1} is the reciprocal of the matrix g_{ij} .

The correlation functions are defined by

$$B_{ij}(\tau) = \langle \alpha_i(t) \alpha_j(t + \tau) \rangle \quad (37)$$

where $\alpha_i(t)$ represents the gross variable as a function of time. The correlation function $B_{ij}(\tau)$ is independent of time according to the ergodic theorem.

For simplicity we shall confine ourselves to the case of even variables, to that the principle of dynamical reversibility of microscopic systems, can be expressed, in terms of the correlation functions, in the form

$$B_{ij}(\tau) = B_{ij}(-\tau) \quad (38)$$

which can also be written in the form

$$B_{ij}(\tau) = B_{ji}(\tau) \quad (39)$$

The correlation functions can be obtained by an alternative procedure. By taking at first fixed values of the variables at time t and averaging the quantities belonging to the time $t + \tau$, and subsequently by averaging over the hitherto fixed parameters, we obtain

$$B_{ij}(\tau) = \langle \alpha_i(t) \langle \alpha_j(t + \tau) \rangle_{\alpha(t)} \rangle \quad (40)$$

The above results have been obtained by straightforward calculations within the method of statistical mechanics. However, Onsager⁴⁰ and Casimir² used a new hypothesis. They assumed that the decay of a fluctuation follows, on the average, the ordinary phenomenological macroscopic laws. The latter equations express linear relations between the flows, which are expressed as the time derivatives of macroscopic variables α_i 's, and the forces, which are also functions of α_i 's. This can be written as

$$J_i \equiv \langle \dot{\alpha}_i \rangle = \sum_{j=1}^f L_{ij} X_j \quad (41)$$

where L_{ij} is the phenomenological coefficient introduced in Eq. 4. The time derivative in the above equation should be considered as a quotient of differences and Eq. 41 should be read

$$(1/\tau) \langle \alpha_i(t + \tau) - \alpha_i(t) \rangle_{\alpha(t)} = \sum_{j=1}^f L_{ij} X_j \quad (42)$$

where the time interval τ is much larger than a characteristic molecular time (for example, the average time between two successive collisions of molecules), and at the same time much shorter than the relaxation time of the macroscopic phenomena. There are many discussions on this hypothesis, but it is impossible to enter into them in the present article.

Multiplying both sides of Eq. 42 by $\alpha_j(t)$, and taking the average over the hitherto fixed parameters, we obtain, according to Eq. 40,

$$B_{ji}(\tau) - B_{ji}(0) = -kL_{ij}\tau \quad (43)$$

in which the relation Eq. 34 has been utilized. From the symmetry relation of the correlation functions, Eq. 39, we obtain the well-known reciprocity relation

$$L_{ij} = L_{ji} \quad (44)$$

Thus Onsager's reciprocity relations have been demonstrated.

B. Principle of Least Dissipation of Energy

We shall consider the system, the macroscopic state of which is determined by the f macroscopic variables $\alpha_1, \dots, \alpha_f$. Let t_1, t_2, \dots, t_p be p instants of time, and $\alpha(t)$ be a set of the f macroscopic variables at the instant t . From the thermodynamic point of view, the changes in the gross variables obey the phenomenological relations Eq. 41. However, from the purely statistical point of view we must expect some deviation with some magnitude of probability, for each instant of time. For example, even in the equilibrium state corresponding to $\alpha = 0$, some of α_i 's take values different from zero by spontaneous fluctuation, although they would always remain zero according to the purely phenomenological law. Then the sets of values at p instants, $\alpha(t_1), \dots, \alpha(t_p)$, are given by the probability distribution function. Since the gross variables are considered to be algebraic sums of molecular variables, these sets of variables have a multivariate Gaussian distribution, according to a kind of central limit theorem*,

* According to Khinchin-Cramer's theorem,^{27a} there exists a Gaussian process of which all first and second moments are equal to those of arbitrary stochastic processes (L^2).

as assumed by Onsager and Machlup.^{29,42} In other words, the temporal development of a gross variable are the Gaussian random processes.

Following Onsager⁴⁰ we shall assume that, as far as the average behavior is concerned, it does not matter whether a state was the result of spontaneous fluctuation or of an imposed constraint. Then, in the case of Gaussian process, as proved by Doob,¹² it must be Markoffian, if it obeys the phenomenological law Eq. 41.

We shall denote the joint probability that $\alpha(t_1)$ lies between $\alpha^{(1)}$ and $\alpha^{(1)} + d\alpha^{(1)}$, and $\alpha(t_2)$ lies between $\alpha^{(2)}$ and $\alpha^{(2)} + d\alpha^{(2)}$, by $f(\alpha^{(2)}, t_2; \alpha^{(1)}, t_1) d\alpha^{(1)} d\alpha^{(2)}$. Since the process is Markoffian, this probability depends only on $\alpha^{(1)}$, $\alpha^{(2)}$ and the time interval $\tau = t_2 - t_1$. Then the conditional probability that $\alpha(t_2) - \alpha(t_1)$ has the value between $\Delta\alpha$ and $\Delta\alpha + d\Delta\alpha$, for a given set of values of $\alpha^{(1)}$, depends only on $\Delta\alpha$, $\alpha^{(1)}$ and τ on account of stationarity. This conditional probability density should be Gaussian and hence is expressed in the form

$$f\left(\alpha^{(1)} + \Delta\alpha \middle| \alpha^{(1)} \right)_{t+\tau} = C \exp \left[-\frac{1}{2} \sum_{i,j} \lambda_{ij} (\Delta\alpha_i - \mu_i) (\Delta\alpha_j - \mu_j) \right] \quad (45)$$

where μ_i is the average of $\Delta\alpha_i$ and may depend on $\alpha^{(1)}$, and λ_{ij} and C are constants.

Here we shall make the postulate that the average of $\Delta\alpha_i/\tau$ obeys the phenomenological equation Eq. 41. Thus we have

$$\mu_i = \tau \sum_{j=1}^f L_{ij} X_j \quad (46)$$

For a Gaussian distribution the second moments are equal⁴ to the elements of the reciprocal matrix of λ_{ij} :

$$\lambda_{ij}^{-1} = \langle (\Delta\alpha_i - \mu_i) (\Delta\alpha_j - \mu_j) \rangle_{\alpha^{(1)}} \quad (47)$$

Then, taking the average over the gross variables which have been fixed, we obtain

$$\lambda_{ij}^{-1} = -\mu_i \mu_j + 2B_{ij}(0) - 2B_{ij}(\tau) \quad (48)$$

where $B_{ij}(\tau)$ is the correlation function given by Eq. 37. If the time interval τ is sufficiently short to neglect the square terms

in τ , comparison of Eq. 48 with Eq. 43 leads to

$$\lambda_{ij}^{-1} = 2k\tau L_{ij} \quad (49)$$

Using the coefficients R_{ij} defined by Eqs. 5 and 6, instead of L_{ij} and Eq. (46), we can express the conditional probability Eq. 45 in the following form:

$$\begin{aligned} \log f \left(\begin{matrix} \alpha^{(1)} + \Delta\alpha \\ t + \tau \end{matrix} \middle| \begin{matrix} \alpha^{(1)} \\ t \end{matrix} \right) \\ = -\frac{1}{4}(\tau/k)[2\Phi(d\alpha/dt, d\alpha/dt) + 2\Psi(X, X) - 2\mathcal{P}] + \text{const} \end{aligned} \quad (50)$$

where $\Phi(d\alpha/dt, d\alpha/dt)$ and $\Psi(X, X)$ are defined by Eqs. 21 and 22, respectively, and \mathcal{P} the entropy production per unit time as expressed in the form of Eq. 1 in which J_i is replaced by $d\alpha_i/dt$. In the above the rate of change $d\alpha/dt$ stands for $[\alpha(t + \tau) - \alpha(t)]/\tau$.

The most probable transition is given by the condition

$$\mathcal{P} - \Phi(d\alpha/dt, d\alpha/dt) - \Psi(X, X) = \text{maximum}. \quad (51)$$

It is evident that, if the reciprocity relations $R_{ij} = R_{ji}$ are valid, Eq. 51 gives the linear relations

$$X_i = \sum_{j=1}^f R_{ij} d\alpha_j/dt \quad (52)$$

This transition probability was first obtained by Onsager⁴⁰ and the probability for the path is obtained from Eq. 50. Hashitsume²¹ and Onsager and Machlup^{29,42} used extensively this probability of path in the theory of thermal fluctuations.

Since the probability distribution has been determined in such a way that the average behavior of $d\alpha/dt$ obeys the phenomenological linear relation, it is rather expected that the linear relation maximizes the probability for change. However, it should be noted that this principle gives the direct statistical significance of the dissipation functions. Since the probability that $\alpha^{(1)}$ lies between $\alpha^{(1)}$ and $\alpha^{(1)} + d\alpha^{(1)}$ is proportional to $\exp[-S(\alpha^{(1)})/k]$ and since the conditional probability density is given by Eq. 50, then the joint probability $f(\alpha^{(2)}, t_2; \alpha^{(1)}, t_1) d\alpha^{(1)} d\alpha^{(2)}$ is given by

$$\begin{aligned} \log f(\alpha^{(2)}, t_2; \alpha^{(1)}, t_1) &= (1/k) \left\{ \left[\frac{1}{2} S(\alpha^{(1)}) + \frac{1}{2} S(\alpha^{(2)}) \right] \right. \\ &\quad \left. - \frac{1}{4} [2\Phi(\Delta\alpha/\tau, \Delta\alpha/\tau) + 2\Psi(X, X)] \right\} \end{aligned} \quad (53)$$

This may be regarded as an extension to time-dependent systems of Boltzmann's relation between probability and entropy.

Since the entropy is a maximum at equilibrium, the extremum property of Eq. 51 corresponds to the maximum entropy at thermodynamic equilibrium. Then this extremal property and the relation 53 are expected to shed light on the microscopic theory of irreversible phenomena.

As shown by Onsager³⁹ $2T\Phi(d\alpha/dt, d\alpha/dt)$ is equal to the rate of dissipation of free energy, and hence the principle expressed in the form of Eq. 51 is called *principle of least dissipation of energy*. This is a generalization of a similar principle in hydrodynamics due to Lord Rayleigh.^{54,55}

Let us consider the case of a continuous system, in which the forces and flows are given as functions of spatial coordinates. Then the total entropy production is given by Eq. 17 over the volume, and the principle of least dissipation becomes

$$\int [\mathbf{X}_u \cdot \mathbf{J}_u + \sum_{\gamma=1}^s \mathbf{X}_\gamma \cdot \mathbf{J}_\gamma + \sum_{\rho=1}^r (A_\rho/T) v_\rho - \varphi(J, J)] dV = \text{maximum} \quad (54)$$

where φ is the dissipation function defined by

$$\begin{aligned} \varphi(J, J) = & \frac{1}{2} [R_{uu} \mathbf{J}_u \cdot \mathbf{J}_u + \sum_{\gamma=1}^s (R_{u\gamma} + R_{\gamma u}) \mathbf{J}_u \cdot \mathbf{J}_\gamma \\ & + \sum_{\gamma=1}^s \sum_{\gamma'=1}^s R_{\gamma\gamma'} \mathbf{J}_\gamma \cdot \mathbf{J}_{\gamma'} + \sum_{\rho=1}^r \sum_{\rho'=1}^r R_{\rho\rho'} v_\rho v_{\rho'}] \end{aligned} \quad (55)$$

in which R_{uu} , $R_{u\gamma}$, $R_{\gamma\gamma'}$ are the phenomenological coefficients given in Eq. 20, and $R_{\rho\rho'}$'s are similarly defined from the coefficients $L_{\rho\rho'}$ of Eq. 13 for the chemical reactions. If the reciprocal relations are valid, the variational principle Eq. 54 is equivalent to the set of linear relations Eq. 20 and

$$A_\rho/T = \sum_{\rho'=1}^r R_{\rho\rho'} v_{\rho'} \quad (56)$$

which is equivalent to Eq. 13.

We must be extremely careful about the condition under which we maximize the left-hand side of Eq. 54. In Onsager's principle of least dissipation of energy, the forces are fixed at

every point of the system and only the flows are varied. The principle of least dissipation of energy is, on the other hand, not restricted to the stationary state. It is connected with the most probable change in thermal fluctuations. If we assume that the irreversible processes in thermodynamic systems are all of quite the same character as that of aged systems, the principle of least dissipation is also applicable to an open system.

Let us consider the case of an open system in the stationary state, for which we have the equations for mass and energy conservation

$$\operatorname{div} \mathbf{J}_u \equiv \nabla \cdot \mathbf{J}_u = \sum_{\gamma=1}^s \mathbf{F}_\gamma \cdot \mathbf{J}_\gamma \quad (57)$$

$$\operatorname{div} \mathbf{J}_\gamma \equiv \nabla \cdot \mathbf{J}_\gamma = \sum_{\rho=1}^s v_{\gamma\rho} M_\rho v_\rho \quad (58)$$

Further, we shall impose the following condition on the variation of the flows:

$$\mathcal{P} = 2 \int \varphi(J, J) dV \quad (59)$$

Then the variational principle Eq. 54 reduces to

$$\int \varphi(J, J) dV = \text{maximum} \quad (60)$$

with the restrictions Eqs. 57, 58, and 59. This variational principle, together with the restrictions, determines the stationary distributions of flows and intensive variables in the interior when the values of the intensive variables are prescribed at the boundary.

It should be noted that the restrictive condition Eq. 59 is not equivalent to the linear relations Eq. 20, although the linear relations satisfy the condition Eq. 59 automatically. That is, the linear relations are sufficient but not necessary for Eq. 59.

IV. VARIATIONAL PRINCIPLES IN THE KINETIC THEORY OF GASES

A. Variational Principle for Mixtures of Dilute Gases

The transport phenomena in a dilute gas are the most typical of the irreversible phenomena that we usually meet. The variational principle which is useful for the calculation of transport coef-

ficients of gases has been established by Hellund and Uehling²² and later developed by Hirschfelder and Curtiss.^{6, 23}

We shall consider a mixture of dilute gases of monatomic molecules. As is well known the state of such a mixture is described by a set of distribution functions $f_\gamma(\mathbf{r}, \mathbf{v}_\gamma, t)$. The function $f_\gamma(\mathbf{r}, \mathbf{v}_\gamma, t)$ is defined in such a way that the probable number of molecules of species γ with the positional coordinates in the range between \mathbf{r} and $\mathbf{r} + d\mathbf{r}$ and the velocity in the range between \mathbf{v}_γ and $\mathbf{v}_\gamma + d\mathbf{v}_\gamma$ is $f_\gamma(\mathbf{r}, \mathbf{v}_\gamma, t) d\mathbf{r} d\mathbf{v}_\gamma$. Then the center of mass velocity, \mathbf{v}_0 , and the diffusion velocity of component γ , $\bar{\mathbf{V}}_\gamma$, are respectively given by

$$\rho \mathbf{v}_0 = \sum_{\gamma=1}^s \int m_\gamma \mathbf{v}_\gamma f_\gamma d\mathbf{v}_\gamma \quad (61)$$

$$n_\gamma \bar{\mathbf{V}}_\gamma = \int \mathbf{v}_\gamma f_\gamma d\mathbf{v}_\gamma \quad (62)$$

where n_γ is the local number density of component γ , m_γ the mass of a γ molecule,

$$\rho = \sum_{\gamma=1}^s n_\gamma m_\gamma$$

the mass density and $\mathbf{V}_\gamma = \mathbf{v}_\gamma - \mathbf{v}_0$ the velocity of a γ molecule relative the center of mass motion. The mass current \mathbf{J}_γ defined in the preceding section is

$$\mathbf{J}_\gamma = m_\gamma n_\gamma \bar{\mathbf{V}}_\gamma \quad (63)$$

The condition of normalization for the distribution function f_γ is

$$\int f_\gamma d\mathbf{v}_\gamma = n_\gamma \quad (64)$$

Further we define the local temperature by

$$\frac{3}{2} nkT = \frac{1}{2} \sum_{\gamma=1}^s \int m_\gamma V_\gamma^2 f_\gamma d\mathbf{v}_\gamma \quad (65)$$

where n is the total number density,

$$n = \sum_{\gamma=1}^s n_\gamma$$

The temperature T defined by Eq. 65 becomes identical with the ordinary one when the system is in thermodynamic equilibrium.

The temporal variation of the distribution functions is subject to the Boltzmann equation

$$\mathcal{D}_\gamma f_\gamma = \sum_{\beta=1}^s \iiint (f'_\gamma f'_\beta - f_\gamma f_\beta) g_{\gamma\beta} b \, db \, d\varepsilon \, d\mathbf{v}_\beta \quad (66)$$

where \mathcal{D}_γ is the differential operator

$$\mathcal{D}_\gamma \equiv \partial/\partial t + \mathbf{v}_\gamma \cdot \nabla + \mathbf{F}_\gamma \cdot \nabla_{\mathbf{v}} \quad (67)$$

\mathbf{F}_γ being the external mechanical force acting upon the unit mass of component γ , and $\nabla_{\mathbf{v}}$ the ∇ -operator in the velocity space. In the right-hand side, which is called the collision term, f'_γ and f'_β represent $f_\gamma(\mathbf{r}, \mathbf{v}'_\gamma, t)$ and $f_\beta(\mathbf{r}, \mathbf{v}'_\beta, t)$ respectively, where \mathbf{v}'_γ and \mathbf{v}'_β are the velocities of the molecules after collision given as the functions of \mathbf{v}_γ and \mathbf{v}_β , the impact parameter b and the azimuthal angle ε . Further, $g_{\gamma\beta}$ is the magnitude of the relative velocity.

Let the Maxwell distribution function for molecules of species γ be f_γ^0 :

$$f_\gamma^0 = n_\gamma (m_\gamma/2\pi kT)^{3/2} \exp [-m_\gamma(\mathbf{v}_\gamma - \mathbf{v}_0)^2/2kT] \quad (68)$$

where T , n_γ and \mathbf{v}_0 are all functions of spatial coordinates in an inhomogeneous system.

In nonuniform gases the Maxwell distribution Eq. 68 does not satisfy the Boltzmann equation Eq. 66. However, Chapman³ and Enskog¹⁴ assumed the Maxwell distribution Eq. 68 may act as the zeroth approximation to the solution of the Boltzmann equation as far as the system is not so far from equilibrium, and write f_γ in the form

$$f_\gamma = f_\gamma^0(1 + \phi_\gamma) \quad (69)$$

where ϕ_γ is considered to be small perturbation.

In terms of ϕ_γ the auxiliary conditions Eqs. 64, 61, and 65 are, respectively, written as

$$\int \phi_\gamma f_\gamma^0 d\mathbf{v}_\gamma = 0 \quad (70)$$

$$\sum_{\gamma=1}^s m_\gamma \int \mathbf{v}_\gamma \phi_\gamma f_\gamma^0 d\mathbf{v}_\gamma = 0 \quad (71)$$

$$\frac{1}{2} \sum_{\gamma=1}^s m_{\gamma} \int V_{\gamma}^2 \phi_{\gamma} f_{\gamma}^0 d\mathbf{v}_{\gamma} = 0 \quad (72)$$

Substituting Eq. 69 into the both sides of the Boltzmann equation 66, we obtain

$$df_{\gamma}^0/dt + d(f_{\gamma}^0 \phi_{\gamma})/dt = \sum_{\beta=1}^s [J(f_{\gamma}^0, f_{\beta}^0 \phi_{\beta}) + J(f_{\gamma}^0 \phi_{\gamma}, f_{\beta}^0)] \quad (73)$$

where

$$J(F_{\gamma}, G_{\beta}) = \iiint (F'_{\gamma} G'_{\beta} - F_{\gamma} G_{\beta}) g_{\gamma\beta} b db d\epsilon d\mathbf{v}_{\beta} \quad (74)$$

In Eq. 74 F_{γ} is a function of \mathbf{v}_{γ} and G_{β} that of \mathbf{v}_{β} , and F'_{γ} and G'_{β} represent $F_{\gamma}(\mathbf{v}'_{\gamma})$ and $G_{\beta}(\mathbf{v}'_{\beta})$, respectively.

If we retain only up to the zeroth order in ϕ_{γ} in the left-hand side, and up to the first order in the right-hand side, we obtain the first approximation equation of Chapman and Enskog^{3, 14, 23, 59}

$$C_{\gamma} f_{\gamma}^0 = \sum_{\beta=1}^s \iiint f_{\gamma}^0 f_{\beta}^0 (\phi'_{\gamma} + \phi'_{\beta} - \phi_{\gamma} - \phi_{\beta}) g_{\gamma\beta} b db d\epsilon d\mathbf{v}_{\beta} \quad (75)$$

where

$$C_{\gamma} = (n_{\gamma}/n) \{ \mathbf{V}_{\gamma} \cdot \mathbf{d}_{\gamma} + (1/kT) (\mathbf{W}_{\gamma} : \nabla \mathbf{v}_0) - [\frac{5}{2} - (m_{\gamma}/2kT) V_{\gamma}^2] \mathbf{V}_{\gamma} \cdot \nabla \log T \} \quad (76)$$

$$\mathbf{d}_{\gamma} = \nabla (n_{\gamma}/n) + (n_{\gamma}/n - n_{\gamma} m_{\gamma}/\rho) \nabla \log p - (n_{\gamma} m_{\gamma}/p\rho) (\rho \mathbf{F}_{\gamma} - \sum_{\beta=1}^s n_{\beta} m_{\beta} \mathbf{F}_{\beta}) \quad (77)$$

$$\mathbf{W}_{\gamma} = m_{\gamma} (\mathbf{V}_{\gamma} \mathbf{V}_{\gamma} - \frac{1}{3} V_{\gamma}^2 \mathbf{U}) \quad (78)$$

p being the hydrostatic pressure and \mathbf{U} the unit tensor. In our case of a mixture of dilute gases p is equal to nkT .

To obtain approximate solutions to the integral equation 75, Hirschfelder and Curtiss^{6, 23} employed the variational principle which will be described below.* Let ψ_{γ} be a trial function which satisfies

* The variational principle presented here appears slightly different from the one originally used by Hirschfelder and Curtiss.

$$\begin{aligned}
 -\sum_{\gamma} \int C_{\gamma} f_{\gamma}^0 \psi_{\gamma} d\mathbf{V}_{\gamma} &= \frac{1}{4} \sum_{\gamma=1}^s \sum_{\beta=1}^s \iiint \iiint f_{\gamma}^0 f_{\beta}^0 (\psi'_{\gamma} + \psi'_{\beta} - \psi_{\gamma} - \psi_{\beta})^2 g_{\gamma\beta} \\
 &\quad \times bdbd\epsilon d\mathbf{v}_{\gamma} d\mathbf{v}_{\beta} \quad (79)
 \end{aligned}$$

where ψ'_{γ} is $\psi_{\gamma}(\mathbf{v}'_{\gamma})$.

On multiplying both sides of the first approximation equation of Chapman and Enskog, 75, by ψ_{γ} , integrating with respect to $d\mathbf{v}_{\gamma}$, summing over γ , and rewriting with use of the well known relation $d\mathbf{v}_{\gamma} d\mathbf{v}_{\beta} = d\mathbf{v}'_{\gamma} d\mathbf{v}'_{\beta}$, we obtain

$$-\sum_{\gamma} \int C_{\gamma} f_{\gamma}^0 \psi_{\gamma} d\mathbf{V}_{\gamma} = \frac{1}{2} \{\phi, \psi\} \quad (80)$$

where

$$\begin{aligned}
 \{\phi, \psi\} &= \frac{1}{2} \sum_{\gamma=1}^s \sum_{\beta=1}^s \iiint \iiint f_{\gamma}^0 f_{\beta}^0 (\phi'_{\gamma} + \phi'_{\beta} - \phi_{\gamma} - \phi_{\beta}) (\psi'_{\gamma} + \psi'_{\beta} - \psi_{\gamma} - \psi_{\beta}) \\
 &\quad \times g_{\gamma\beta} bdbd\epsilon d\mathbf{v}_{\gamma} d\mathbf{v}_{\beta} \quad (81)
 \end{aligned}$$

Comparing Eq. 79 with Eq. 80, we find the relations

$$\{\phi, \psi\} = \{\psi, \phi\} = \{\psi, \psi\} \quad (82)$$

From Eqs. 81 and 82, and the positive-definiteness of $\{\psi, \psi\}$, we immediately obtain

$$\begin{aligned}
 \{\phi, \phi\} - \{\psi, \psi\} &= \{\phi, \phi\} - 2\{\phi, \psi\} + \{\psi, \psi\} \\
 &= \{\phi - \psi, \phi - \psi\} \geq 0 \quad (83)
 \end{aligned}$$

Thus it is seen that the solution of the first approximation equation of Chapman and Enskog, Eq. 75, is given by a solution of the variational principle

$$\{\psi, \psi\} = \text{maximum} \quad (84)$$

with the condition Eq. 79. It can also be shown that the equality sign applies only when ψ is ϕ , if those trial functions are compatible with the auxiliary conditions, Eqs. 70, 71, and 72. This is the statement of the variational principle which has been utilized in calculating the approximate values of the transport coefficients of gases.³⁶

B. Thermodynamic Interpretation

We shall now consider the physical implications of the variational principle presented above.³⁸ At first, concerning the brace symbol, let us consider the statistical expression of the entropy per unit volume

$$s = k \sum_{\gamma=1}^s \int f_{\gamma} (1 - \log f_{\gamma}) d\mathbf{v}_{\gamma} \quad (85)$$

From this relation, we obtain, as shown by Prigogine,⁴⁸

$$\begin{aligned} ds/dt = & -k \operatorname{div} \mathbf{v}_0 \sum_{\gamma=1}^s \int f_{\gamma} (1 - \log f_{\gamma}) d\mathbf{v}_{\gamma} \\ & - k \operatorname{div} \sum_{\gamma=1}^s \int f_{\gamma} (1 - \log f_{\gamma}) \mathbf{V}_{\gamma} d\mathbf{v}_{\gamma} - k \sum_{\gamma=1}^s \int \log f_{\gamma} (df_{\gamma}/dt) d\mathbf{v}_{\gamma} \end{aligned} \quad (86)$$

The first two summations represent the flow of entropy and the last summation corresponds to the local entropy production. If we substitute df_{γ}/dt from the Boltzmann equation 66 and rewrite with use of the relation $d\mathbf{v}_{\gamma} d\mathbf{v}_{\beta} = d\mathbf{v}'_{\gamma} d\mathbf{v}'_{\beta}$, we find

$$\sigma = \frac{1}{4} k \sum_{\gamma=1}^s \sum_{\beta=1}^s \iiint \iiint [\log (f'_{\gamma} f'_{\beta} / f_{\gamma} f_{\beta})] (f'_{\gamma} f'_{\beta} - f_{\gamma} f_{\beta}) g_{\gamma\beta} b db d\epsilon d\mathbf{v}_{\gamma} d\mathbf{v}_{\beta} \quad (87)$$

The above expression is nonnegative and this is nothing else than Boltzmann's H -theorem in local form.

Let an arbitrary perturbation of the distribution of molecules of species γ be ψ_{γ} , and the distribution function is given by $f_{\gamma}^0 (1 + \psi_{\gamma})$. If the deviation from the Maxwell distribution f_{γ}^0 is so small that we may drop the terms involving the products of perturbation ψ_{γ} , the local entropy production given by Eq. 87 is, in terms of the brace notation Eq. 81, reduced to

$$\sigma = \frac{1}{2} k \{\psi, \psi\} \quad (88)$$

The physical implications of the brace $\{\psi, \psi\}$ were first discussed by Enskog.^{16, 59} Thus we have found that the integral expression is the entropy production, apart from a numerical factor, and that the entropy production also plays an important role in the variational method in the kinetic theory of gases.

We shall next consider the physical implication of the condition Eq. 79. The right-hand side is evidently the statistical expression for the local entropy production apart from the constant factor. To rewrite the left-hand side in a more apparent form, we shall recall the thermodynamical relation for the chemical potential (per mole) of a mixture of perfect gases:

$$\mu_\gamma = -\frac{5}{2}kT \log T + kT \log p + kT \log (n_\gamma/n) + \text{const} \quad (89)$$

With the help of Eqs. 81 and 89, we can rewrite Eq. 79 in the form

$$\mathbf{J}_u \cdot \nabla (1/T) - (\mathbf{p}\mathbf{U} - \mathbf{P}) : \nabla \mathbf{v}_0/T + \sum_\gamma [\mathbf{F}_\gamma/T - \nabla (\mu_\gamma^+/T)] \cdot \mathbf{J}_\gamma = \frac{1}{2}k\{\psi, \psi\} \quad (90)$$

where $\mathbf{J}_\gamma = m_\gamma n_\gamma \bar{\mathbf{V}}_\gamma$ is the flow of matter of component γ with respect to the center of mass motion, μ_γ^+ the chemical potential per unit mass of component γ , and \mathbf{J}_u and \mathbf{P} are the energy flow with respect to the center of mass motion and the pressure tensor as defined, respectively, by

$$\mathbf{J}_u = \frac{1}{2} \sum_{\gamma=1}^s \int m_\gamma V_\gamma^2 \mathbf{V}_\gamma \psi_\gamma f_\gamma^0 d\mathbf{V}_\gamma \quad (91)$$

$$\mathbf{P} = p\mathbf{U} + \sum_{\gamma=1}^s m_\gamma \int \mathbf{V}_\gamma \mathbf{V}_\gamma \psi_\gamma f_\gamma^0 d\mathbf{V}_\gamma \quad (92)$$

Then we can easily see that the left-hand side of Eq. 90 is the thermodynamical definition of the local entropy production as given by Eq. 17, although, in the present case, it includes the second summation corresponding to the production due to the viscous flow, but does not include the term for the chemical reactions. Thus the condition Eq. 79 implies, that the phenomenological entropy production does agree with the statistical expression of the entropy production, which is given as the brace symbol. This was first pointed out by the author.³⁸

In the above-mentioned variational principle the intensive variables are kept constant as in the case of Onsager's least dissipation of energy and contrary to the case of the principle of minimum entropy production, which will be dealt with in the latter part of this chapter. Further, it is easily seen that the variational principle Eq. 84 is closely connected with the principle

of least dissipation of energy expressed in the form of Eq. 60. The constraint for the present case, Eq. 90, corresponds evidently to Eq. 59. The theorems derived in the present section are given in local form, whereas the principle of least dissipation concerns the total production of entropy. However, if the forces such as $\nabla(1/T)$ are all uniform throughout the system, there will be no difference between the local and the integral forms, and the conditions for stationarity are automatically fulfilled.

The flows are expressed in terms of the perturbation as seen in Eq. 91, the brace notation does not contain the intensive variables as in the case of a dissipation function, the brace $\frac{1}{2}k\{\psi, \psi\}$ playing a similar role to the dissipation function $\varphi(J, J)$ given by Eq. 55.

It has been pointed out by Murakami³⁵ that this variational principle can be expressed in a form without restriction, corresponding to Eq. 54. Since $\frac{1}{4}k\{\psi, \psi\}$ corresponds to the dissipation function, in analogy with Eq. 54 our variational principle may be written as

$$\xi(\psi, \psi) \equiv -k \sum_{\gamma} \int C_{\gamma} \psi_{\gamma} f_{\gamma}^0 d\mathbf{V}_{\gamma} - \frac{1}{4}k\{\psi, \psi\} = \text{maximum} \quad (93)$$

Since we have the relation Eq. 80 for the solution of the first approximation equation, ϕ_{γ} , and the arbitrary perturbation ψ_{γ} , then we have

$$\xi(\psi, \psi) = \frac{1}{2}k[\{\phi, \psi\} - \frac{1}{2}\{\psi, \psi\}] \quad (94)$$

Thus we immediately obtain the inequality

$$\begin{aligned} \xi(\phi, \phi) - \xi(\psi, \psi) &= \frac{1}{4}k[\{\phi, \phi\} - 2\{\phi, \psi\} + \{\psi, \psi\}] \\ &= \frac{1}{4}k\{\phi - \psi, \phi - \psi\} \geq 0 \end{aligned} \quad (95)$$

This is the proof of the variational principle that Eq. 93 gives the solution of the Chapman-Enskog equation. The variational principle given in the form of Eq. 93 is much more convenient for practical purposes, because we need not consider restrictions other than simple ones such as the auxiliary conditions, Eqs. 70, 71, and 72. In the case of thermal conduction in a simple gas, Eq. 93 reduces to

$$\nabla(1/T) \cdot \int mV^2 \mathbf{V} \psi f d\mathbf{V} - \frac{1}{4}k \int \int \{\psi(\mathbf{v}') + \psi(\mathbf{v}_1) - \psi(\mathbf{v}) - \psi(\mathbf{v}_1)\}^2 \quad (96)$$

$$\times f^0(\mathbf{v})f^0(\mathbf{v}_1)g b d b d \varepsilon d\mathbf{v} d\mathbf{v}_1 = \text{maximum}$$

where the suffices indicating molecular species are omitted.

As seen in the above $\frac{1}{2}k\{\psi, \psi\}$ has certain features analogous to the dissipation function, but there are essential differences between these two functions. The brace $\{\psi, \psi\}$, contains no empirical transport coefficients but depends only on the intermolecular forces, whereas the dissipation function is a quadratic form with the empirical transport coefficients as its coefficients. Then in the case of Eq. 84, the variational principle leads to the maximum values of the transport coefficients compatible with the restrictions. This is the principle of maximum transport coefficients stated in Nakai's paper³⁶ on the kinetic theory of gases. On the other hand, Onsager's principle of least dissipation of energy is merely a mathematical reformulation of the linear relations and hence is independent of the magnitude of these coefficients.

Finally we shall mention another characteristic feature of the principle of this section. The variation for ψ_γ is taken in the velocity space, while the variation for the flows in Eq. 54 is taken in the ordinary space, when the intensive variables are inhomogeneous inside the system.

Our principle seems to be quite different from E. Einstein's early attempt^{13,63} to deduce the distribution function in the stationary state from the variational principle by maximizing the entropy locally, subject to a prescribed energy flow, etc.

C. Application to Dense Gases

We have shown that the approximate values of the transport coefficients of a dilute gas can be calculated by the variational method. It seems to be desirable to generalize such a principle to the case of a dense gas. A generalization has been done by Murakami³⁵ for dense gases consisting of rigid sphere molecules without attraction, based upon Enskog's modification of the Boltzmann equation.¹⁵

The modified Boltzmann equation is

$$\mathcal{D}f = \iint [\chi(\mathbf{r} + \frac{1}{2}\sigma\mathbf{k})f'(\mathbf{r})f'_1(\mathbf{r} + \sigma\mathbf{k}) - \chi(\mathbf{r} - \frac{1}{2}\sigma\mathbf{k})f(\mathbf{r})f_1(\mathbf{r} - \sigma\mathbf{k})] \times \sigma^2 \mathbf{g} \cdot \mathbf{k} d\mathbf{k} dv_1 \quad (97)$$

where we consider a one-component gas consisting of the rigid spheres of diameter σ , \mathbf{k} being the unit vector in the direction of the line connecting two centers. Notations similar to those used in Eq. 66 are used without subscripts indicating molecular species. If the density is so high that the molecular diameter σ becomes comparable with the intermolecular distance, the χ -factor is necessary to take account of the change in the number of collision. Thus the frequency of collision differs by χ from that in a gas made up of point particles.

For the system in equilibrium the equation of state for one mole of gas is, in terms of the χ -factor, expressed as

$$pV/RT = 1 + (N_0 b/V)\chi \quad (98)$$

where $N_0 b = \frac{2}{3}\pi N_0 \sigma^3$ is the second virial coefficient, N_0 being the Avogadro number. Then for the system in equilibrium the χ -factor is given by²³

$$\chi = 1 + 0.6250(N_0 b/V) + 0.2869(N_0 b/V)^2 + 0.115(N_0 b/V)^3 + \dots \quad (99)$$

in connection with the virial expansion of equation of state. We shall assume that the difference in the χ -factor for equilibrium and the state slightly deviating from equilibrium is negligible. The entropy per mole is given by

$$S = -R \log V + RN_0 b \int^v (\chi/V^2) dV + \text{const} \quad (100)$$

Let us denote the entropy per unit volume by s and the part of s due to gas imperfection by Δs . Then Δs is, according to Eq. 100

$$\Delta s = -nkb \int \chi dn + \text{const} \quad (101)$$

If the conditions in the gas are slowly varying, $f(\mathbf{r} + \sigma\mathbf{k})$ and $\chi(\mathbf{r} + \frac{1}{2}\sigma\mathbf{k})$ may be expanded in a Taylor series. Then we can

define the energy flow and the pressure tensor in accordance with this approximation. For the case where the distribution function f is given in terms of the local Maxwell distribution, Eq. 68, and the perturbation, ϕ just as in Eq. 69, it has been demonstrated by Murakami³⁵ that the energy flow and the pressure tensor are

$$\mathbf{J}_u = (1 + \frac{2}{5}nb\chi) \int \frac{1}{2}mV^2 \mathbf{V}\phi f^0 d\mathbf{V} + (3kT\omega/2m) \nabla(1/T) \quad (102)$$

$$\mathbf{P} = [p^0 - \omega(\nabla \cdot \mathbf{v}_0/T)] \mathbf{U} + (1 + \frac{2}{5}nb\chi)m \int \mathbf{V}\mathbf{V}\phi f^0 d\mathbf{V} - \frac{6}{5}\omega \mathbf{G}/T \quad (103)$$

where p^0 is the hydrostatic pressure given by Eq. 98, which is written as

$$p^0 = nkT(1 + nb\chi) \quad (104)$$

and

$$\omega = \frac{4}{9}n^2\sigma^4\chi(\pi mkT^3)^{\frac{1}{2}} \quad (105)$$

$$\mathbf{G} = \frac{1}{2}[\nabla \mathbf{v}_0 + (\nabla \mathbf{v}_0)^\dagger] - \frac{1}{3}(\nabla \cdot \mathbf{v}_0)\mathbf{U} \quad (106)$$

in which \dagger indicates the transposed tensor.

In the expressions Eqs. 102 and 103 there appear the contributions of collisional transfer, in addition to the usual kinetic contributions which are solely responsible for the energy flow and the pressure tensor in the case of a dilute gas.

The entropy production per unit volume according to the thermodynamic definition Eq. 17, to which the terms due to the viscous force are added, is

$$\begin{aligned} \sigma &= \mathbf{J}_u \cdot \nabla (1/T) - (\mathbf{P} - p^0 \mathbf{U}) : \nabla \mathbf{v}_0 / T \\ &= (1 + \frac{2}{5}bn\chi) \mathbf{J}_{uK} \cdot \nabla (1/T) - (1 + \frac{2}{5}bn\chi) (\mathbf{P}_K - nkT\mathbf{U}) : (\nabla \mathbf{v}_0 / T) \\ &\quad + (3kT/2m) \omega [\nabla(1/T)]^2 + \frac{6}{5} \omega \mathbf{G}/T : \mathbf{G}/T + \omega [(\nabla \cdot \mathbf{v}_0)/T]^2 \end{aligned} \quad (107)$$

where \mathbf{J}_{uK} and \mathbf{P}_K are the kinetic parts of \mathbf{J} and \mathbf{P} , and are given by the same expressions for the energy flow and the pressure tensor of dilute gas in Eqs. 91 and 92, respectively.

The statistical expression of entropy for an imperfect gas is not yet known in terms of the distribution functions. In this section we shall assume that the deviation from equilibrium is slight and the gas imperfection is also small, and hence that Eq. 101 for a gas in equilibrium may be adopted as this part of

entropy without appreciable errors. Then the entropy per unit volume is given as a sum of two contributions given by Eqs. 85 and 101:

$$s = k \int f(1 - \log f) d\mathbf{v} + nkb \int_0^n \chi dn \quad (108)$$

Starting from the time derivative of Eq. 108, we obtain, after lengthy calculations, the statistical expression of the local entropy production:

$$2\varphi(\phi, \phi) = \frac{1}{2}k\chi\{\phi, \phi\} + (3kT/2m)\omega[\nabla(1/T)]^2 + \frac{6}{5}\omega \mathbf{G}/T : \mathbf{G}/T + \omega[(\nabla \cdot \mathbf{v}_0)/T]^2 \quad (109)$$

where we use the symbol 2φ for the local production to distinguish it from the thermodynamic expression, Eq. 107, corresponding to the dissipation function. The brace notation is given by

$$\begin{aligned} \{\phi, \psi\} = & \frac{1}{2} \iiint [\phi(\mathbf{v}') + \phi(\mathbf{v}'_1) - \phi(\mathbf{v}) - \phi(\mathbf{v}_1)] \\ & \times [\psi(\mathbf{v}') + \psi(\mathbf{v}'_1) - \psi(\mathbf{v}) - \psi(\mathbf{v}_1)] \\ & \times f^0(\mathbf{v}) f^0(\mathbf{v}_1) \sigma^2 \mathbf{g} \cdot \mathbf{k} d\mathbf{k} d\mathbf{v} d\mathbf{v}_1 \end{aligned} \quad (110)$$

In analogy with Eq. 93 of a dilute gas, we shall consider the function which is determined by the variational principle:

$$\sigma - \varphi(\phi, \phi) = \text{maximum} \quad (111)$$

Using σ given by Eq. 107, we may rewrite Eq. 111 in the form

$$\begin{aligned} \xi(\psi, \psi) = & (1 + \frac{2}{5}nb\chi) \int (\frac{1}{2}mV^2 - \frac{5}{2}kT) [\mathbf{V} \cdot \nabla(1/T)] \psi f^0 d\mathbf{V} \\ & - (1 + \frac{2}{5}nb\chi) \int m(\mathbf{V}\mathbf{V} - \frac{1}{3}V^2\mathbf{U}) : [(\nabla\mathbf{v}_0)/T] \psi f^0 d\mathbf{V} \\ & - \frac{1}{4}k\chi\{\psi, \psi\} = \text{maximum} \end{aligned} \quad (112)$$

where the perturbation function is denoted by ψ .

Alternatively, if we insert $f = f^0(1 + \phi)$ in the modified Boltzmann equation 97 and retain only up to the zeroth order in ϕ in the left-hand side and the first order in the right-hand side, the first approximation equation of Chapman and Enskog for a dense gas is obtained:

$$\begin{aligned}
 f^0 \left\{ \left(1 + \frac{2}{5} nb\chi \right) (mV^2/2kT - \frac{5}{2}) \mathbf{V} \cdot \nabla \log T \right. \\
 \left. + \left(1 + \frac{2}{5} nb\chi \right) m(\mathbf{V}\mathbf{V} - \frac{1}{3}V^2\mathbf{U}) : \nabla v_0/kT \right\} \\
 = \chi \int \int f^0(\mathbf{v})f^0(\mathbf{v}_1) \{ \phi(\mathbf{v}') + \phi(\mathbf{v}'_1) - \phi(\mathbf{v}) - \phi(\mathbf{v}_1) \} \sigma^2 \mathbf{g} \cdot \mathbf{k} d\mathbf{k} d\mathbf{v}_1,
 \end{aligned} \quad (113)$$

which corresponds to Eq. 75 for a dilute gas.

We shall now prove that the solution of Eq. 113 maximizes the function $\xi(\psi, \psi)$ and is the solution of the variational problem Eq. 111. Multiplying Eq. 113 by ψ and integrating with respect to the velocity \mathbf{v} , we obtain

$$\xi(\psi, \psi) = \frac{1}{2}k\chi[\{\phi, \psi\} - \frac{1}{2}\{\psi, \psi\}] \quad (114)$$

Then we can immediately show

$$\xi(\phi, \phi) - \xi(\psi, \psi) = \frac{1}{4}k\chi\{\phi - \psi, \phi - \psi\} \geq 0 \quad (115)$$

Thus we can get the approximate solution of Eq. 113 by choosing suitable trial functions for the variational principles, Eq. 112. Especially in the case of a dense gas, this variational method seems to be useful, because it is not so easy to get the solution directly solving Eq. 113, though the present method is unfortunately restricted to the case of rigid-sphere molecules.

V. PRINCIPLE OF MINIMUM PRODUCTION OF ENTROPY

A. Discontinuous Systems

Let us consider a discontinuous system, of which the entropy production is given by Eq. 1. If the irreversible processes in this system is linear and the flows obey the phenomenological relations Eq. 4, we have

$$\mathcal{P} = \sum_{ij} L_{ij} X_i X_j \geq 0 \quad (116)$$

We meet much of typical stationary nonequilibrium state in the theory of linear irreversible processes. In the thermomolecular pressure difference, which is a typical example of the stationary state, the transfer of matter is zero, but the transfer of energy between the two chambers is still remaining.

It has been shown by Prigogine⁴⁵⁻⁴⁷ that the stationary states are characterized by the variational principle that in stationary

states the production of entropy per unit time is a minimum compatible with some constraints to be specified in each case. This is Prigogine's *principle of minimum production of entropy*, and is the best known variational principle in the theory of irreversible processes. This principle was also applied to biological problems.⁴⁶ It has been studied by Denbigh,⁷ de Groot,¹⁸ Haase^{19,20} and Mazur³⁰ in some detail.

Let us consider the stationary state, in which only n forces out of the f forces, are kept constant. Thus we have

$$J_{n+1} = \dots = J_f = 0 \quad (117)$$

It is easily shown that, if Onsager's reciprocity relations $L_{ij} = L_{ji}$ are valid, Eq. 117 is deduced from the condition of the minimum production of entropy. Indeed, the forces X_{n+1}, \dots, X_f remain free, and then the condition to minimize the entropy production given by Eq. 116 is written as

$$\partial \mathcal{P} / \partial X_i = \sum_{j=1}^f (L_{ij} + L_{ji}) X_j = 0 \quad (i = n+1, \dots, f) \quad (118)$$

With use of the relations $L_{ij} = L_{ji}$ and the linear relations Eq. 4 we get immediately Eq. 117. Let us note that the extremum given by Eq. 118 refers to a minimum, because \mathcal{P} is nonnegative. The states of minimum production of entropy were named by de Groot stationary states of first, second, etc., order when one, two, etc., parameters are fixed at constant values.¹⁸

This is the same for the chemical reactions,* for which the entropy production is given by

$$\mathcal{P} = \sum_{\rho=1}^r \sum_{\rho'=1}^r L_{\rho\rho'} (A_{\rho}/T) (A_{\rho'}/T) \quad (119)$$

as easily obtained from Eqs. 12 and 13.

We shall now inquire under what kind of external condition the stationary state becomes the state of minimum production of entropy. In the case of the thermomolecular pressure difference,

* For simplicity we treat discontinuous systems without chemical reactions and homogeneous chemical reactions separately, but this separation is not essential.

the energy flow from one chamber to another is maintained in such a way that the temperature difference between two chambers may be kept constant. On the other hand, no flows of matter take place in the system. Such a stationary state is possible only when the temperatures of the chambers are kept constant and there exist no flows of matter from or to the environment. However, in the same external circumstance, many types of complicated irreversible processes, which are not stationary, are also possible.

Let us consider in more detail the external environment required to maintain the stationary state. In the case of a thermomolecular pressure difference, we have to put these chambers in contact with the heat baths to keep them at prescribed temperatures. In this case we should take account of the irreversible production of entropy of two external transports from and to the heat baths. For the stationary state in which the flows of matter are maintained, we have to deal with an open system, which is in contact with the material reservoirs.

Let us consider the two connected chambers, I and II, both of which are connected to their respective material and heat reservoirs. We shall denote the forces needed to cause the flow from one of the reservoirs to the chamber I by X_i^E and the ones from the chamber II to another reservoir by X_i^F . Further, let us denote the external flows to the chamber I and those from the chamber II by J_i^E and J_i^F , respectively. We now assume that, out of the f flows, only n flows are permitted, as the heat flow in thermomolecular pressure difference

$$\begin{aligned} J_{n+1}^E &= \dots = J_f^E = 0 \\ J_{n+1}^F &= \dots = J_f^F = 0 \end{aligned} \quad (120)$$

Furthermore, the external transport processes are also assumed to be linear:

$$\begin{aligned} J_i^E &= \sum_{j=1}^n L_{ij}^E X_j^E \\ J_i^F &= \sum_{j=1}^n L_{ij}^F X_j^F \end{aligned} \quad (i = 1, 2, \dots, n) \quad (121)$$

The entropy production including the one due to the external

transport processes is

$$\mathcal{P} = \sum_{i=1}^f X_i J_i + \sum_{i=1}^n X_i^E J_i^E + \sum_{i=1}^n X_i^F J_i^F \quad (122)$$

Using the linear relations Eqs. 4 and 121, we obtain

$$\frac{1}{2} d\mathcal{P}/dt = \sum_{i=1}^f J_i dX_i/dt + \sum_{i=1}^n J_i^E dX_i^E/dt + \sum_{i=1}^n J_i^F dX_i^F/dt \quad (123)$$

In the case where the intensive variables in both reservoirs are kept constant, we have the relation

$$X_i^E + X_i + X_i^F = \text{const} \quad (i = 1, 2, \dots, n) \quad (124)$$

The system can be in the stationary state only under this condition. For the case of a thermomolecular pressure difference, the constant of Eq. 124 is the difference in the reciprocal temperature of the two heat reservoirs.

Let the macroscopic variables for chambers I and II be α_i^I and α_i^{II} , respectively. By the definition of flows given by Eq. 25 for an isolated system, we have

$$\begin{aligned} d\alpha_i^I/dt &= J_i^E - J_i \\ d\alpha_i^{II}/dt &= J_i - J_i^F \end{aligned} \quad (i = 1, 2, \dots, n) \quad (125)$$

and

$$-d\alpha_i^I/dt = d\alpha_i^{II}/dt = J_i \quad (i = n+1, \dots, f) \quad (126)$$

Using Eqs. 124, 125, and 126, we rewrite Eq. 123 in the form

$$\begin{aligned} \frac{1}{2} d\mathcal{P}/dt &= \sum_{i=1}^n (dX_i^E/dt) (d\alpha_i^I/dt) - \sum_{i=1}^n (dX_i^F/dt) (d\alpha_i^{II}/dt) \\ &\quad + \sum_{i=n+1}^f (dX_i/dt) (d\alpha_i/dt) \end{aligned} \quad (127)$$

where $d\alpha_i/dt = d\alpha_i^{II}/dt$ ($i = n+1, \dots, f$)

To make further progress it is rather convenient to go back to the original expressions for the forces, Eqs. 2 and 3. Then we have*

* This condition may be expressed as $J_\gamma = \dot{\alpha}_\gamma = 0$ for $\gamma \geq n$, and seems to be a rather specialized one, but the results are the same for the more generalized conditions of constraint.

$$\begin{aligned} X_u^E &= 1/T^I - 1/T^E \\ X_u^F &= 1/T^F - 1/T^{II} \end{aligned} \quad (128)$$

$$\begin{aligned} X_\gamma^E &= \mu_\gamma^E/T^E - \mu_\gamma^I/T^I \\ X_\gamma^F &= \mu_\gamma^{II}/T^{II} - \mu_\gamma^F/T^F \quad (\gamma = 1, 2, \dots, n-1) \end{aligned} \quad (129)$$

where T^E and μ_γ^E are the temperature and the chemical potential of component γ in the first reservoir and T^F and μ_γ^F the corresponding ones in the second reservoir.

We have

$$(\partial/\partial t)(1/T^I) = \partial U^I/\partial t (\partial/\partial U^I)(1/T^I) + \sum_{\gamma=1}^s \partial N_\gamma^I/\partial t (\partial/\partial N_\gamma^I)(1/T^I) \quad (130)$$

$$(\partial/\partial t)(\mu_\gamma^I/T^I) = \partial U^I/\partial t (\partial/\partial U^I)(\mu_\gamma^I/T^I) + \sum_{\gamma=1}^s \partial N_\gamma^I/\partial t (\partial/\partial N_\gamma^I)(\mu_\gamma^I/T^I) \quad (131)$$

and similar relations for II. On the other hand, the following thermodynamic relations are known:

$$\begin{aligned} 1/T &= \partial S/\partial U \\ \mu_\gamma/T &= -\partial S/\partial N_\gamma \end{aligned} \quad (132)$$

where the volume is constant. Using Eqs. 2, 3, 128, 129, 130, 131, and 132, we can rewrite Eq. 127 in the form

$$\frac{1}{2}d\mathcal{P}/dt = \frac{1}{2}d\mathcal{P}^I/dt + \frac{1}{2}d\mathcal{P}^{II}/dt \quad (133)$$

where

$$\begin{aligned} \frac{1}{2}d\mathcal{P}^I/dt &= (\partial^2 S^I/\partial U^{I2})(dU^I/dt)(dU^I/dt) \\ &+ 2 \sum_{\gamma=1}^s (\partial^2 S^I/\partial N_\gamma^I \partial U^I)(dU^I/dt)(dN_\gamma^I/dt) \\ &+ \sum_{\gamma=1}^s \sum_{\gamma'=1}^{s'} (\partial^2 S^I/\partial N_\gamma^I \partial N_{\gamma'}^I)(dN_\gamma^I/dt)(dN_{\gamma'}^I/dt) \end{aligned} \quad (134)$$

$$\begin{aligned} \frac{1}{2}d\mathcal{P}^{II}/dt &= (\partial^2 S^{II}/\partial U^{II2})(dU^{II}/dt)(dU^{II}/dt) \\ &+ 2 \sum_{\gamma=1}^s (\partial^2 S^{II}/\partial N_\gamma^{II} \partial U^{II})(dU^{II}/dt)(dN_\gamma^{II}/dt) \\ &+ \sum_{\gamma=1}^s \sum_{\gamma'=1}^{s'} (\partial^2 S^{II}/\partial N_\gamma^{II} \partial N_{\gamma'}^{II})(dN_\gamma^{II}/dt)(dN_{\gamma'}^{II}/dt) \end{aligned} \quad (135)$$

the intensive variables in the reservoirs being kept constant.

By the condition of the thermodynamic stability, the symmetric matrix formed by $-\partial^2 S/\partial U^2$, $-\partial^2 S/\partial N_\gamma \partial N_{\gamma'}$, etc. are positive definite, and hence Eqs. 134 and 135 are both negative. Thus we have

$$d\mathcal{P}/dt \leq 0 \quad (136)$$

where the equality sign applies only to the stationary state in which all the intensive quantities are independent of time. We can conclude from the above-mentioned that, under the *stationary* circumstance, the entropy production per unit time never increases with time, and reaches the state of minimum production of entropy.

We can show that the above conclusion is true in the case of chemical reactions.⁵¹ These results give full importance to the physical implications of the principle of minimum entropy production. As is well known, the entropy is a maximum at the equilibrium state, and it increases monotonically with time as demonstrated by Boltzmann's and Gibbs' H -theorems. The present theorem states that the entropy production is not only a minimum at the stationary state, but also that it decreases monotonically until it attains the stationary value.

It is also concluded from the above-mentioned that, if the system under the stationary external condition deviates from the stationary state by a spontaneous fluctuation which takes place with a certain probability from the molecular point of view, it always returns to the stationary state. Such a stability of the stationary state has been studied by means of an extension of Le Chatelier and Braun's principle.^{18, 47}

B. Minimum Production in Continuous Systems

The principle of minimum entropy production has been generalized to a continuous system by Mazur³⁰. Although his generalization has also been made for the case of electric current, we shall confine ourselves to the systems in which the thermal conduction and the diffusion take place together with chemical reactions.

Since the mass produced by chemical reactions is given by Eqs. 9 and 10, the mass balance equation for component γ is^{32, 33, 47}

$$\partial \rho_\gamma / \partial t = -\operatorname{div} \rho_\gamma \mathbf{v}_0 - \operatorname{div} \mathbf{J}_\gamma + \sum_{\rho=1}^r v_{\gamma\rho} M_\gamma v_\gamma \quad (\gamma = 1, 2, \dots, s) \quad (137)$$

where ρ_γ is the density of component γ , $\rho_\gamma = n_\gamma m_\gamma$, \mathbf{J}_γ the flow of component γ with respect to the mass-center motion, and \mathbf{v}_0 the center of mass velocity. The equation of energy balance is

$$\partial e / \partial t = -\operatorname{div} e \mathbf{v}_0 - p \operatorname{div} \mathbf{v}_0 - \operatorname{div} \mathbf{J}_u + \sum_\gamma \mathbf{F}_\gamma \cdot \mathbf{J}_\gamma \quad (138)$$

where e is the internal energy per unit volume, p the hydrostatic pressure and \mathbf{J}_u the energy flow as defined in the beginning of this article. The viscous term is neglected here.

The equation of entropy balance in terms of the entropy per unit volume, s , is

$$\partial s / \partial t = -\operatorname{div} s \mathbf{v}_0 - \operatorname{div} \mathbf{S} + \sigma \quad (139)$$

where \mathbf{S} and σ are the entropy flow and the local entropy production defined by Eqs. 18 and 17, respectively.

The total entropy production per unit time is given by the integration of Eq. 17 over the volume,

$$\mathcal{P} = \int_V [\mathbf{X}_u \cdot \mathbf{J}_u + \sum_{\gamma=1}^s \mathbf{X}_\gamma \cdot \mathbf{J}_\gamma + \sum_{\rho=1}^r (A_\rho / T) v_\rho] dV \geq 0 \quad (140)$$

Following Prigogine and Glansdorff¹⁷ we shall divide the variation of the entropy production into two parts:

$$\delta \mathcal{P} = \delta_X \mathcal{P} + \delta_J \mathcal{P} \quad (141)$$

$$\delta_X \mathcal{P} = \int_V [\mathbf{J}_u \cdot \delta \mathbf{X}_u + \sum_{\gamma=1}^s \mathbf{J}_\gamma \cdot \delta \mathbf{X}_\gamma + \sum_{\rho=1}^r v_\rho \delta (A_\rho / T)] dV \quad (142)$$

$$\delta_J \mathcal{P} = \int_V [\mathbf{X}_u \cdot \delta \mathbf{J}_u + \sum_{\gamma=1}^s \mathbf{X}_\gamma \cdot \delta \mathbf{J}_\gamma + \sum_{\rho=1}^r (A_\rho / T) \delta v_\rho] dV \quad (143)$$

where $\delta_X \mathcal{P}$ is the variation due to the change in forces and $\delta_J \mathcal{P}$ the one due to the change in flows.

Hereafter we shall restrict ourselves to systems which are in mechanical equilibrium without a center of mass motion. Then, first let us consider the condition

$$\delta_X \mathcal{P} = 0 \quad (144)$$

According to the definitions of A_ρ , \mathbf{X}_u and \mathbf{X}_γ , Eqs. 11, 15 and 16, we transform Eq. 144 into

$$-\int_V [(\operatorname{div} \mathbf{J}_u - \sum_{\gamma=1}^s \mathbf{J}_\gamma \cdot \mathbf{F}_\gamma) \delta(1/T) - \sum_{\gamma=1}^s (\operatorname{div} \mathbf{J}_\gamma - \sum_{\rho=1}^r \nu_{\gamma\rho} M_\rho v_\rho) \delta(\mu_\gamma/T)] dV \\ + \int_\Omega [\mathbf{J}_u \delta(1/T) - \sum_{\gamma=1}^s \mathbf{J}_\gamma \delta(\mu_\gamma/T)] \cdot d\Omega = 0 \quad (145)$$

where $d\Omega$ is the vectorial surface element of the boundary surface Ω , pointing to the outward normal, and Gauss's divergence theorem has been used.

We shall consider two kinds of boundary conditions which are compatible with stationarity. One of these is to prescribe each of the intensive variables such as temperature, a chemical potential everywhere at the boundary surface. These boundary values should be independent of time. However, it is not necessary to give these intensive quantities everywhere, when some part of the boundary is made of an adiabatic and impenetrable wall. As intermediate of the above two conditions, it is also possible to use the semipermeable membrane and to give, at the same time, some of variables at this portion of boundary.

Thus we have either of the following two conditions at the boundary of system:

$$\delta(1/T) = \delta(\mu_\gamma/T) = 0 \quad (\gamma = 1, 2, \dots, s) \quad (146)$$

or

$$\mathbf{J}_u \cdot \mathbf{n} = \mathbf{J}_\gamma \cdot \mathbf{n} = 0 \quad (\gamma = 1, 2, \dots, s) \quad (147)$$

where \mathbf{n} is the unit vector in the direction of the outward normal to the boundary surface.

Then the variational principle given by Eq. 144 with the boundary condition furnishes the relations

$$\operatorname{div} \mathbf{J}_u = \sum_{\gamma=1}^s \mathbf{F}_\gamma \cdot \mathbf{J}_\gamma \quad (148)$$

$$\operatorname{div} \mathbf{J}_\gamma = \sum_{\rho=1}^r \nu_{\gamma\rho} M_\rho v_\rho \quad (149)$$

As immediately seen from Eqs. 137 and 138, the above two

equations are the balance equations for the stationary state. According to the definitions of the local entropy production and the entropy flow, Eqs. 17 and 18, we obtain, from Eqs. 148 and 149, the stationary equations for entropy:

$$\sigma = \operatorname{div} \mathbf{S} \quad (150)$$

Thus we have learned that the stationary state is deduced from the variational condition given by Eq. 144.

Let us now consider the linear irreversible process, of which the flows and the forces are connected by the phenomenological relations 13 and 19. If the transport coefficients are entirely independent of any of the intensive variables and if they are subject to the reciprocity relations, then we can show that

$$\begin{aligned} \delta_X \mathcal{P} &= \delta_J \mathcal{P} \\ \delta \mathcal{P} &= 2\delta_X \mathcal{P} \end{aligned} \quad (151)$$

Hence, in the linear dissipative systems, the conditions in Eq. 144 are expressed in the forms

$$\delta \mathcal{P} = 0 \quad \mathcal{P} = \text{minimum} \quad (152)$$

This implies that Eq. 145 and hence the stationary state are obtained from the variational principle Eq. 152 as shown by Mazur.³⁰ In other words, the stationary state is characterized as the state of minimum entropy production as in the case of a discontinuous system. Thus we have demonstrated the principle of minimum entropy production is still valid for continuous systems. The extremum is a minimum because of the positive-definiteness of the entropy production.

In linear case, the time rate of entropy production is, according to Eqs. 142 and 151,

$$\begin{aligned} \frac{1}{2} \partial \mathcal{P} / \partial t &= - \int_V [(\operatorname{div} \mathbf{J}_u - \sum_{\gamma=1}^s \mathbf{J}_\gamma \cdot \mathbf{F}_\gamma) (\partial / \partial t) (1/T) \\ &\quad - \sum_{\gamma=1}^s (\operatorname{div} \mathbf{J}_\gamma - \sum_{\rho=1}^r r_{\gamma\rho} M_\rho v_\rho) (\partial / \partial t) (\mu_\gamma / T)] dV \end{aligned} \quad (153)$$

of which the derivation is similar to that for Eq. 145 and where at every point of the boundary surface either of the conditions

146 or 147 is applied. This can be transformed, with the use of Eqs. 137, 138 and the Gibbs-Duhem relations, into

$$\begin{aligned} \frac{1}{2} \partial \mathcal{P} / \partial t = & - \int_V [(\rho c_p / T^2) (\partial T / \partial t)^2 \\ & + \sum_{\gamma=1}^s \sum_{\gamma'=1}^s (\partial \mu_{\gamma} / \partial \rho_{\gamma'}) (\partial \rho_{\gamma} / \partial t) (\partial \rho_{\gamma'} / \partial t)] dV \end{aligned} \quad (154)$$

where $c_p > 0$ is the specific heat. The second summation in the integrand is also positive according to the stability condition with respect to diffusion.⁴⁹ Then we have³⁰

$$\partial \mathcal{P} / \partial t \leq 0 \quad (155)$$

Thus we find that the entropy production decreases monotonically with time* in exactly the same manner as in the case of a discontinuous system as shown by Eq. 136.

At first sight, the principle of minimum entropy production, especially in the case of a continuous system, seems to have some intimate connection with the principle of least dissipation of energy. However, these two principles are of rather different characters. In the case of least dissipation of energy the flows are varied by keeping the intensive variables at every point constant, while the forces and flows are varied at the same time in accordance with the phenomenological relations under the prescribed boundary values in the case of the principle of minimum production of entropy.

There seems to be a slightly formal relation between these two principles when the principle of least dissipation of energy is expressed in the form of Eq. 60. If the linear relations are used, the dissipation function $\varphi(J, J)$ is numerically equal to the local entropy production and hence the minimum value of Eq. 152 agrees with the maximum of Eq. 59 compatible with the conditions 57 and 58. However, in the case of Eq. 60, the J 's are varied under the conditions 57 and 58, in contrast with Eq. 152 for which the forces are varied and which gives the stationarity conditions 57 and 58, being identical with Eqs. 148 and 149, respectively. Both of these principles determine the spatial

* The same is true in the case of electrical and electrochemical processes.³⁰

distribution of flows and forces inside of the system with chemical reactions.

In connection to the above results, we should pay attention to the other type of variational principle proposed by Haase.^{19, 20} He discussed the condition to minimize the local entropy production when the temperature is prescribed at every point of the interior of the system. In this case the state of minimum production of entropy does not correspond to the stationary state in the presence of chemical reactions. Haase's condition does not, however, seem to be physically realizable, since the gradient of the intensive quantities changes in the temporal evolution of the system under the given boundary condition.

Before concluding this section, we should mention the boundary conditions given by Eqs. 146 and 147. These conditions correspond clearly to Eqs. 124 and 126, respectively, in the case of a discontinuous system. Let us now consider the case where the values of the intensive variables are left free at a certain portion of the boundary surface Ω_1 . Then let us determine the boundary condition so as to get the minimum entropy production compatible with the boundary condition at the remaining portion of the boundary. The general theorem of the calculus of variation states that the entropy production becomes a minimum when the flows across Ω_1 vanish, i.e., $\mathbf{J}_u \cdot \mathbf{n} = \mathbf{J}_\gamma \cdot \mathbf{n} = 0$ at Ω_1 . This implies that if we replace any part of the boundary by an insulating wall, the entropy production is always diminished by such a replacement, provided the prescribed intensive variables at the remaining portion of the boundary are unchanged. The above result is applicable also to replacement by a conducting but impenetrable wall. These results are in accordance with the theorem by Onsager that the restrictions can only decrease the entropy production, since an insulating or impenetrable wall acts certainly as a restriction to flows.

When the boundary values are left free for the whole boundary surface, the minimum production of entropy leads to the equilibrium state for which the entropy production vanishes.

C. Nonlinear Irreversible Processes

In the previous section, the principle of minimum production of entropy is extended to a continuous system, but this extension is legitimated only when the phenomenological coefficients of Eq. 19 are entirely independent of any of intensive variables. This condition is rather restrictive for the practical purpose.

As with Eq. 141, we shall divide the temporal change of \mathcal{P} into two parts:

$$d\mathcal{P}/dt = d_X\mathcal{P}/dt + d_J\mathcal{P}/dt \quad (156)$$

in which $d\mathcal{P}_X/dt$ is change due to the temporal evolution of forces and $d\mathcal{P}_J/dt$ the one due to the temporal evolution of flows. If the boundary condition is subject to Eq. 146 or 147, the first term in the right-hand side of Eq. 156 is expressed as

$$\begin{aligned} d_X\mathcal{P}/dt = & - \int_V [(\operatorname{div} \mathbf{J}_u - \sum_{\gamma=1}^s \mathbf{J}_\gamma \cdot \mathbf{F}_\gamma) (\partial/\partial t) (1/T) \\ & - \sum_{\gamma=1}^s (\operatorname{div} \mathbf{J}_\gamma - \sum_{\rho=1}^r v_{\gamma\rho} M_\rho v_\rho (\partial/\partial t) (\mu_\gamma/T))] dV \end{aligned} \quad (157)$$

which is obtained in exactly the same manner as in derivation of Eq. 145 or Eq. 153. From the nonpositive character of the right-hand side of Eq. 154 we obtain

$$d_X\mathcal{P}/dt \leq 0 \quad (158)$$

Then, at the stationary state,

$$d_X\mathcal{P}/dt = 0 \quad (159)$$

If we denote the flows at the stationary state by \mathbf{J}_u^0 , \mathbf{J}_γ^0 and v_ρ^0 , the condition for the stationarity is

$$\int_V [\mathbf{J}_u^0 \cdot (\partial \mathbf{X}_u / \partial t) + \sum_{\gamma=1}^s \mathbf{J}_\gamma^0 \cdot (\partial \mathbf{X}_\gamma / \partial t) + \sum_{\rho=1}^r v_\rho^0 (\partial/\partial t) (A_\rho/T)] dV = 0 \quad (160)$$

In general another part of the time rate of entropy production $d_J\mathcal{P}/dt$ is considered probably positive, but we may expect this is also negative under a certain condition. This problem is considered for the case of simple chemical reactions by Nielsen^{37, 51} and Mel.³⁴ It has been shown for this example that $d_J\mathcal{P}/dt$ cannot be positive when the state is near to equilibrium and that it is

negative for the state far enough from stationary state. Then we may expect the entropy production rate to decrease with time even when we cannot apply the linear relations between the forces and flows.

However it seems to be also possible that there exists another state of minimum production of entropy at the intermediate stage between the above two extreme cases, as pointed out by Klein²⁷ for a simplified model of irreversible process, which will be seen later in this article.

Although the principle given in Eqs. 159 and 160 is more general than the principle of minimum entropy production, this cannot be used as a variational principle.⁵² To consider this situation in more detail let us write Eq. 159 in a discrete form:

$$\delta_X \mathcal{P} = \sum_{i=1}^f J_i \delta X_i = 0 \quad (161)$$

where the J_i 's are functions of X_i 's.

A Pfaff form (Eq. 161) is, in general, not integrable, except when

$$\partial J_i / \partial X_j = \partial J_j / \partial X_i \quad (162)$$

Even when $d_X \mathcal{P}$ is not integrable, it is possible to find the potential Φ of which the minimum corresponds to the stationary state if there exists an integrating factor, and then we can derive the stationary state from the variational principle. However, the necessary and sufficient condition for the existence of the integrating factor is

$$J_k (\partial J_j / \partial X_i - \partial J_i / \partial X_j) + J_j (\partial J_i / \partial X_k - \partial J_k / \partial X_i) + J_i (\partial J_k / \partial X_j - \partial J_j / \partial X_k) = 0 \quad (163)$$

which is not always required in thermodynamics.

If the flows and the forces do not satisfy the above condition, it is impossible to find the function which decreases monotonically and which agrees with the entropy production for the stationary state. In this case the condition for the stationarity is written, according to Eqs. 141 and 161, as

$$\delta \mathcal{P} = \delta_J \mathcal{P} \quad (164)$$

This equation presents a certain analogy with Lagrange's principle in mechanics of a nonholonomic system, as pointed out by Glansdorff and Prigogine.¹⁷

Even in the linear case, if the phenomenological coefficients do not satisfy the reciprocity relations, the condition 152 is not satisfied. Prigogine and Balescu⁵³ have dealt with the purely antisymmetric case of coefficients, $L_{ij} = -L_{ji}$, and they have shown that such a system make the rotation about the stationary state in the J - X plane. They called such a kind of processes cyclic processes and studied in detail. Volterra's model⁵⁸ of interacting biological populations is considered to be an example of these cyclic processes. It should be noted that the rotation in a cyclic process has a definite sign which is uniquely determined by the process, while the sign of rotation of a mechanical system depends on the initial state.

Let us now see that there exists a function \mathcal{W} with the following properties

$$\mathcal{W} \geq 0 \quad (165)$$

$$d\mathcal{W}/dt \leq 0 \quad (166)$$

$$\mathcal{W} = \text{minimum at a stationary state} \quad (167)$$

and \mathcal{W} is proportional to the entropy production in the linear cases with the reciprocity relations.

Although such functions do not always exist for the case $f > 2$, according to the general theorem mentioned above, Prigogine^{50,51} has found the \mathcal{W} functions for some of the simplest cases. For the isotropic thermal conduction, he has shown that the \mathcal{W} function is given by

$$\mathcal{W} = \frac{1}{2} \int_V \mathbf{J}_u^2 dV \quad (168)$$

where \mathbf{J}_u is the heat flow related to the temperature gradient by the relation

$$\mathbf{J}_u = -\kappa(T) \nabla T \quad (169)$$

the thermal conductivity $\kappa(T)$ being an arbitrary positive-definite function of the temperature. The entropy production retains the minimum character only when $\kappa(T) = \lambda/T^2$. The minimum character of \mathcal{W} is proved in the following manner.

We obtain from Eqs. 168 and 169

$$\partial \mathcal{W} / \partial t = \int_V \{ \kappa(T) (\nabla T)^2 [\partial \kappa(T) / \partial T] (\partial T / \partial t) + [\kappa(T)]^2 \nabla T \nabla (\partial T / \partial t) \} dV \quad (170)$$

If the temperature is time-independent at the boundary except the portion where no heat flow across it is present, the above equation is transformed, by partial integration, into

$$\partial \mathcal{W} / \partial t = - \int_V \{ \kappa(T) \nabla [\kappa(T) \nabla T] \partial T / \partial t \} dV \quad (171)$$

Using the energy balance equation which is a special case of Eq. 138, we obtain from Eq. 171

$$\partial \mathcal{W} / \partial t = - \int_V [\kappa(T) / c_P] (\partial T / \partial t)^2 dV \leq 0 \quad (172)$$

c_P being the specific heat. Thus we have proved that \mathcal{W} decreases monotonically with time until it reaches the minimum value at the stationary state.

The same type of variational principle has been proved for the cases of diffusion processes and consecutive chemical reactions.⁵¹ In the case of thermal conductivity or diffusion the meaning of the function \mathcal{W} is rather simple. It expresses the average of the square of the heat flow or diffusion flow and has its smallest value in the stationary state. In any case the function \mathcal{W} is closely related to the entropy production.

VI. STATISTICAL THEORY OF THE MINIMUM ENTROPY PRODUCTION PRINCIPLE

A. Microscopic Description of Entropy Production in an Ideal Gas

As the principle of minimum entropy production has wide range of applicability, it seems useful to derive this principle by the statistical-mechanical method. This approach will show that the minimum entropy production principle holds in a microscopic description of the system. However, since it is rather complicated to deal with general cases, we shall restrict ourselves to the case of a simple system. Following Klein and Meijer²⁴ we shall consider a system consisting of two identical chambers, I and II, which contain a total number of N molecules of an ideal

gas. The two chambers are connected through a narrow capillary tube, of which the dimensions are so chosen that collisions between molecules in the tube may be neglected. Further collisions of the molecules with the walls of the tube do not affect the energy of these molecules. Each chamber is in good thermal contact with a heat bath having temperature T^I and T^{II} , respectively.

Let us denote the energy levels of a molecule in one of the box of volume V by ε_i ($i = 1, 2, \dots$). Since the chambers are identical the energy levels are the same in both chambers. We can specify the state of the system at any time by the values of the two sets of occupation probabilities p_i and q_i at that time. Here p_i is the probability of finding a molecule in the i th energy state in I and q_i is that of finding a molecule in the i th state in II.

We shall now restrict ourselves to the case of a closed system consisting of particles which obey Maxwell-Boltzmann statistics, though the proof has been given by Klein²⁶ for more general cases where the particles obey Bose-Einstein or Fermi-Dirac statistics and where the total number of molecules are not constant as in a grand canonical ensemble. Following Klein and Meijer²⁴ we shall employ a generalization of the method used by Pauli⁴⁴ to derive the H -theorem from quantum mechanics. This method was rather extensively studied to derive the second law by Thomsen,⁵⁷ though he treated only isolated systems, for which the state of minimum entropy production leads to equilibrium. Then for the time rates of change of probabilities are given⁵⁶ by*

$$dp_i/dt = \sum_j (a_{ji}p_j - a_{ij}p_i) + b_{ii}(q_i - p_i) \quad (173)$$

$$dq_i/dt = \sum_j (c_{ji}q_j - c_{ij}q_i) + b_{ii}(p_i - q_i) \quad (174)$$

In the above equations a_{ij} is the probability per unit time that a molecule in I, originally in state i makes a transition to state j , remaining in I. We define c_{ij} as the corresponding transition probability per unit time for a molecule in II. The probability expressed by b_{ii} is the one per unit time that a molecule in state i moves from I to II or conversely, and this transition is symmetric. We need not consider the transition between the states

* The rates given by Eqs. 173 and 174 do not change $\sum_i (p_i + q_i) = 1$.

with different energy as we assumed that the energy is conserved for a molecule passing through the capillary.

Here we shall recall that the chambers I and II are well in contact with the heat baths having the temperature T^I and T^{II} . If the gases in these container are in good thermal contact with heat baths, the probabilities p_i and q_i are almost Maxwellian. This is the role of the heat baths. In the absence of the probability of migration between the chambers, we get the stationary state when p_i and q_i are Maxwellian. This condition requires for the transition probabilities

$$\begin{aligned} a_{ij} \exp(-\varepsilon_i/kT^I) &= a_{ji} \exp(-\varepsilon_j/kT^I) \\ c_{ij} \exp(-\varepsilon_i/kT^{II}) &= c_{ji} \exp(-\varepsilon_j/kT^{II}) \end{aligned} \quad (175)$$

The entropy of the gas given as the Boltzmann H -function multiplied by $-k$ and is expressed by

$$S = -Nk \sum_i (p_i \log p_i + q_i \log q_i) + Nk \log N \quad (176)$$

The change in entropy is split into two parts: the entropy flow from the heat baths and the internal production of entropy. The former part is evaluated from the energy received from the heat baths. Let us consider the first chamber I, of which energy is

$$U^I = N \sum_i \varepsilon_i p_i$$

We can evaluate the increase in the energy U^I due to the interaction with the heat bath by omitting the last term of Eq. 173, obtaining

$$d_e U^I/dt = N \sum_i \varepsilon_i \sum_j (a_{ji} p_j - a_{ij} p_i) \quad (177)$$

and a similar expression for $d_e U^{II}/dt$ for the gas in II.

Since the gas is in good contact with the heat baths the external part of the entropy increase is

$$\begin{aligned} d_e S/dt &= (1/T^I) d_e U^I/dt + (1/T^{II}) d_e U^{II}/dt \\ &= (N/T^I) \sum_i \varepsilon_i \sum_j (a_{ji} p_j - a_{ij} p_i) \\ &\quad + (N/T^{II}) \sum_i \varepsilon_i \sum_j (c_{ji} q_j - c_{ij} q_i) \end{aligned} \quad (178)$$

From Eqs. 173, 174, 176, and 178, we obtain the entropy production in the form

$$\begin{aligned}
\mathcal{P} &= dS/dt - d_e S/dt \\
&= -Nk \sum_i [(\log p_i + \varepsilon_i/kT^I) \sum_j (a_{ji} p_j - a_{ij} p_i) \\
&\quad + (\log q_i + \varepsilon_i/kT^{II}) \sum_j (c_{ji} q_j - c_{ij} q_i) + b_{ii} (\log p_i - \log q_i) (q_i - p_i)]
\end{aligned} \tag{179}$$

Furthermore, using Eq. 175, we can easily prove that \mathcal{P} is the nonnegative quantity.

We shall next evaluate the time rate of entropy production. We obtain, from Eqs. 173, 174, 175, and 179,

$$\begin{aligned}
d\mathcal{P}/dt &= -Nk \sum_i \{ [(1/p_i) (dp_i/dt)^2 + (1/q_i) (dq_i/dt)^2] \\
&\quad + (dp_i/dt) [\sum_j \log \{ (p_j \exp \varepsilon_j/kT^I) / (p_i \exp \varepsilon_i/kT^I) \} a_{ij} - b_{ii} \log p_i/q_i] \\
&\quad + (dq_i/dt) [\sum_j \log \{ (q_j \exp \varepsilon_j/kT^{II}) / (q_i \exp \varepsilon_i/kT^{II}) \} c_{ij} - b_{ii} \log q_i/p_i] \}
\end{aligned} \tag{180}$$

Up to now we have not used the fact that the temperature difference is so small and that the distributions in the both chambers are not so far from equilibrium one. If the gas is in thermal equilibrium, the distributions are Maxwellian with respect to their temperatures, and we have

$$p_j \exp \varepsilon_j/kT^I = p_i \exp \varepsilon_i/kT^I$$

and

$$q_j \exp \varepsilon_j/kT^{II} = q_i \exp \varepsilon_i/kT^{II}$$

Let us summarize these restrictions by introducing the notation:

$$\begin{aligned}
q_r/p_r &= 1 + \delta_r \\
(p_j \exp \varepsilon_j/kT^I) / (p_i \exp \varepsilon_i/kT^I) &= 1 + \rho_{ij} \\
(q_j \exp \varepsilon_j/kT^{II}) / (q_i \exp \varepsilon_i/kT^{II}) &= 1 + \sigma_{ij}
\end{aligned} \tag{181}$$

If the deviation from Maxwell distribution is slight and $(T^I - T^{II})/T^I$ are small, we may neglect the terms second order in δ_r , ρ_{ij} , and σ_{ij} . Then we have

$$\begin{aligned}
&\log [(p_j \exp \varepsilon_j/kT^I) / (p_i \exp \varepsilon_i/kT^I)] a_{ij} - b_{ii} \log p_i/q_i \\
&= (1/p_i) [\sum_j (a_{ji} p_j - a_{ij} p_i) + b_{ii} (q_i - p_i)]
\end{aligned} \tag{182}$$

and a similar expression for the second chamber II.

Then, from Eqs. 180, 173, 174, and 182, we obtain

$$d\mathcal{P}/dt = -2Nk \sum_i [(1/p_i) (dp_i/dt)^2 + (1/q_i) (dq_i/dt)^2] \quad (183)$$

This implies that the time rate of entropy production decreases monotonically with time until it attains to the stationary state. Then we can conclude that the stationary state is the state to minimize the entropy production and thus the principle of minimum entropy production has been demonstrated by the statistical method. This is a certainly a extension of Pauli's H -theorem to nonequilibrium stationary state. Furthermore, we can directly see from Eq. 183 that the entropy production does decrease unless all the occupation probabilities are time-independent. It should be noted that this derivation of the principle does not explicitly depend on the thermodynamic relations such as the reciprocity and the Gibbs relations.

Rather lately, an attempt to generalize this principle to a nonlinear irreversible process has been made by Klein,²⁷ based on a statistical method for a simplified model. He demonstrated that the minimum production properties are also a useful approximation criterion for the stationary state even when the latter is very far from equilibrium. According to a simple example of an irreversible process given in his calculation, it has been found that the entropy production does not decrease monotonically, but passes through its minimum en route to the stationary state. We have already mentioned these results in connection with the variational principle in nonlinear irreversible processes.

B. Application to Magnetic Resonance

In the present section we wish to show that the principle of minimum entropy production is applicable also to the stationary state in a magnetic resonance experiment, in which a collection of spin magnetic moments are subject to a circularly polarized magnetic field perpendicular to a constant magnetic field. Application to this type of phenomenon is done by a reinterpretation and modification of Klein and Meijer's method.²⁴ This has been done by Klein²⁵ and he has shown that Overhauser processes⁴³ of producing nuclear polarization satisfy the principle of minimum

entropy production in the stationary state. Later more general treatment to a magnetic resonance type process was done by Wangness.⁶¹

We shall consider the system of N identical molecular moments comprising a gas in which we assume that strong collisions between the molecules provide the only relaxation mechanism. Let the components of the external magnetic field be

$$\begin{aligned} H_z &= H_0 \\ H_+ &= H_x + iH_y = H_1 \exp(-i\omega t) \end{aligned} \quad (184)$$

The moments are in good thermal contact with a heat bath at temperature T , the other molecular degrees of freedom being considered as a part of a heat bath.

Let Ψ be the state function of a system in the Schrodinger representation. This function is, in general, expanded in the form

$$\Psi = \sum_m a_m \varphi_m \quad (185)$$

where the φ_m 's form a complete orthonormal set of functions. For a mixture of quantum states, the matrix element of the density matrix is defined by

$$\rho_{mn} = \langle a_n^* a_m \rangle \quad (186)$$

where $\langle \rangle$ indicates the ensemble average.

Let the spin angular momentum of a molecule in units of \hbar be \mathbf{I} and the eigenfunctions of I_z be u_m in such a way that $I_z u_m = m u_m$. Here we shall restrict ourselves to the case of spin $\frac{1}{2}$, so that $m = \pm \frac{1}{2}$. In our present case, it is convenient to choose the set of u_m 's as the orthonormal set to represent the state vector. It is also convenient to form the density matrix in the coordinate system rotating with the resultant field, so that in this system all the fields are constant. Then Eq. 184 in the rotating coordinate system becomes

$$\Psi = \sum_m b_m(t) \exp(im\omega t) u_m \quad (187)$$

where ω is the frequency of the rotating coordinate system.

Let μ be the magnetic moment of a molecule, and we have

$$\mu = \gamma \hbar \mathbf{I} \quad (188)$$

where γ is the gyromagnetic ratio. The density matrix ρ_{mn} in the rotating system is defined by

$$\begin{aligned}\rho_{++} &= \langle b_+^* b_+ \rangle = \frac{1}{2} + \varepsilon \\ \rho_{-+} &= \langle b_+^* b_- \rangle = \delta \\ \rho_{--} &= \langle b_-^* b_- \rangle = \frac{1}{2} - \varepsilon \\ \rho_{+-} &= \langle b_-^* b_+ \rangle = \delta^*\end{aligned}\quad (189)$$

where $+$ and $-$ stand for $m = \frac{1}{2}$ and $m = -\frac{1}{2}$, respectively, and we have the normalization condition $\rho_{++} + \rho_{--} = 1$. The b 's are considered to be the functions of $t = t' + \tau'$ and the average is taken both over t' and τ' . The first is the time average over the possible initial states and the second is smoothing out the sudden change of the variables due to molecular collisions, and we express b as a function of the average collision time τ . Thus Wangsness^{60,61} calculated the average expectation values of the spin components:

$$\begin{aligned}\langle I_z \rangle &= (1 + \alpha^2 \tau^2)^{-1} [(1 + \Delta^2 \tau^2) E \\ &\quad + \frac{1}{2} i \omega_1 \tau (1 - i \Delta \tau) P - (1 + i \Delta \tau) P^*] = \varepsilon\end{aligned}\quad (190)$$

$$\begin{aligned}\langle I_+ \rangle &= \exp(-i \omega t) (1 + \alpha^2 \tau^2)^{-1} [i \omega_1 \tau (1 - i \Delta \tau) E \\ &\quad + (1 + \frac{1}{2} \omega_1^2 \tau^2 - i \Delta \tau) P + \frac{1}{2} \omega_1^2 \tau^2 P^*] = \exp(-i \omega t) \delta\end{aligned}\quad (191)$$

where

$$\begin{aligned}E &= \langle b_+^{0*} b_+^0 \rangle - \frac{1}{2} \\ P &= \langle b_+^{0*} b_-^0 \rangle\end{aligned}\quad (192)$$

b_m^0 is the values of the $b_m(t)$ for the particular spin at the last collision and

$$\begin{aligned}\omega_1/\gamma &= H_1 \\ \omega_0/\gamma &= (\Delta + \omega)/\gamma = H_0 \\ \alpha^2 &= \Delta^2 + \omega_1^2\end{aligned}\quad (193)$$

H_1 being the amplitude of the oscillating magnetic field and H_0 the constant field.

In general, the average quantities E and P are functions of time. Their time derivations are given by the equation of motion

of the average expectation value of the spin to be given by

$$(d/dt)\langle \mathbf{I} \rangle = \gamma \langle \mathbf{I} \rangle \times \mathbf{H} + (1/\tau)[\chi_s \mathbf{H} - \langle \mathbf{I} \rangle] \quad (194)$$

where χ_s is the spin susceptibility for spin $\frac{1}{2}$, and is given by

$$\chi_s = \chi_0/\gamma\hbar = \mu^2/kT\gamma\hbar = \gamma\hbar/4kT \quad (195)$$

From Eqs. 190, 191, and 194, it is obtained, as shown by Wangsness^{60,61}, that

$$\begin{aligned} \tau \dot{E} &= \chi_s \omega_0/\gamma - E + \frac{1}{2}i\omega_1\tau(P - P^*) \\ \tau \dot{P} &= (\chi_s \omega_0/\gamma)(1 - i\omega\tau) + i\omega_1\tau E - (1 + i\Delta\tau)P \\ \tau \dot{P}^* &= (\chi_s \omega_0/\gamma)(1 + i\omega\tau) - i\omega_1\tau E - (1 - i\Delta\tau)P^* \end{aligned} \quad (196)$$

and

$$\begin{aligned} \tau \dot{\varepsilon} &= \chi_s \omega_0/\gamma - E \\ \tau \dot{\delta} &= \chi_s \omega_1/\gamma - P \end{aligned} \quad (197)$$

It is easily seen that the stationary-state solutions of the above equations are

$$E_s = \chi_s \omega_0/\gamma \quad (198)$$

and

$$P_s = \chi_s \omega_1/\gamma$$

We shall next consider the statistical definition of entropy in magnetic resonance. According to usual definition introduced by von Neumann, the quantum statistical definition of entropy is

$$S = -k \text{trace} (\rho \log \rho) \quad (199)$$

which reduces to the same form as Eq. 176 for an ideal gas, if all the off-diagonal elements vanish. However, in the case of a magnetic resonance experiment, we should take account of the off-diagonal elements. Wangsness⁶¹ assumed the entropy of the spin system to be given by

$$S = -k[\rho_{++} \log \rho_{++} + \rho_{--} \log \rho_{--}] - k[(\rho_{-+})^2 + (\rho_{+-})^2] \quad (200)$$

The terms in the first bracket are the usual statistical expressions for entropy and in the absence of the rotating field, Eq. 200 reduces to the usual one. Using Eq. 189 we obtain from Eq. 200:

$$dS/dt = -k\dot{\varepsilon} \log [(1 + 2\varepsilon)/(1 - 2\varepsilon)] - 2k\{\dot{\delta}\delta + \delta^*\dot{\delta}^*\} \quad (201)$$

As in the case of an ideal gas dealt with in the previous section, we have to calculate the external change of entropy due to the energy flow from a heat bath. This energy flow can be evaluated from the energy of the spins in the field given by $-\gamma\hbar\langle\mathbf{I}\rangle \cdot \mathbf{H}$. Using Eqs. 194, 190, and 191, we obtain:

$$\begin{aligned} d_e S/dt &= -(\hbar/T\tau)[\gamma\chi_s \mathbf{H}^2 - \gamma\mathbf{H} \cdot \langle\mathbf{I}\rangle] \\ &= -(4k/\tau)[(\chi_s/\gamma)^2(\omega_0^2 + \omega_1^2) - \varepsilon_s E - \frac{1}{2}(\delta_s P + \delta_s^* P^*)] \end{aligned} \quad (202)$$

where ε_s and δ_s are the stationary-state values for ε and δ . Then subtracting Eq. 202 from Eq. 201, we get the entropy production

$$\begin{aligned} \tau\mathcal{P} &= -k(E_s - E) \log [(1 + 2\varepsilon)/(1 - 2\varepsilon)] - 2k[(P_s - P)\delta + (P_s - P^*)\delta^*] \\ &\quad + 4k[(\chi_s/\gamma)^2(\omega_0^2 + \omega_1^2) - \varepsilon_s E - \frac{1}{2}(\delta_s P + \delta_s^* P^*)] \end{aligned} \quad (203)$$

In practically all magnetic resonance experiments, the following inequalities are extremely well satisfied:

$$\begin{aligned} \hbar\omega_0/4kT &\ll 1 \\ \hbar\omega_1/4kT &\ll 1 \end{aligned} \quad (204)$$

Then E , P and P^* are themselves small compared with unity and we may replace $\log [(1 + 2\varepsilon)/(1 - 2\varepsilon)]$ by 4ε . If we make this replacement for the logarithm it is easily shown that E_s , P_s and P_s^* , and ε_s , δ_s and δ_s^* , the stationary state solutions of Eqs. 196 and 197, satisfy the equations

$$\begin{aligned} \partial\mathcal{P}/\partial E &= 0 \\ \partial\mathcal{P}/\partial P &= 0 \\ \partial\mathcal{P}/\partial P^* &= 0 \end{aligned} \quad (205)$$

This implies that the entropy production is a minimum when parameters E , P , and P^* assume their stationary state values, and hence that the principle of minimum production of entropy holds in a magnetic resonance experiment.

It may be shown that \mathcal{P} is actually a minimum in the same way that we have seen in the previous sections.

The most important result obtained by Wangsness⁶¹ is that the definition of entropy in magnetic resonance Eq. 200 leads to

consistent result, Wangsness' choice of entropy is different from the usual one as pointed out by Lurcat.²⁸ The validity of his choice has, however, been confirmed by Meijer³¹ in applying Casimir's considerations² on even and odd variables.

C. Generalized Minimum Production Principle

The principle of minimum entropy production holds in the macroscopic description in which the entropy is considered to be a function of the diagonal density matrix, as seen from Klein and Meijer's theory. An attempt has been made by Callen¹ to generalize this principle for the cases where the contribution of the off-diagonal elements of the density matrix to the entropy cannot be neglected.

We shall start from von Neumann's definition of entropy in quantum-statistical mechanics given by Eq. 199. Since the entropy is defined as a function of the matrix elements, we may define a flow and a force corresponding to each matrix element. A force associated with ρ_{mn} is defined by

$$X_{mn} = \partial S / \partial \rho_{mn} \quad (206)$$

where the entropy S is given by Eq. 199. The above definition corresponds to Eq. 28 for the macroscopic forces, and a set of flows are, corresponding to Eq. 25, defined by

$$J_{mn} = \dot{\rho}_{mn} \quad (207)$$

In equilibrium state both of X_{mn} and J_{mn} vanish, since the entropy is a maximum and the density matrix is time-independent. The flows are functions of forces such that the flows vanish when the forces all vanish. Then, for sufficiently small values of the forces the flows are linear functions of the forces, and we may therefore write

$$J_{mn} = \sum_{rs} L_{mn,rs} X_{rs} \quad (208)$$

where $L_{mn,rs}$ is the microscopic transport coefficient. Callen¹ has shown that the coefficients $L_{mn,rs}$ is symmetric, by repetition of the proof of Onsager's reciprocity relations with some considerations of the effect of Casimir's antisymmetry:²

$$L_{mn,rs} = L_{rs,mn} \quad (209)$$

Let us now denote the deviation of matrix element from its equilibrium value ρ_{mn}^0 by Δ_{mn} :

$$\Delta_{mn} = \rho_{mn} - \rho_{mn}^0 \quad (210)$$

Then the entropy is expressed as

$$S = S_0 - \frac{1}{2} \sum_{mn, rs} g_{mn, rs} \Delta_{mn} \Delta_{rs} \quad (211)$$

The force X_{mn} associated with a set of Δ_{mn} is given, corresponding to Eq. 24 in macroscopic case, by

$$X_{mn} = \partial S / \partial \Delta_{mn} = - \sum_{rs} g_{mn, rs} \Delta_{rs} \quad (212)$$

The flows are, according to Eqs. 207, 208, and 212,

$$J_{mn} = \dot{\Delta}_{mn} = \sum_{rs} L_{mn, rs} X_{rs} \quad (213)$$

Finally, the entropy production is

$$\begin{aligned} \mathcal{P} &= \sum_{mn} X_{mn} J_{mn} = \sum_{mn, rs} L_{mn, rs} X_{mn} X_{rs} \\ &= \sum_{mn, rs} \sum_{ab, cd} L_{mn, rs} g_{mn, ab} g_{rs, cd} \Delta_{ab} \Delta_{cd} \end{aligned} \quad (214)$$

which is obtainable from Eqs. 211, 212 and 213.

In the macroscopic theory of stationary state, some of forces are kept constant. For the present case, following Callen, we impose a set of constraints given in the form, with the help of constant matrices $b_{mn}^{(\kappa)}$, ($\kappa = 1, 2, \dots, K$),

$$\sum_{mn} b_{mn}^{(\kappa)} X_{mn} = 1 \quad (\kappa = 1, 2, \dots, K) \quad (215)$$

of which a special case gives the macroscopic constraints. From the normalization condition for the density matrix, we have

$$\text{trace } \mathbf{\Delta} = \sum_m \Delta_{mm} = 0 \quad (216)$$

With use of Eq. 212, the above condition is rewritten as

$$\sum_{mn} \sum_r g_{rr, mn}^{-1} X_{mn} = 0 \quad (217)$$

It is always possible to write the condition Eq. 215 together with Eq. 217 in the set of equations

$$\sum_{mn} a_{mn}^{(\kappa)} X_{mn} = A^{(\kappa)} \quad (\kappa = 1, 2, \dots, K+1) \quad (218)$$

where $a_{mn}^{(\kappa)}$'s are orthogonal in the sense

$$\sum_{mn} a_{mn}^{(\kappa)} a_{mn}^{(\kappa')} = \delta_{\kappa\kappa'} \quad (219)$$

and the $A^{(\kappa)}$'s are constants and $A^{(K+1)} = 0$.

Let us employ these $a_{mn}^{(\kappa)}$'s as the coordinate axes to represent the matrix, which hereafter regarded as a vector. The components referred to the new coordinate axis are denoted by the prime and Greek suffix, which correspond to a set of two roman suffices.

Thus we have

$$\begin{aligned}\Delta'_{\kappa} &= \sum_{mn} \mathbf{a}_{\kappa, mn}^{-1} \Delta_{mn} \\ \Delta_{mn} &= \sum_{\kappa} \mathbf{a}_{mn, \kappa} \Delta'_{\kappa}\end{aligned}\quad (220)$$

The entropy is expressed in the form, according to Eqs. 211 and 212

$$S = S_0 + \frac{1}{2} \sum_{mn} X_{mn} \Delta_{mn} = S_0 + \sum_{\kappa} X'_{\kappa} \Delta'_{\kappa} \quad (221)$$

where X'_{κ} is the new coordinate given by

$$X'_{\kappa} = \sum_{mn} \mathbf{a}_{mn, \kappa} X_{mn} \quad (222)$$

From Eqs. 213, 219, and 222, we obtain

$$J'_{\kappa} = \dot{\Delta}_{\kappa} = \sum_{mn} \mathbf{a}_{\kappa, mn}^{-1} J_{mn} = \sum_{\kappa'} \sum_{mn, rs} \mathbf{L}_{mn, rs} \mathbf{a}_{\kappa, mn}^{-1} \mathbf{a}_{\kappa', rs}^{-1} X'_{\kappa'} \quad (223)$$

Finally, the entropy production is

$$\mathcal{P} = \sum_{mn} X_{mn} J_{mn} = \sum_{\kappa} X'_{\kappa} J'_{\kappa} = \sum_{\kappa, \kappa'} \sum_{mn, rs} \mathbf{L}_{mn, rs} \mathbf{a}_{\kappa, mn}^{-1} \mathbf{a}_{\kappa', rs}^{-1} X'_{\kappa} X'_{\kappa'} \quad (224)$$

and the condition of constraints, Eq. 215, is written as

$$X'_{\kappa} = A^{(\kappa)} \quad (\kappa = 1, 2, \dots, K+1) \quad (225)$$

The actual stationary state realized under the constraints, Eq. 225, is given by

$$J'_{\kappa} = 0 \quad (\kappa > K) \quad (226)$$

The solution is determined by Eqs. 225 and 226.

We shall now show that the state of minimum production of entropy leads to the actual stationary state. The equation 225 implies only that $\delta X'_{\kappa}$'s must be zero in the subspace $\leq K$, and the condition for minimization of \mathcal{P} under this condition is expressed in the form

$$\begin{aligned}\sum_{\kappa'} \sum_{mn, rs} (\mathbf{L}_{mn, rs} \mathbf{a}_{\kappa, mn}^{-1} \mathbf{a}_{\kappa', rs}^{-1} + \mathbf{L}_{mn, rs} \mathbf{a}_{\kappa', mn}^{-1} \mathbf{a}_{\kappa, rs}^{-1}) X'_{\kappa'} &= 0 \\ (\kappa > K)\end{aligned}\quad (227)$$

If we use the microscopic reciprocity $\mathbf{L}_{mn, rs} = \mathbf{L}_{rs, mn}$, we obtain, from Eqs. 223 and 227,

$$J'_\kappa = \sum_{\kappa'} \sum_{m\eta,rs} L_{m\eta,rs} a_{\kappa,m\eta} a_{\kappa',rs} X_{\kappa'} = 0 \quad (\kappa > K) \quad (228)$$

which is identical with Eq. 226 for the actual stationary state. This fact proves that the principle of minimum entropy production holds, in the absence of a magnetic field, the elements of the density matrix assume the value which minimize the entropy production compatible with the constraints.

This demonstration of generalized minimum production principle has been given by Callen.¹ This theorem is very general and seems to have wide applicability. However, the proof of this theorem is so closely connected with the reciprocity relations that some restriction will appear in applying it to practical problems, whereas the principle of minimum entropy production in the macroscopic description holds even when the reciprocal relations are not used.

In connection with the above-mentioned theorem, it seems to be desirable in giving a quantum-mechanical version of the least dissipation principle, to mention the purely quantum-mechanical proof of the reciprocity relations by Watanabe,⁶² but a discussion of this would be beyond the scope of the present article.

References

1. Callen, H. B., in I. Prigogine, ed., *Proceedings of the International Symposium on Transport Processes in Statistical Mechanics*, Interscience, New York, 1958; Phys. Rev. **105**, 360 (1957).
2. Casimir, H. B. G., *Revs. Modern Phys.* **17**, 343 (1945).
3. Chapman, S., and Cowling, T. G., *Mathematical Theory of Non-uniform Gases*, Cambridge Univ. Press, Cambridge, 1939.
4. Cramér, H., *Mathematical Methods of Statistics*, Princeton Univ. Press, Princeton, 1951.
5. Curie, P., *Oeuvres*, Gauthier-Villars, Paris, 1908, p. 27.
6. Curtiss, C. F., and Hirschfelder, J. O., *J. Chem. Phys.*, **17**, 550 (1949).
7. Denbigh, K. G., *Trans. Faraday Soc.* **48**, 389 (1952).
8. Donder, Th. de, *Leçon de thermodynamique et de chimie physique*, Gauthier-Villars, Paris, 1920.
9. Donder, Th. de, *L'affinité*, Gauthier-Villars, Paris, 1928.
10. Donder, Th. de, *L'affinité* (2nd part), Gauthier-Villars, Paris, 1931.
11. Donder, Th. de, *L'affinité*, (3rd part), Gauthier-Villars, Paris, 1934.
12. Doob, J. L., *Stochastic Processes*, Wiley, New York, 1953.
13. Einstein, E., *Ann. Physik* **69**, 241 (1922).

14. Enskog, D., *Kinetische Theorie der Vorgänge in mässig verdünnten Gase, I. Allgemeine Teil*. Diss., Upsala, 1917.
15. Enskog, D., *Kungl. Svenska Vetenskapsakad.* **63**, No. 4 (1922).
16. Enskog, D., *Z. Physik*, **54**, 498 (1929).
17. Glandsdorff, P., and Prigogine, I., *Physica* **20**, 773 (1954).
18. Groot, S. R. de, *Thermodynamics of Irreversible Processes*, North-Holland, Amsterdam, 1951.
19. Haase, R., *Z. Naturforsch.* **6a**, 522 (1951).
20. Haase, R., *Ergebnisse d. exakt. Naturwiss.* **26**, 56 (1952).
21. Hashitsume, N., *Progr. Theoret. Phys. (Japan)*, **8**, 461 (1952).
22. Hellund, E. J., and Uehling, E. A., *Phys. Rev.* **56**, 818 (1939).
23. Hirschfelder, J. O., Curtiss, C. F., and Bird, R. B., *Molecular Theory of Gases and Liquids*, Wiley, New York, 1954.
24. Klein, M. J., and Meijer, P. H. E., *Phys. Rev.* **96**, 250 (1954).
25. Klein, M. J., *Phys. Rev.* **98**, 1736 (1955).
26. Klein, M. J., *Phys. Rev.* **103**, 839 (1956).
27. Klein, M. J., in I. Prigogine ed., *Proceedings of the International Symposium on Transport Processes in Statistical Mechanics*, Interscience, New York, 1958.
- 27a. Khinchin, A., *Math. Ann.* **109**, 604 (1933).
28. Lurcat, F., *Compt. rend.* **242**, 1686 (1956).
29. Machlup, S., and Onsager, L., *Phys. Rev.* **91**, 1512 (1953).
30. Mazur, P., *Bull. acad. roy. Belg. Cl. Sci.* **38**, 182 (1952).
31. Meijer, P. H. E., in I. Prigogine ed., *Proceedings of the International Symposium on Transport Processes in Statistical Mechanics*, Interscience, New York, 1958.
32. Meixner, J., *Ann. Physik* **43**, 244 (1943).
33. Meixner, J., *Z. phys. Chem. (B)* **53**, 235 (1943).
34. Mel, H. C., *Bull. acad. roy. Belg. Cl. Sci.* **40**, 834 (1954).
35. Murakami, T., *J. Phys. Soc. Japan* **15**, 60 (1960).
36. Nakai, S., in K. Husimi, ed., *Quantum Statistical Mechanics*, Kyoritsu Shuppan, Tokyo, 1948 [in Japanese].
37. Nielsen, A. E., *Bull. acad. roy. Belg. Cl. Sci.* **40**, 539 (1954).
38. Ono, S., *Sci. Papers Coll. Gen. Educ. Univ. Tokyo* **5**, 87 (1955).
39. Onsager, L., *Phys. Rev.* **37**, 405 (1931).
40. Onsager, L., *Phys. Rev.* **38**, 2265 (1931).
41. Onsager, L., *Ann. N. Y. Acad. Sci.* **46**, 241 (1945).
42. Onsager, L., and Machlup, S., *Phys. Rev.* **91**, 1505 (1953).
43. Overhauser, A. W., *Phys. Rev.* **92**, 411 (1953).
44. Pauli, W., *Festschrift zum 60. Geburtstage A. Sommerfelds*, Hirzel, Leipzig, 1928, p. 30.
45. Prigogine, I., *Bull. acad. roy. Belg. Cl. Sci.*, **31**, 600 (1945).
46. Prigogine, I., and Wiame, J. M. *Experientia (Basel)* **2**, 451 (1946).

47. Prigogine, I., *Étude thermodynamique des phénomènes irréversibles*, Desoer, Liège, 1947.
48. Prigogine, I., *Physica* **15**, 272 (1949).
49. Prigogine, I., and Defay, R., *Thermodynamique chimique*, Desoer, Liège, 1950, Chap. XV.
50. Prigogine, I., *Bull. acad. roy. Belg. Cl. Sci.* **40**, 471 (1954).
51. Prigogine, I., *Introduction to Thermodynamics of Irreversible Processes*, Thomas, Springfield, 1955.
52. Prigogine, I., and Balescu, R., *Bull. acad. roy. Belg. Cl. Sci.* **41**, 917 (1955).
53. Prigogine, I., and Balescu, R., in I. Prigogine, ed., *Proceedings of the International Symposium on Transport Processes in Statistical Mechanics*, Interscience, New York, 1958; *Bull. acad. roy. Belg. Cl. Sci.* **42**, 256 (1956).
54. Rayleigh, Lord, *Proc. Math. Soc. London* **4**, 357 (1873).
55. Rayleigh, Lord, *Theory of Sound*, 1st ed., MacMillan, London, 1877.
56. Siegert, A. J. F., *Phys. Rev.* **76**, 1708 (1949).
57. Thomsen, J. S., *Phys. Rev.* **91**, 1263 (1953).
58. Volterra, V., *Théorie mathématique de la lutte pour la vie*, Gauthier-Villars, Paris, 1931.
59. Waldmann, L., *Handbuch der Physik*, **12**, 295 (1958).
60. Wangsness, R. K., *Phys. Rev.* **98**, 927 (1955).
61. Wangsness, R. K., *Phys. Rev.* **101**, 1 (1956).
62. Watanabe, S., in I. Prigogine, ed., *Proceedings of the International Symposium on Transport Processes in Statistical Mechanics*, Interscience, New York, 1958.
63. Wergeland, H., in I. Prigogine, ed., *Proceeding of the International Symposium on Transport Processes in Statistical Mechanics*, Interscience, New York, 1958.

ELECTRON DIFFRACTION IN GASES AND MOLECULAR STRUCTURE

O. BASTIANSEN and P. N. SKANCKE, *Institute of Theoretical
Chemistry, The Technical University of Norway, Trondheim, Norway*

CONTENTS

I. Introduction	323
II. Theory	325
III. Experimental Method and Calculation Procedure	328
IV. Molecular Structure Determinations	335
A. Precision Determination of Internuclear Distances	336
B. Various Molecular Structure Problems	347
C. Conformational Analysis.	353
V. Molecular Vibrations	357
VI. Future Prospects	359
References	360

I. INTRODUCTION

It is now 32 years since Davisson and Germer⁴⁰ did their first experiment on the diffraction of electrons and thus gave the proof for the validity of the de Broglie relation. Since then the electron diffraction method has been open for the study of the structure of matter, and a large number of problems have been treated with this method, using both the diffraction from solid material and from gases.

During the first few years following the Second World War the electron diffraction method seemed to get into a crisis. As to the use of electron diffraction in the crystalline phase, the method did not seem to be able to compete with the X-ray method that was so well developed. Further, the method of neutron diffraction, a newcomer in the scientific arena, seemed to be full of promises and able to take over a great many of the problems from the electron

diffraction method. As to the use of electron diffraction in gases, still more serious objections could be put forth. The microwave method began to supply chemistry with high-precision structure data, and in spite of its well-known limitation it seemed to be able to take over a substantial part of the field of structure chemistry earlier covered by the electron diffraction method, particularly if it were combined with other spectroscopic methods. At the same time the method of low-temperature X-ray crystallography was introduced, and that method seemed to be able to solve molecular structure problems for practically all kinds of volatile compounds. In 1950 it was stated that electron diffractionists should be prepared to face unemployment problems. This statement should of course not be taken too seriously, but it did certainly reflect some doubt among several structure chemists about the future of the electron diffraction method for structure studies.

At the same time that this scepticism was expressed, the electron diffraction method had a revival and entered a phase of new possibilities. Its application in crystallography was greatly accelerated, particularly by the work of J. Cowley in Australia, G. Pinsker and B. Weinstein in Russia, H. Raether in Germany, and several groups in Japan. The application of the electron diffraction method for gases went also into a phase of renewal, stimulated by the construction of new and better experimental equipment. The application of new apparatuses increased the accuracy of the method considerably and also extended the applicability of the method to structural problems of greater complexity.

The present article, which deals exclusively with electron diffraction in gases, does not pretend to give a complete survey or review of the field. The authors' intention is, by a rather arbitrary choice of examples, mainly taken from the work done in Norway, to try to give an idea of what kind of problems we can hope to solve by the electron diffraction method. This, we hope, should be of greater value for those interested in the field of molecular structure than a more detailed theoretical introduction or a comprehensive review of all structure results obtained by electron diffraction during the last few years.

The choosing of examples mainly from the work done in Oslo

and Trondheim is at the expressed request of the Editor. The authors want, at this stage, to emphasize the important contribution to the development of the field made by American scientists such as L. Bartell, L. O. Brockway, K. Hedberg, J. Ibers, I. and J. Karle, R. L. Livingston, V. Schomaker, and their collaborators. Of great value for the development of the modern electron diffraction gas method is the voluminous literature from Japan of both theoretical and experimental nature. Among the Japanese gas electron diffractionists the name of Y. Morino should be mentioned first. In the last few years a very active electron diffraction gas group has been set up in Moscow under the leadership of P. A. Akishin. The most important contribution of this group is probably the considerable extension of the temperature interval for electron diffraction gas studies to higher temperatures. To obtain an up-to-date understanding of the field, the work of the above-mentioned investigators and their groups should be carefully studied.

II. THEORY

The following theoretical outline is limited to a presentation of the definitions and equations necessary for the description of the diffraction of electrons from free molecules. More detailed theoretical surveys, including the deduction of the equations, have been given by various authors.^{41, 42, 45, 64, 80}

An electron diffraction experiment consists primarily in the determination of the diffracted intensity, $I_t(s)$, as a function of the angle of diffraction. The theoretical expression for $I_t(s)$ is the following

$$I_t(s) = (K/s^4) \left\{ \sum_i [(Z_i - F_i)^2 + S_i] + \sum_{i \neq j} (Z_i - F_i)(Z_j - F_j) [(\sin R_{ij}s)/(R_{ij}s)] \right\} \quad (1)$$

Instead of the diffraction angle, it is convenient to use $s = (4\pi/\lambda) \sin \theta$ as independent variable, where λ is the wave length and θ the Bragg angle (one half the diffraction angle).

As to the other symbols in Eq. 1, K is an uninteresting constant at constant electron velocity, Z_i is the atomic number of the i th

atom, F_i is the scattering amplitude of the i th atom, S_i is the incoherent scattering factor, and R_{ij} is the distance between the i th and the j th atom in the molecule.

The amplitudes F_i in Eq. 1 are here the same as the atomic form factors used in X-ray diffraction, and depend upon the electron distribution in the atoms.

The expression for $I_b(s)$ is composed of two terms

$$I_b(s) = (K/s^4) \sum_i [(Z_i - F_i)^2 + S_i] \quad (2)$$

which represents the background scattering, and

$$I_m(s) = (K/s^4) \sum_{i \neq j} \sum (Z_i - F_i)(Z_j - F_j) [(\sin R_{ij}s)/(R_{ij}s)] \quad (3)$$

which is the expression for the molecular scattering.

The first term, $I_b(s)$, contains only the atomic and incoherent scattering and does, therefore, not supply any information about the molecular structure. Such information, however, is present in the second term which is, therefore, the important one for the molecular structure studies.

The validity of Eqs. 1 and 3 is limited by the following assumptions:

1. The molecule is rigid;
2. No phase shift occurs during the scattering process.

The first assumption must always be corrected for, since the thermal vibration of the molecules influences the expression for the molecular scattering rather drastically. A good approximation is obtained if small harmonic oscillations of the atoms are assumed. In that case the expression for the molecular scattering is

$$I_m(s) = (K/s^4) \sum_{i \neq j} \sum (Z_i - F_i)(Z_j - F_j) \exp [-(1/2)u_{ij}^2 s^2] [(\sin R_{ij}^e s)/(R_{ij}^e s)] \quad (4)$$

R_{ij}^e is the equilibrium distance between the i th and j th atom. The root-mean-square deviation from the equilibrium distance is u_{ij} , usually called "mean amplitude":

$$u_{ij} = \langle (R_{ij} - R_{ij}^e)^2 \rangle_{av}^{1/2} \quad (5)$$

R_{ij} is the instantaneous distance.

The second assumption is merely a consequence of the first Born approximation which implies a real scattering amplitude. A quantum mechanical treatment of the scattering process leads to a complex scattering amplitude containing a phase factor which is a function of the scattering angle.⁶⁵ The phase-shift effect depends upon the difference $Z_i - Z_j$. This means that a distance between two atoms of the same kind will not be effected by phase-shift phenomena. For small differences in atomic numbers the effect can usually be neglected. When large differences in atomic numbers occur, as for instance in UF_6 , there is a considerable effect, and corrections have to be carried out for the determination of the interatomic distances R_{ij}^e and for the mean amplitudes u_{ij} .^{72, 71, 24, 47, 52}

In cases where the phase-shift effect can be neglected it is convenient to define a radial-distribution function as follows:

$$\mu(r) \equiv [\sigma(r)/r] = (2/\pi) \int_0^\infty s^5 I_m(s) \varphi(s) \sin rs \, ds \quad (6)$$

where $\varphi(s)$ is a modification function that has to be chosen in a special way to simplify the radial-distribution curve. It can now be shown that

$$\mu(r) = \sum_{\text{dist}} (n_{ij}/R_{ij}^e) Z_i \cdot Z_j \cdot N_{ij}(R_{ij}^e - r) \quad (7)$$

The sum is taken over all the different distances in the molecule. n_{ij} is the number of times equivalent distances occur. The function $N_{ij}(\rho)$ (the normal function) where $R_{ij}^e - r$ is substituted by ρ , has the form

$$N_{ij}(\rho) = (1/\pi) \int_0^\infty [1 - (F_i/Z_i)] [1 - (F_j/Z_j)] \varphi(s) \exp [-(1/2) u_{ij}^2 s^2] \cos \rho s \, ds \quad (8)$$

It is seen that the modification function, $\varphi(s)$, earlier introduced, appears also here in the theoretical expression. If the $\varphi(s)$ function is chosen to be of the form

$$\varphi(s) = \frac{[\exp (-ks^2)]}{[1 - (F_i/Z_i)][1 - (F_j/Z_j)]} \quad (9)$$

the expression for the normal function for the distance between

the i th and j th atom will be simplified to

$$N_{ij}(\rho) = (1/\pi) \int_0^\infty \exp\{-[k + (1/2)u_{ij}^2]s^2\} \cos \rho s ds \quad (10)$$

k is a constant, usually chosen between 0 and approximately 0.004 Å².

By performing the integration we obtain

$$N_{ij}(\rho) = [1/(2\pi)^{\frac{1}{2}}] [1/(u_{ij}^2 + 2k)]^{\frac{1}{2}} \exp[-(\rho^2)/(2u_{ij}^2 + 4k)] \quad (11)$$

This means that the contributions to the radial-distribution curve from distances between atom type i and atom type j are Gaussian peaks with a weight factor equal to

$$(n_{ij}/R_{ij}^e) Z_i \cdot Z_j$$

The contributions from the other types of distances are not exactly Gaussian. As all F curves have nearly similar forms the deviation from the Gaussian shape is not very large, but should be taken into account.

III. EXPERIMENTAL METHOD AND CALCULATION PROCEDURE

Molecular structure studies by the electron diffraction method are based upon comparison between an experimental curve and a theoretical curve. The theoretical curve contains molecular structural data, namely the interatomic distances and the u values. The interatomic distances are obtained from an assumed structure model by simple geometry. The u values are considerably more difficult to obtain from a structure model. In a completely rigid molecular model all u values are equal to zero. Only in a diatomic molecule where the molecule is approximated to a harmonic oscillator is the u value easily obtainable from the force constant. The study of the u values for more complex molecules is going to be considered later in this article.

The comparison between an experimentally obtained curve and a theoretical one can either be based upon intensity curves or radial-distribution curves. One could, for instance, compare the experimentally obtained I_m curve, or better $I_m \cdot s^4$, by one calculated

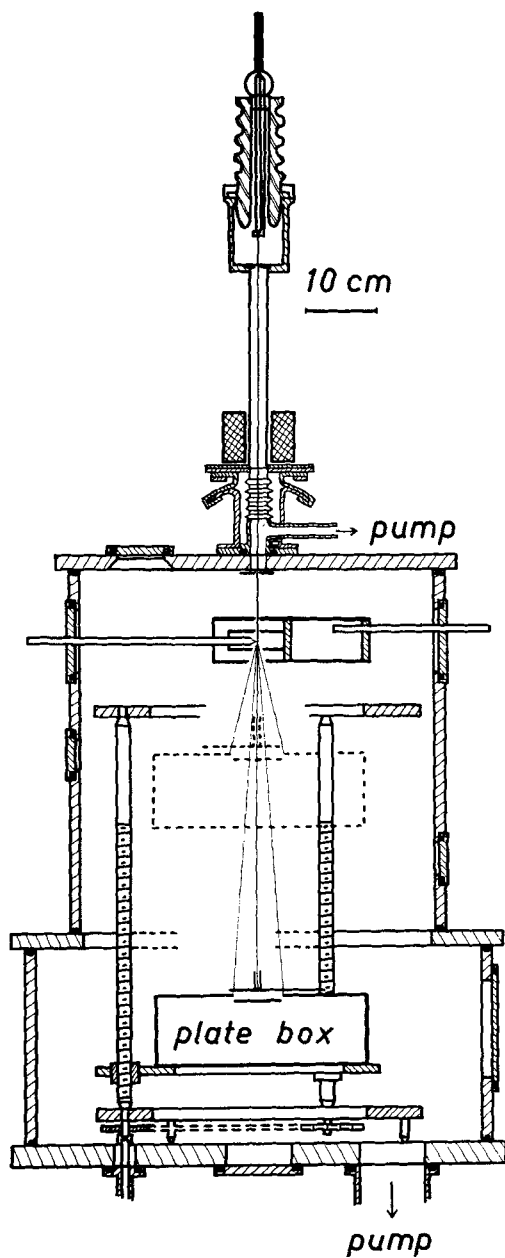


Fig. 1. A simplified section sketch of the Oslo electron diffraction apparatus.

from Eq. 4. Another alternative is to compare the radial-distribution curve obtained from Eq. 6 with the one obtained from Eqs. 7 and 8. The first of these radial-distribution curves contains the experimental curve I_m and the other one the structure data of a molecular model.

Whatever the calculation procedure, the molecular intensity has to be obtained from the experiments. It is convenient to operate with a function I_E which is the experimental representation of the expression $I_m \cdot s^4$.

In Fig. 1 an oversimplified sketch of a section of the Oslo electron diffraction apparatus is presented. The vacuum chamber consists of two steel cylinders, the inner diameter of which are 50 and 63 cm respectively. The total height is 80 cm. The main opening giving access to the chamber is a door in the bottom cylinder. Through this door the photographic plate box is inserted. In the top and bottom plates of the chamber and in the side wall of the upper cylinder there exists a series of openings for the attachment of pumps, gauges, cooling trap, gas nozzle, and other auxiliary equipment.

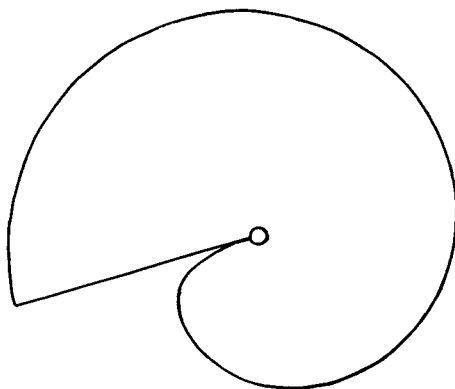


Fig. 2. A modified s^3 sector for electron diffraction gas work.

In the upper part of the sketch the electron gun and the magnetic focussing lens are shown. The electron beam entering the upper cylinder hits the gas beam at the gas nozzle.

This is a gas jet surrounded by a liquid air trap to avoid the

spreading out of the gas in the apparatus. This assembly has been constructed with great care, for the quality of the electron diffraction diagrams is critically dependent upon this part of the apparatus.

Immediately before the electron beam reaches the photographic plate it is screened by a rotating sector, with axis of rotation along the incident electron beam.^{78, 46, 43} A model of such a sector is given in Fig. 2.

The object of the sector is easily understood by inspection of Eq. 1. The $1/s^4$ factor in the expression for I_t is responsible for a steep fall off in the total intensity curve. A photometer curve of a non-sectored diagram is almost completely dominated by this steep slope, and the diffraction rings are practically lost. The steep fall-off of the intensity curve is compensated by the rotating sector. The sector that is most frequently used effects a multiplication by a factor of approximately s^3 . A photometer curve of a sectored diagram of coronene is given as an example in Fig. 3.

In the sketch of Fig. 1 the plate box is shown in two alternative positions. The plate-box mounting can be moved up and down in

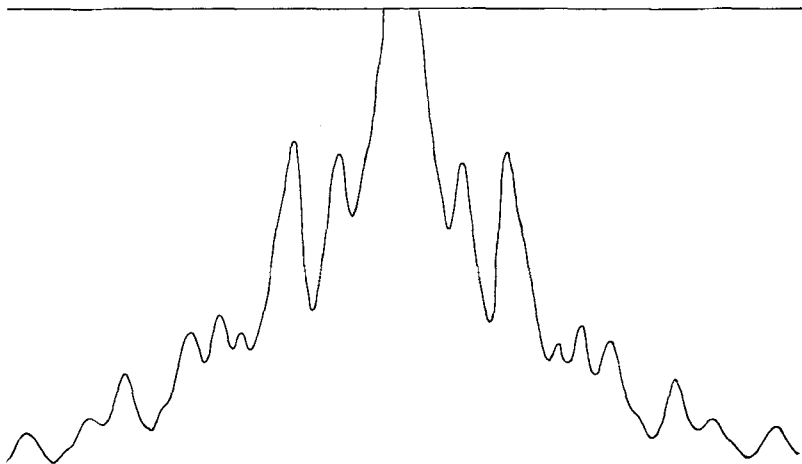


Fig. 3. Photometer curve of a sector electron diffraction diagram of coronene. Distance between diffraction point and photographic plate equal to approximately 49 cm.

the cylinder and the distance between the diffraction point and the photographic plate can thus be varied. Usually diagrams are taken at three various distances, namely approximately 12, 19, and 49 cm.

To obtain the I_E curve from the photometer curve several corrections have to be carried out. There are corrections for photographic effects, corrections for the exact form of the sector and corrections for the fact that we are dealing with flat photographic plates. The intensity curves taken at the three different distances between diffraction point and photographic plate are all used to obtain the final experimental curve. For each distance the average of a whole series of curves is used. The overlap intervals of the intensity curves from the three various distances are rather large and the final curve covers the s range from approximately 1 \AA^{-1} up to 65 \AA^{-1} in the most favorable cases. Examples of experimental I_E curves are given in Fig. 4 along with corresponding calculated curves.

For the calculation of the radial-distribution curve from the experimental intensity curve, according to Eq. 6, the intensity range from zero to infinity is required. The effect of the two integration limits on the radial-distribution curve should therefore be studied carefully. The effect of the outer integration limit can be controlled by using various k values in the chosen φ function in Eq. 9.

With a large damping factor the value of the intensity curve at the outer integration limit is negligible. The k values used in practice lie usually between $k = 0$ and 0.004 \AA^2 . As a general rule the radial-distribution curves with small k values are more reliable at small r values and those with large k values more reliable at large r values.

The effect of the inner integration limit is taken care of after the Fourier transform has been carried through. This is perhaps best illustrated by an example. Figure 5 shows a radial-distribution curve of benzene⁸ obtained by using the following modification function

$$\varphi(s) = [\exp(-0.0009 s^2)]/[1 - (F_C/Z_C)^2]$$

The curve is given in the r interval from 0.9 to 4.1 Å. The curve is

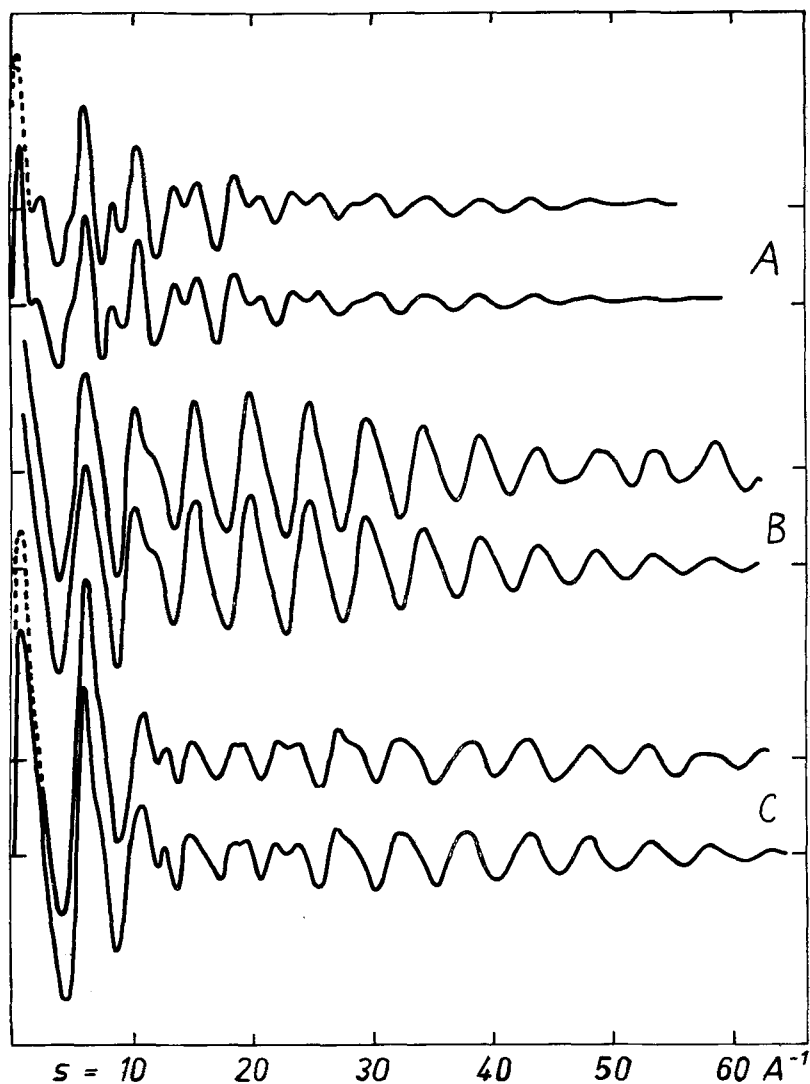


Fig. 4. Experimental and theoretical molecular intensity curves I_E . (A) cyclooctatetraene, (B) allene, (C) vinylacetylene.

composed of Gaussian-like peaks and the position of the maxima of the peaks correspond to the interatomic distances in the benzene molecule. The minima of the curve do, however, not lie on the zero

line. The negative areas in the curve are due to the lost inner part of the intensity curve. This effect can be compensated for simply by drawing in an envelope as indicated by the broken line. If this

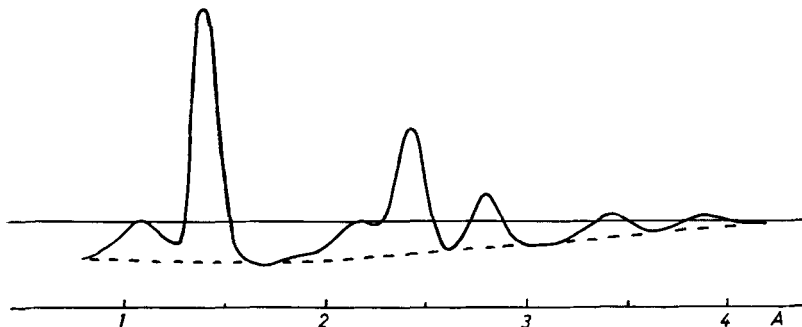


Fig. 5. Radial-distribution curve of benzene as obtained directly from the intensity curve ($k = 0.0009 \text{ \AA}^2$).

line is used as the zero line the radial-distribution curve in Fig. 6 is obtained and this curve should be free of the effect of the inner break off.

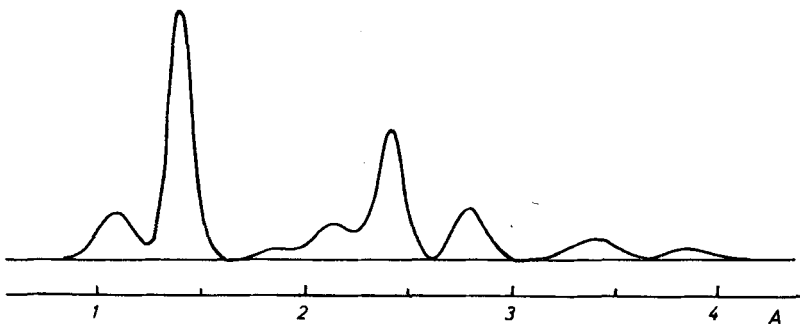


Fig. 6. Radial-distribution curve after subtraction of the envelope.

From the radial-distribution curve as that given in Fig. 6 the first structure model is calculated. The position of the maximum of the first peak at 1.085 Å corresponds to the C—H bond distance in benzene, the next one at 1.397 Å corresponds to the C—C bond distance and so forth. In Fig. 6 only the peaks corresponding to

the C—H and C—C distances are present. The H₁—H₃ and H₁—H₄ distances are also observable beyond the r interval given in the figure. The areas of the corresponding peaks are, however, too small to be recognized in a scale practical for the presentation of the rest of the curve. (The contribution of the H₁—H₂ distance is completely lost, as this distance is too close to the C₁—C₃ distance.)

The u values of the internuclear distances are determined, for instance, by reading off the half-widths of the Gaussian-shaped peaks, and using the formula

$$u = [(B^2/8 \ln 2) - 2k]^{\frac{1}{2}}$$

A more accurate determination of the internuclear distances and the u values are obtained by resolving parts of the radial-distribution curve into sums of Gaussian peaks using the method of the least squares. This is of particularly great interest when the peaks overlap.

When the first set of structure parameters has been obtained, theoretical radial-distribution curves and theoretical intensity curves are computed. These curves are compared with the corresponding experimental curves as earlier mentioned. For this comparison least-squares calculations are frequently applied.

IV. MOLECULAR STRUCTURE DETERMINATIONS

Usually the molecular structure of a substance is said to be determined when a rigid static geometrical model has been given. To determine this model a certain number of molecular structure parameters have to be known. The structure parameters usually presented are bond distances, valency angles, and angles describing how various groups are mutually oriented.

A static model does, however, not give a complete description of the molecule. It does not tell anything about the intramolecular movements. A more elaborate structure model has to be introduced in order to describe the more or less restricted intramolecular rotation that often takes place, or to describe the molecular vibrations. Force constants determining the intramolecular movements must also be considered as molecular structure parameters, along with the geometrical molecular structure parameters. So far no single

method has been developed that can give all these parameters for all kind of molecules with the highest precision in one type of experiment. Still the various information of importance for molecular structure theory has to be gathered together from various kinds of experimental and theoretical methods. The object of the following paragraphs is to show what kind of information has been obtained or may be expected to be obtained from electron diffraction gas work.

A. Precision Determination of Internuclear Distances

For the evaluation of the electron diffraction gas method as a precision method for internuclear distance determination, two questions have to be answered: (1) What is the reproducibility of the method? and (2) What does the determined distance mean?

Principally, the first question should be easy to answer. A repetition of a complete structure determination, until statistical material is available, should solve the problem of reproducibility. In practice, however, this is impossible to do. One electron diffraction structure determination including experiment and necessary computation requires at least several months work for one person. Consequently, as a rule, complete structure determination for one molecule is carried out only once. However, a number of times it has been done twice, of course using entirely different sets of diagrams, preferably taken at least at one year intervals. These experiments together with the study of different molecules containing the same structure feature have given a good basis for judging the reproducibility.

Of course a single example does not give much information concerning the reproducibility. In spite of this it might be of interest to present a representative example of two independent electron diffraction studies. The compound chosen is benzene.⁸ The purpose of this example is not only to demonstrate the reproducibility in a typical case but also to show what kind of informations can be obtained from radial-distribution curves.

The two sets of radial-distribution curves were obtained from electron diffraction diagrams taken at an interval of more than one year. The calculations were done by two different persons at two

different places without their knowing about each other. One of the radial-distribution curves was given in Fig. 6. The corresponding curve from the other experiment is so similar to the one presented that difference can hardly be observed in the scale of the presented figure. By inspection of the seven maxima in each of the radial-distribution curves the C—C and C—H distances were obtained. They were obtained by approximating each of the peaks with a Gaussian peak. The internuclear distances thus obtained from the two investigations are listed in Table I. The upper half of the table

TABLE I. Experimental and Calculated Internuclear Distances in Benzene⁸

	Obs. dist.	Bond dist.	Calc. dist.	Exp. — calc., %
<i>Investigation I</i>				
C ₁ —C ₂	1.3975	1.3975	1.3974	+0.007
C ₁ —C ₃	2.4190	1.3966	2.4204	—0.058
C ₁ —C ₄	2.7964	1.3982	2.7948	—0.057
C ₁ —H ₁	1.0850	1.085	1.082	+0.27
C ₁ —H ₂	2.1460	1.074	2.153	—0.33
C ₁ —H ₃	3.4045	1.086	3.401	+0.10
C ₁ —H ₄	3.8737	1.079	3.877	—0.08
<i>Investigation II</i>				
C ₁ —C ₂	1.3971	1.3971	1.3968	+0.021
C ₁ —C ₃	2.4195	1.3969	2.4193	+0.008
C ₁ —C ₄	2.7929	1.3965	2.7936	—0.025
C ₁ —H ₁	1.0821	1.082	1.084	—0.21
C ₁ —H ₂	2.1515	1.081	2.154	—0.13
C ₁ —H ₃	3.4050	1.088	3.402	+0.09
C ₁ —H ₄	3.8890	1.095	3.878	+0.28

contains the first investigation (I), the lower half contains the second investigation (II). The observed internuclear distances are given in the first column of each half of the table. The next column of each half presents bond distances calculated from the corresponding internuclear distances. The C—C bond distance values were calculated under the assumption of hexagonal symmetry. The C—H bond distance values were obtained using the

average C—C-bond distance obtained for the actual investigation together with the assumption of hexagonal symmetry. In both investigations the three values obtained for the C—C bond distance are very close together. It should be remembered that the three values are obtained from three different peaks in the radial-distribution curve, and the good correspondence therefore indicates a high degree of self-consistency of the method. Further, the average values in the two investigations are only 0.0006 Å apart. In the case of the C—H bond distance neither the self-consistency in each experiment nor the reproducibility is as high as for the C—C bond distances. This is to be expected as the C—H peaks in the radial-distribution curve are broader and have less area than the C—C peaks. On the other hand, the difference of the two average C—H bond distances is only 0.002 Å, which is very good compared to what can be obtained in similar structure studies by other methods.

It should be pointed out that the values obtained by the electron diffraction method are in very good accordance with the values obtained by Stoicheff based upon Raman spectroscopic studies.⁷³

In the fourth column of each half of Table I the calculated C—C and C—H distances based upon the average bond distances in each of the two investigations are listed. In the last columns the percentage difference for each internuclear distance is given.

As stated above, one single example is of very limited value for the evaluation of the reproducibility of the method. The mentioned example is, however, one of a number of similar examples. It is of little value to describe these cases. They do support the impression of several electron diffractionists that the predominating bond distances in simple organic molecules can be reproduced to an accuracy of 0.001 to 0.002 Å, and in some cases even better. It is hard to say definitely what is the limiting factor in the electron diffraction method. In the Oslo apparatus the high voltage equipment is no doubt the bottle-neck for the precision. An improvement at this point might increase the reproducibility still more.

As already mentioned, the H₁—H₃ and H₁—H₄ distances in the benzene molecule are also observable in the radial-distribution curve. The calculated values for these two distances are 4.292 and 4.956 Å respectively. The distances obtained for the first investi-

gation are 4.294 and 4.959 Å and for the second investigation 4.299 and 4.964 Å.

So far we have only discussed the reproducibility of the electron diffraction method and have not been concerned with what the determined distance really means. This is of course a question of greatest importance but also of considerable complexity. As pointed out by several investigators, the term "internuclear distance" today needs careful specification as to the method applied and the corrections made.^{23,4} This need will be more urgent the greater the improvements of the experimental methods. When a comparison of results obtained from spectroscopic studies with electron diffraction data is carried out, it should be remembered that these two methods in fact give principally two different values. In spectroscopic work the average of the inverse-square of the internuclear distance is measured. In electron diffraction work the most natural thing to do is to give the position of the maximum of the peak in the radial-distribution curve as was done in the example already presented. Because of the anharmonicity of the molecular vibrations neither of these types of values correspond to the equilibrium distance. A close examination shows that practically all peaks in the radial-distribution curve deviates a trifle from the symmetric Gaussian form, the slope on the left-hand side being usually slightly steeper than on the right-hand side. In special cases this effect can be particularly pronounced. For instance in a molecule like ammonia the H—H peak (or the D—D peak in heavy ammonia) is notably unsymmetric. In this case the conversion mechanism might contribute substantially to the effect. The maximum of the H—H peak in ammonia occurs at 1.584 Å. The average r value obtained by measuring the "center of gravity" of the peak is 1.668 Å.³

In the case of a diatomic molecule like Br₂ the effect can be studied theoretically using spectroscopical information about anharmonicity.⁶⁸ A comparison between values thus obtained and electron diffraction data leads to the same order of magnitude for the anharmonicity effect. L. S. Bartell²³ has studied the anharmonicity effect on electron diffraction and has found that conventional procedures lead to values which are likely to differ from the true equilibrium internuclear distance by the order of 0.01 Å.

Bartell and collaborators, therefore, give both the position of the maxima on the radial-distribution curve and the "center of gravity."

The straight-forward but perhaps naive approach to this problem is to have a set of compounds simultaneously studied with the electron diffraction method and with another precision method. This has been done with a series of molecules, and the result for a group of them is presented in Table II. The electron diffraction work is all done by the Oslo apparatus, the other part of the work is done by microwave spectroscopy, Raman spectroscopy or X-ray crystallography. The correspondence is in most cases surprisingly good. This is of course no guarantee that the results from electron diffraction data principally are the same as those obtained by the other methods. We might have a scale error that by accident makes the correspondence look too good.

Unfortunately, we must at the present stage of development admit that a series of unresolved problems still plague the absolute determination of internuclear distances. However, the values that can be obtained for bond distances from the electron diffraction method are in most cases accurate enough to provide valuable information for the theory of valency. In the following examples of bond distance measurements will be given.

The bond distance is usually considered as the most fundamental structure parameter. Perhaps the most interesting chemical bond is the carbon—carbon bond. This bond exists in a great variety of forms, and the bond distance ranges from approximately 1.20 Å in the triple bond up to 1.54 Å in the single bond. The carbon—carbon bond presents the theoreticians with a series of problems. One of the most important contributions of the experimentalists to the solution of these problems is to provide distance values with the highest possible accuracy. An increasing number of carbon—carbon distance values exist in the literature. It has been emphasized by several investigators that the bond lengths for a given bond environment are nearly the same in different molecules. Tables of average carbon—carbon distances obtained from various methods have been published, among others by C. Costain and B. Stoicheff,³² I. Hjalmar, ⁵¹ and B. Bak.²⁰ In Table III of the

TABLE II. Various Examples of Comparison between Electron Diffraction Data and Data Obtained by Other Methods

Molecule	State	Method	Bond lengths, A, and angles, deg.	Ref.
$\text{H}_2\text{C}=\text{CH}-\text{CH}=\text{CH}_2$	Gas	E.D.	C—C: 1.483, C=C: 1.337, C—H: 1.082, C—C=C: 122°4	16
	Gas	R	C—C: 1.485, C=C: 1.337 (ass.), C—H: 1.08 (ass.), C=C=C: 122°5	76
Pyridine	Gas	E.D.	(N—C ₂ , C ₂ —C ₃ , C ₃ —C ₄) _{av} : 1.377, (H ₂ —C ₂ , H ₃ —C ₃ , H ₄ —C ₄) _{av} : 1.078	10
	Gas	M.W.	(N—C ₂ , C ₂ —C ₃ , C ₃ —C ₄) _{av} : 1.377, (H ₂ —C ₂ , H ₃ —C ₃ , H ₄ —C ₄) _{av} : 1.081	21
Furan	Gas	E.D.	(O—C ₂ , C ₂ —C ₃ , C ₃ —C ₄) _{av} : 1.377, (H ₂ —C ₂ , H ₃ —C ₃) _{av} : 1.075	10
	Gas	M.W.	(O—C ₂ , C ₂ —C ₃ , C ₃ —C ₄) _{av} : 1.378, (H ₂ —C ₂ , H ₃ —C ₃) _{av} : 1.075	22
Benzene	Gas	E.D.	C—C: 1.397, C—H: 1.083	8
	Gas	R	C—C: 1.397 _s , C—H: 1.084	73
NH_3	Gas	E.D.	N—H: 1.016	4
	Gas	I.R.	N—H: 1.014	49
ND_3	Gas	E.D.	N—D: 1.017	4
$\text{H}_3\text{C}-\text{C}\equiv\text{C}-\text{C}\equiv\text{C}-\text{CH}_3$	Gas	E.D.	C=C: 1.208, C ₁ —C ₂ : 1.450, C ₃ —C ₄ : 1.377, C ₁ —H ₁ : 1.09, H—C—C: 111°6	12
	Crystal	X-ray	C=C: 1.199, C ₁ —C ₂ : 1.466, C ₃ —C ₄ : 1.375	50
$\text{H}_2\text{C}=\text{C}=\text{CH}_2$	Gas	E.D.	C=C: 1.312, C—H: 1.082, H—C=C: 120°8	17
	Gas	R	C=C: 1.309, C—H: 1.07 (ass.), H—C—H: 117°	74
Hexachlorobenzene	Gas	E.D.	C—C: 1.398, C—Cl: 1.718	15
	Crystal	X-ray	C—C: 1.39, C—Cl: 1.70	79

present article, non-aromatic carbon—carbon distances have been listed. In the second column values obtained from spectroscopic studies of various authors are given. Some of these values are average values from several investigators. In the third column of the table values obtained from the Norwegian electron diffraction group are given. Some of the electron diffraction data are not determined with the highest possible accuracy. This is the case for ethane for instance. Further, the values for butatriene are preliminary values that might be altered by refinements.

TABLE III. C—C Bond Distances Obtained from Spectroscopic Methods and from Electron Diffraction

Type of bond	Bond distance, Å spectroscopic	Ref.	Bond distance, Å electron diffraction	Ref.
$\text{—C}\equiv\text{C—}$	1.207		1.207 vinylacetylene 1.208 dimethyldiacetylene	66 12
$\diagup\text{C}=\text{C}\diagdown$	1.338		1.337 butadiene 1.334 cyclooctatetraene 1.336 vinylacetylene	16 29 66
$=\text{C}=\text{C}=\text{}$	1.284	75	1.283 carbon suboxide 1.283 butatriene	66 18
$\diagup\text{C—C}\diagdown$	1.543, 1.534	48, 2a	1.536 ethane	3
$\diagup\text{C—C}\diagup$	1.485	76	1.483 butadiene 1.462 cyclooctatetraene	16 29
$\equiv\text{C—C}\equiv$	1.377	31, 77, 81	1.377 dimethyldiacetylene	12
$\diagup\text{C}=\text{C}=\text{}$	1.311	53, 74	1.312 allene 1.318 butatriene	17 18
$\diagup\text{C—C}\diagup$	1.501	55		
$\diagup\text{C—C}\equiv$	1.459		1.450 dimethyldiacetylene	12
$\diagup\text{C—C}\equiv$	1.426	32	1.425 vinylacetylene	66

It would no doubt have been very desirable to know the error limits for the bond distances. Unfortunately, reliable error estimates are difficult to give. Of course standard-deviation values can be given as a result of a least-squares calculation. This would, however, not give a real description of the total probable error in an electron diffraction study. In error evaluations it is difficult to avoid subjective estimates. Error limits given from electron diffraction measurements should, therefore, always be taken with reservations. From the study of the electron diffraction method and from estimation of the various sources of errors one feels safe in most cases in giving an error range of ± 0.005 Å. For some distances this estimation is probably too pessimistic. The general correspondence between the spectroscopically obtained values and the electron diffraction values is satisfactory, and the values for the same kind of distance for various compounds are, within any reasonable error limit, the same. The single bond in 1,3-butadiene¹⁶ and 1,3,5,7-cyclooctatetraene²⁹ seems to be an exception. This distance is found to be 0.021 Å larger in butadiene than in cyclooctatetraene. Reservations should be taken as to accidental errors in one or both of these compounds. Such errors seem, however, rather unlikely, particularly on the basis of the fact that the double bonds in the two compounds were found to be only 0.003 Å apart. There are, therefore, good reasons to believe that the result is real. It is rather surprising that the C—C distance in the planar butadiene is larger than in the puckered cyclooctatetraene. Using the simple argument of *p*-orbital overlap one would expect butadiene to have the stronger C—C single bond and therefore have the shorter bond length. The effect is perhaps related to the cyclic form of cyclooctatetraene that might favor the dislocation of the *p*-electron. The distance of the bridge bond connecting neighboring rings in biphenyl and related compound might also be considered in this connection. This bond as well is an *sp*²—*sp*² bond with possibilities for *p*-orbital overlap. It is interesting to note that the C—C bridge bond in the non-planar biphenyl is found to be 1.489 Å,⁵ i.e., only slightly larger than the C—C bond distance in the planar 1,3-butadiene. On the other hand the bridge bond in hexaphenylbenzene, with the interplanar angle of approximately

90°, is found equal to 1.52 Å.¹³ Again the effect is not convincingly large compared to the expected errors, particularly because of the fact that the bridge bond distance is determined indirectly from the larger interatomic distances of the molecules. However, a pessimistic error estimate leads to a maximum error of 0.01 Å for the two given bridge bond distances.

TABLE IV. Covalent Radii of the C-Atom for Different Types of Hybridization

Bond multiplicity	C—	C=	C≡
sp^3	0.767		
sp^2	0.737	0.669	
sp	0.687	0.642	0.604

As pointed out by I. Hjalmarsson⁵¹ it is possible to give a set of covalent radii for the carbon atom. If aromatic molecules, small cyclic rings, and other special kinds of molecules are excluded altogether, six covalent radii for carbon can be given, one related to the triple bond, two related to the double bond (sp , and sp^2 hybridization), and three related to the single bond (sp , sp^2 , and sp^3 hybridization). The radii derived from the total average of the distances given in Table III are listed in Table IV. It is of great importance for the study of molecular structures to find out to what extent these radii are generally applicable. Only further endeavor for increased accuracy in a larger number of molecular structure studies can form the basis for empirical rules along the indicated line.

It has been emphasized that molecules containing small cyclic rings have to be excluded in the group of distances given in Table III. For instance the C—C distance in cyclopropane is found to be shorter than the corresponding distance in an open chain. A recent preliminary electron diffraction study leads to a value of 1.509 Å⁹ which is no doubt significantly smaller than the ethane distance. The great deviation from the usual tetrahedral angle in the case of

cyclopropane makes it easy to accept a difference in the C—C distance.

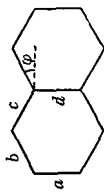
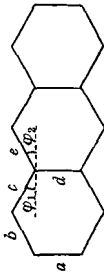
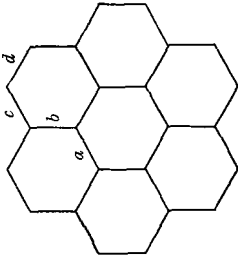
The aromatic distances that also have been excluded so far are of special interest in valency theory. A series of aromatic molecules have been studied by the electron diffraction method. It is interesting to note that the average C—C distance in the aromatic rings of a series of molecules is about the same. This has been demonstrated in Table V. The condensed aromatic molecules seem to have an average bond distance a trifle larger than benzene. In coronene the average C—C distance approaches the C—C distances in graphite of 1.421 Å.⁶⁷

TABLE V. The Average Aromatic C—C Bond Distance in Various Aromatic Molecules

Molecule	C—C distance, Å	Ref.
Benzene	1.397	8
Hexachlorobenzene	1.398	15
Biphenyl	1.396	5
Hexaphenylbenzene	1.400	13
Naphthalene	1.401	6
Anthracene	1.408	7
Coronene	1.415	6

One of the most important problems connected to the carbon—carbon distances of aromatic rings is the determination of the lengths of the different individual bonds in condensed aromatic systems. Extensive X-ray work^{34, 33, 70} has been carried through in order to give accurate values for the bond distances in molecules like naphthalene, anthracene, and coronene. These three molecules have also been studied in this institute using the electron diffraction method.^{6, 7} Elaborate studies including least-squares calculations have led to the result presented in third column of Table VI. The X-ray data are also included. As for naphthalene, the correspondence between the electron diffraction results and those obtained from X-ray studies is satisfactory. For the two other compounds there is a deviation that has to be explained. There are a series of

TABLE VI. Individual C—C Bond Distances and Valency Angles in Condensed Aromatic Molecules

Molecule	Type of distance and valency angle	Electron diffraction $R_E, \text{ \AA}; \varphi_E, \text{ deg}$	Ref.	X-ray diffraction $R_X, \text{ \AA}; \varphi_X, \text{ deg}$	Ref.	$\Delta = \begin{cases} R_E - R_X \\ \varphi_E - \varphi_X \end{cases}$
Naphthalene		$a = 1.412$ $b = 1.371$ $c = 1.422$ $d = 1.420$ $\varphi = 29^\circ 42$	6	$a = 1.415$ $b = 1.364$ $c = 1.421$ $d = 1.418$ $\varphi = 29^\circ 13$	34, 34a	-0.003 +0.007 +0.001 +0.002 +0.29
Anthracene		$a = 1.419$ $b = 1.390$ $c = 1.420$ $d = 1.425$ $e = 1.404$ $\varphi_1 = 29^\circ 28$ $\varphi_2 = 29^\circ 42$	7	$a = 1.419$ $b = 1.368$ $c = 1.436$ $d = 1.428$ $e = 1.399$ $\varphi_1 = 29^\circ 00$ $\varphi_2 = 29^\circ 51$	33, 34a	0.000 +0.022 -0.016 -0.003 +0.005 +0.28 -0.09
Coronene		$a = 1.438$ $b = 1.381$ $c = 1.444$ $d = 1.362$	6	$a = 1.430$ $b = 1.430$ $c = 1.415$ $d = 1.385$	70	+0.008 -0.049 +0.029 -0.023

explanations that present themselves: (1) The electron diffraction method is not well suited for the study of this kind of molecules. Though the average distance no doubt is accurately determined the individual distances are difficult to obtain. For instance in coronene the two distances b and c are particularly sensitive for errors in the larger internuclear distances of the molecule in such a way that one of the distances may come out too large and the other one too small, the sum $b + 2c$ being approximately constant. (2) The accuracy of the X-ray studies might not be sufficient for the comparison. (3) Out-of-planarity vibrations might obscure the electron diffraction studies, that to a great extent are based upon determination of the larger carbon—carbon distances in the molecules. (4) There might be real differences in the structure of the molecules in the gaseous state and in the solid state.

The carbon—hydrogen bond is of nearly the same theoretical importance as the carbon—carbon bond. Unfortunately electron diffraction studies generally do not give carbon—hydrogen distances with the same accuracy as carbon—carbon distances. In spite of this the electron diffraction method no doubt may contribute to the study of the carbon—hydrogen bond distance and its dependence upon the hybridization and the neighboring bonds.

At the same time as the accuracy of bond distance measurements by the electron diffraction method has increased, the applicability of the method has also been enlarged. A new technique developed by Akishin *et al.*¹ at Moscow State University makes possible the study of compounds with boiling points over 1000°C. The molecules first studied by this technique are of the type MX_2 , where M represents atoms of Group II metals and X represents halogen atoms.

B. Various Molecular Structure Problems

As pointed out earlier the valency angle may be considered as one of the fundamental molecular structure parameters. Again the situation related to the carbon atom may serve as an example. According to well-established concepts the symmetry around a carbon atom depends upon the nature of the hybridization. The

effect of the hybridization and the steric effect can be favorably studied by the electron diffraction method.

Studying the three main types of hybridization around the carbon atom, interest may first be concentrated upon the validity of the angle-relation rule that demands tetrahedral symmetry in case of sp^3 hybridization, 120° angle in case of sp^2 hybridization, and 180° angle in case of sp hybridization. For the sp^3 hybridization tetrahedral angles are usually found. Moderate steric effects lead to a deviation of a few degrees. Of course drastic deviations from the tetrahedral angle occur in exceptional cases as, for instance, cyclopropane, cyclobutane and their derivatives. In the case of the sp hybridization, linear molecules are almost always observed. Such compounds as dimethyldiacetylene, allene, and butatriene may serve as examples in which electron diffraction studies lead to linear equilibrium configurations. As it occurs in aromatic compounds, sp^2 hybridization leads to a valency angle very close to 120° . In benzene itself, of course, this value is, by symmetry, a necessity. In other aromatic molecules like those earlier mentioned (Table VI) the deviation from the ideal 120° angle seems to be less than 1° . In non-aromatic compounds the angle between the double bond and one of the single bonds seems to be slightly larger than 120° . In Table VII a few examples of this valency angle have been listed. The value for ethylene is the average of the two best spectroscopic values.^{2,44} The other values are electron diffraction values obtained in Norway. The $C=C-H$ angle value for 1,3-butadiene is less accurate than the other ones for there is serious overlap in the radial-distribution curve in the area of the crucial carbon—hydrogen distances. The value for butatriene is preliminar but will hardly change much by refinements. The deviation from the average value of 121.2° is within the limits of error for all angle values except perhaps for the $C=C-C$ angle in 1,3-butadiene. The deviation of 1.2° in 1,3-butadiene is probably significant, though the error analysis does not lead to a decisive result. A larger value for the $C=C-C$ angle is consistent with the smaller value for the $C=C-H$ angle in the same molecule. The angle between the two single bonds are thus found to be 117.6° which is very nearly the same value as the average value of 117.8° .

In cyclopropane the unusual C—C—C angle of 60° influences the other valency angles of the molecule. Preliminary value found for the C—C—H angle is 118.3° and for the H—C—H angle, 113.6° .⁹

TABLE VII. Experimental Valency Angles Associated with an sp^2 Hybridization

Compound	Valency angle	Exp. value	Ref.	Deviation from ave. value, deg
Ethylene	CCH	121.3	2, 44	+0.1
1,3-Butadiene	CCH	119.8	16	—1.4
1,3-Butadiene	CCC	122.4	16	+1.2
Allene	CCH	120.8	17	—0.4
Butatriene	CCH	121.5	18	+0.3

As a whole, it is a molecular structure problem of considerable interest to try to form better empirical rules for the valency angles, analogous to those existing for the bond distances. In spite of the greater accuracy of the spectroscopic methods, the electron diffraction method might be superior for this purpose. The electron diffraction method usually allows the determination of a larger number of structure parameters with fewer assumptions.

For a great number of molecules the bond distances and the valency angles are sufficient to describe the geometry of the molecule. However, for the majority of the molecules information concerning the mutual orientation of various groups is required as well. The ethane molecule may serve as an example of this. The most direct proof of the predominating *trans* form in gaseous ethane is given using the electron diffraction method.³ Both the *trans*-H—H distance as well as the *gauche*-H—H distance can be derived from the radial distribution curve. The position of these two distances are found to be 3.09 and 2.44 Å, respectively, corresponding to the calculated distances from the *trans* model of 3.09 and 2.50 Å. Of course the obtained accuracy of H—H distances as compared to the C—C and C—H distances is not very high.

Another example of considerable theoretical interest is presented

by the 1,3-butadiene molecule. Electron diffraction studies show that the two halves of the molecule lie in one plane.¹⁶ A series of molecules that exhibit an analogous kind of problems are the biphenyls and related molecules.^{5, 13, 14, 25, 26} A series of such compounds have been studied by electron diffraction. These studies have led to unplanar molecular configurations. In the case of 2,2'-bipyridyl there are some doubts left as to the equilibrium form of the molecule but in the rest of the molecules studied an equilibrium angle between the rings is given. The result for a series of molecules is listed in Table VIII. To understand these results in

TABLE VIII. Interplanar Angles in Biphenyl and Some Related Molecules

Compound	Angle of twist	Ref.
Biphenyl	41°6	5
1,3,5-Triphenylbenzene	46°4	26
Hexaphenylbenzene	90°0	13
4,4'-Bipyridyl	37°2	5
2,2'-Bithienyl	34°2	14
2,2'-Dichlorobiphenyl	74°	25
2,2'-Dibromobiphenyl	75°	25
2,2'-Diiodobiphenyl	79°	25

contrast to planarity of the 1,3-butadiene molecule the effect of the hydrogen—hydrogen interaction has to be considered. To obtain the best possible *p*-orbital overlap the molecule will always tend towards the planar form. This tendency is opposed by the hydrogen—hydrogen repulsion. In case of the 1,3-butadiene molecule the H—H distance that might influence the planarity of the molecule is equal to about 2.48 Å. This value is close to the most favorable packing distance between two hydrogen atoms. Probably the forces between the hydrogen atoms are still attractive at this distance, and it seems therefore natural to include the hydrogen—hydrogen attraction as one of the effects stabilizing the planar configuration. According to the best bond distance parameters of biphenyl the distance between the *ortho* hydrogen atoms of the two

different rings is 1.81 Å in a planar model. The corresponding value for 4,4'-bipyridyl is 1.95 Å. These values are no doubt too short, and the forces between the corresponding hydrogen atoms are accordingly repulsive. In the observed non-planar form the distance between the *ortho* hydrogen atoms is increased to 2.36 Å, both for biphenyl and 4,4'-bipyridyl. This distance is again in the neighborhood of the best packing distance between two hydrogen atoms. There is, therefore, good reason to believe that also in these molecules the interaction between non-bonded hydrogens is of importance for the molecular structure.

In the molecules listed in Table VIII the angle of twist is primarily influenced by the interaction of atoms in two rings directly linked together. One exception is formed by the hexaphenylbenzene.¹³ For this molecule the arrangement of the peripheral rings around the central ring is almost entirely determined by the repulsion of the atoms in the different outer rings. It is interesting to note in this connection that the outer rings seem to oscillate, with no appreciable restriction, in a limited angular interval of approximately $\pm 10^\circ$ from the orthogonal form. This result that was obtained by electron diffraction studies is easily understood from arguments based upon steric considerations. If two neighboring peripheral rings are rotated symmetrically towards each other, hydrogen—hydrogen contact is reached at about 10° from orthogonality. If a "propeller" model is assumed, steric conflicts will not lead to serious difficulties until a rotation of approximately 40° is performed. In order to realize such a conformation it is necessary to rotate all the peripheral rings in the same direction. If only one ring is out of order the rest would have to assume an arrangement near the orthogonal conformation. The probability of the symmetrical 40° "propeller" should, therefore, be rather small for pure statistical reasons. On the other hand, this symmetrical form might well be present in the crystalline state.

In most of the compounds discussed so far there seems to be a distinct equilibrium position determined by a certain angle of twist. The case of hexaphenylbenzene with the apparent unrestricted freedom of rotation in a limited angular interval may be considered to present an example of a transitional case, inter-

mediate between the case of a fixed orientation and the case of an entirely free rotation. It is questionable whether entirely free internal rotation exists at all in the sense that the potential energy is strictly constant throughout the whole angular interval from 0° to 360° . If one searches for cases with free rotation one might profitably study molecules like dimethylacetylene and their derivatives. The 1,4-dibromobutyne-2 is particularly favorable from the electron diffraction point of view.¹¹ In the radial-distribution curve all the distances that are independent of the internal rotational angle can be subtracted, leaving a difference radial-distribution curve for the variable distances. In Fig. 7 the fully

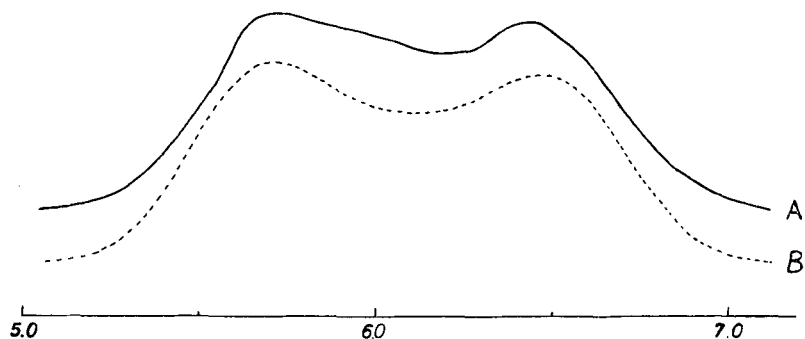


Fig. 7. Experimental (A) and theoretical (B) radial-distribution difference curve for 1,4-dibromobutyne-2.¹¹

drawn curve represents the experimental radial-distribution contribution from the Br—Br distance and the variable H—Br distances in the 1,4-dibromobutyne-2. The broken curve represents the calculated Br—Br contribution for a molecule with free rotation. The main points of deviation between these two curves can be explained by the H—Br distances that have not been included in the calculated curve. Though the electron diffraction studies thus strongly favor the assumption of free rotation, it can not exclude possible existence of a small potential barrier of say 100 to 200 cal./mole. These results are conformable with electron diffraction⁵⁶ and dipole moment⁶² studies carried out on the corresponding chloroderivative.

C. Conformational Analysis.

Strictly speaking, any molecular structure study involving determination of the spatial arrangement of the atoms may be termed as conformational analysis. The study of free and restricted rotation as mentioned previously is, for instance, closely related to the study of "rotational isomerism" which at least must be considered as a part of the conformational analysis.

Of particular interest in this connection is the study of molecules where either well-established theories or pure chemical intuition presents more than one alternative conformation for a given molecule. The problem of the conformational analysis in such a case is to find which conformation or conformations are present, describe the geometry of them, and if possible give the energy difference between the existing alternatives.

Ethane may serve as an example of a molecule with only one equilibrium conformation. Even though there exists an infinite number of conformations, if all intermediate forms between two energy minima are included, there exists only one equilibrium conformation (as long as all the hydrogen atoms are of only one kind of isotopes) namely the *trans* conformation.

An example of two equilibrium conformations is presented by the *trans*-1,2-dibromocyclohexane molecule. The electron diffraction radial-distribution curve exhibits C—Br and Br—Br distances for both the *ee* and the *aa* conformations.²⁸ As this molecule was studied at an early stage of the development of the electron diffraction method, very little could be said beside the fact that two conformations existed. To be able to give a quantitative statement concerning the relative stability of two conformations, quantitative studies of the areas under the various peaks in the radial-distribution curve must be carried out. For the use of the electron diffraction method in conformational analysis it is, therefore, of great importance to gather information about the reproducibility of the area determinations of the peaks in the radial-distribution curve. This information can be obtained by studying easily interpretable cases where the existence of only one conformation is undisputable. Benzene may be used as an example. In Table IX the areas under the C—C and C—H peaks in benzene are given.⁸ Both

the calculated values and two independently measured values are presented. The values were normalized to the same arbitrary scale by making the total area under the whole curve in each of the two experimental curves equal to the total area under the theoretical curve. This example indicates, that the errors in area determinations vary from 1 to 10 %, depending upon the relative value of the areas. In cases with a larger number of distances the expected error of the areas of the smaller peaks may be greater, particularly in cases with severe overlap. Difficulties in drawing in the envelope may also obscure an accurate determination of the area.

TABLE IX. Experimental and Calculated Areas of the Peaks in the Radial-Distribution Curve of Benzene⁸

Distances	Calc.	Exp. (invest. I)	Exp. (invest. II)
C ₁ —C ₂	154.6	155.3	156.4
C ₁ —C ₃	89.3	89.1	90.4
C ₁ —C ₄	38.6	40.4	39.6
C ₁ —H ₁	41.6	41.7	41.7
C ₁ —H ₂	41.8	41.5	39.9
C ₁ —H ₃	26.5	24.2	24.4
C ₁ —H ₄	11.6	12.0	11.6

If the 1,3-butadiene molecule is reconsidered in this connection the question as to another alternative conformation in addition to the planar *trans* conformation may be raised. Arguments have been set forth as to the possibility of the existence of a *cis* conformation or a "near-*cis*" conformation. The analysis of the areas of the peaks specific for the *trans* conformation and comparison with the peaks that exist for any conformation, exclude the possibility of more than 10 % contribution of other conformations than the *trans*.¹⁶ This means that a hypothetical *cis* conformation, if present, must be at least 1.3 kcal./mole less stable than the *trans* form.

A particularly illustrative example of the application of electron diffraction for conformational analysis is the study of *trans*-1,4-

dichlorocyclohexane and the corresponding bromocompound.¹⁹ The procedure is best demonstrated by Figs. 8 and 9. These figures give experimental radial-distribution curves for the two compounds together with various calculated radial-distribution curves. The calculated curves correspond to the pure *ee* and the *aa* conformations as well as the 50 % mixture of each of them. The curve for

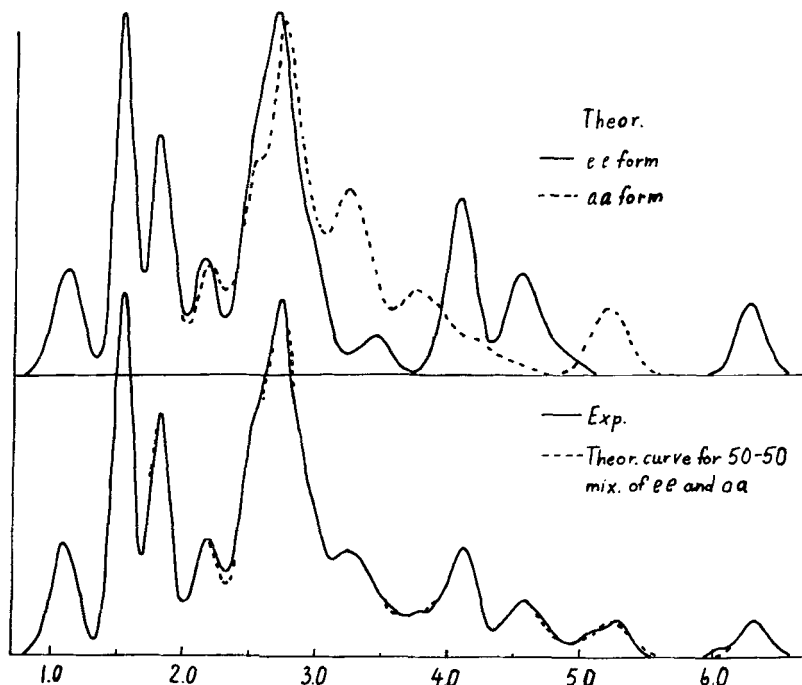


Fig. 8. Theoretical and experimental radial-distribution curve for 1,4-*trans*-dichlorocyclohexane.¹⁹

the last alternative is in very good agreement with the experimental curve. The conformational analysis thus give as a result an equal mixture of the two conformations. A least-squares procedure comparing the areas of the experimental curve with the calculated ones showed that the composite radial-distribution curve giving the best agreement with the experimental curve should have 51 % *ee* conformation and 49 % *aa* conformation. Studying the standard

deviation for the error in the ratio of the two conformations, the energy difference between the two conformations is shown to be less than 170 cal/mole.

An other example of a successful conformational analysis is the electron diffraction study of *n*-butane carried out independently by Bonham and Bartell³⁰ and Kuchitsu⁵⁷ in Morino's laboratory. Both find 60 % of the *trans* conformation and 40 % of the *gauche* conformation, a result leading to an energy difference of 650

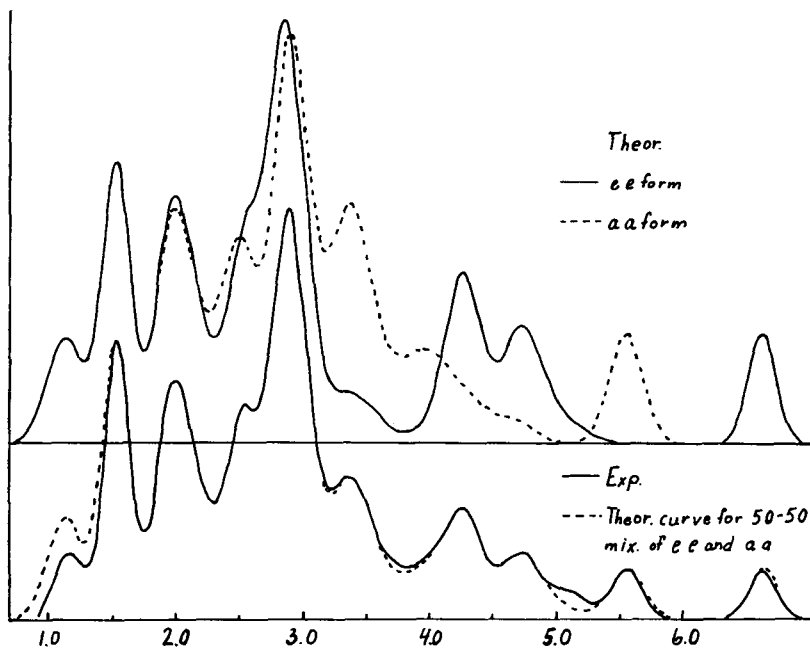


Fig. 9. Theoretical and experimental radial-distribution curve for 1,4-*trans*-dibromocyclohexane.¹⁹

cal/mole, the *trans* conformation being the more stable one. It is interesting to note in this connection that in the case of *n*-propyl chloride the *gauche* form is the more stable conformation.⁵⁹

A series of successful conformational analyses have been carried out using electron diffraction studies. Here, as anywhere else throughout this article, only a few examples have been chosen to illustrate the method.

V. MOLECULAR VIBRATIONS

As mentioned previously in this article, an electron diffraction study leads to the determination of (1) interatomic distances, and (2) the mean amplitudes of vibration u . So far the discussion has been based upon the interatomic distances, as they are of importance for the study of bond distances, valency angles and the molecular geometry as a whole. In the following a few comments on the study of the u values will be made.

The electron diffraction determination of the u values is based upon the study of the natural damping of the various sine terms making up the electron diffraction intensity curve. This damping of the sine terms can be measured from the radial-distribution curve by studying the width of the corresponding Gaussian-like peak. As mentioned earlier, the u value may be obtained either directly from the intensity curve or from the radial-distribution curve using least-squares calculations.

The first u -value determinations from electron diffraction data were reported by I. and J. Karle⁵⁴ who followed the treatment of P. Debye.⁴² Now a whole series of molecules have been studied.

The u values give informations about the "rigidity" of the molecule or the internal "mobility" of the molecule. Small u values correspond to high rigidity or small mobility. The u values may, therefore, be considered as physical properties of the molecule. These properties can also be derived from the force constants of the molecule. This means that the u values may principally be obtained from two entirely different experimental methods, namely electron diffraction and vibration spectra.

The calculations of mean amplitudes from spectroscopic data are almost entirely carried out using harmonic potential fields. The methods used for these calculations have, in particular, been studied by Morino and collaborators^{60, 61, 58} and by Cyvin.^{37, 38}

Unfortunately, a complete set of normal frequencies obtained from the vibrational spectrum of a molecule is not always sufficient for the calculations of the u values. Therefore, certain assumptions based upon general knowledge of force constants often have to be made. In certain cases the additional information may be obtained from the spectra of various isotope-substituted molecular species.

An increasing number of electron diffraction and spectroscopic u values have been calculated. A complete list of values gathered by Cyvin from the literature up to recent date is under publication.³⁹ In Table X only two examples are presented, namely benzene^{8, 27, 35} and allene.^{17, 36} In the case of benzene two independent sets of values were obtained from the electron diffraction study. The values are well-reproduced and in good agreement with the spectroscopic values. In the case of allene the correspondence between the electron diffraction values and the spectroscopic values is satisfactory except for the C_1C_3 distance where a significant discrepancy seems to be present. This discrepancy can be satisfactorily explained by taking into account out-of-linearity vibration. The spectroscopic calculations were based upon the assumption of a model with linear carbon skeleton.

TABLE X. Calculated and Measured Mean Amplitudes of Vibration u in Benzene^{8, 35} and Allene^{17, 36}

Molecule	Distances	Obs. u values (E.D.), Å		Calc. u values (spectr.); $T = 298^\circ\text{K}$
		Invest. I	Invest. II	
Benzene	C_1-C_3	0.0455	0.0453	0.0459
	C_1-C_3	0.054	0.054	0.0547
	C_1-C_4	0.062	0.059	0.0597
	C_1-H_1	0.073	0.073	0.0771
	C_1-H_2	0.094	0.092	0.1004
	C_1-H_3	0.094	0.087	0.0960
	C_1-H_4	0.097	0.099	0.0942
Allene	C_1-H_1	0.0795		0.0772
	C_1-C_2	0.0390		0.0401
	C_2-H_1	0.105		0.102
	C_1-C_3	0.052		0.045
	C_3-H_1	0.127		0.114

The question has been raised several times whether increased accuracy in electron diffraction measurements may lead to u values accurate enough for use in force-constant calculations. So far the obtainable accuracy does not generally seem to be sufficient.

However, the continuing improvement in the experimental methods gives good promises for the future.⁶³

Further development of the spectroscopic studies necessitates a more thorough study of the effect of anharmonicity. Besides the introductory work of Bartell²³ the influence of anharmonicity has also been studied by A. Reitan.^{68, 69}

For usual molecular structure studies the influence of vibrations may often be neglected. In special cases, however, detectable influences upon internuclear distances are observed. For instance in the case of dimethyldiacetylene a systematic difference between the observed internuclear distances, and those obtained using a model with linear carbon skeleton is detected.¹² The comparison shows that the largest internuclear distances, as observed from the radial-distribution curve, are a trifle shorter than the corresponding distances in the linear model. The same effect has been observed for allene¹⁷ and for butatriene.¹⁸ This effect can be explained by out-of-linearity vibrations. These vibrations should make the longer internuclear distances, as an average, shorter than the corresponding distances in a rigid linear molecule. The effect leads to an apparently unlinear molecule and might cause difficulties in molecular structure determinations. It seems to be difficult, if not impossible, to distinguish between such an apparent unlinearity and a small but real deviation from linearity of the equilibrium conformation. This kind of difficulty will also enter into other molecular structure problems, and has, as a matter of fact, already been encountered earlier in this article in the discussion of the C—C bond distance studies of large aromatic molecules.

VI. FUTURE PROSPECTS

Generally it is difficult and dangerous to prophesy, and in science it is still more so. Unknown factors always have to be anticipated. However, electron diffractionists at least seem to believe in the future of their method for the study of gas molecules. Unless an entirely new method is developed that can take over great parts of what electron diffraction is doing today, one must expect that electron diffraction studies are going to extend and improve lists of bond distances and valency angles, that electron

diffraction conformational analysis is going to enlarge our understanding of molecular geometry, and that *u*-value measurements are going to throw more light on the dynamics of the free molecule.

The authors want to thank lic. techn. S. Cyvin, civ. ing. F. Dyvik, and lic. techn. M. Trætteberg for valuable help. Special thanks are due to Professor H. Breed, Rensselaer Polytechnic Institute for critical reading of the manuscript.

References

1. Akishin, P. A., and Spiridonov, V. P., *Kristallografiya, U.S.S.R.*, **2**, 475 (1957).
2. Allen, H. C., and Plyler, E. K., *J. Am. Chem. Soc.*, **80**, 2673 (1958).
- 2a. Allen, H. C., and Plyler, E. K., *J. Chem. Phys.*, **31**, 1062 (1959).
3. Almenningen, A., and Bastiansen, O., *Acta Chem. Scand.*, **9**, 815 (1955).
4. Almenningen, A., and Bastiansen, O., *Research Correspondence*, **9** (Sept. 1956).
5. Almenningen, A., and Bastiansen, O., *Kgl. Norske Videnskab. Selskabs Skrifter*, **No. 4** (1958).
6. Almenningen, A., Bastiansen, O., and Dyvik, F., *Annual Technical Report (1958—1959)*, Contract No. AF 61(052)-72, Air Research and Development Command, U.S. Air Force.
7. Almenningen, A., Bastiansen, O., and Dyvik, F. (unpublished).
8. Almenningen, A., Bastiansen, O., and Fernholt, L., *Kgl. Norske Videnskab. Selskabs Skrifter*, **No. 3** (1958).
9. Almenningen, A., Bastiansen, O., Fernholt, L., and Skancke, P. N. (unpublished).
10. Almenningen, A., Bastiansen, O., and Hansen, L., *Acta Chem. Scand.*, **9**, 1306 (1955).
11. Almenningen, A., Bastiansen, O., and Harshbarger, F., *Acta Chem. Scand.*, **11**, 1059 (1957).
12. Almenningen, A., Bastiansen, O., and Munthe-Kaas, T., *Acta Chem. Scand.*, **10**, 261 (1956).
13. Almenningen, A., Bastiansen, O., and Skancke, P. N., *Acta Chem. Scand.*, **12**, 1215 (1958).
14. Almenningen, A., Bastiansen, O., and Svendsås, P., *Acta Chem. Scand.*, **12**, 1671 (1958).
15. Almenningen, A., Bastiansen, O., and Strand, T. (unpublished).
16. Almenningen, A., Bastiansen, O., and Trætteberg, M., *Acta Chem. Scand.*, **12**, 1221 (1958).
17. Almenningen, A., Bastiansen, O., and Trætteberg, M., *Acta Chem. Scand.*, **13**, 1699 (1959).

18. Almenningen, A., Bastiansen, O., and Trøttemberg, M. (unpublished).
19. Atkinson, V., and Hassel, O., *Acta Chem. Scand.* **13**, 1737 (1959).
20. Bak, B., *Acta Vålådalensia*, p. 7 (1958).
21. Bak, B., Hansen, L., and Rastrup-Andersen, J., *J. Chem. Phys.*, **22**, 2013 (1954).
22. Bak, B., Hansen, L., and Rastrup-Andersen, J., *Disc. Farad. Soc.*, **No. 19**, 30 (1955).
23. Bartell, L. S., *J. Chem. Phys.*, **23**, 1219 (1955).
24. Bartell, L. S., and Brockway, L. O., *Nature*, **171**, 978 (1953).
25. Bastiansen, O., *Acta Chem. Scand.*, **4**, 926 (1950).
26. Bastiansen, O., *Acta Chem. Scand.*, **6**, 205 (1952).
27. Bastiansen, O., and Cyvin, S. J., *Nature*, **180**, 980 (1957).
28. Bastiansen, O., and Hassel, O., *Tidsskr. Kjem., Bergv., Met.*, **6**, 96 (1946).
29. Bastiansen, O., Hedberg, L., and Hedberg, K., *J. Chem. Phys.*, **27**, 1311 (1957).
30. Bonham, R. A., and Bartell, L. S., *J. Am. Chem. Soc.*, **81**, 3491 (1959).
31. Callomon, J. H., and Stoicheff, B. P., *Can. J. Phys.*, **35**, 373 (1957).
32. Costain, C. C., and Stoicheff, B. P., *J. Chem. Phys.*, **30**, 777 (1959).
33. Cruickshank, D. W. J., *Acta Cryst.*, **9**, 915 (1956).
34. Cruickshank, D. W. J., *Acta Cryst.*, **10**, 504 (1957).
- 34a. Cruickshank, D. W. J., and Sparks, R. A., *Proc. Roy. Soc.* (In press).
35. Cyvin, S. J., *Acta Chem. Scand.*, **11**, 1499 (1957).
36. Cyvin, S. J., *J. Chem. Phys.*, **29**, 583 (1958).
37. Cyvin, S. J., *Spectrochim. Acta*, **56** (1959).
38. Cyvin, S. J., *Spectrochim. Acta*, **828** (1959).
39. Cyvin, S. J., *Kgl. Norske Videnskab. Selskabs Skrifter No. 2* (1959).
40. Davisson, C. J., and Germer, L. H., *Phys. Rev.*, **30**, 705 (1927).
41. Debye, P., *Ann. Physik*, **46**, 809 (1915).
42. Debye, P., *J. Chem. Phys.*, **9**, 55 (1941).
43. Debye, P. P., *Physik. Z.*, **40**, 404 (1939).
44. Dowling, J. M., and Stoicheff, B. P., *Can. J. Phys.*, **37**, 703 (1959).
45. Ehrenfest, P., *Amsterdam Acad.*, **23**, 132 (1915).
46. Finbak, Chr., *Avhandl. Norske Videnskaps-Akad. Oslo. I. Mat.-Naturv.* **Kl. 13** (1937).
47. Glauber, R., and Schomaker, V., *Phys. Rev.*, **89**, 667 (1953).
48. Hansen, G. E., and Dennison, D. M., *J. Chem. Phys.*, **20**, 313 (1952).
49. Herzberg, G., *Infrared and Raman Spectra of Polyatomic Molecules*, p. 439, New York, 1945.
50. Himes, R. C., and Harris, P. M., *Technical Report No. 3*, R. F. Project 355, Ohio State University, 1953.
51. Hjalmar, I., *Acta Vålådalensia*, p. 29 (1958).
52. Hoerni, J. A., and Ibers, J. A., *Phys. Rev.*, **91**, 1182 (1953).
53. Johnson, H. R., and Strandberg, M. N. P., *J. Chem. Phys.*, **20**, 687 (1952).

54. Karle, I. L., and Karle, J., *J. Chem. Phys.*, **17**, 1052 (1949).
55. Kilb, R. W., Lin, C. C., and Wilson, E. B., Jr., *J. Chem. Phys.*, **26**, 1695 (1957).
56. Kuchitsu, K., *Bull. Chem. Soc. Japan*, **30**, 399 (1957).
57. Kuchitsu, K., *Bull. Chem. Soc. Japan*, **32**, 748 (1959).
58. Morino, Y., and Hirota, E., *J. Chem. Phys.*, **23**, 737 (1955).
59. Morino, Y., and Kuchitsu, K., *J. Chem. Phys.*, **28**, 175 (1958).
60. Morino, Y., Kuchitsu, K., and Shimanouchi, T., *J. Chem. Phys.*, **20**, 726 (1952).
61. Morino, Y., Kuchitsu, K., Takahashi, A., and Maeda, K., *J. Chem. Phys.*, **21**, 1927 (1953).
62. Morino, Y., Miyagawa, I., Chiba, T., and Shimozawa, T., *Bull. Chem. Soc. Japan*, **30**, 222 (1957).
63. Morino, Y., Nakamura, Y., and Iijima, T., *J. Chem. Phys.* **32**, 643 (1960).
64. Mott, N. F., *Proc. Roy. Soc.*, **127**, 658 (1930).
65. Mott, N. F., and Massey, H. S. W., *The Theory of Atomic Collisions* (Oxford University Press, London, 1949) second edition.
66. Munthe-Kaas, T., *Thesis, Oslo University* (1955).
67. Nelson, J. B., and Riley, D. P., *Proc. Phys. Soc.*, **57**, 477 (1945).
68. Reitan, A., *Kgl. Norske Videnskab. Selskabs Skrifter*, **No. 2** (1958).
69. Reitan, A., *Acta Chem. Scand.*, **12**, 785 (1958).
70. Robertson, J. M., and White, J. G., *J. Chem. Soc.*, p. 607 (1945).
71. Schomaker, V., and Glauber, R., *Nature*, **170**, 290 (1952).
72. Schomaker, V., Glauber, R., Bastiansen, O., Sheehan, W. F., Jr., Felsenfeld, G., and Ibers, J. A., *Report Calif. Inst. of Technology*, p. 7 (1951—1952).
73. Stoicheff, B. P., *Can. J. Phys.*, **32**, 339 (1954).
74. Stoicheff, B. P., *Can. J. Phys.*, **33**, 811 (1955).
75. Stoicheff, B. P., *Can. J. Phys.*, **35**, 837 (1957).
76. Stoicheff, B. P., Private communication (1959).
77. Thomas, L. F., Heeks, J. S., and Sheridan, J., *Arch. sci. (Geneva)* **10**, 180 (1957).
78. Trendelenburg, F., *Wiss. Veröffentl. Siemens-Konzern*, **13**, 48 (1933).
79. Tulinsky, A., and White, J. G., *Acta Cryst.*, **11**, 7 (1958).
80. Viervoll, H., *Acta Chem. Scand.*, **1**, 120 (1947).
81. Westenberg, A. A., and Wilson, E. B., Jr., *J. Am. Chem. Soc.*, **72**, 199 (1950).

AUTHOR INDEX*

- Abbott, J. A., 189, 207 (ref. 1), 235
 Adams, E. N., II, 88, 91, 92, 128, 219, 235
 Adamson, A. F., 223 (ref. 17), 230, 235
 Akamatsu, H., 223, 235
 Akishin, P. A., 325, 347, 360
 Albright, C. H., 28 (ref. 23), 30
 Allen, H. C., 348 (ref. 2), 349 (ref. 2), 360
 Almenningen, A., 332 (ref. 8), 336 (ref. 8), 337 (ref. 8), 339 (refs. 3, 4), 341 (refs. 4, 8, 10, 12, 15-17), 342 (refs. 3, 12, 16-18), 343 (refs. 5, 16), 344 (refs. 9, 13), 345 (refs. 5-8, 13, 15), 346 (refs. 6, 7), 349 (refs. 3, 9, 16-18), 350 (refs. 5, 13, 14, 16), 351 (ref. 13), 352 (ref. 11), 353 (ref. 8), 354 (refs. 8, 16), 358 (refs. 8, 17), 359 (refs. 12, 17, 18), 360
 Angus, W. R., 205, 235
 Atkinson, V., 355 (ref. 19), 356 (ref. 19), 361
 Badger, R. M., 142, 169
 Bak, B., 340, 341 (refs. 21, 22), 361
 Bak, T. A., 33-57
 Balescu, R., 54, 57, 305 (ref. 52), 306, 321
 Barnett, M. P., 86 (ref. 4), 104 (ref. 4), 128
 Bartell, L. S., 325, 327 (ref. 24), 339, 340, 356, 359, 361
 Bastiansen, O., 323-362
 Bates, L. F., 172 (ref. 5), 235
 Baudet, J., 187, 189, 199, 200, 235, 236
 Bell, R. P., 131, 148, 150, 164, 166, 167, 169
 Benis, L., 249 (ref. 2), 264
 Bergmann, E. D., 27 (ref. 1), 30, 195 (ref. 9), 196 (ref. 9), 235
 Berthier, G., 25 (ref. 22), 26 (ref. 22), 27 (refs. 1, 22), 30, 193 (ref. 63), 194, 235, 237
 Bhatnager, S. S., 205, 206, 235
 Bigeleisen, J., 138, 164, 169
 Birchard, J. R., 153 (ref. 34), 170
 Bird, R. B., 61-63 (ref. 11), 79 (ref. 11), 86 (ref. 11), 128, 282 (ref. 23), 284 (ref. 23), 290 (ref. 23), 320
 Bitter, F., 185, 189, 205, 235
 Blayden, H. E., 223, 230, 235, 238
 Boato, G., 168 (ref. 5), 169
 Bogoliubov, N., 51, 54, 57
 Bolton, H. C., 189, 207 (ref. 1), 235
 Bonet, J. V., 184, 235
 Bonham, R. A., 356, 361
 Bonner, W. A., 139 (ref. 16), 169
 Bowers, R., 235
 Bray, W. C., 57
 Breiter, M., 13 (ref. 2), 23 (ref. 2), 30
 Breuzen, H., 254 (ref. 6), 264
 Brezina, M., 10
 Brockway, L. O., 325, 327 (ref. 24), 361
 Broersma, S., 173, 205, 235
 Brooks, H., 194, 235
 Buckingham, R. A., 185, 207 (ref. 22), 235
 Bulawa, J., 265
 Busch, G., 234, 235
 Bushkovitch, A. V., 184, 235
 Cabrera, B., 205, 206, 235
 Callen, H. B., 316, 317, 319, 319
 Callomon, J. H., 342 (ref. 31), 361
 Calus, H., 240
 Campbell, D. E., 87 (ref. 12), 128
 Campbell, E. S., 100, 128
 Careri, G., 168 (ref. 5), 169
 Carver, T. R., 220, 221 (ref. 89), 237
 Casimir, H. B. G., 274, 276, 316, 319
 Chaberski, A., 226 (ref. 68), 237
 Chapman, S., 283, 284, 319
 Chiba, T., 352 (ref. 62), 362
 Cimino, A., 168 (ref. 5), 169
 Corner, J., 88, 89, 128
 Coryell, C. D., 12 (ref. 27), 31

* *Italic numbers refer to the bibliographies of the different papers.*

- Costain, C. C., 340, 342 (ref. 32), 361
 Cottrell, T. L., 155 (ref. 6), 169
 Coulson, C. A., 185, 235
 Cowley, J., 324
 Cowling, T. G., 283 (ref. 3), 284 (ref. 3), 319
 Cramér, H., 278 (ref. 4), 319
 Crawford, J. H., 234, 238
 Cross, P., 136 (ref. 38), 138 (ref. 38), 170
 Cruickshank, D. W. J., 345 (refs. 33, 34), 346 (refs. 33, 34), 361
 Cruickshank, J. H., 205, 211, 236
 Curie, P., 273, 319
 Curtiss, C. F., 59-129, 282, 284, 290 (ref. 23), 319, 320
 Cyvin, S. J., 357, 358, 361
 Dail, H. W., 231, 236
 Dainton, F. S., 168, 169
 Davis, T. W., 153 (ref. 19), 154 (ref. 19), 170
 Davisson, C. J., 323, 361
 Debye, P., 325 (refs. 41, 42), 33 (ref. 43), 357, 361
 Decius, J. C., 136 (ref. 38), 138 (ref. 38), 170
 Defay, R., 302 (ref. 49), 321
 Delahay, P., 13 (ref. 2), 14 (ref. 3), 20 (ref. 3), 22 (ref. 3), 23 (ref. 2), 30
 Denbigh, K. G., 294, 319
 Dennison, D. M., 342 (ref. 48), 361
 Dingle, R. B., 219, 236
 Döring, W., 104, 128
 Donder, Th. de, 270, 319
 Donovan, B., 219, 236, 237
 Doob, J. L., 278, 319
 Dorfman, L. M., 153 (ref. 8), 169
 Dowling, J. M., 348 (ref. 44), 349 (ref. 44), 361
 Dyvik, F., 345 (refs. 6, 7), 346 (refs. 6, 7), 360
 Eckart, C., 137, 149, 169
 Ehrenfest, P., 325 (ref. 45), 361
 Einstein, E., 289, 319
 Elving, P. J., 1-31
 Enskog, D., 283, 284, 286, 289, 320
 Espe, I., 186, 236
 Evans, M. G., 9, 30, 194, 196, 236
 Eyring, H., 132 (ref. 12), 134 (ref. 12), 139, 142, 149 (refs. 10, 12, 13), 169
 Fahlenbrach, H., 205, 206, 235
 Farkas, A., 168 (ref. 11), 169
 Farkas, L., 168 (ref. 11), 169
 Farquharson, J., 205, 236
 Felsenfeld, G., 327 (ref. 72), 362
 Fernholt, L., 332 (ref. 8), 336 (ref. 8), 337 (ref. 8), 341 (ref. 8), 344 (ref. 9), 345 (ref. 8), 349 (ref. 9), 353 (ref. 8), 354 (ref. 8), 358 (ref. 8), 360
 Finbak, Chr., 331 (ref. 46), 361
 Frackiewicz, A., 240, 264
 Franck, A., 183, 184, 186, 238
 François, H., 185 (ref. 78), 189 (ref. 78), 205 (ref. 78), 207-209 (ref. 78), 210, 237
 Frank-Kamenetzki, D. A., 57
 Fujii, S., 198, 236
 Galt, J. K., 231, 236
 Ganguli, N., 222, 225, 229, 236
 Gans, R., 187, 236
 Gergely, J., 194, 196, 236
 Germer, L. H., 323, 361
 Giddings, J. C., 87 (ref. 7), 96 (refs. 6, 7), 128
 Glansdorff, P., 39, 47, 54, 57, 299, 306, 320
 Glasstone, S., 132 (ref. 12), 134 (ref. 12), 139 (ref. 12), 142 (ref. 12), 149 (refs. 12, 13), 169
 Glauber, R., 327 (refs. 47, 72), 361, 362
 Goldman, J. E., 237
 Gordon, A. S., 153, 154 (ref. 19), 170
 Gray, F. W., 205, 211, 236
 Groot, S. R. de, 57, 294, 298 (ref. 18), 320
 Guy, J., 181, 187, 189, 199, 200, 235, 236, 238
 Haase, R., 294, 303, 320
 Haering, R. R., 226, 231, 236
 Ham, F. S., 219, 236
 Hansen, G. E., 342 (ref. 48), 361
 Hansen, L., 341 (refs. 10, 21, 22), 360, 361

- Hansen, N., 254 (ref. 6), 264
Harris, P. M., 341 (ref. 50), 361
Harshbarger, F., 352 (ref. 11), 360
Hartmann, H., 185, 236
Hashitsume, N., 279, 320
Hassel, O., 353 (ref. 28), 355 (ref. 19), 356 (ref. 19), 361
Hazato, G., 212, 238
Hearon, J. Z., 47, 57
Hector, L. G., 184, 185, 189, 236, 238
Hedberg, K., 325, 342 (ref. 29), 343 (ref. 29), 361
Hedberg, L., 342 (ref. 29), 343 (ref. 29), 361
Heeks, J. S., 342 (ref. 77), 362
Heer, J. de, 194, 196, 236
Heilbronner, E., 27 (ref. 24), 30
Hellund, E. J., 282, 320
Henkel, J., 88 (ref. 8), 91 (ref. 8), 128
Herrman, E., 240, 264
Herschbach, D. R., 132 (ref. 15), 136 (ref. 15), 139 (ref. 14), 169
Herzberg, G., 341 (ref. 49), 361
Hill, W. H., 205, 235
Himes, R. C., 341 (ref. 50), 361
Hirota, E., 357 (ref. 58), 362
Hirschfelder, J. O., 59-129, 184, 186, 196 (ref. 42), 236, 282, 284, 290 (ref. 23), 319, 320
Hjalmars, I., 340, 344, 361
Hoarau, J., 171-238
Hoerni, J. A., 327 (ref. 52), 361
Hoijsink, G. J., 5 (ref. 10), 27 (ref. 11), 28 (ref. 12), 30
Honda, H., 223, 236
Houwalt, A., 265
Hove, J. E., 226, 236
Hückel, W., 190, 236
Hüttig, G. F., 240, 264
Hurewicz, W., 51, 57
Hush, N. S., 9, 23, 27 (ref. 13), 29, 30
Ibers, J. A., 325, 327 (refs. 52, 72), 361, 362
Ijima, T., 359 (ref. 63), 362
Iley, R., 223 (ref. 120), 238
Inokuchi, H., 223 (ref. 3), 235
Itoh, T., 198, 236
Jankowska, H., 253 (ref. 8), 264, 265
Johnson, H. R., 342 (ref. 53), 361
Johnston, D. F., 236
Johnston, H. S., 131-170
Jousot-Dubien, J., 173, 176, 237
Jurewicz, A., 256 (ref. 10), 257 (ref. 10), 264, 265
Kabadi, M. B., 185, 238
Kambe, K., 198, 236
Kamieński, B., 249, 264
Karczewski, K., 249 (ref. 3), 264
Karle, I. L., 325, 357, 361
Karle, J., 325, 357, 361
Kassel, L. S., 139, 169
Kemble, E. C., 184, 236
Khinchin, A., 277, 320
Kiive, P., 223, 237
Kilb, R. W., 342 (ref. 55), 362
Kimball, G. E., 149 (ref. 10), 169
Kirkwood, J. G., 127, 128, 129
Kistiakowsky, G. B., 144 (ref. 18, 151 (ref. 18), 170
Kjeldaa, T., Jr., 219, 221, 236
Klein, F. S., 164 (ref. 4), 169
Klein, G., 95, 100, 128
Klein, M. J., 305, 307, 308, 311, 320
Kleinerman, M., 13 (ref. 2), 23 (ref. 2), 30
Klemm, W., 172 (ref. 52), 236
Kocot, D., 265
Koefoed, J., 37, 57
Kohn, W., 219, 221, 236
Koutecký, J., 2
Krishnan, K. S., 195 (ref. 55), 196 (ref. 55), 222, 225, 229, 236
Kryloff, N., 51, 54, 57
Kuchitsu, K., 352 (ref. 56), 356, 357 (refs. 60, 61), 362
Laidler, K. J., 132 (ref. 12), 134 (ref. 12), 139 (ref. 12), 142 (ref. 12), 149 (refs. 12, 13), 169
Laitinen, H. A., 5, 9, 30
Landau, L., 215, 236
Lemanceau, B., 173, 176, 237
Leone, J. T., 12 (ref. 6), 15-18 (ref. 6), 30
Lewicki, W., 264, 265

- Libus, Z., 264
 Lidiard, A. B., 236
 Lin, C. C., 342 (ref. 55), 362
 Linder, B., 128, 129
 Lipka, B., 256 (ref. 10), 257 (ref. 10), 264, 265
 Livingston, R. L., 325
 London, F., 181, 191, 192, 194, 236
 Lonsdale, K., 195, 196 (ref. 55), 236
 Lotka, 52
 Lumbroso, N., 185 (ref. 78), 189 (ref. 78), 195 (ref. 43a), 205 (ref. 78), 207-210 (ref. 78), 236, 237
 Lurcat, F., 316, 320

 McClure, J. W., 231, 236
 Maccoll, A., 26 (ref. 16), 30
 McCone, A., Jr., 68, 79 (ref. 13), 128
 McElcheran, D. E., 168 (ref. 7), 169
 Machlup, S., 39 (ref. 12), 41 (ref. 12), 57, 278, 279, 320
 McNesby, J. R., 153, 154 (ref. 19), 170
 McWeeny, R., 194, 236
 Maeda, K., 357 (ref. 61), 362
 Mahieu, M., 33 (ref. 17), 57
 Mandelcorn, L., 153 (ref. 20), 170
 March, N. H., 219, 236, 237
 Marchand, A., 171-238
 Marcus, R. A., 28, 30
 Marjury, T. G., 153 (ref. 21), 155, 170
 Markowitz, J. M., 11 (ref. 7), 30
 Martin, A. J., 11 (ref. 8), 12 (ref. 8), 30
 Massey, H. S. W., 185, 207 (ref. 22), 235, 327 (ref. 65), 362
 Matsen, F. A., 27 (ref. 25), 31
 Matsunaga, Y., 223 (ref. 3), 235
 Mayot, M., 193 (ref. 63), 194, 235, 237
 Mazur, P., 294, 298, 301, 302 (ref. 30), 320
 Meijer, P. H. E., 307, 308, 311, 316, 320
 Meixner, J., 298 (refs. 32, 33), 320
 Mel, H. C., 298 (ref. 34), 304, 320
 Miazek, M., 264
 Minc, S., 241, 264
 Mitra, N. G., 205, 206, 235
 Miwa, M., 222, 237
 Miyagawa, I., 352 (ref. 62), 362
 Molinari, E., 168 (ref. 5), 169
 Mooser, E., 234, 235
 Morino, Y., 325, 352 (ref. 62), 356 (ref. 59) 357, 359 (ref. 63), 362
 Morrow, J. C., 184, 237
 Mott, N. F., 325 (ref. 64), 327 (ref. 65), 362
 Mrowka, B., 184, 186, 187, 236, 237
 Mrozowski, S., 226, 230, 237
 Müller, F., 246, 264
 Munthe-Kaas, T., 341 (ref. 12), 342 (refs. 12, 66), 359 (ref. 12), 360, 362
 Murakami, T., 288, 289, 291, 320

 Nakai, S., 285 (ref. 36), 289, 320
 Nakamura, Y., 359 (ref. 63), 362
 Nelson, J. B., 345 (ref. 67), 362
 Neumann, J. v., 104, 129
 Newell, G. F., 184, 237
 Nicholson, A. J. C., 153 (ref. 22), 170
 Nielsen, A. E., 304, 320
 Noyes, W. A., Jr., 153 (ref. 8), 169
 Nozières, P., 231, 237

 Odell, T., 128
 Ohno, K., 198, 236
 Oleszczyk, Z., 241, 264
 Ono, S., 267-321
 Onsager, L., 34, 35, 39, 41, 57, 273, 274, 276, 278-280, 320
 Osborne, M. F. M., 219, 237
 Oswin, H. G., 153 (ref. 23), 170
 Ouchi, K., 223 (ref. 44), 236
 Overhauser, A. W., 311, 320

 Pacault, A., 171-238
 Palczewska, W., 264
 Paramasivan, S., 222 (ref. 76), 237
 Pascal, P., 185, 189, 203-205, 207-211, 237
 Pauli, W., 308, 320
 Pauling, L., 141, 170, 190, 237
 Pease, R. N., 100, 129
 Peierls, R. E., 105, 217, 237
 Perceau, R., 210
 Pines, D., 219, 221, 237
 Pinnick, H. T., 223, 237
 Pinsker, G., 324
 Pitzer, K. S., 132, 139 (ref. 14), 169, 170
 Plyler, E. K., 348 (ref. 2), 349 (ref. 2), 360

- Polanyi, J. C., 139 (ref. 26), 147, 170
 Powell, R. E., 139 (ref. 14), 169
 Pressman, D., 12 (refs. 26, 27), 31
 Prigogine, I., 33, 39, 41, 47, 54, 57, 286, 293, 294 (ref. 46), 298 (refs. 47, 51), 299, 302 (ref. 49), 304 (ref. 51), 305 (ref. 52), 306, 307 (ref. 51), 320, 321
 Probulski, S., 265
 Prokopowicz, M., 253 (ref. 8), 264, 265
 Pugh, E. W., 237
 Pullman, A., 25 (refs. 21, 22), 26 (refs. 21, 22), 27 (refs. 1, 21, 22), 28 (refs. 19-21, 21a), 30
 Pullman, B., 1-31, 193 (ref. 63), 194, 195 (ref. 9), 196 (ref. 9), 235, 237
 Raether, H., 324
 Ramsey, N. F., 186, 237
 Rao, S. R., 222 (ref. 86), 237
 Rapp, D., 132 (ref. 15), 136 (ref. 15), 149, 169, 170
 Rastrup-Andersen, J., 341 (refs. 21, 22), 361
 Rayleigh, Lord, 273, 280, 321
 Rebbert, R., 153 (ref. 23), 170
 Reitan, A., 339 (ref. 68), 359, 362
 Reuther, H., 246, 264
 Rice, F. O., 153, 154 (ref. 28), 170
 Rice, O. K., 37, 57
 Rienaecker, G., 254, 264
 Riley, D. P., 345 (ref. 67), 362
 Robertson, J. M., 345 (ref. 70), 346 (ref. 70), 362
 Rosen, N., 184, 237
 Rosenthal, I., 11 (refs. 7, 8), 12 (ref. 8), 28 (ref. 23), 30
 Salzberg, Z., 128, 129
 Sanchez, M., 264
 Sastri, M. V. C., 205, 236
 Sato, S., 139, 164, 170
 Schalit, L. M., 100, 128
 Scherr, G. W., 189, 237
 Schmid, R. W., 27 (ref. 24), 30
 Schomaker, V., 325, 327 (refs. 47, 72), 361, 362
 Schooten, J. van, 28 (ref. 12), 30
 Schumacher, R. T., 220, 221 (refs. 89, 90), 237
 Selwood, P. W., 172 (ref. 91), 238
 Semenov, N. N., 170
 Sheehan, W. F., Jr., 327 (ref. 72), 362
 Sheridan, J., 342 (ref. 77), 362
 Shiba, H., 212, 238
 Shida, S., 198, 236
 Shimanouchi, T., 357 (ref. 60), 362
 Shimozawa, T., 352 (ref. 62), 362
 Shoenberg, D., 231, 238
 Siegert, A. J. F., 308 (ref. 56), 321
 Sinanoglu, O., 132 (ref. 31), 170
 Skancke, P. N., 323-362
 Slichter, C. P., 220, 221 (refs. 89, 90), 237
 Slonczewski, J. C., 227, 231, 238
 Sojecki, W., 265
 Sone, T., 184, 189, 238
 Spalding, D. B., 83, 129
 Spaulding, W. P., 88 (ref. 8), 91 (ref. 8), 128
 Spiridonov, V. P., 347 (ref. 1), 360
 Sriraman, S., 238
 Steacie, E. W. R., 131 (ref. 32), 153, 154 (ref. 37), 155, 170
 Steele, M. C., 219, 237
 Steensholt, G., 184, 238
 Stevens, D. K., 234, 238
 Stoicheff, B. P., 327 (ref. 74), 338, 340, 341 (refs. 73, 74, 76), 342 (refs. 31, 32, 74-76), 348 (ref. 44), 349 (ref. 44), 361, 362
 Stoner, E. C., 216, 238
 Strand, T., 341 (ref. 15), 345 (ref. 15), 360
 Strandberg, M. N. P., 342 (ref. 53), 361
 Strazesco, D. M., 259 (ref. 7), 264
 Svendsås, P., 350 (ref. 14), 360
 Takahashi, A., 357 (ref. 61), 362
 Takahashi, H., 223 (ref. 3), 235
 Tanford, B. C., 100, 129
 Taylor, G. I., 105, 129
 Thomas, L. F., 342 (ref. 77), 362
 Thomsen, J. S., 308, 321
 Tibbs, S. T., 185, 207 (ref. 22), 235
 Tillieu, J., 181, 187, 189, 199, 200, 235, 236, 238
 Tomassi, W., 239-265

- Trætteberg, M., 341 (refs. 16, 17), 342 (refs. 16-18), 343 (ref. 16), 349 (refs. 16-18), 350 (ref. 16), 354 (ref. 16), 358 (ref. 17), 359 (refs. 17, 18), 360
 Trendelenburg, F., 331 (ref. 78), 362
 Treszczanowicz, E., 256, 257 (ref. 10), 264
 Trew, V. C. G., 185, 238
 Trotman-Dickenson, A. F., 131 (ref. 33), 151 (ref. 33), 153 (refs. 34, 35), 170
 Tuli, G. D., 205, 206, 235
 Tulinsky, A., 341 (ref. 79), 362
 Ubbelohde, A. R., 190, 238
 Uehling, E. A., 282, 320
 Unger, S., 254 (ref. 6), 264
 Vaidyanathan, V. I., 185, 189, 205, 222 (ref. 104), 238
 Van Artsdalen, E. R., 144 (ref. 18), 151 (ref. 18), 170
 Vanderslice, T. A., 153, 154 (ref. 28), 170
 Van Meersche, M., 168 (ref. 36), 170
 Van Vleck, J. H., 181-184, 186, 187, 238
 Venkatachalam, K. A., 185, 238
 Venkateswarlu, K., 238
 Viervoll, H., 325 (ref. 80), 362
 Volpi, G. G., 168 (ref. 5), 169
 Volterra, V., 48, 51, 52, 57, 306, 321
 Waldmann, L., 284 (ref. 59), 286 (ref. 59), 321
 Wallace, P. R., 226, 231, 236
 Walter, J., 149 (ref. 10), 169
 Wang, S. C., 184, 238
 Wangsness, R. K., 312-316, 321
 Watanabe, S., 319, 321
 Watson, A. T., 27 (ref. 25), 31
 Wawrzyniak, I., 253 (ref. 9), 264, 265
 Wawzonek, S., 5, 9, 30
 Weinstein, B., 324
 Weiss, P. R., 227, 231, 238
 Weltner, W., 184, 186, 238
 Wergeland, H., 289 (ref. 63), 321
 Westenberg, A. A., 342 (ref. 81), 362
 Weston, R. E., Jr., 164 (ref. 4), 169
 White, J. G., 341 (ref. 79), 345 (ref. 70), 346 (ref. 70), 362
 Whittle, E., 153 (ref. 37), 154 (ref. 37), 155, 170
 Wiame, J. M., 293 (ref. 46), 294 (ref. 46), 320
 Wick, G. C., 184, 186, 238
 Wilde, K. A., 88, 91-93, 129
 Wills, A. P., 184, 189, 238
 Wilson, A. H., 217, 219, 238
 Wilson, D. J., 139 (refs. 16, 39), 144, 165 (ref. 39), 169, 170
 Wilson, E. B., Jr., 136 (ref. 38), 138 (ref. 38), 170, 342 (refs. 55, 81), 362
 Winstein, S., 12 (ref. 26), 31
 Witmer, E. E., 184, 186, 238
 Wolfsberg, M., 138 (ref. 3), 164 (ref. 4), 169
 Wood, W. W., 124, 125, 127, 128, 128, 129
 Woodbridge, D. B., 205, 238
 Wrobel, H., 264, 265
 Wynne-Jones, W. F. K., 223 (ref. 120), 238
 Xhrouet, E., 33 (ref. 18), 57
 Yager, W. A., 231, 236
 Yang, T. Y., 211, 238
 Yoshizumi, H., 198, 236
 Young, W. G., 12 (refs. 26, 27), 31
 Zeldovitch, Y. B., 104, 129
 Zener, C., 184, 236
 Ziedlecka, Z., 265
 Zuman, P., 10

SUBJECT INDEX

- Absorbents, potentiometric investigations of, 258
- Adams and Wilde approximations for the flame equations, 91
- Additivity law of magnetic properties, 202
- Alkalies and alkaline earths, magnetic susceptibility of a metallic crystal, experimental results and interpretation, 220
- Aromatic molecules, diamagnetic anisotropy of, London's quantitative theory, 190
- Arrhenius kinetics and detonations in real gases, 121
- Arrhenius kinetics, model of unimolecular reactions producing flames, 76
- Atomic magnetic susceptibilities, determination of, 204
- Bond dissociation energy, evaluation of the index p from symmetrical activated complex, 167
- Bond rupture, in organic electrode reactions, 3
- Broersma apparatus for measuring diamagnetic susceptibilities, 173
- Carbon blacks and polycrystalline graphite, magnetism of mono- and polycrystalline graphite, 226
- Carbon-halogen bond fission, 11, 14
- CH_2 group, magnetic susceptibility of, 204
- Chemical reaction mechanism, 5ff. (*See also* Electrochemical reaction mechanism)
- carbon-halogen bond fission, 11
- ketone reduction, 12
- Chemical reaction rates, calculated, applications to experimental data, 151
- parameter needed from the potential energy surface, 139
- tunnelling corrections in, 131ff.
- Chemical reactions, number of essential coordinates to describe, 132
- tunnelling factors, 148
- Conformational analysis, molecular structure determination, 353
- Contact substances, investigation of by means of powder electrodes, 253
- Continuous systems, and minimum entropy production, 298
- Coordinates to describe chemical reactions, number of essential, 132
- Corner approximation for the flame equations, 89
- Dense gases, variational principles in the kinetic theory of gases applied to, 289
- Detonation equations, 110
- Detonation produced by single-step unimolecular reaction, 104ff.
- Arrhenius kinetics and detonations in real gases, 121
- detonation equations, 110
- ignition temperature model, 115
- Detonations and flames, theory of the propagation of, 59ff. (*See also* Hydrodynamic equations of change)
- Diamagnetic anisotropy of aromatic molecules, London's quantitative theory, 190
- London's theory compared with experiment, 194
- Diamagnetic susceptibilities, measurements of, 172ff. (*See also* Magnetic susceptibility)
- theories of, 178ff.
- Diamagnetism of semi-free electrons, 214ff.
- Diffraction of electrons (*See* Electron diffraction)
- Dilute gases, mixtures of, variational principle in the kinetic theory of

- gases, 281
- Discontinuous systems and minimum entropy production, 293
- Dispersed-crystal organic substances, investigations of, 261
- Dissipation of energy, principle of least, 274, 277
- Effective masses of charged particles, determination of, using their magnetic properties, 234
- Electrochemical reaction mechanism, 13ff. (*See also* Chemical reaction mechanism)
 - carbon-halogen bond fission, 14
 - ketone reduction, 16
- Electrode reactions, organic, bond rupture, 3
 - chemical reaction mechanism, 5
 - electrochemical reaction mechanism, 13
 - energetic reaction mechanism, 19
 - mechanisms, 3ff.
 - processes involving more than two electrons, 4
- Electron diffraction, in gases, and molecular structure, 323ff.
 - determination of mean amplitude of vibration of molecules, 357
 - from free molecules, theoretical outline, 325
 - method for the precision determination of internuclear distances, 336
 - method of studying molecular structure, experimental method and calculation procedure, 328
 - future prospects, 359
- Energetic reaction mechanism, of organic electrode reactions, 19
 - quantum mechanical approach, 24
 - thermodynamic-kinetic approach, 19
- Energy, principle of least dissipation of, 274, 277
- Entropy, generalized minimum production principle, 316
 - principle of minimum production of, 293
 - application to magnetic resonance, 311
 - in an ideal gas, 307
 - in continuous systems, 298
 - in discontinuous systems, 293
 - nonlinear irreversible processes, 304
 - statistical theory of the principle of the minimum production of, 307
- Flames and detonations, theory of the propagation of, 59ff. (*See also* Hydrodynamic equations of change)
- Flames produced by an exothermic unimolecular reaction, 68
 - approximate solutions of equations for, 88ff.
 - Arrhenius kinetics applied to, 76
 - effect of kinetic energy terms on equations for, 86
 - flame equations for, 69
 - ignition temperature model for, 74
- Flames supported by complex systems of chemical reaction chains, 96
- Free molecules, electron diffraction from, theoretical outline, 325
- Graphite, magnetism of mono- and polycrystalline, 222, 226 (*See also* magnetism)
 - theoretical studies, Gonguli and Kreshman, 225
- Guy and Tellieu method of calculating magnetic susceptibility, 187
- Half-wave potential, significance in electrochemical reaction mechanism of pH-dependence of, 15
- Hirschfelder approximations for the flame equations, 93
- Hydrodynamic equations of change and the theory of the propagation of flames and detonations, 60
 - boundary conditions, 66
 - one-dimensional steady-state equations, 65
 - one-dimensional time-dependent equations, 63
- Ideal gas, microscopic description of entropy production in, 307
- Ignition temperature approximation for

- the flame equations, 88
- Ignition temperature model, for single-step unimolecular reactions that produce detonations, 115
 - for unimolecular reactions that produce flames, 74
- Increments of structure, 208
- Internuclear distances, precision determination of, 336
- Irreversible processes, nonlinear, 33ff., 304
 - nonlinear problems in thermodynamics of, 33ff.
 - oscillating reactions, 47
 - thermodynamics of linear systems, 35
 - thermodynamics of nonlinear systems, 39
 - variational principles in thermodynamics and statistical mechanics of, 267ff.
- Ketone reduction, chemical reaction mechanism, 12
 - electrochemical reaction mechanism, 16
- Kinetic energy terms, effect on equations for flames produced by an exothermic unimolecular reaction, 86
- Kinetic theory of gases, variational principles in, 281ff., 286, 289
- Klein approximation for the flame equations, 95
- Linear systems, irreversible processes of, 35, 301 (*See also* Continuous systems; Discontinuous systems)
- London, quantitative theory of diamagnetic anisotropy of aromatic molecules, 190, 194
- Magnetic properties of charged particles, determination of effective masses using, 234
- Magnetic resonance, application of the theory of the minimum entropy production principle to, 311
- Magnetic susceptibility, 204ff. (*See also* Diamagnetic anisotropy; Diamagnetic susceptibilities)
 - determination of atomic, 204
 - introduction of increments of structure, 208
 - susceptibility of the CH₃ group, 204
 - Tellieu and Guy method of calculating, 187
 - Van Vleck method of calculating, 181
- Magnetic susceptibility of a metallic crystal, 215
 - experimental results and interpretation, 220
 - alkalies and alkaline earths, 220
 - other metals, 221
 - transition elements, 220
 - theory of, 215
- Magnetism of mono- and polycrystalline graphite, 222
 - experimental results, 222
 - theoretical studies, 224-226
- Magnetochemical systematizations, experimental, 202, 204, 211
 - experimental and theoretical, comparison with experiment, 213
 - theoretical, 199, 213
- Metallic crystal, magnetic susceptibility of, 215 (*See also* Magnetic susceptibility)
- Molecular structure determination, 335ff.
 - conformational analysis, 353
- Molecular structure, electron diffraction, 323ff.
- Molecular structure problems, 347
- Molecular vibration electron diffraction method of studying, 357
- Nonlinear irreversible processes, 33ff., 39, 304 (*See also* Continuous systems; Discontinuous systems)
- Nonlinear systems, thermodynamics for irreversible processes of, 39
- Onsager's reciprocity relations, 274
- Organic electrode reactions, rate constant calculation, 29
- Oscillating reactions in irreversible processes, 47
- p*, the index (*See* Bond dissociation energy)

- Pacault, Lemanceau, and Jousset-Dubien apparatus for measuring diamagnetic susceptibilities, 174
- Partition functions, molecular, new method of expressing, 134
- Partition functions, new method of expressing molecular, 134
- pH-dependence of half-wave potential, significance in electrochemical reaction mechanism, 15
- Polycrystalline graphite and carbon blacks, magnetism of mono- and polycrystalline graphite, 222, 226
- Potential energy surface, parameters needed to calculate chemical reaction rates from, 139
- Potentiometric investigations of adsorbents, 258
- Powder electrodes, compound, 246
 mechanism of establishing the potential of, 251
 principles of the correct construction of, 247
 construction of, 239
 investigation of contact substances by means of, 253
 investigation of Fe—C and Fe—Zn systems, 256
- Powder electrodes of the first kind, 241
- Powder electrodes without a powered substance, 263
- Reaction rates (*see* Chemical reactions; Chemical reaction mechanism; Chemical reaction rates)
 calculated, applications to experimental data, 151
 parameters needed from the potential energy surface for chemical, 139
 tunnelling corrections in chemical, 131ff.
- Reactions, chemical, number of essential coordinates to describe, 132
- Semi-free electrons, diamagnetism of, 214ff.
 experimental results and interpretation, 220
 theory, 215
- Single-step unimolecular reaction detonation, 104 (*See also* Detonation produced by single-step unimolecular reaction)
- Quantum mechanical approach to the problem of the energetic reaction mechanism, 24
- Rate constant calculation in organic electrode reactions, 29
- Reaction mechanism (*See* Chemical reaction mechanism; Electrochemical reaction mechanism)
- Structure determinations, of molecules, 335ff.
- Thermodynamic-kinetic approach to the problem of the energetic reaction mechanism, 19
- Thermodynamics of linear systems for irreversible processes, 35
- Thermodynamics of nonlinear systems, for irreversible processes, 39
- Transition elements, magnetic susceptibility of a metallic crystal, experimental results and interpretation, 220
- Tunnelling corrections in chemical reaction rates, 131ff.
- Tunnelling factors in chemical reactions, 148
- Unimolecular reactions that produce detonation (*See* Detonation produced by single-step unimolecular reaction)
- Unimolecular reactions that produce flames (*See* Flames produced by an exothermic unimolecular reaction)
- Van Vleck method of calculating magnetic susceptibility, 181